ISSN 0861-0509

Acta morphologica et anthropologica (10)

10• Sofia• 2005• Institute of Experimental Morphology and Anthropology

Contents

Anthropology

EDITORIAL

Koprivshtitsa Morphological Days, 5th National Conference on Anthropology (June 4-6, 2004)

Institute of Experimental Morphology and Anthropology Bulgarian Academy of Sciences, Sofia

From June 4th to 6th in the town of Koprivshtitsa was held Fifth National Conference on Anthropology with international participation and the Koprivshtitsa Morphological Days devoted to the 125th anniversary of the passing of the eminent founder of Bulgarian Renaissance Lyuben Karavelov.

These scientific meetings were organized by the Institute of Morphology and Anthropology at BAS together with the Bulgarian Anthropological Society and the Bulgarian Anatomical Society. 130 scientists from Bulgaria, Turkey, Holland and Germany took part in the conference.

A total of 49 reports and 40 posters have been presented.

The town of Koprivshtitsa has for the first time played host to a scientific forum.

The exceptionally warm cooperation of the town municipality has greatly helped the organization and realization of the conference.

On the day of the official opening ceremony, June 4th 2004, in the presence of the local authorities the chairman of the Bulgarian Anthropological Society and Head of the Institute of Experimental Morphology and Anthropology at BAS corresponding member prof. Dr. Yordan Yordanov bestowed on the part of BAS a plastic anthropological reconstruction of the head by the skull of Lyuben Karavelov.

The conference was opened by prof. Dr. Vassil Vassilev — chairman of the Bulgarian Anatomical Society. A welcome address to the participants was extolled by the mayor of the town of Koprivshtitsa Mr. Nikola Kamenarov the stress being placed on the rich historical past of the town and a major tourist venue of Bulgaria.

Greeting addresses were presented by prof. J. Koebke on the part of the German participants, prof. R. Mesut from Turkey, prof. K-H. Korfsmeier from the Anatomische Geselschaft and Mrs. Iskra Shipeva from the Directorate of the Town History Museums.

The communications and posters at the conference were presented by collaborators of the Chairs of Anatomy, Histology and Embryology and the Chairs of General Biology at the Medical and Veterinary Departments, Institutes of BAS, Chairs of Sofia University "St. Kliment Ohridski", Plovdiv University "Paisiy Hilendarski", etc.

The presentations of all reports were accompanied by animated and fruitful discussions.

The management of IEMA—BAS and the editorial board of Acta Morphologica et Anthropologica have decided on their publication in vol. 10 of the journal.

Institute of Experimental Morphology and Anthropology

Acta morphologica et anthropologica, 10
Sofia • 2005

Morphology

Keratan-Sulfate Immunohistochemistry: a New Tool for Characterization of Microglial Morphology and Topography

D. Kadiysky, M. Svetoslavova*, N. Sales**, C. Lasmezas**, J.-Ph. Deslys***

* *Institute of Experimental Morphology and Anthropology, Bulgarian Academy of Sciences, Sofia*
** *Groupe d'Inovation Diagnostique et Therapeutique sur Infections a Prions (GIDTIP), Laboratoire de Neurovirologie, Commissariat a l'Energie Atomique, Fontenay aux Roses, France*

Recently discovered anti-keratan-sulfate monoclonal antibody 5D4 selectively stains ramified microglia *in situ* both in paraffin and cryostat sections. Using this antibody are studied and discussed in this work both the structural polymorphism of microglia and their heterogenous density throughout the CNS (topography).

Key words: keratan-sulfate immunohistochemistry, microglia, 5D4 monoclonal antibodies, central nervous system (CNS).

Introduction

Microglia are distinct cell type in the CNS [5] but at the same time many evidences indicate that they are one of the components of the brain mononuclear phagocytes [7, 10]. Regularly spaced microglia in brain as "resting" type under physiological conditions they adopt ramified morphological appearance and serve the role of immune surveillance and host defence [4]. Microglia are the sole cells in CNS expressing immune functions [11]. Since Del Rio Hortega's studies on microglia in 1932 [6] till now many questions about cellular size, exact shape or about not so-uniform microglial morphology aren't dissolved clearly. Keratan-sulfate immunohistochemistry using 5D4 monoclonal antibodies was proposed last decade as specific marker for the most numerous subgroup of brain mononuclear phagocytes-ramified microglia [8, 9]. 5D4 monoclonal antibodies are directed against human keratan sulfate [2]. Keratan sulfate as a sulfated mucopolysaccharide is found in skeletal tissues and

cornea, and it contains D-galactose and D-glucosamine-6-O-sulfate. Our study shows the specific labelling features of keratan sulfate immunohistochemistry in CNS and some new data about microglial morphology.

Material and Methods

Animals: 10 adult female hamsters 5 weeks old are used. Anaesthetized hamsters were sacrificed and the brains were fixed in Carnoy's solution at room temperature overnight. After embedding in paraffin transversal sections 7 μm were obtained using. Commercially available monoclonal *antibodies* 5D4 (Calbiochem-San Diego CA), clone 5-D-4, isotype IgG1, k, were used for immunohistochemical procedure. Optimal working dilution of monoclonal antibodies is 1:1000 for overnight incubation at 4°C. The next day a procedure, using PicTure Polymer Detection System — a horseradish peroxidase/Fab polymer conjugate (ZYMED), was performed for 45 min at room temperature. DAB substrate kit for peroxidase (VECTOR) is applied as diaminobenzidine chromogen for 5-10 min. *Studied CNS regions*: immunohistochemistry of cerebral cortex, hippocampus, cerebellum, thalamus. *Controls*: Whole immunostaining procedure without 5D4 mAb and whole procedure with 5D4 mAb 1:1000 in PBS with 100 μg type I and II keratan sulfate.

Results

Keratan-sulfate immunohistochemistry applied in healthy hamster CNS shows that 5D4(+) cells are located in all studied by us regions: cortex, hippocampus, thalamus and cerebellum (Fig. 1). 5D4(+) microglial cells are characteristic with their ramified shape and multiple branched cellular processes and immunopositivity is expressed equally by highly ramified and by not so well ramified microglial cells (Fig. 2). In the cerebellum, cortex and thalamus are distributed smaller (8-12 μm), oval, and visually non-well ramified 5D4(+) microglial cells. The density of this type microglia increases essentially in molecular layer of cerebellum (Fig. 3). Keratan sulfate immunohistochemistry visualizes a specific for the brain parenhyma cellular association: cell-to-cell direct contact between a highly ramified and widespread microglial cell with one (or several) big neuron(s). A centrally located very thin blood vessel (8-10 μm in diameter) is always found in the middle of this cellular complex (Fig. 4). This finding that cellular and vascular elements interact in clusters is equally demonstrated in hamster brain cortex, hippocampus and thalamus.

Discussion

The specificity of this immunohistochemical procedure for ramified microglia is confirmed previously [1, 2, 3]. Keratan-sulfate epitope is expressed only by this microglial subpopulation [2] but not by all microglia. According to Wilms H. et al. [12] the smaller 5D4(+) cells (with not-well ramified shape) are probably microglia in the early stages of morphological transformation into ramified state. Our finding that many 5D4(+) microglial cells in the mature brain are in direct contact with neuronal population shows the large variety of the cell interactions in CNS. The specific localization of the neuron/microglia complexes next to adjacent microvascular network point to their eventual activities in blood brain barrier functions but this remains an open issue for further studies.

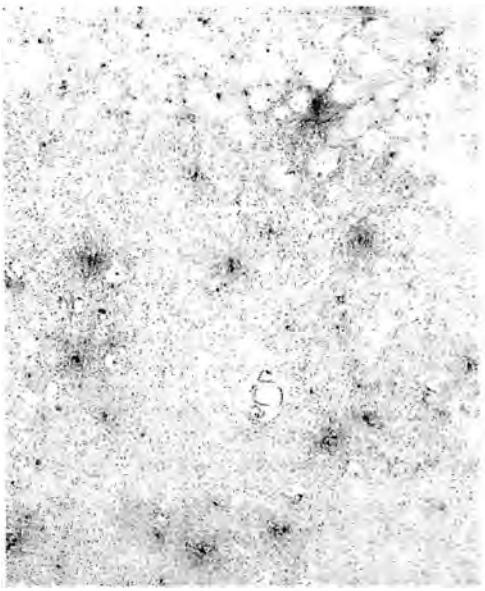

Fig. 1. Topographical distribution of 5D4(+) ramified microglia in mature hamster CNS. Hippocampus area (× 200)

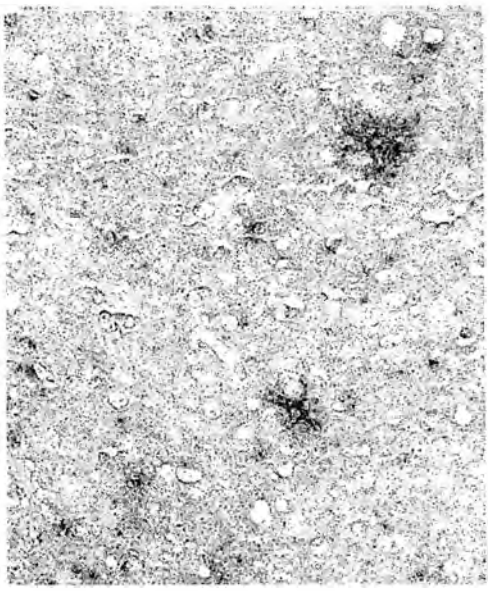

Fig. 2. Keratan-sulfate immunohistochemistry of two kind 5D4(+) microglia: large, highly ramified and smaller (not so well ramified) cells. Thalamus area. Adult hamster (× 400)

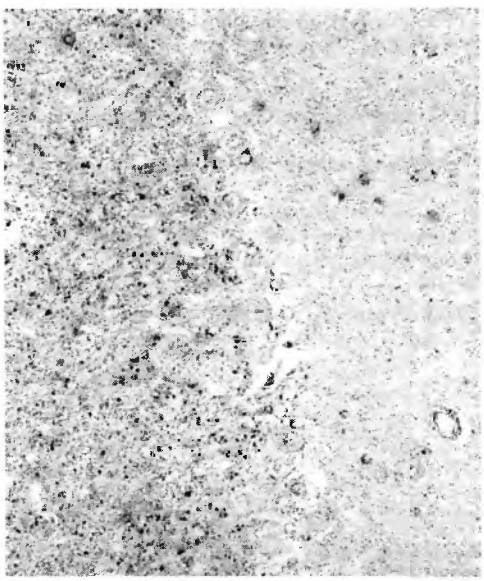

Fig. 3. Density of the smaller (not so well ramified) subclass of 5D4(+) microglia throughout molecular layer of cerebellum. Adult hamster (× 200)

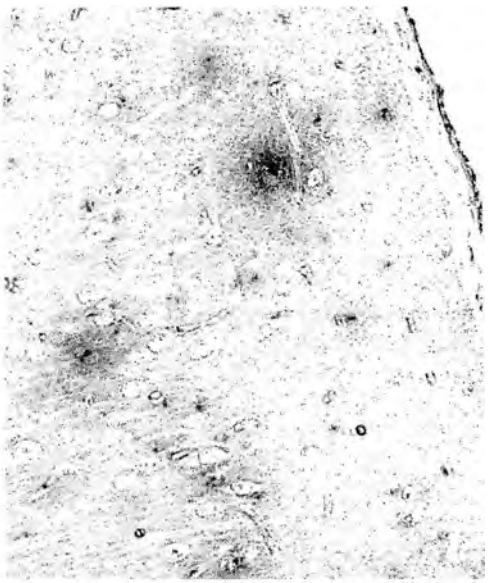

Fig. 4. Microglia/neuron cell-to-cell complexes associated to fine brain vasculature. Occipital cortex. Adult hamster (× 400)

Conclusion

Our data obtained by keratan-sulfate immunohistochemistry for ramified microglia reinforce the knowledge about morphology, tissue distribution (topography) and microenvironmental interrelationships of ramified microglia — a basic member of exclusively heterogenous family of brain mononuclear phagocytes.

References

1. Bertolotto, A. et al. 5D4 keratan sulfate epitope identies a subset of ramified microglia in normal central nervous system parenhyma. — J. Neuroimmunol., **85**, 1998, 69-77.
2. Bertolotto, A., B. Katerson, G. Canavese, A. Migheli, D. Schiffer. Monoclonal antibodies to keratan sulfate immunolocalize ramified microglia in paraffin and cryostat sections of rat brain. — J. Histochem. Cytochem., **41**, 1993, 481-487.
3. Bertolotto, A. et al. Keratan sulfate is a marker of ramified microglia. — Dev. Brain. Res., **26**, 1995, 233-241.
4. Bin, L., J. S. Hong. Role of microglia in inflammation-mediated neurodegenerative diseases: mechanisms and strategies for therapeutic intervention. — J. Pharm. Exp. Therap., **304**, 2003, 1-7.
5. Del Rio Hortega, P. Estudios sobre la neuroglia. La glia de escasas radiaciones (oligodendroglia). — Biol. Real. Soc. Espan. Hist. Nat., **21**, 1921, 63-92.
6. Del Rio Hortega, P. Microglia. — In: Cytology and cellular pathology of the nervous system. (Ed. W. Penfield). New York, Hoeber, 1932, 481-543.
7. Graeber, M., G. Kreutzberg, W. Streit. Foreword to Glia. — Glia, **7**, 1993, 2-4.
8. Janders, S., G. Stol. Downregulation of microglial keratan sulfate proteoglycans coincident with lymphomonocytic infiltration of the rat central nervous system. — Am. J. Pathol., **148**, 1966, 71-78.
9. Janders, S., G. Stol. Strain-specific expression of microglial keratan sulfate proteoglicans in the normal rat CNS: correlation with expression of MHC class II antigens. — Glia, **18**, 1966, 255-260.
10. Savada, M., A. Susumura, H. Yamamoto, T. Marunouchi. Activation and proliferation of microglia by CSF-1 and involvement of protein kinase C. — Brain. Res., **509**, 1990, 119-124.
11. Streit, W. Microglia as protective, immunocompetent cells of the CNS. — Glia, **40**, 2002, 133-139.
12. Wilms, H., M. A. Wollmer, J. Sievers. In vitro-staining specifity of the antibody 5D4 for microglia but not for monocytes and macrophages indicates that microglia are unique subgroup of the myelomonocytic lineage. — J. Neuroimmunol., **98**, 1999, 89-95.

This work was supported by grant N9/2003 from PAI (Programme d'Actions Integrees) franco-bulgares — RILA.

Institute of Experimental Morphology and Anthropology

Acta morphologica et anthropologica, 10
Sofia • 2005

GT1b Ganglioside Brain Changes in Chronic Relapsing Experimental Allergic Encephalomyelitis Induced in the Lewis Rats

E. Zaprianova, D. Deleva, A. Filchev, V. Kolyovska, B. Sultanov

Institute of Experimental Morphology and Anthropology, Bulgarian Academy of Sciences, Sofia

Ganglioside GT1b was suggested to play a role in mediating the interactions between oligodendroglia and axons. Relations between neurons, axons, myelin and glia have been proved to be complex in multiple sclerosis (MS). In this study, the relative distribution of GT1b was determined in the brain of Lewis rats during the early stages of chronic relapsing experimental allergic encephalomyelitis (CREAE), an animal model of MS. A significant decrease of relative portion of GT1b in the brain was detected just before the onset of clinical signs and during the first clinical episode of CREAE. This finding provides evidence of disturbed relationship between axons and oligodendroglia in CREAE. Our data support the new widely accepted hypothesis that axonal damage begins very early in MS pathogenesis.

Key words: ganglioside GT1b, chronic relapsing experimental allergic encephalomyelitis, multiple sclerosis, brain, axon-glia interactions.

Introduction

Chronic relapsing experimental allergic encephalomyelitis (CREAE) is an animal model reproducing many features of human demyelinating disorder multiple sclerosis (MS). In MS the myelin sheath has traditionally been regarded as the primary target and an autoimmune inflammatory component has dominated the description of the disease. Recent studies has brought axonal pathology into the focus regarding the research of MS. Current questions involve the mechanisms, extent, timing and clinical significance of axonal damage in MS. Axonal injury considered at one time to be a late phenomenon, is now recognized as an early occurrence in MS pathogenesis [2, 4, 8, 9, 13]. Investigations of functional interactions between axons and glia have revealed the extent and complexity of neuronal-glial communication during development, adult function and central nervous system disorders [3, 11, 16, 17]. Ganglioside GT1b was suggested to play a role in mediating the interactions between oligodendroglia and axons [9]. Therefore, in this study we determined the relative distribution of GT1b in the brain of Lewis rats during the early development of CREAE (preclinical stage and the first clinical episode).

Materials and Methods

CR EAE was induced in the Lewis rats by inoculation with purified guinea-pig myelin and complete Freund's adjuvant followed by treatment with low-dose cyclosporin A as previously described in detail [14]. Control rats were inoculated as above except that inoculum did not contain myelin. The animals were weighed and examined daily from the seventh days post-inoculum (DPI) for clinical symptoms of EAE and killed at various stages of CREAE as follows: I group — preclinical stage — at 10 DPI (12 animals); II group — first clinical episode of EAE — hindlimb paralysis (12 animals); III group — control rats (12 animals). The total lipids were extracted from the brain by three step extraction with chloroform/methanol/water (4:8:3 by vol.) as described previously [14]. Purification of gangliosides from the total lipid extract was performed according procedure of Ladish and Gillard [6]. The gangliosides were analysed by HPTLC — fractionation and quantified densitometrically at 555 nm. The relative distribution of four major brain gangliosides from Lewis rats with CREAE and from control animals at the various stage of the disease, was determined. The Student's test was used to determine statistical differences between the groups using $P < 0.05$ as the level of confidence.

Results

Clinical findings

The majority of rats inoculated with myelin and complete Freund's adjuvant followed by treatment with CsA developed neurological signs commencing 11-18 DPI. Most of the affected animals recovered fully by 18-22 DPI. The control rats did not develop neurological signs during a period of observation of 40 days after inoculation/initiation of CsA treatment.

Ganglioside profile by HPTLC

The relative percentage of the four major gangliosides (GM1,GD1a,GD1b and GT1b) in Lewis rats during different stages of CREAE and in control rats was recalculated on the basis of the densitograms (Fig. 1 — *A*, *B*, *C*). The relative proportion of GT1b decreases from 21.7% in the control group to 12.9 % just before the onset of clinical signs (preclinical stage) and 7.2 % during the first clinical episode of CREAE (Table 1). The decrease of GT1b during the preclinical stage of CREAE and the first clinical episode of the disease is statistically significant.

Discussion

The data in this study documented a statistically significant decrease of relative portion of GT1b in the brains of Lewis rats with CREAE just before the onset of the clinical signs (the preclinical stage) and during the first clinical episode in comparison to control brains. As it was mentioned above CREAE, because of its histopathology and pronounced demyelination, is considered as an animal paradigm for human MS. Axonal injury and neuronal loss are nw recognized to be hallmarks of MS [13] and to appear during the earliest stages of the disease[2, 4, 7, 10]. Primary axonal injury in the brain and spinal cord of Lewis rats with CREAE has been

A

Peak	height	area
1	40.4	1182.9
2	36.3	1264.5
3	68.7	1845.7
4	25.5	1151.8

B

Peak	height	area
1	26.6	709.7
2	34.8	1143.9
3	68.1	2071.2
4	61.6	1598.7

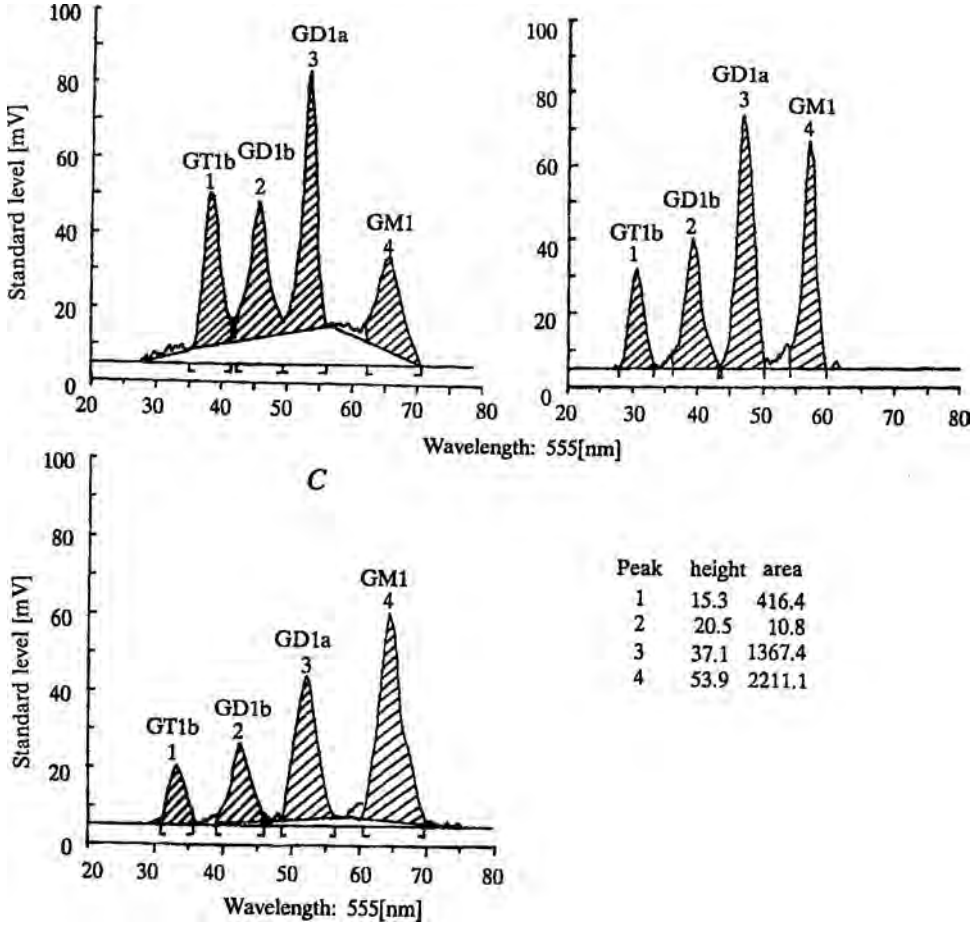

C

Peak	height	area
1	15.3	416.4
2	20.5	10.8
3	37.1	1367.4
4	53.9	2211.1

Fig.1. Densitograms of brain gangliosides of Lewis rats during different stages of the disease: *A* — control animals; *B* — preclinical stage; *C* — first clinical episode of EAE

demonstrated by our electronmicroscopic studies [15]. We could suggest that the decrease of relative portion of GT1b revealed in the present study is connected with the disturbance of axonal-oligodendroglial interactions very early in the pathogenesis of CREAE. Our results corresponds well with the data concerning GT1b changes in two neurodegenerative disorders — Alzheimer's disease and Creutzfeld-Jakob disease. K r a c u n et al. [5] found in Alzheimer's disease GT1b to be decreased in regions involved in its pathogenesis. In Creutzfeld-Jakob disease the percentage distribution of individual gangliosides was characterized by severe decrease in GT1b [8] throughout the patients' nervous tissues.

In conclusion, the findings in this investigation reveal for the first time that GT1b relative portion decreases in the brain of Lewis rats with CREAE at the first stages of CREAE suggesting very early disturbance of axonal-oligodendroglial relationship. They further support the new hypothesis that axonal damage begins early in MS pathogenesis.

Table 1
Relative Percentage of Major Brain Gangliosides in Lewis Rats During Different Stages of CREAE and in Control Rats

Ganglioside	I group (12)	II group (12)	III group (12)
GT1b	21.7 ± 0.5	12.9 ± 0.6	7.2 ± 0.4
GD1b	23.2 ± 0.9	20.7 ± 0.7	19.4 ± 0.7
GD1a	33.9 ± 1.0	37.5 ± 0.6	28.9 ± 0.5
GM1	21.2 ± 0.8	28.9 ± 0.5	44.5 ± 1.0

Numbers in parentheses represent number of different animals analysed individually: I group — control animals; II group — preclinical stage; III group — first clinical episode of EAE.

References

1. Ando, S. et al. Alterations in brain gangliosides and other lipids of patients with Creutzfeldt-Jakob disease and subacute sclerosing panencephalitis (SSPE). — Jpn. J. Exp. Med., **54**, 1984, 229-234.
2. De Stefano, N. et al. Evidence of axonal damage in the early stages of multiple scerosis and its relevance to disability. — Arch. Neurol., **58**, 2001, 65-70.
3. Doyle, J., D. Colman. Glial-neuron interactions and the regulation of myelin formation. — Current Opinion in Cell Biology, **5**, 1993, 779-785.
4. Ferguson, B. et al. Axonal damage in acute multiple sclerosis lesions. — Brain, **120**, 1997, 393-399.
5. Kracun, I. et al. Cortical distribution of gangliosides in Alzheimer's disease. — Neurochem. Int., **20**, 1992, No 3, 433-438.
6. Ladish, S., B. Gillard. A solvent partition method for microscale ganglioside purification. — Anal. Biochem., **146**, 1985, 220-231.
7. Miller, D., A. Thompson, M. Filippi. Magnetic resonance studies of abnormalities in the normal appearing white matter and grey matter in multiple sclerosis. — J. of Neurology, **250**, 2003, 1407-1419.
8. Ohtani, Y. et al. Ganglioside alterations in the central and peripheral nervous system of patients with Creutzfeldt-Jakob disease. — Neurodegeneration, **5**, No 4, 1996, 331-338.
9. Tiemeyer, M., P. Swank-Hill, R. Schnaar. A membrane receptor for gangliosides is associated with central nervous system myelin. — J. Biol. Chem., **265**, 1990, 11990-11999.
10. Trapp, B., J. Peterson, J. Mcdonough. Mechanisms of axonal loss and neuronal dysfunction in MS. — Multiple Sclerosis, **10**, 2004, 89-98.
11. Vernadakis, A. Neuron-glia interrelations. — International Review of Neurobiology, **30**, 1988, 149-224.
12. Waxman, S. G. Multiple sclerosis as neuronal disease. — Arch. Neurol., **57**, 2000, 22-24.
13. Yong, V. Prospects for neuroprotection in multiple sclerosis. — Frontiers in Bioscience, **9**, 2004, 864-872.
14. Zaprianova, E. et al. Ganglioside spinal cord changes in chronic relapsing experimental allergic encephalomyelitis induced in the Lewis rats. — Neurochem. Research, **22** (2), 1997, 175-179.
15. Zaprianova, E. et al. Axonal reaction precedes demyelination in experimental models of multiple sclerosis. — Morphology (in Russian), **5**, 2002, 54-59.
16. Zaprianova, E. Central nervous system myelin sheath. Abstr. Regional South-East Europ. Conf. Neurol. Psych., Varna, 1984, 107.
17. Запрянова, Е. Миелинизация в централната нервна система. С., БАН, 1980.

Institute of Experimental Morphology and Anthropology

Acta morphologica et anthropologica, 10
Sofia • 2005

Fos Expression in the Arcuate POMC-Neurons after Gastric Stimulation in the Rat

I. Stoyanova[*], *C. Phifer*[**], *H. Zheng*[***], *L. Patterson*[***], *H. R. Berthoud*[***]

[*] *Department of Anatomy, Faculty of Medicine, Thracian University, Stara Zagora*
[**] *Louisiana Scholars College, Northwestern State University of Louisiana, Natchitoches 71497, USA*
[***] *Neurobiology of Nutrition Laboratory, PBRC, LSU, Baton Rouge, LA 70808, USA*

The arcuate nucleus (AR) of the hypothalamus is a critical component of forebrain pathways that regulate a variety of neuroendocrine functions and plays a particularly important role in the regulation of feeding and metabolism. Expression of the immediate early gene product c-Fos is considered to be a marker for neuronal activation in different brain regions in response to afferent input. To determine neurochemical phenotype of hypothalamic arcuate neurons receiving input from the stomach, we carried out gastric stimulation in combination with c-Fos/peptide double-labelling immunocytochemistry. A fairly high number of α-MSH-immunoreactive (IR) neuronal perikarya and a high density of α-MSH-IR fibers are present in the hypothalamic AR. Quantitative analysis revealed that gastric distension upregulates the POMC derived α-MSH expression alone as well as c-Fos/α-MSH staining in AR neurons. These results demonstrate that arcuate α-MSHergic neurons are implicated in the dissemination of gastric distension signals in the brain.

Key words: arcuate nucleus, gastric stimulation, α-MSH, c-Fos-expression, rat.

Introduction

The arcuate nucleus (AR) of the hypothalamus is a critical component of forebrain pathways that regulate a variety of neuroendocrine functions [1]. The AR sends strong projections to other hypothalamic nuclei implicated in the regulation of feeding and metabolism. It consists of two neuronal populations: one of them stimulates food intake and expresses neuropeptide Y (NPY) and agouti-related peptide (AgRP) [2], while the other suppresses feeding and expresses proopiomelanocortin (POMC) and cocaine-amphetamine-related transcript (CART) [3]. Alpha-melanocytostimulating hormone (α-MSH) is one of the bioactive peptides derived from the prohormone POMC, which also participates in the control of food intake and body weight [1]. Therefore, it is important to understand the POMC gene regulation in the brain, as pharmacological manipulations of POMC expression/processing could be a potential strategy to combat obesity.

During the last decade, a new method for activity stains was developed [4], which allows expressing the immediate early gene product c-Fos and thus distinguishing functionally identified subpopulations of neurons.

The aim of the study was to assess quantitatively the distribution of c-Fos immunoreactive neurons in the hypothalamic arcuate nucleus after gastric distension, and to determine the proportion of α-MSHergic neurons activated by this stimulus.

Material and Methods

Twelve rats were anesthetized with ketamine (80 mg/kg i.p.). Cannulas were implanted in the stomach. After two a weeks latex balloon was inserted in the stomach and it was distended by filling the balloon with warm water. Rats were left for 60 min to allow c-Fos expression, and then they were perfused with fixative (4% phosphate-buffered saline paraformaldehide). Brains were removed, post fixated and 30 μm thick sections were cut in a cryostat at — 20°C. Sections were incubated for 24 h for double labelling, first with anti-c-Fos anti-serum, then with anti-α-MSH-antibody according to the protocol for avidin-biotin complex method. C-Fos staining reaction product was brown, while α-MSH was visualized with the SG chromogen as gray staining of the cytoplasm of the immunoreactive cells.

Results

A fairly high number of α-MSH-immunoreactive (IR) neuronal perikarya were present in the AR. In addition, a high density of α-MSH-IR fibers was particularly impressive. Numerous α-MSH-containing varicose neuronal fibers were found projecting to various parts of the hypothalamus — paraventricular nucleus, dorsomedial hypothalamic nucleus, perifornical area, lateral hypothalamus (LH), zona incerta etc. We found α-MSH-IR neurons mainly in the ventrolateral part of the AR. The overwhelming majority of distension-induced c-Fos-expression was in the lateral region of AR, where POMC neurons reside (Fig. 1). Many of the c-Fos-IR neurons were α-MSH/c-Fos double labelled. The absolute numbers of c-Fos-, α-MSH-positive neurons and double-labelled cells in each section were expressed as percentage from the total numbers of neuronal perikarya. The corpus distension produced significant increases in numbers of neurons expressing α-MSH (37.4%) above the control conditions (26-27.7%). The proportion of double-labelled cells in the AR of the stimulated group was higher (20.3% vs.17.3%) than in the control animals without gastric distension.

Discussion

The present study demonstrates that gastric distention, in the absence of other stimuli, leads to expression of c-Fos in the AR neurons. The vast majority of distension-induced c-Fos-expression was in the lateral part of AR, where neuronal perikarya expressing the POMC derived anorexigenic peptide α-MSH are situated. Gastric distention also increases the number of α-MSH neurons (37.4%) vs. 26% in animals with no distention. This effect leads to decreased appetite and food ingestion. Heisler et al. (5) have revealed that central serotonin (SER) systems are involved in the α-MSH activation via direct release of SER in the AR and binding to POMC neurons.

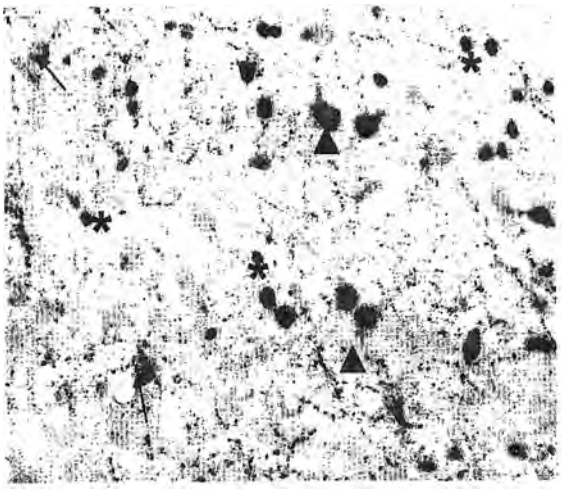

Fig. 1. Light microscope image of a frontal section of rat AR after gastric distension, processed for double immunocytochemistry for c-Fos and α-MSH. Neurons that were counted as α-MSH-positive but not activated by gastric distension (arrows), neurons that were α-MSH-negative but activated or c-Fos positive (asterisks), and neurons that were double-labelled (arrowheads) are indicated. × 160

The numerous α-MSH-containing fibers, we observed distributed throughout various hypothalamic nuclei, suggest that the neurotransmitter may influence the function of other brain structures, involved in the final physiological regulation of eating, and thus play a pivotal role in the control of energy balance and body weight. Our present findings suggest that populations of α-MSH neurons in the AR may provide a link between mediobasal hypothalamic satiety and LH phagic centers. These α-MSH-IR projections may underlie some of the extremely complex responses associated with hunger, food intake, and satiety.

In summary, we concluded that α-MSH arcuate neurons may be activated by stimuli that excite gastric mechanoreceptors (e.g., gastric balloon distension or ingestion of a large meal) and lead to cessation of feeding behavior.

References

1. Berthoud, H. R. et al. Neuroanatomy of extrinsic afferent supplying the gastrointestinal tract. — Neurogastroenterol. Motil., **16** (Suppl. 1), 2004, 28-33.
2. Bagnol, D. et al. Anatomy of an endogenous antagonist: relationship between Agouti-related protein and proopiomelanocortin in brain. — J. Neurosci., **19**, 1999, RC26.
3. Elias, C. F. et al. Chemically defined projections linking the mediobasal hypothalamus and the lateral hypothalamic area. — J. Comp. Neurol., **402**, 1998, 442-459.
4. Olson, B. R. et al. c-Fos expression in rat brain and brainstem nuclei in response to treatments that alter food intake and gastric motility. — Mol. Cell. Neurosci., **4**, 1993, 93-106.
5. Heisler, L. K. et al. Activation of central melanocortin pathways by fenfluramine. — Science, **297**, 2002, 609-611.

Institute of Experimental Morphology and Anthropology

Acta morphologica et anthropologica, 10
Sofia•2005

Substance P and Calcitonin Gene-Related Peptide Containing Neurons in the Feline Spinal and Superior Mesenteric Ganglia Projecting to the Distal Ileum

I. Stoyanova, N. Lazarov

Department of Anatomy, Faculty of Medicine, Thracian University, Stara Zagora

Combined retrograde tracing with the fluorescent tracer Fast Blue (FB) and immunofluorescent cytochemical methods were used to study the distribution and neurochemical identification of the neurons innervating the distal part of the ileum in cats. As revealed by retrograde tracing, FB-positive neurons projecting to the small intestine were located in the prevertebral superior mesenteric ganglion (SMG) and the dorsal root ganglia (DRG) at the level Th_{7-12}. In the SMG, the majority of the projecting neurons resided in the upper part of the ganglion, suggesting a somatotopic organization within the ganglion. Immunocytochemistry revealed two populations of retrogradely labelled neurons: substance P (SP)- and calcitonin gene-related peptide (CGRP)-positive. We concluded that the SMG and DRG Th_{7-12} should be considered as a prominent source of SP- and CGRP-immunoreactive sympathetic and sensory projections to the distal ileum of the cat.

Key words: superior mesenteric ganglion, dorsal root ganglia, retrograde tracing, immunohistochemistry, cat.

Introduction

The innervation of the distal ileum was studied in different animals. The sympathetic supply originates from the prevertebral ganglia: the coeliac ganglion provides the major input to the proximal gut regions, while the distal gut receives input from the superior and inferior mesenteric and hypogastric ganglia. The parasympathetic and sensory neuronal perikarya projecting to this part of the gut are located in the vagal dorsal motor nucleus and in the nodose ganglion and in dorsal root ganglia (DRG) [1], respectively.

Apart from the classical neurotransmitters acetylcholine and noradrenalin, a large number of the neurons in the sympathic ganglia contain small biologically active peptides, which act as neurotransmitters or neuromodulators in the autonomic nervous system: substance P, somatostatin, NPY, VIP, and CGRP [2]. The distribution of some of these transmitters through a feline SMG was described by Stoyanova et al. [3].

Although some peptidergic pathways to the gastrointestinal tract have been identified, in certain species our knowledge about the origin and projections of all

these fibres is still incomplete and some of the data are contradictory. The present work was undertaken to determine the distribution and neuropeptide contents of the neurons and neuronal fibres in feline SMG and DRG, projecting to the distal part of the small intestine.

Material and Methods

Five adult cats were anesthetized and a solution of 2% retrograde neuronal tracer FB was injected into the wall of the distal ileum. The animals were perfused after 35-40 days, with 2 L 4% paraformaldehyde and 0.2% picric acid in 0.1 M phosphate buffered saline. The SMG and DRG Th_6-L_2 were removed, postfixed, frozen and 20 μm thick sections were cut on a cryostat at –20°C. The indirect immunofluorescent technique was applied with primary antibodies, rabbit anti-SP- or CGRP-antiserum and secondary antibody donkey-anti-rabbit IgG conjugated to fluorescein isothiocyanate.

Results

In the SMG the tracer was found in neurons located predominantly in the upper part of the ganglion (Fig. 1). Two types of FB-labelled neurons were differentiated: magnocellular multipolar ganglionic cells, which were often clustered and a second group of parvocellular neurons with a less pronounced multipolar shape. A fairly high number of the FB-marked cells were CGRP-immunoreactive (Fig. 2 — *a*, *b*). In addition, numerous FB/CGRP-containing varicose neuronal fibres were found surrounding CGRP-negative magnocellular ganglionic cells. Less parvocellular SMG neurons projecting to the ileum were SP-positive. However, more often FB/SP-IR neuronal fibres were detected. In the investigated spinal ganglia FB-labelled primary sensory neurons were found at levels $Th_{7\text{-}12}$. Relatively large proportions of them were SP- or CGRP-positive.

Fig. 1. A large number of FB-labelled neurons in the upper part of the SMG (× 50)

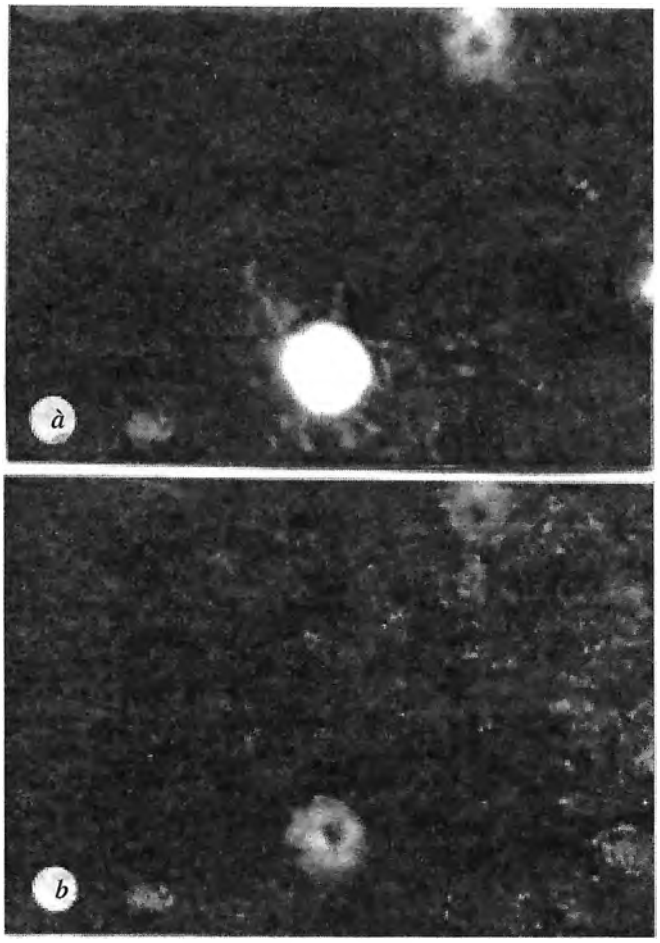

Fig. 2. Double labelling of parvocellular SMG projecting neurons — *a* FB; *b* CGRP (× 250)

Discussion

The present work reveals that the distal ileum in the cat receives both autonomic and sensory innervation. As already reported in a previous study [4], an organotopic arrangement of nerve cell bodies within the SMG is present: those innervating the distal part of the ileum are located in the upper part of the ganglion.

It was found that in the rat the primary afferents projecting to the ileum are located in DRG $Th_{10\text{-}13}$ [5], whereas in the cat we detected FB-labelled cells at level $Th_{7\text{-}12}$. CGRP is one of the major neuropeptides, expressed in the sensory relaying regions of the nervous system. CGRP is generally co-localized with SP in the primary afferent nociceptors, and both neuropeptides play a role in mediating visceral nociceptive transmission [6].

We concluded that the SMG and DRG $Th_{7\text{-}12}$ should be considered as a prominent source of SP- and CGRP-immunoreactive sympathetic and sensory projections to the distal ileum of the cat. Most of the SMG and DRG projecting neurons are CGRPergic, and a few of these are SPergic.

References

1. Pidsudko, Z. et al. The influence of inflammation on the expression of neuropeptides in the ileum-projecting primary sensory neurons in the pig. — Folia Morphol. (Warsz.), **62**, 2003, 235-237.
2. Hokfelt, T. et al. On the occurrence of substance P-containing fibres in sympathetic ganglia: immunohistochemical evidence. — Brain Res., **132**, 1977, 29-41.
3. Stoyanova, I., D. W. Scheuermann, C. Chouchkov. Neurochemical features of feline superior mesenteric ganglion. — It. J. Anat. Embryol., **103**, 1998, 35-43.
4. Stoyanova, I., C. Chouchkov, D. W. Scheuermann. Immunocytochemical localization of the neurons in the superior mesenteric ganglion innervating the small intestine of the cat. — Ann. Anat., **179**, 1997, 517-523.
5. Cervero, F., K. A. Sharkey. An electrophysiological study of intestinal afferent fibres in the rat. — J. Physiol., **401**,1988, 381-397.
6. Levin, J. D., H. L. Fields, A. I. Basbaum. Peptides and the primary afferent nociceptor. — J. Neurosci., **13**, 1993, 2273-2286.

Institute of Experimental Morphology and Anthropology

Acta morphologica et anthropologica, 10
Sofia•2005

Different Forms of the Amyloid β Peptide Affect Differentially the Electrical Activity of Cultured Neuronal Networks

L. Kirazov, E. Kirazov*, L. Venkov*, E. Vassileva*, S. Stuewe**, D. G. Weiss***

* *Institute of Experimental Morphology and Anthropology, Bulgarian Academy of Sciences, 1113 Sofia, Bulgaria*
** *Institute of Cell Biology and Biosystems Technology, University of Rostock, Albert-Einstein-Str., D-18051 Rostock, Germany*

The amyloid β peptide (Aβ) has a central role in the pathology of the Alzheimer's disease. A number of cytotoxic effects have been attributed to it. There are several recent reports about the impact of Aβ on electrophysiological events in neurons. In a previous study we have shown that Aβ affects the electrical activity of cultured neuronal networks. In this work we compare the effects of different Aβ forms — $Aβ_{1-42}$, $Aβ_{1-40}$, and the fragment $Aβ_{25-35}$. The obtained results show that $Aβ_{1-40}$ affects the electrical activity of the neurons differently compared to $Aβ_{1-42}$ and $Aβ_{25-35}$.

Key words: Alzheimer's disease, amyloid β peptide forms, electrical activity of neurons.

Introduction

One of the morphological hallmarks of Alzheimer's disease are the senile plaques. Their core is built up from insoluble Aβ aggregates and is surrounded with degenerated neurons. For a long time it was assumed that it is these aggregated Aβ fibrils that are neurotoxic [3]. Numerous contradictory data stemming from research on Alzheimer's disease raised the question whether the aggregated Aβ fibrils have a central role or are only an element in the etiology of the disease.

It is known that Aβ is derived from its precursor protein as monomers which then aggregate in dimers, oligomers and fibrils, which can precipitate to form the core of the senile plaques. The location where these aggregation steps take place is unknown. A hypothesis postulates that the first aggregation steps occur intracellularly, because of the possibility to attain higher Aβ concentrations within cell compartments. Thereafter Aβ oligomers could be secreted out in the extracellular space where they act as an aggregation core.

There are a lot of controversial reports regarding the toxicity of Aβ in different aggregation states. Some authors attribute toxicity to monomeric Aβ species [10],

while others point out Aβ aggregates such as dimers [9], Aβ derived diffusible ligands [2], oligomers and fibrils as the carrier of toxicity [4].

The two basic endogenic forms of the Aβ monomer differ in the length of their amino-acid sequence. In the non-Alzheimer's brain the main form is $A\beta_{1-40}$ (ca. 90%) and some $A\beta_{1-42}$ is also secreted (ca. 10%). In the diseased brain this ratio switches so that $A\beta_{1-42}$ prevails, and this is the form found predominantly in the core of the senile plaques.

In a previous study we have reported that soluble Aβ inhibits the electrical activity of cultured neuronal networks in a concentration-dependent manner [6]. The aim of the present study is to compare the effects of the two forms — $A\beta_{1-42}$, $A\beta_{1-40}$, and the biologically active fragment $A\beta_{25-35}$.

Material and Methods

The effects of $A\beta_{25-35}$, $A\beta_{1-40}$ and $A\beta_{1-42}$ on the electrical activity of neuronal networks (frontal cortex cell culture from mouse embryos seeded on microelectrode arrays) were studied employing a neurotoxicity assay system described previously [5]. To ensure that in the employed solutions $A\beta_{(25-35;\ 1-40;\ 1-42)}$ are in their monomeric (soluble) form, we adopted a modification of the methods described by Butterfield et al. [1] and Zagorski et al. [12]. Individual networks were used for treatment with one form of the Aβ peptide.

Results and Discussion

It has been shown that the sequence from amino acid 25 to 35 carries the biological activity of Aβ [11]. Interestingly, although this sequence is present in both major endogenous forms of Aβ, they have different biological effects and show clear pharmacological differences [8]. Together with the switch in the ratio between $A\beta_{1-42}$ and $A\beta_{1-40}$ in healthy and diseased brain this guided us to compare their effect on the electrical activity of cultured neuronal networks.

In preliminary studies we could see that $A\beta_{25-35}$ has the strongest inhibitory effect, followed by $A\beta_{1-42}$ and $A\beta_{1-40}$ [7]. It was interesting to observe that during the incubation with $A\beta_{1-40}$ the electrical activity of the neurons tended to recover from the inhibitory effect.

In the present study we performed a set of experiments to verify our preliminary results and tested the Aβ-peptides and the Aβ-fragment at the most effective concentration — 50 μM.

The results show that $A\beta_{25-35}$ and $A\beta_{1-42}$ inhibit reversibly the electrical activity of the neurons (Fig. 1 and 2). The effect of $A\beta_{1-40}$ differs from these of the other two peptides. We observed initial inhibition followed by recovery to almost native activity (Fig. 3).

The difference between the action of the three peptides raises the question — are they acting through the same or through different mechanisms/sites? If they act through the same site it could be the difference in their structure that causes differences in their binding affinities, or steric factors become involved, thus resulting in differential effects. The structure of $A\beta_{1-42}$ could favor the stabilization of the hypothetic binding. If they act through different sites the mechanism of $A\beta_{1-40}$ action could implicate a feedback which alleviates the initial inhibition.

The exact mode of action of the tested Aβ peptides remains unclear and presents a challenge for further studies.

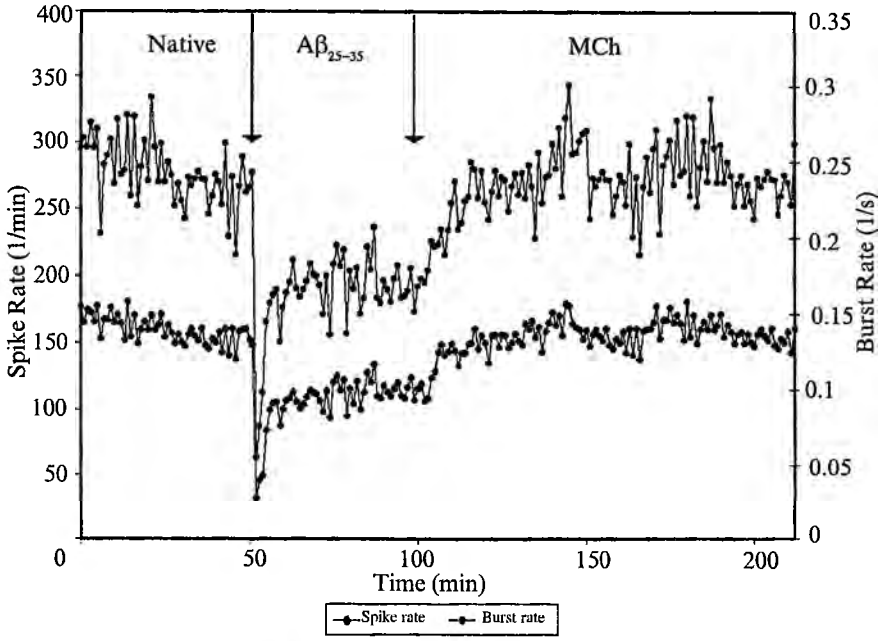

Fig. 1. Effect of 50 μM $A\beta_{25-35}$ on the spike and burst rates of a neuronal network. Burst rate is extracted using analog spike integration and is presented as bursts per second. Filled circles — spike rate; open circles — burst rate. Arrows indicate the time of onset of treatment of the network. Native — native electrical activity of the network; $A\beta_{25-35}$ — treatment with 50 μM $A\beta_{25-35}$; MCh — medium change, incubating medium replaced with fresh conditioned medium, lacking Aβ

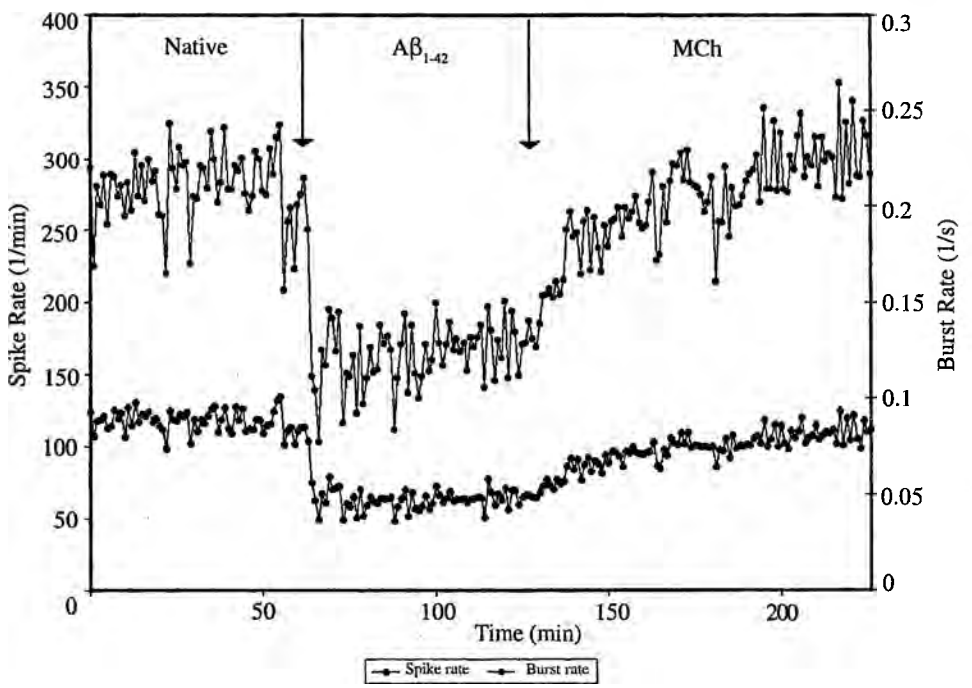

Fig. 2. Effect of 50 μM $A\beta_{1-42}$ on the spike and burst rates of a neuronal network. For details see Fig. 1

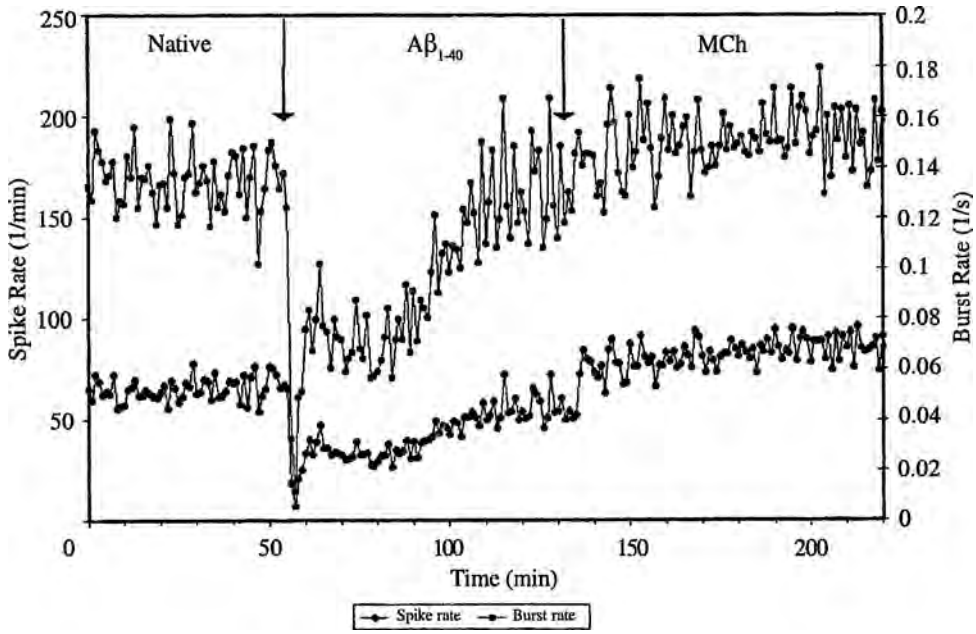

Fig. 3. Effect of 50 μM $A\beta_{1-40}$ on the spike and burst rates of a neuronal network. For details see Fig. 1

References

1. Butterfield, D. A. et al. Amyloid β-peptide associated free radical oxidative stress, neurotoxicity, and Alzheimer's disease. — Meth. Enzymol., **309**, 1999, 746-769.
2. Gong, Y. et al. Alzheimer's disease-affected brain: Presence of oligomeric A beta ligands (ADDLs) suggests a molecular basis for reversible memory loss. — Proc. Natl. Acad. Sci. USA, **100**, 2003, 10417-10422.
3. Hardy, J., G. Higgins. Alzheimer's disease: the amyloid cascade hypothesis. — Science, **256**, 1992, 184-185.
4. Kayed, R. et al. Common structure of soluble amyloid oligomers implies common mechanism of pathogenesis. — Science, **300**, 1993, 486-489.
5. Kirazov, L. et al. The amyloidogenic Aβ peptide affects the electric activity of neuronal cells. — Compt. rend. Acad. bulg. Sci., **55**, 2002, 103-108.
6. Kirazov, E. et al. Studies on the effects of the amyloidogenic Aβ peptide on the electrical activity of neuronal networks cultured on microelectrode arrays. — Acta morphol. Bulg., **7**, 2002, 9-16.
7. Kirazov, L. et al. Comparison of the effect of different forms of the amyloidogenic β peptide on the electrical activity of cultured neuronal networks. — Compt. rend. Acad. bulg. Sci., **57**, 2004, 91-96.
8. Lee, D. H., H. Y. Wang. Differential physiologic responses of alpha7 nicotinic acetylcholine receptors to beta-amyloid1-40 and beta-amyloid1-42. — J. Neurobiol., **55**, 2003, 25-30.
9. Roher, A. E. et al. Morphology and toxicity of Aβ-(1-42) dimer derived from neuritic and vascular amyloid deposits of Alzheimer's disease. — J. Biol. Chem., **271**, 1996, 20631-20635.
10. Taylor, B. M. Spontaneous aggregation and cytotoxicity of the beta-amyloid Abeta1-40: a kinetic model. — J. Protein Chem., **22**, 2003, 31-40.
11. Whitson, J. S. β-Amyloid protein promotes neuritic branching in hippocampal cultures. — Neurosci. Lett., **110**, 1990, 319-324.
12. Zagorski, M. G. Methodological and chemical factors affecting amyloid β peptide amyloidogenicity. — Meth. Enzymol., **309**, 1999, 189-207.

Institute of Experimental Morphology and Anthropology

Acta morphologica et anthropologica, 10
Sofia•2005

Plastic Capacity of Growing and Regenerating Myelin Sheaths

S. Dolapchieva

Department of Anatomy and Histology, Medical University Sofia

According to the generally accepted theory of Betty Geren, the myelin sheath develops as an elongation of the glial plasma membrane. Data about an incorporation of membranous material from the glial cytoplasm to the outer and inner mesaxons have been presented in the literature. In this study, developing and regenerating peripheral nerves were investigated by conventional electron microscopy. We have shown another group of membranes of the sheath, which are able to incorporate cytoplasm components. From the inner or outer surface of the compact myelin disintegrate segments of the lamellae, which acquire the morphological and cytochemical characteristics of the myelin-forming membranes. The disintegration of segments from the "rigged" compact myelin, that increases the possibility of the myelin sheaths to develop and regenerate, indicates their significant plastic capacity.

Key words: nerve fibers, myelin sheath, postnatal development, regeneration, plasticity.

Introduction

1971 Webster [8] has established that the myelin lamellae grow exponential quickly than the glial plasmalemma, the source of the myelin sheath [5]. The non-compact membranes of the myelin sheath (mesaxons, paranodal and Schmidt-Lanterman lamellae) were proposed to be sites for incorporation of glial cytoplasm material to the growing sheath [2, 7, 9]. In the present study, we demonstrate additional membranes, dynamic disintegrated segments of the compact myelin, which we believe to belong to the myelin-forming membranes. The segments, likely the myelin-forming membranes, are strongly positive for the myelin-associated enzymes (5`-nucleotidase and Na+, K+-ATPase), moderately positive towards ruthenium red and cationized ferritin, and negative towards lectins [9].

Material and Methods

Group A. Rabbits of 8 age groups (newborn — 4 months) were used. Segments of ventral and dorsal spinal roots were removed and investigated. Group B. Tibial nerves of adult rabbits were cut and restored by primary grafting. Segments 1 cm

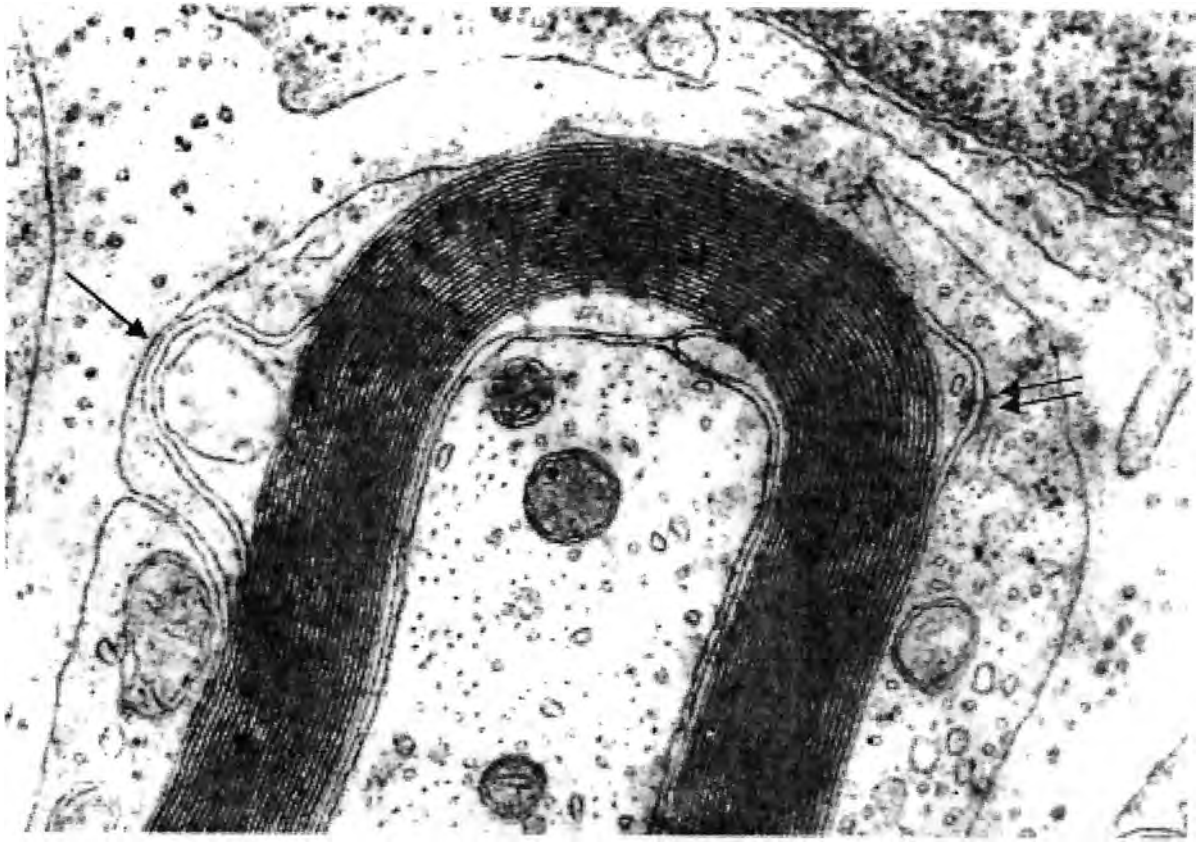

Fig. 1. 15-day-old rabbit. A transversal section through radix anterior. A disintegrated peripheral segment near the outer mesaxon (arrow). The split segment at the opposite side of the myelin sheath in association with desmosome-like structure (double arrow). EM Siemens I × 60 000

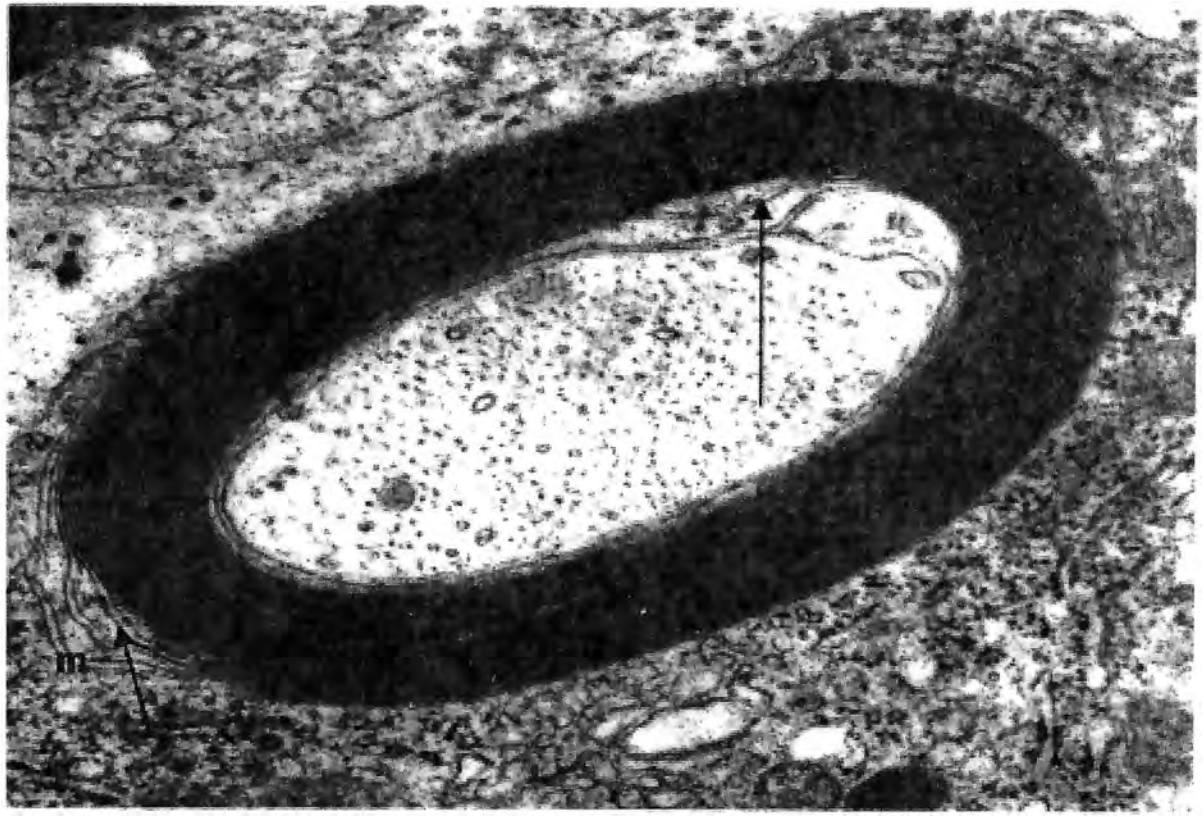

Fig. 2. 15-day-old rabbit. A transversal section through radix anterior. A disintegrated segment from the inner surface of the myelin sheath (long arrow). Two segments disintegrated from the outer surface of the sheath near the outer mesaxon m (short arrow). EM Siemens I (× 60 000)

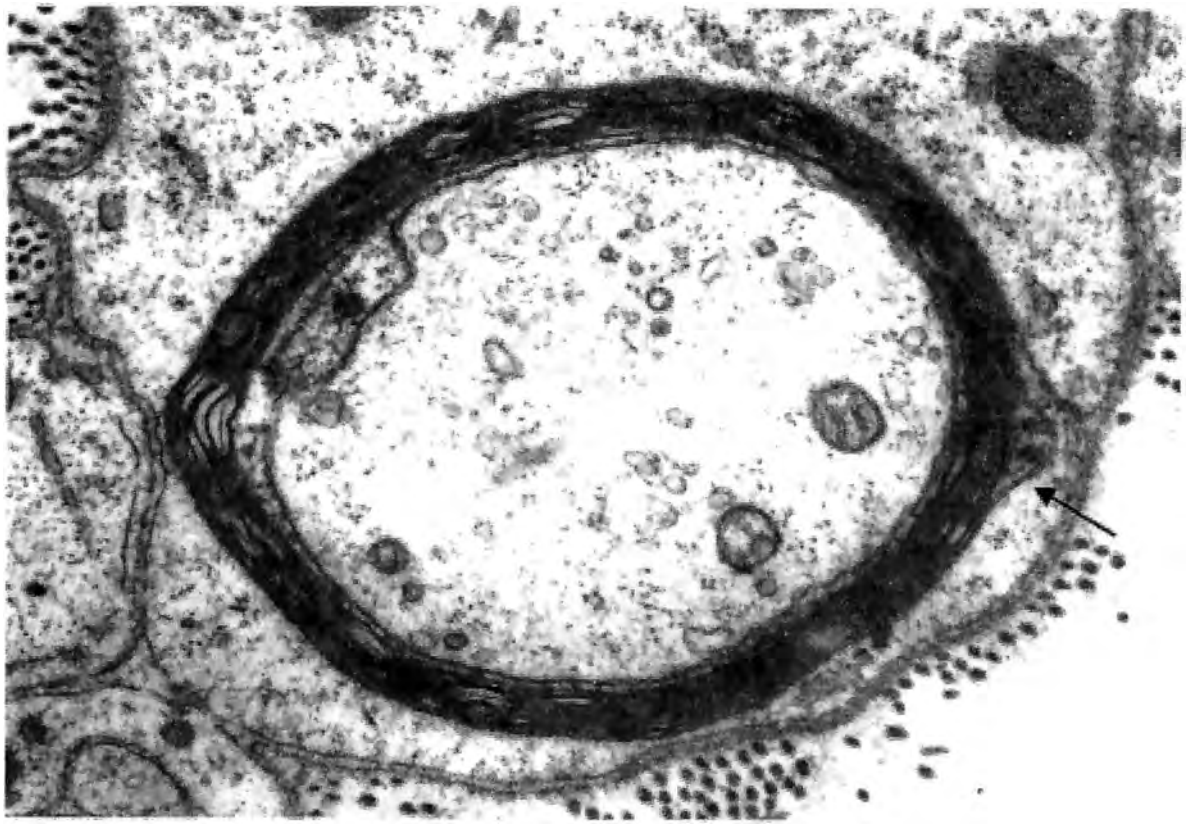

Fig. 3. A transversal section through regenerating n. tibialis 30 days after primary grafting, 1cm distal to the graft. A disintegrated segment from the outer surface of the myelin sheath near the mesaxon (arrow). EM Hitachi H500 (× 32 000)

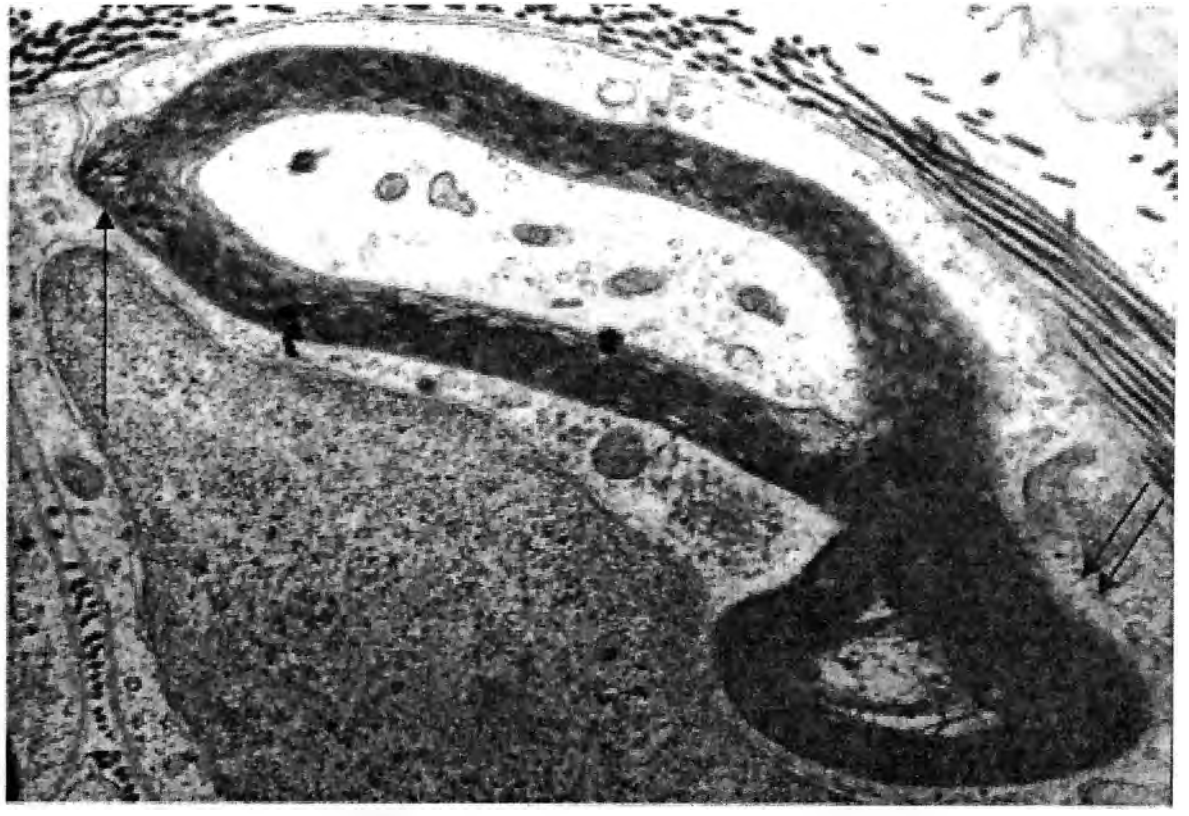

Fig. 4. A transversal section through regenerating n. tibialis 28 days after primary grafting, 1cm distal to the graft. Disintegrated myelin lamellae near the outer mesaxon (arrow). Overproduced myelin (double arrow). EM Hitachi H500 (× 23 000)

distal to the graft were removed 28, 30 and 40 days after grafting. The material from both investigated groups of animals was prepared for EM according to the routine protocol. Transversal sections were examined under SiemensI and Hitachi H500 EM.

Results

In developing and mature myelinated nerve fibers, we have quite frequently seen disintegrated segments from the compact myelin. More frequently appeared split peripheral myelin lamellae, near the outer mesaxon or at the opposite side of the myelin sheath (Fig. 1). More rarely appeared inner disintegrated myelin lamellae, as a rule near the inner mesaxon (Fig. 2). Desmosome-like structures were often associated with the split segments (Fig. 1). In Fig. 2 could be seen developing desmosome-like structures between the outer mesaxon and the next two split myelin segments. In regenerating myelin sheaths, the disintegrated segments have shown similar dispositions (Figs. 3, 4). During the regeneration, we have frequently observed an overproduced myelin (Fig. 4).

In all cases, close interrelations were seen between the split myelin segments and membranous profiles of the Schwann cell cytoplasm (Figs. 1-4).

Discussion

The dynamic disintegration of inner and outer lamellae was observed in the animals of all investigated age groups, in regenerating myelinated nerve fibers, in growing and mature myelin sheaths. We believed that these split lamellae are sites of incorporation of glial cytoplasm material to the growing myelin sheaths, such as the mesaxons [2, 9]. In adult animals, the myelin sheath is considered to renew constantly [7]. The desmosome-like structures of the disintegrated myelin lamellae might take part in the mechanism of incorporation of cytoplasm profiles to the myelin sheaths. The cytochemical characteristics of the structures [3, 4, 9] show, that they are more similar to the gap junctions, accelerating repeatedly the metabolic exchange between the territorial units connected by them [1]. We suppose that the overproduced myelin (Fig. 4) called "aberrant" myelin [6] results from an intensive incorporation of cytoplasm material to the disintegrated lamellae. We can see similar images in the transversally cut paranodal areas. In the present case, however, the section of the myelinated fiber contains the nucleus of the Schwann cell, indicating the middle part of the internode. We have observed aberrant myelin significantly frequently in the regenerating nerve fibers than in the growing fibers.

References

1. Balice-Gordon, R. J., L. J. Bone, S. S. Scherer. Functional gap junctions in the Schwann cell myelin sheath. — J. Cell Biol., **142**, 1998, 1095-1104.
2. Bunge, R. P., M. B. Bunge, B. Bates. Movements of the Schwann cell nucleus implicate progression of the inner (axon-related) Schwann cell process during myelination. — J. Cell Biol., **109**, 1989, 273-284.
3. Fannon, A. M. et al. Novel E-cadherin-mediated adhesion in peripheral nerve: Schwann cell architecture is stabilized by autotypic adherens junctions. — J. Cell Biol., **129**, 1995, 189-202.
4. Fujimoto, K. et al. Distribution of anionic sites on intracellular organelles: A study by labelling frozen thin-section with cationized ferritin. — Acta Histochem. Cytochem., **18**, 1985, 455-463.

5. G e r e n, B. B. The formation from the Schwann cell surface of myelin in peripheral nerves of chick embryos. — Exp. Cell Res., 7, 1954, 558-562.
6. P e r e y r a, P. M., P. E. B r a u n. Studies on fractions, which are involved in myelin assembly: Isolation from developing mouse brain, and characterization by enzyme markers, electron microscopy, and electrophoresis. — J. Neurochem., **41**, 1983, 957-973.
7. S a m o r a j s k i, T., R. L. F r i e d e. A quantitative electron microscopic study of myelination in the pyramidal tract of rat. — J. Comp. Neurol., **134**, 1968, 323-338.
8. W e b s t e r, H. de F. The geometry of peripheral myelin sheaths during their formation and growth in rat sciatic nerves. — J. Cell Biol., **48**, 1971, 348-367.
9. Д о л а п ч и е в а, С. Аксон-миелин-Швановоклетъчният комплекс в развитие и експеримент. Дисерт. труд, София, 2001.

Institute of Experimental Morphology and Anthropology

Acta morphologica et anthropologica, 10
Sofia • 2005

Characteristics and Formation of the Peripheral Myelinated Nerve Fiber Paranodes

S. Dolapchieva

Department of Anatomy and Histology, Medical University, Sofia

The paranodes restrict bilaterally the nodal axolemma abundant of sodium channels. The glial paranodal loops build together with the axolemma the heterotypic axo-glial septate-like junctions. Unique autotypic adherent junctions, named desmosome-like junctions, attach the membranes of the loops to each other. Developing myelinated fibers of rabbit spinal roots were examinated by conventional electron microscopy. As a rule, the axo-glial junctions appear after beginning of compact myelin formation. The adnodal loops form first their septate junctions. The process continues to the internode. At the same time, develop the autotypic adherens junctions. The interrelated development of both junctions is obviously of significance for achievement of the regular organization of the myelinated fibers. The findings put the question about the developmental priority of the axo-glial junctions or the desmosome-like junctions, i.e. about the leading role of the neuron or the glial Schwann cell in the formation of the mature paranodes.

Key words: nerve fibers development, paranode, axo-glial junctions, desmosome-like junctions.

Introduction

The myelin sheath is a unique and fundamental adaptation of vertebrates. The physiological end product of myelination is saltatory conduction where the nerve impulse rapidly "jumps" from node to node. The myelinated axon can be divided into three domains: the internodal axon covered by compact myelin; the paranodal axon connected to the terminal ends or paranodal loops of the myelin internode; and the nodal axon which is apposed by Schwann cell finger-like processes in the peripheral nerves. The paranodal loops tightly adhere to the axon through a continuous spiral of axo-glial or septate-like junctions [1]. They form a physical barrier that prevents diffusion of nodal Na+ channels and juxtaparanodal K+ channels [6]. The adherent or desmosome-like (D-L) junctions [2, 4, 8] connect multiple layers of paranodal loops in their middle region. The single tight junctions [3, 5] appear between the paranodal loops in their adaxonal area of. The interrelated development of all these contacts of the paranode was not investigated.

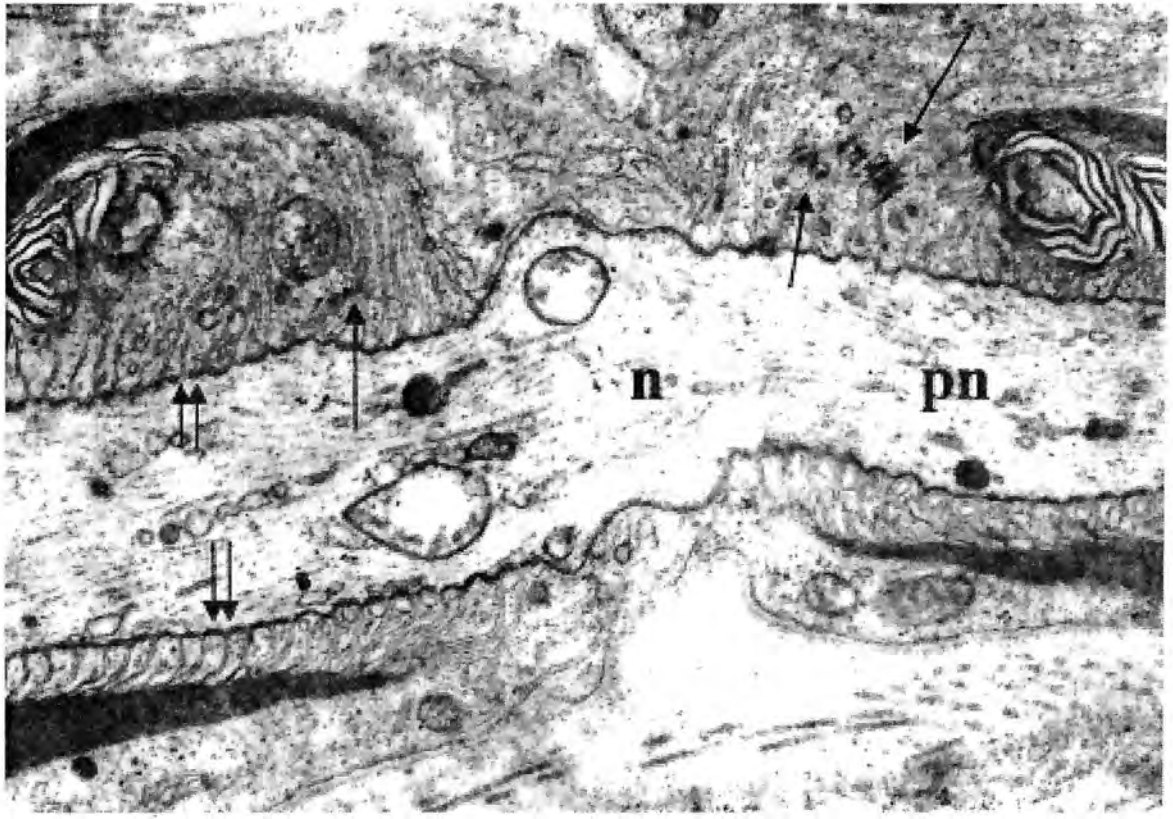

Fig. 1. Newborn rabbit. A longitudinal section through the ventral root. Axo-glial junctions of paranode pn (double arrows). D-L junctions between the membranes of neighboring paranodal loops (arrows). At the right paranodal zone, the D-L junctions are disposed in two rows, n — node. EM Siemens I × 24 000

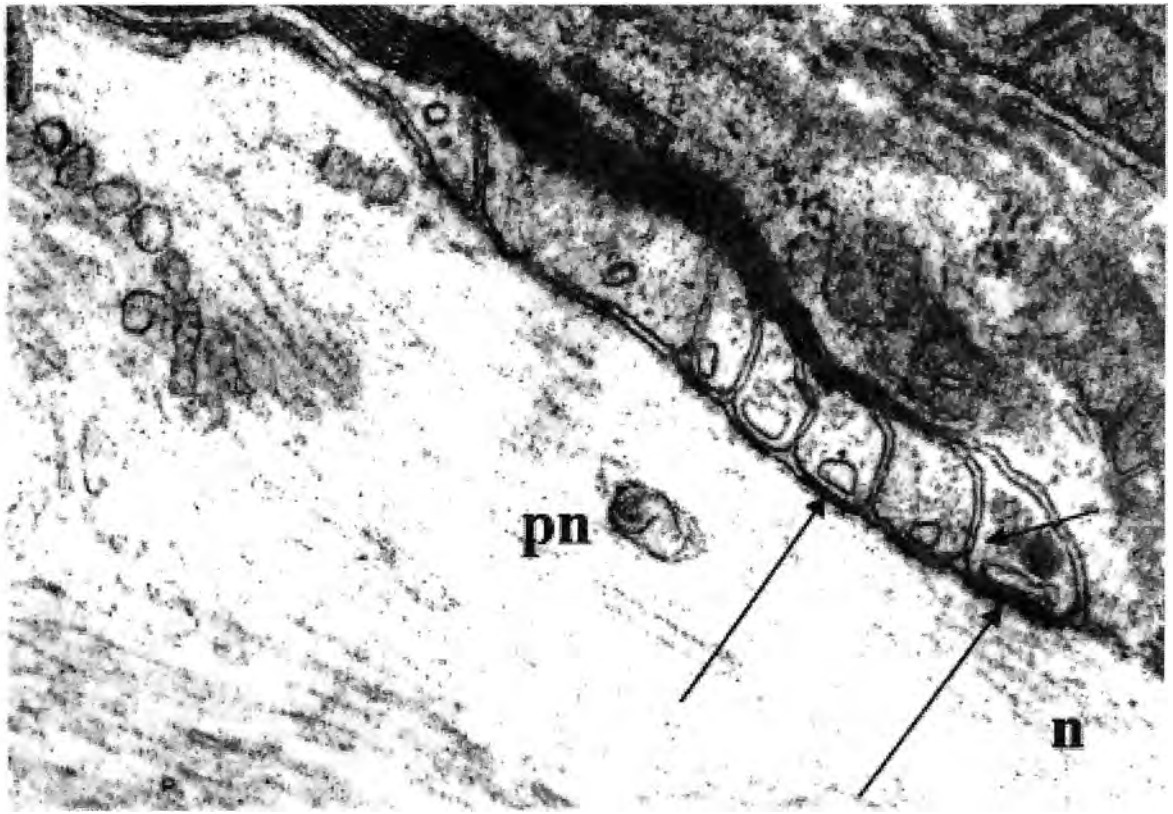

Fig. 2. Newborn rabbit. A longitudinal section through the dorsal root. Adnodal axo-glial junctions (long arrows). Tight junction between membranes of two neighboring paranodal loops (short arrow), n — node, pn — paranode. EM Siemens I × 70 000

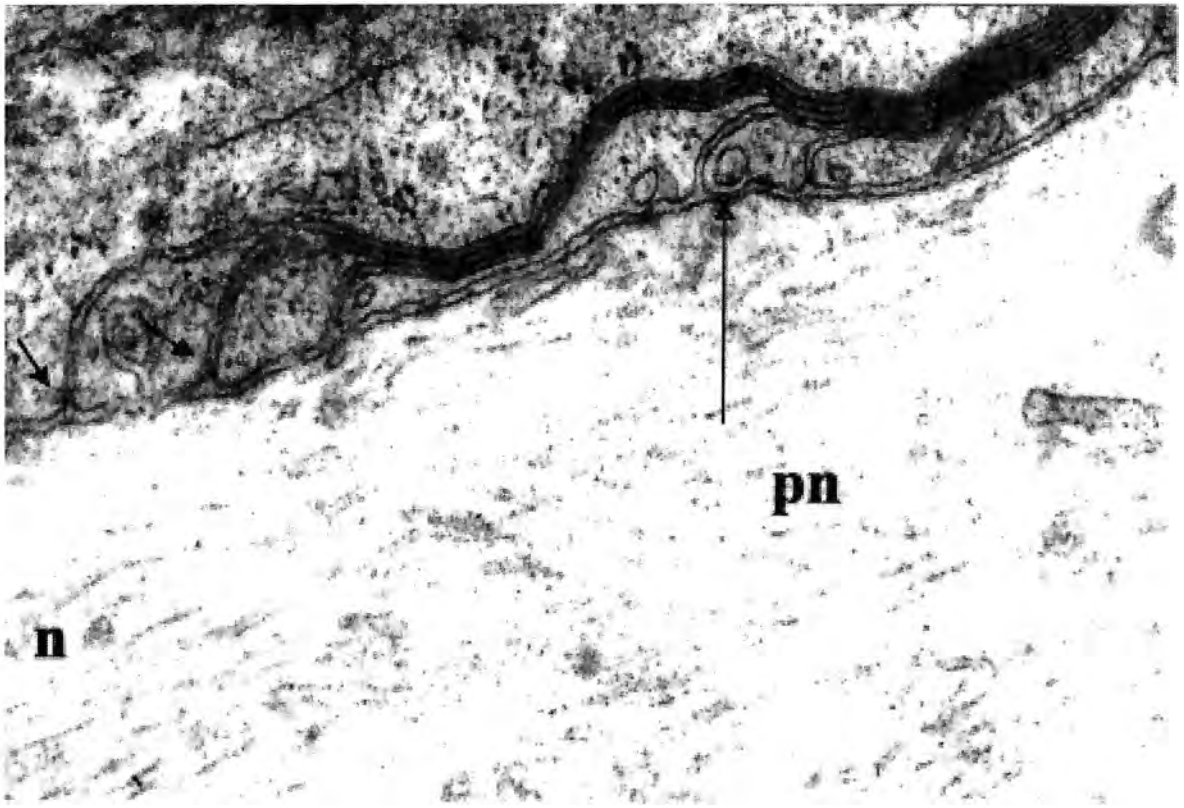

Fig. 3. Newborn rabbit. A longitudinal section through the dorsal root. An initial formation of axo-glial junction in the middle of the paranode **pn** (long arrow). Tight junctions between the adaxonal paranodal membranes (short arrows), **n** — node. EM Siemens I × 60 000

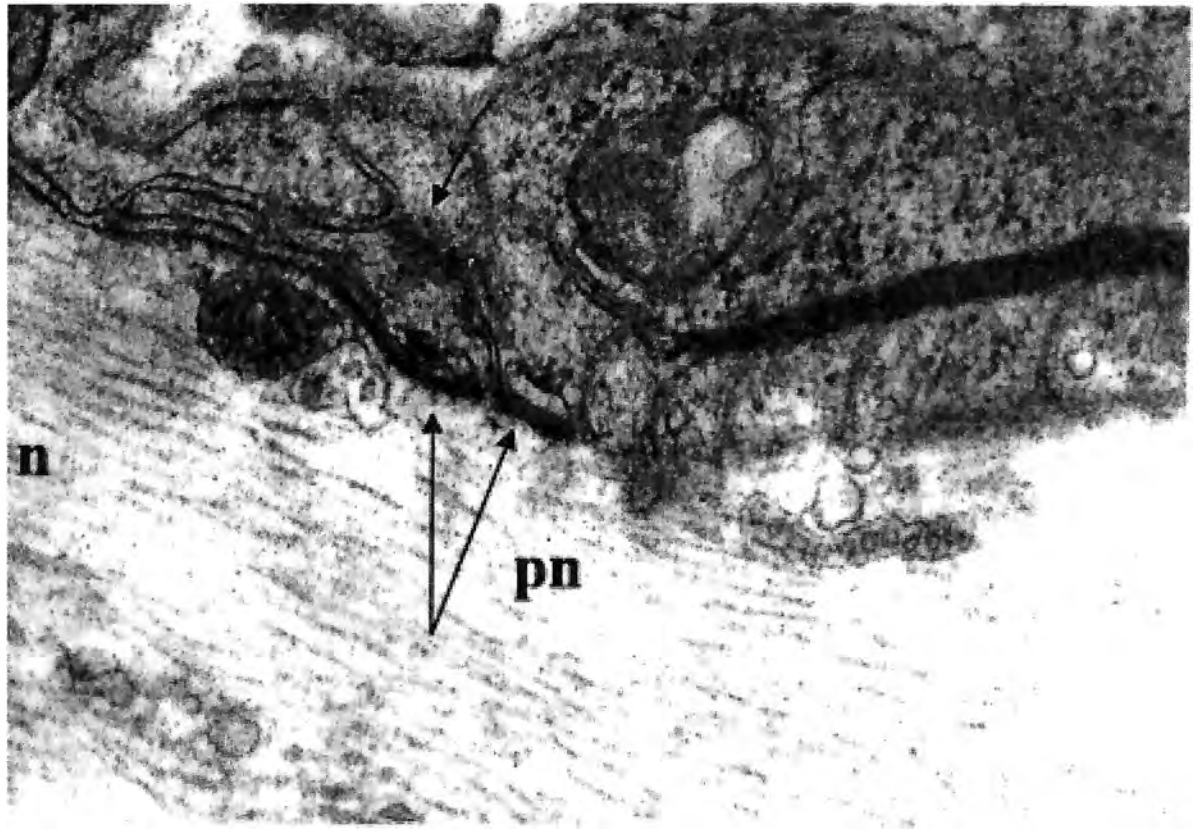

Fig. 4. Newborn rabbit. A longitudinal section through the dorsal root. Axo-glial junctions of two adnodal loops of the paranode **pn** (long arrows). Formation of D-L junctions (short arrow), **n** — node. EM Siemens I × 70 000

Material and Methods

Rabbits of 9 age groups (newborn — 8 months) were used. Segments of ventral and dorsal spinal roots were removed and prepared for EM according to the routine protocol. Longitudinal sections were examined under Siemens I EM.

Results

In well-developed myelin sheaths, the axo-glial junctions appeared as uniform thickenings between axolemma and all paranodal loops (Fig. 1). In appropriate sections, D-L junctions appeared in one or two rows between the neighboring membranes of the paranodal loops (Fig. 1). In nonmature myelin sheaths, the axo-glial junctions have first appeared at the adnodal loops of the paranode (Figs. 2, 4). Short tight junctions were visualized between adaxonal segments of neighboring paranodal loops (Figs. 2, 3). In a single case, we have seen an initial formation of axo-glial junction in the middle of the paranode, constituting of three dense particles (Fig. 3). In appropriate sections, it could be observed a simultaneous development of the first adnodal axo-glial junctions and D-L junctions, belonging to the same paranodal loop membranes (Fig. 4).

Discussion

Our findings have supported the data of Yamamoto et al. [7] that the axo-glial junctions develop from the node to the internode. However, we have shown that the rule is not absolute. In some cases, first develops axo-glial junction at a loop in the middle zone of the paranode (Fig. 3). During the formation of axo-glial junctions, in the paranode develop also tight junctions. Similarly to the D-L junctions, they connect the membranes of the paranodal loops. That connection, however, is limited to the membranes. The outer layers of both contacting unit membranes only fuse to each other. Hence, the tight junctions are not able to draw together the neighboring loops. The adherens, D-L junctions, develop simultaneously with the axo-glial junctions, also from the node to the internode. The D-L junctions are able to draw together the paranodal loops owing of their solid cytoplasm densities, which fuse to each other and build a complete spiral on the length of the paranode. At the other hand, the first D-L junctions develop in close interrelation with the adjacent D-L structure of the outer mesaxon (Fig. 4). The mesaxons are often associated with such structures, before and during the myelinization [8]. I.e., the D-L junctions as a whole have a priority in their genesis and formation. Taking into account all these findings, we may suppose that the adherent junctions have developmental priority in comparison to the axo-glial junctions. Nevertheless, additional studies in this aspect are necessary.

References

1. Arroyo, E. J., S. S. Scherer. On the molecular architecture of myelinated fibers. — Histochem. Cell Biol., **113**, 2000, 1-18.
2. Fannon, A. M. et al. Novel E-cadherin-mediated adhesion in peripheral nerve: Schwann cell architecture is stabilized by autotypic adherens junctions. — J. Cell Biol., **129**, 1995, 189-202.

3. Sandri, C., J. M. Van Buren, K. Akert. Membrane morphology of the vertebrate nervous system. — Prog. Brain Res., 46, 1982, 201-265.
4. Scherer, S. S. Nodes, paranodes, and incisures: from form to function. — Ann. N. Y. Acad. Sci., 883, 1999, 131-142.
5. Scherer, S. S., E. J. Arroyo. Recent progress on the molecular organization of myelinated axons. — J. Periph. Nerv. Syst., 7, 2002, 1-12.
6. Trapp, B. D., G. J. Kidd. Axo-glial septate junctions: the maestro of nodal formation and myelination? — J. Cell Biol., 150, 2000, F97-F99.
7. Yamamoto, K., A. C. Merry, A. A. Sima. An orderly development of paranodal axoglial junctions and bracelets of Nageotte in the rat sural nerve. — Brain Res. Dev. Brain Res., 96, 1996, 36-45.
8. Долапчиева, С. Аксон-миелин-Швановоклетъчният комплекс в развитие и експеримент. Дисерт. труд, София, 2001.

Institute of Experimental Morphology and Anthropology

Acta morphologica et anthropologica, 10
Sofia•2005

Morphometric Analysis of Neuronal Changes During Chronic Relapsing Experimental Allergic Encephalomyelitis

V. Ormandjieva, E. Zaprianova, D. Deleva

Institute of Experimental Morphology and Anthropology, Bulgarian Academy of Sciences, Sofia

In the present study we used morphometric method to investigate the early changes of hypoglossal nerve neurons of Lewis rats during the first clinical episode of chronic relapsing experimental allergic encephalomyelitis (CREAE). The surface area of the hypoglossal nerve neurons increased statistically significant during the first clinical episode of CREAE in comparison to control rats. These morphometric changes reflect the early degeneration of the neurons and support the notion that neuronal degeneration can begin very early in the pathogenesis of the disease. Our findings provide another evidence of the concept of multiple sclerosis (MS) as a neuronal disease.

Key words: chronic relapsing experimental allergic encephalomyelitis, Lewis rat, hypoglossal nerve, neurons, morphometry.

Introduction

Chronic relapsing experimental allergic encephalomyelitis (CREAE) shares histological, immunological and clinical parameters with multiple sclerosis (MS), a human central nervous system (CNS) demyelinating disease of not elucidated etiology. MS is considered to be prototype of primary demyelinating disease in the CNS in every textbook of neurology. However, in the past few years a considerable body of evidence indicates that neurons are also targets of the disease process [6]. Furthermore, in 2000 Editorial paper of W a x m a n [8] in Archives of Neurology was entitled "Multiple Sclerosis as a Neuronal Disease".

Early neuronal damage in patients with MS has been observed in vivo by magnetic resonance spectroscopy which showed decreased levels of the neuronal specific marker N-acetylaspartate (NAA) in early stages of MS [1]. By assessing central brain NAA in MS patients with a wide range of disability and disease duration De S t e f a n o et al. [1] showed that diffuse cerebral axonal damage begins in the early stage of relapsing-remitting MS and develops more rapidly in the earlier clinical stage of the disease. Pathological studies of F e r g u s o n et al. [2] and T r a p p et al. [7], applying morphological techniques, have provided evidence of axonal injury throughout active MS lesions.

In order to obtain more information concerning the neuronal damage in early MS we performed morphometric investigations on the hypoglossal nerve neurons of Lewis rats during the first clinical episode of CREAE.

Material and Methods

Chronic relapsing experimental allergic encephalomyelitis (CREAE) was induced in Lewis rats by inoculation with purified guinea-pig myelin and complete Freund's adjuvant followed by treatment with low-dose cyclosporin A, as previosly described in detail [9]. Control rats were inoculated and treated as above except that the inoculum did not contain guinea-pig myelin. The animals were weighed and examined daily from the seventh day post-inoculum (DPI) and killed during the first clinical episode of CREAE.

The morphometric studies were performed on paraffin sections (6 μm) stained with Nissl of the medulla oblongata at the level of the hypoglossal nerve nucleus of the experimental animals during the first clinical episode of CREAE as well as of control healthy rats. The surface area of the hypoglossal nerve neurons was measured by using the point-counting method of Автандилов [11] under the magnification of 630. The Student's test was used to determine statistical differences between the rats with CREAE and control animals.

Results

Clinical findings

The majority of the Lewis rats inoculated with myelin and complete Freund's adjuvant and given CsA developed neurological signs commencing 11-16 DPI (first clinical episode). Most of the affected animals recovered fully by 18-27 DPI (first remission).

Morphometric findings

The surface area of hypoglossal nerve neurons of Lewis rats increased significantly during the first clinical episode of CREAE in comparison with the control Lewis rats (Table 1 and 2).

TABLE 1. SURFACE AREA OF THE HYPOGLOSSAL NERVE NUCLEUS NEURONS (in μm^2) OF THE LEWIS RATS WITH CREAE IN COMPARISON WITH CONTROL ANIMALS

RATS WITH CREAE	CONTROL RATS
274.22 ± 7.75	226.15 ± 8.0

TABLE 2. NUMBER OF MEASURED HYPOGLOSSAL NERVE NUCLEUS NEURONS OF THE LEWIS RATS WITH CREAE AND OF CONTROL ANIMALS

RATS WITH CREAE	CONTROL RATS
520	494

Discussion

Our morphometric study revealed a significant increase of the surface area of hypoglossal nerve neurons during the first clinical episode of CREAE. This finding reflects the first sign of primary degeneration of the neuron — the swelling of neuronal cell body. In this investigation using a suitable model of MS [10] we present for the first time data concerning the early degeneration of the neurons of a motor nerve in CREAE. They are in concordance with the results of Hobom et al. [3] on neuronal degeneration of the sensory optic nerve in experimental autoimmune encephalomyelitis (EAE) induced by myelin olygodendrocyte glycoprotein. The retinal ganglion cell death occurred before the onset of clinical symptoms of the disease. Early neuronal dysfunction in EAE has been also revealed in the studies of Nicot et al. [4] on the regulation of gene expression in the Lewis rats lumbar spinal cord during the clinical course of acute EAE.

A degenerative component to MS was always apparent, but was underestimated until recently. It is widely accepted now that the degenerative response is an integral and early component of MS [5]. The fact that neuronal damage occurs very early in the pathogenesis of MS has important implications for therapeutic strategies, which aim at preventing neuronal loss.

In conclusion, we have shown in chronic relapsing EAE, a suitable animal model for the study of MS pathogenesis, using morphometric method, a degeneretion of hypoglossal nerve neurons during the first clinical episode of the disease. This finding, supports the notion that neuronal degeneration can begin very early in MS. It provides another evidence of the concept of MS as a neuronal disease.

References

1. De Stefano, N. et al. Evidence of axonal damage in the early stages of multiple sclerosis and its relevance to disability. — Arch. Neurol., **58**, 2001, 65-70.
2. Ferguson, B. et al. Axonal damage in acute multiple sclerosis lesions. — Brain, **120**, 1997, 393-399.
3. Hobom, M. et al. Mechanisms and time course of neuronal degeneration in experimental autoimmune encephalomyelitis. — Brain Pathol., **14**, 2004, 2, 148-157.
4. Nicot, A. et al. Regulation of gene expression in experimental autoimmune encephalomyelitis indicates early neuronal dysfunction. — Brain, **126**, 2003, 398-412.
5. Owens, T. The enigma of multiple sclerosis: inflammation and neurodegeneration cause heterogeneous dysfunction and damage. — Curr. Opin. Neuro., **16**, 2003, No 3, 259-265.
6. Sultanov, B. Neuronal and Axonal Damage in Early Multiple Sclerosis. — Acta Morphol. et Anthropol., **9**, 2004, 208-210.
7. Trapp, B. D. et al. Axonal transection in the lesion of multiple sclerosis. — N. Engl. J. Med., **338**, 1998, 278-285.
8. Waxman, S. G. Multiple sclerosis as neuronal disease. — Arch. Neurol., **57**, 2000, 22-24.
9. Zaprianova, E. et al. Ganglioside Spinal Cord Changes in Chronic Relapsing Experimental Allergic Encephalomyelitis Induced in the Lewis Rat. — Neurochem. Res., **22**, 1997, No 2, 175-179.
10. Zaprianova, E. et al. Chronic remmiting experimental allergic encephalomyelitis in Lewis rats as a model of multiple sclerosis. — Neurosci. Behav. Physiol., **29**, 1999, No 1, 7-10.
11. Автандилов, Г. Г. Медицинская морфометрия. М., Медицина, 1990.

Institute of Experimental Morphology and Anthropology

Acta morphologica et anthropologica, 10
Sofia•2005

General Peculiarities of the Structure of the Sinusoidal Capillaries of the Adrenal Gland

A. Petrova

Department of Anatomy, Histology and Embryology, Medical University of Varna, Varna

The adrenal gland was electron microscopically investigated. In the cortical part of the gland both arterial and venular areas of the sinusoid capillaries were identified while in the medullar part there were typical sinusoid capillaries and venous sinusoids as well as arterial capillaries. These data correspond to the concepts about the construction of the terminal vascular bed in the adrenal gland. The sinusoid capillaries in the adrenal gland possess as basic peculiarities common for its two parts the following: a fenestrated endothelium, an continuous basal membrane and optional (occasional) extraendothelial cellular and fibrillar elements. The differences between both parts of the gland concern the presence of microvilli and processes of the parenchymal cells in the pericapillary space and in the wall of the sinusoid capillaries, the extent of endothelial fenestratedness, and the activity of micropinocytosis.

Key words: sinusoid capillaries, adrenal cortex, adrenal medulla.

Terminal blood vessels in both parts of the adrenal gland designed as sinusoid capillaries or sinusoids represent the object of our investigations. We identify as sinusoid capillaries the vessels with a fenestrated endothelium, that as a rule, is surrounded by a basal membrane. To them belong some vessels of different shape and size of the lumen. It is rounded when it contains erythrocytes but irregular in their absence because of deformation induced by the surrounding parenchymal cells.

In the wall of the sinusoid capillaries some permanent components such as endothelium and basal membrane and provisory extraendothelial cellular and fibrillary elements can be distinguished.

Every endothelial cell could be, conditionally, divided into two zones: a nucleus containing and a peripheral zone. The latter is relatively thin and presents with non-fenestrated and fenestrated areas showing definite differences between the cortex and the medulla. In the cortical part the thickness of the non-fenestrated areas varies between 200 and 800 nm while that of the fenestrated ones — between 40 and 120 nm. They occupy the larger part of the cellular surface and contain numerous fenestrae closed by a membrane or by pores without any membrane. In the medullar part the non-fenestrated areas of the endothelium are strongly attenuated reaching up to 20 nm. Among the attenuated parts thickenings being sometimes of large size can be observed. The fenestrated areas of the endothelium in the medulla are considerably

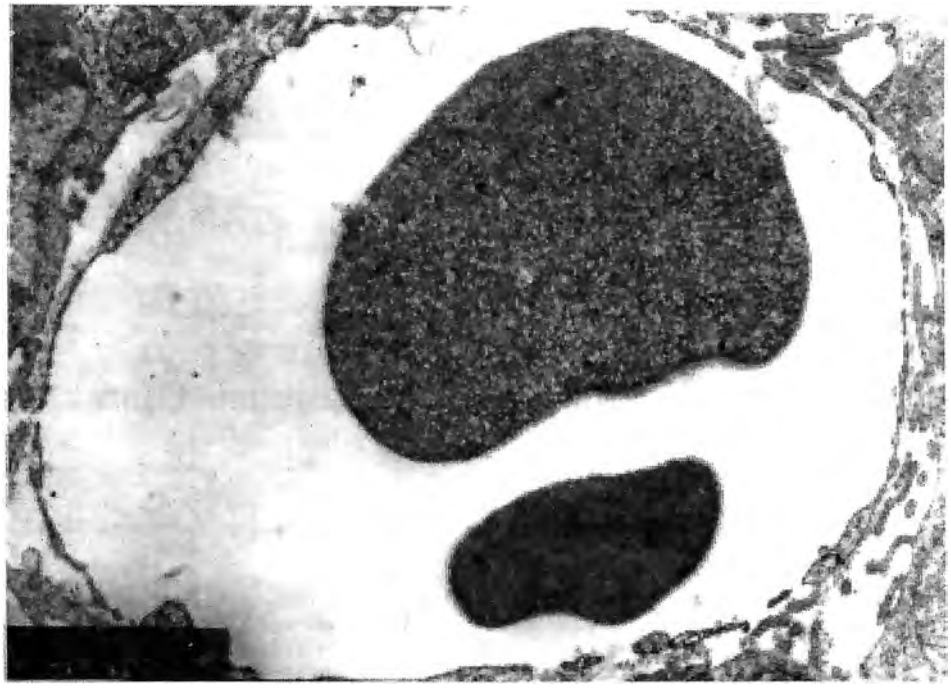

Fig. 1. Adrenal cortex. Sinusoidal capillary. Electron microscope magnification (× 16 000)

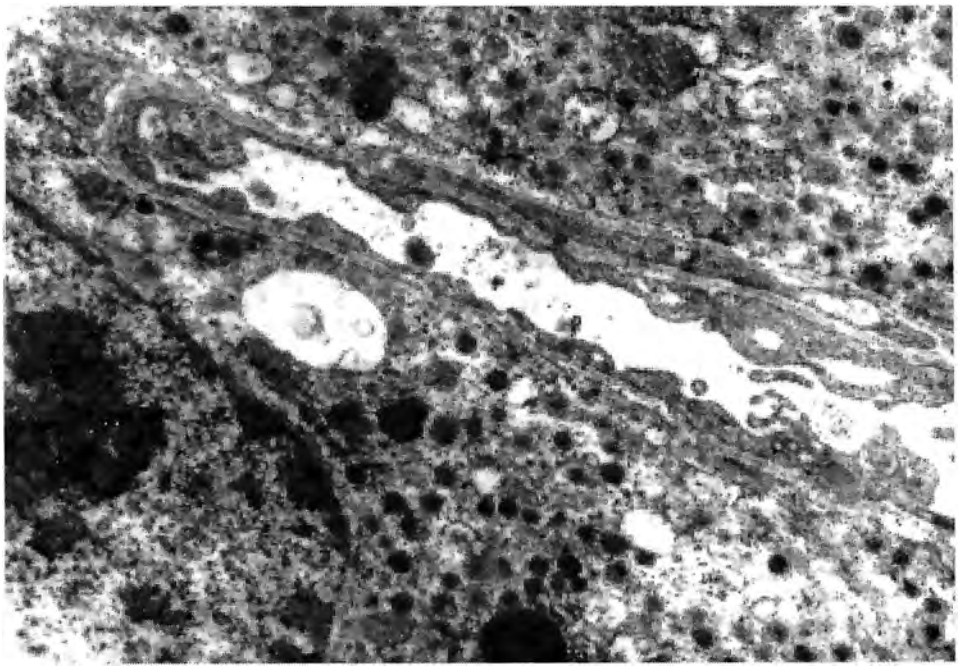

Fig. 2. Adrenal medulla. Sinusoidal capillary. Electron microscope magnification (× 8000)

smaller in size than these in the cortex (Fig. 1, 2). The fenestrae in both glandular parts are closed by one-layer membrane with a centrally located dense material.

Our data indicate the presence of a significant micropinocytotic activity in the non-fenestrated peripheral areas of the endothelial cells that is, in general, stronger in the medulla than in the cortex. The presence of forming and opening vesicles on the surface argues for a two-directional transport (Fig. 3). In relation with the transendothelial transport some peculiar formations of the fenestrated endothelial areas are of undoubted interest. The fenestrated plate bends and prominates into the lumen thus moving away from the basal membrane. Some evaginations of the glandular cells can penetrate into the formed enlargement of the subendothelial space (Fig. 4) [4].

As a rule, the wall of the sinusoid capillaries in the cortex and medulla does not possess any continuous layer of extraendothelial cellular and fibrillar elements. Single cells and fibrillar elements occur comparatively seldom and along a restricted distance only. In the pericapillary space of the cortical part one can also observe evaginations of the endothelial cells of different shape and size as well as processes and microvilli of the parenchymal cells (Fig. 1). The pericapillary space in the medullar part is distinguished by that in the cortical one mainly through the absence of processes and microvilli of the parenchymal cells. That is why the parenchymal cells are located along a significant distance in the close proximity to the sinusoid capillary as both basal membranes, i.e. the endothelial and the parenchymal, are merged into one membrane (Fig. 2).

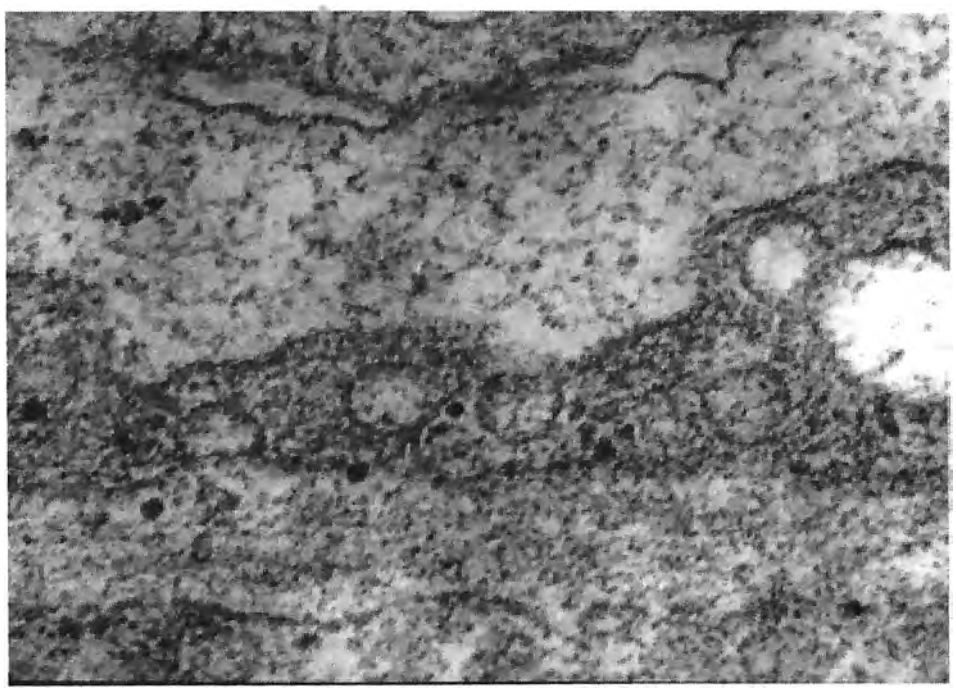

Fig. 3. Adrenal medulla. Forming and opening micropinocytic vesicles. Electron microscope magnification (× 87 500)

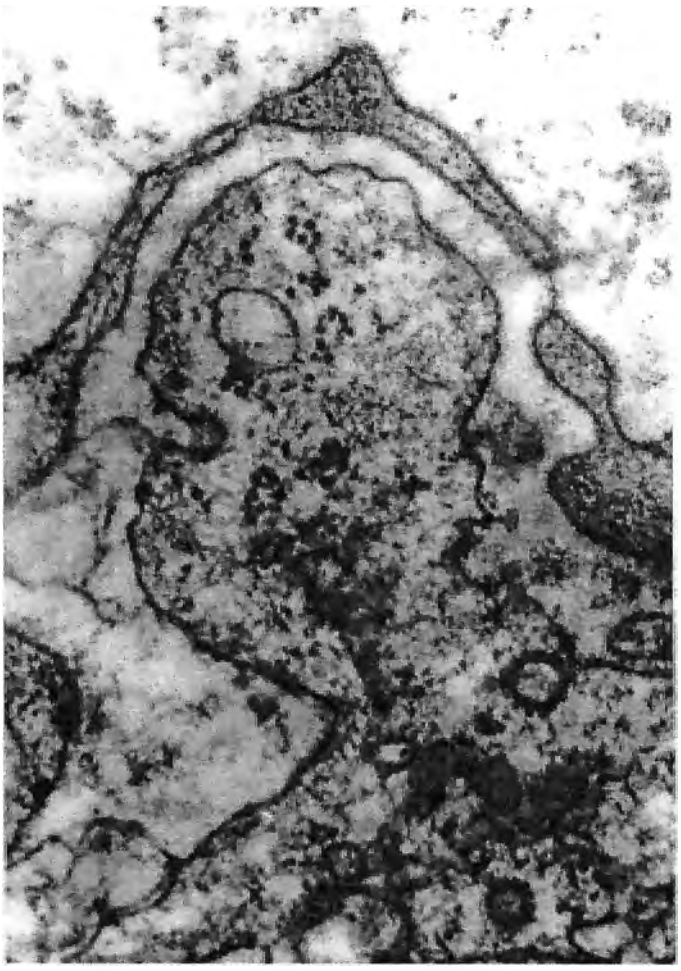

Fig. 4. Adrenal cortex. Electron microscope magnification (× 50 000)

The results from our studies disprove the general validity of certain signs incorporated into the classification characteristics of the capillaries of the endocrine organs: an continuous layer of periendothelial cells [7], permanent parenchymal basal membrane as an obligatory borderline of the pericapillary space [1, 2], size of the fenestrae [1, 3], and three-layer structure of the fenestral membrane [7]. Literature data about the presence of a fenestrated endothelim within the medulla are contradictory [5,6].

Our investigations demonstrate that the sinusoid capillaries of the adrenal cortex and medulla are of a qualitatively equal structure but they differ concerning the amount of the single ultrastructural devices designed for a transendothelial transport. They possess the whole possible set of structural mechanisms determining the capacity for an intensive transendothelial transport under stress conditions.

References

1. D a v i d, H. Vergleichende submikroskopische Morphologie der Kapillaren versciedener Organe und Organismen. — Dtsch. Gesundh.-Wes., **21**, 1966, 1319-1328.
2. E n r i c o, A. Lo spazio pericapillare nell' ghiandole endocrine. — Arch. Ital. Anat. Embriol., **80**, 1975, 37-56.
3. M a j n o, G. Ultrastructure of the vascular membrane. — In: Handbook of Physiology, sect. 2, vol. III. Washington, 1965.
4. P e t r o v a, A., V. N. V a n k o v. On some luminal formations of endothelial cells in the adrenal cortex. — Compt. Rrend. Acad. Bbulg. Scien., **30**, 1977, No 1, 153-156.
5. R y a n, U. S. et al. Fenestrated endothelium of the adrenal gland: freeze-fracture studies. — Tissue Cell, **7**, 1975, 181-190.
6. С а п и н, М. П. Сосуды надпочечных желез. Москва, 1974.
7. Ш а х л а м о в, В. А. Каппиляры. Москва, 1971.

Institute of Experimental Morphology and Anthropology

Acta morphologica et anthropologica, 10
Sofia • 2005

Ultrastructural Observation of the Human Milky Spots

K. N. Michailova

Department of Anatomy and Histology, Faculty of Medicine, Medical University, Sofia

The structure of the milky spots were investigated by transmission electron microscopy on surgically removed specimens of the great omentum of 15 patients from 35 to 67 years old. Thin mesothelium without stomata openings on inconstant basal lamina covered extremely complicated contour over milky spots. The human milky spots were smaller and the cell components were disposed very sparsely. Significant differences in cell nature and number, as well as lack of constant order characterized the neighbouring milky spots. The present study demonstrated that largest population of macrophages, following lymphocytes and group of mast cells were principal cell types in norm. Other cell clusters consisted numerous neutrophilic leucocytes, large groups of mast cells and macrophages or in cell accumulations predominated connective tissue component. The microvasculature of milky spots was composed by large groups of blood vessels with different size, continuous capillaries and cistern-like lymphatic vessels with extremely flat lumens, oriented near to peritoneal surface.

Key words: electron microscopy, man, great omentum, milky spot, peritoneum.

Introduction

The great omentum has numerous tiny white lymphoid nodules, known as milky spots and for their protective role they have been called the "policemen of the abdomen". In Fawcett's book of histology they are described as round or oval patches of macrophages and other free cells along the blood vessels [1]. Since Ranvier named "taches laiteuse" [8] such milky spots, many workers have investigated them in different animals [6, 7]. Seifert reported for the first time milky spots in the human great omentum [9]. Data from the last twenty years widened the extra-omental localization of milky spots on the mediastinal pleura (Kampmeier' foci), chest wall, pericardium, uterine fringe, pancreatic peritoneum, gastrosplenic ligament, splenoportal fat bands and mesenteric root [10, 11]. The number of milky spots per unit area gradually decreases with age [3]. Its microvasculature consists of an arteriole precapillary, postcapillary, collecting venule, venule, and beginnings of blind lymphatic capillaries, surrounded with cell clusters of macrophges (47.5%), B and T lymphocytes (40.8%) and rare mast cells (6.1%) [1, 2].

Material and Methods

Samples of different sectors of the great omentum peritoneum with the underlying tissue were obtained after laparatomy from 15 patients from both sexes (9 males and 6 females), aged 35 — 67 years (< 40 years: 2 cases; 40 -50: 3 cases; 50 — 60: 6 cases; > 60 years: 4 cases). Five patients had pancreatic, gastric and rectal carcinoma (without previous chemo- or radiotherapy), 3 echinoccoses, 4 cholelithiasis, 2 liver abscesses and 1metastases after lung carcinoma. The blocks, measuring 3×1×1 mm were fixed in 1% glutaraldehyde in 0.1 M Na cacodylate buffer (pH 7.4) for 1h at room temperature and were postfixed for 1h in 1.5% OsO_4 (pH 7.4) in the same buffer. After dehydratation the blocks were embedded in Durcupan ACM (Fluka). The regions without pathologic alterations (with continuous mesothelial covering and intact cells as vessels in the submesothelial layer) were identified on light microscopically on semithin sections, stained with 1% Toluidine blue. The contrasted thin specimens were examined in Hitachi 500 electron microscope.

Results

The largest surface of the human great omentum showed wide and shallow folds, separated by fine concavities. The serous covering was composed of continuous mesothelium over basal lamina and submesothelial layer. The mesothelial layer

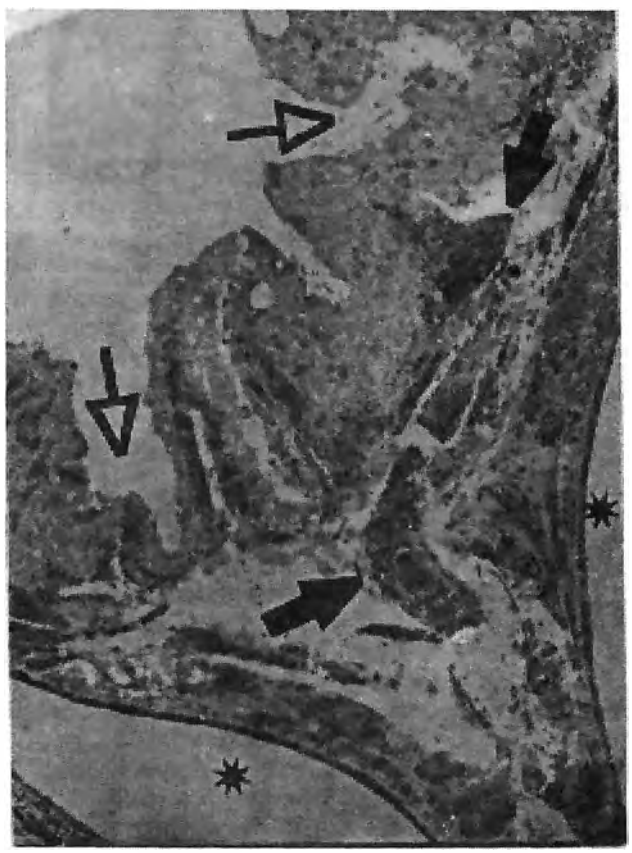

Fig. 1. Invaginations (empty arrows) between protrusions in the mesothelial layer. Fine collagen bundles (arrows) surrounded large intercellular spaces. Two lipocytes (asterisks) (× 7700)

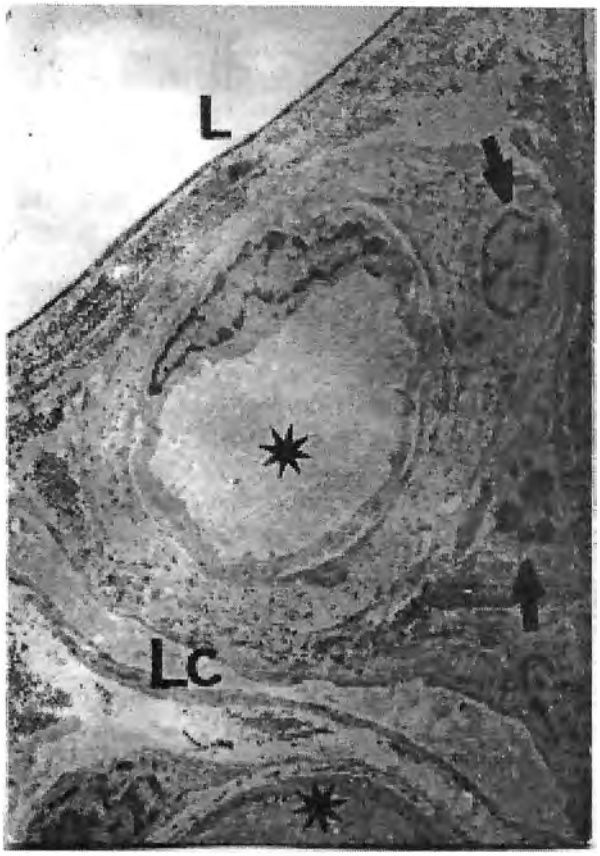

Fig. 2. Cells (arrows) in vicinity of lymphatic capillary (Lc) with extremely flat lumen and two blood capillaries (asterisks). Lipocytes (L) (× 7700)

predominantly consisted of flat cells. They exhibited slightly protruded central portions with elongated nucleus and a scant perinuclear cytoplasm. A poor organelle apparatus was disposed in extremely thin peripheral zones. The cubic mesothelial cells occurred in small groups. The nuclear portions of the most cubic cells repeated the contour of the nucleus and were located in the submesothelial invaginations. The rich organelle apparatus occupied the perinuclear cytoplasm. In wide zones it was difficult to distinguish the mesothelial basal lamina. The superficial part of the submesothelial layer was composed by single cells (fibrocytes and free cells), blood capillaries and small group of smooth muscle cells. The largest portion of the same zone was occupied of loosely arranged collagen with different size, surrounded wide intercellular spaces. The adipose tissue built the entire thickness of the submesothelial layer in wide areas or filled its deep part only.

The mesothelium formed large ridges with a complicated contour, limited by deep furrows with different length and width over cell clusters and densely packed vessels, which were located in the superficial part of the submesothelial layer and more rarely in the deep adipose tissue (Fig. 1). Blood vessels with different size and continuous capillaries formed large groups in the cell accumulations (Fig. 2). Cistern-like lymphatic vessels with extremely flat lumens or with complicated contour, were oriented near to the peritoneal surface. The extremely thin, electron-lucent endothelium without basal lamina built the lymphatic capillaries. The free cells in the cell accumulations densely distributed and surrounded exclusively thin intercellular

spaces, while in other ones they were disposed sparsely over a net of fibrocytes and fine collagen bundles. The most numerous cell types were the macrophages, followed by lymphocytes and mast cells. Neutrophilic leucocytes, macrophages and groups of mast cells were observed in other clusters. Bundles of thin unmyelinated or occasional myelinated fibers were observed in vicinity of the vessels and the cells.

Discussion

The present study of the human great omentum confirm the general peritoneal structure in norm, as previously were described for other organs of the abdominal cavity [5]. The zones of milky spots represent significant morphological differences — mesothelium with complicated contour over inconstant basal lamina and submesothelial layer with cell accumulations in vicinity of vessels (blood and lymphatic), as compared with the remaining parts of the great omentum. In contrast with other studies [6] we did not observed stomata, which formed opening in the mesothelial layer. We consider that stomata in norm involve close contact between the mesothelial and endothelial cells and observed their typical image only in pathological conditions [4]. The structural complexity, allow us to propose, that the human milky spots are constant appearance, but they are smaller and the cell components are very sparsely disposed, as compared with the animals ones [6, 7]. Large differences in cell nature and number without constant order characterize the neighbouring milky spots. Our results are in contrast with the data of S h i m o t s u m a et al. [10], that the macrophages cover milky spots, while lymphocytes are found in the central portion. It is difficult to define the exact cell composition and vessel participation in the present routine observation, if do not pay attention of the age of the patients and an undefinable inflammatory alterations [2, 10]. The structural complexity of these zones are like the diaphragmatic units and suggest that both organs represent most specialized regions in the supporting of the peritoneal homeostasis.

References

1. F a w c e t t, D. W. Textbook of Histology. 11th Edition. Philadelphia, W.B. Saunders, 1986, p. 164.
2. K r i s t, L. F. et al. Cellular composition of milky spots in the human great omentum: an immunochemical and ultrastructural study. — Anat. Rec., **241**, 1995, 163-174.
3. K r i s t, L. F. et al. Ontogeny of milky spots in the human great omentum: an immunochemical study. — Anat. Rec., **249**, 1997, 399-404.
4. M i c h a i l o v a, K. N. Postinflammatory changes of the diaphragmatic stomata. — Ann. Anat., **183**, 2001, 309-317.
5. M i c h a i l o v a, K., W. W a s s i l e v, T. W e d e l. Scanning and transmission electron microscopic study of visceral and parietal peritoneal regions in the rat. — Ann. Anat., **181**, 1999, 253-260.
6. M i r o n o v, V. A., S. A. G u s e v, A. F. B a r a d i. Mesothelial stomata overlying omental milky spots: Scanning electron-microscopic study. — Cell Tissue Res., **201**, 1979, 327-330.
7. M i x t e r, R. L. On macrophagal foci ("milky spots") in the pleura of different mammals, including man. — Am. J. Anat., **69**, 1941, 159-186.
8. R a n v i e r, L. Du developpement et de l'accroissement des vaisseaux sanguins. — Arch. Physiol. Norm. Path., **6**, 1874, 429-449.
9. S e i f e r t, E. Zur Biologie des menschlichen grosen Netzes. — Arch. Klin. Chir., **116**, 1921, 510-517.
10. S h i m o t s u m a, M. et al. Morpho-physiological function and role of omental milky spots as omentum-associated lymphoid tissue (OALT) in the peritoneal cavity. — Lymphology, **26**, 1993, 90-101.
11. T a k e m o r i, N. et al. Light and electron microscopic study of splenoportal milky spots in New Zealand black mice: comparison between splenoportal milky spots and aberrant spleens. — J. Anat., **186**, 1995, 287-299.

Institute of Experimental Morphology and Anthropology

Acta morphologica et anthropologica, 10
Sofia•2005

Ultrastructural Differences of the Medial Meniscus Depending on the Sites of Insertion

M. Kalniev, N. Vidinov, K. Vidinov, N. Kondov, G. Georgiev

Department of Anatomy and Histology. MF, MU, Sofia

The aim of our study was to trace out the structure of the sites of insertion of medial meniscus and his close parts in Wistar rats. The existent investigations concern only the layers of the menisci, but not their sites of insertion. The electron microscopy investigation we have made showed the presence of an electron dark stripe situated between the articular matrix and the collagen bundles. That stripe was very much folded and formed thin digit-like growths. The tense zone of the meniscus bears resemblance to the the transitional zone between articular cartilage ad synovial membrane. The cells from the zone lack a typical chondroblast character. They represent transient cellular forms with fibroblast phenotype, assigned the task to regulate the demands of cartilage matrix.

Key words: meniscus, proteoglycans, collagen, computer analysis.

Introduction

The structure of the sites of insertion of the menisci determines their steadiness to different abnormal mechanical influences [10]. Their individual structural characteristic defines various individual possibilities of the menisci to be injured and teared. The existent investigations concern only the layers of the menisci, but not their sites of insertion [5, 1, 2, 3, 6, 9, 11]. The aim of our study was to trace out the structure of the sites of insertion of medial meniscus and his close parts in Wistar rats.

Material and Methods

The materials of the investigation were 15 Wistar rats of both sexes, aged between 8 and 12 months. The material was taken from the anterior point of insertion (API) and the posterior point of insertion (PPI) and then was compared. The samples were investigated by routine light microscopy after staining in Mason. Routine transmission and scanning electron microscopy were used, as well as ultracytochemical examination with Safranin O was performed in order to prove the presence of proteoglycans. The electronograms were analyzed by Image analyzer "Olympus", Version 4.5. Electronograms with the same enlargement and taken down under equal

conditions were used for that purpose. They were calibrated for a size, intensity and density. The received data were worked up by a computer with a special program and then charts (barohistograms) were produced.

Results

The results from light microscopic examination in Mason showed that the meniscus was built on four zones: a sliding zone, a pressure zone, a tense zone and a paramenisical zone. It was established on bigger enlargement, the collagen bundles contacted directly with the articular cartilage or they separated on the articular cartilage by thin clefts. The electron microscopy investigation of the API showed the presence of an electron dark stripe situated between the articular matrix and the collagen bundles. That stripe was very much folded and formed thin digit-like growths (Fig. 1). Proteoglycan complexes were arranged between these growths. Sometimes the growths were situated densely and even contacted each other. Peripheral collagen structures were arranged in groups. These groups were in parallel and formed bundles. Their ultrastructural characteristic was of collagen type I. The parallel investigation by scanning electron microscopy confirmed those special features (Fig. 2). The examination of the structures of the PPI showed that the border electron dark stripe was not very much folded and it contacted with fibroblast-like cells. On their outside surface were situated crystalline calcium precipitations (Fig. 3). The collagen fibers situated peripheral on the site of insertion were unorganized and formed a collagen network. The scannogram showed that they were different in form and size. Sometimes the collagen fibers contacted each other.

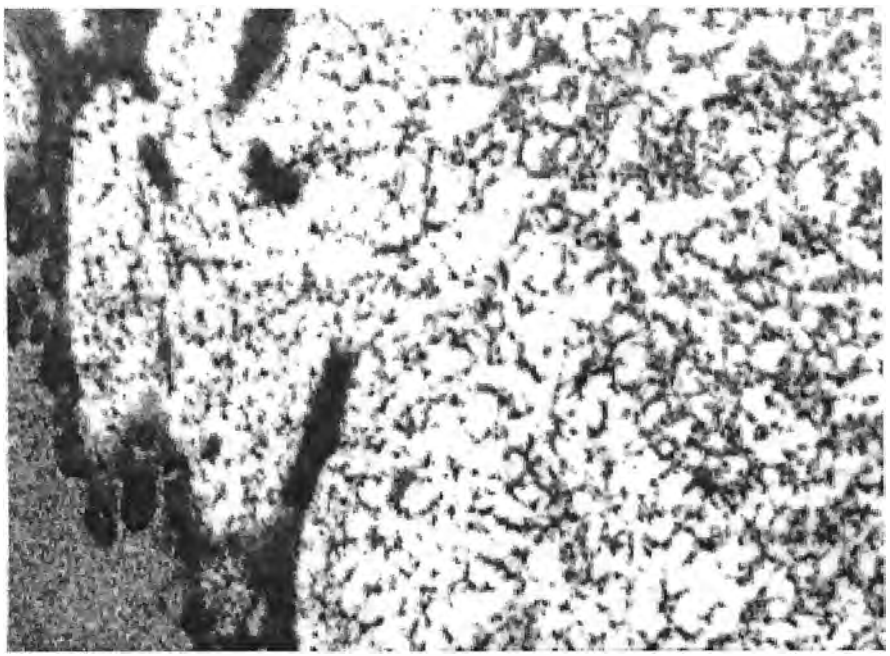

Fig. 1. The electron microscopy investigation of the API showed the presence of an electron dark stripe situated between the articular matrix and the collagen bundles. It was very much folded and formed thin digit-like growths (× 15 000)

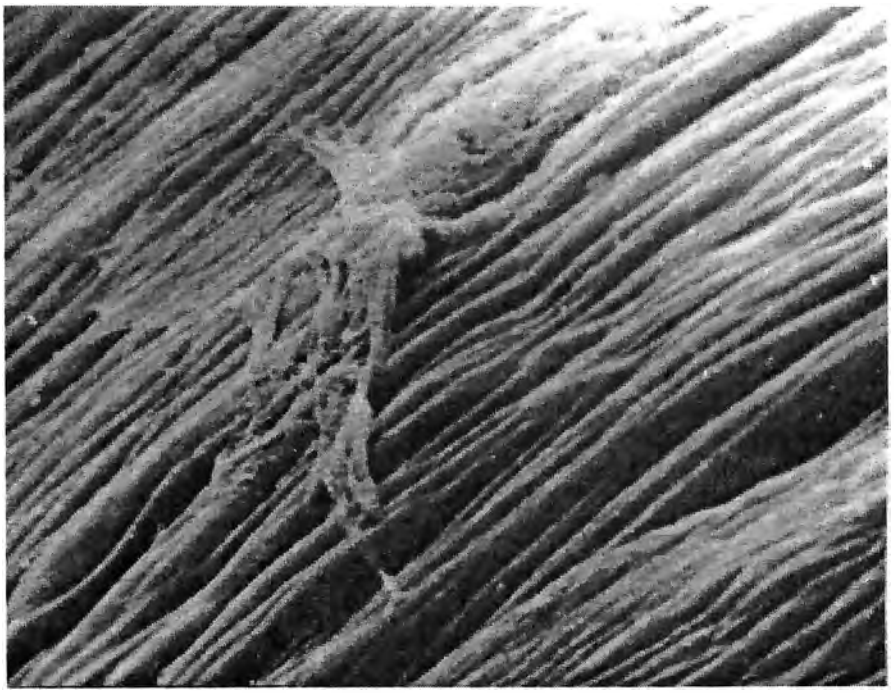

Fig. 2. SEM — the ultrastructural characteristic of the fibers was of collagen type I (× 6000)

Fig. 3. Fibroblast-like cells. On their outside surface were situated crystalline calcium precipitations (× 10 000)

Discussion

The results of our experiments show that there is a great percentage of variations in the insertion of the menisci. The impaired biomechanics clarifying different types of traumas. As shown by the study results, the tense zone of the meniscus bears resemblance to the the transitional zone between articular cartilage ad synovial membrane of the articular cartilage [12]. The cells from the zone lack a typical chondroblast character. Obviously, they represent transient cellular forms with fibroblast phenotype, assigned the task to regulate the demands of both cartilage and synovial matrix. Such duplicity of the cells defines their excessive metabolic involvement owing to which they undergo rapid wearing out with ensuing degeneration [5, 7, 8]. As in the articular cartilage, initially the cells of the zone react by activation becoming manifest with enhanced proteoglycan synthesis, documented by increased concentration of proteoglycans in the territorial matrix of the cells. The transient nature of the elements in the insertion of the meniscus determines the pronounced lability of this zone. That must be always taken into account when clarifying the causes for the pain in the knee joint and in the surgical interventions on the menisci in different types of traumas.

References

1. Arnoczky, S. P. et al. The meniscus. In: Buckwalter, Jr, J. A., Woo, SL-Y, Eds. The injury and repair of musculosceletal soft tissue. Park Ridge. IL: Am. Acad. Orthop. Surg., **34**, 1988; 487-537.
2. Berlet, G. C, P. J. Fowler. The anterior horn of the medial meniscus. An anatomic study of its insertion. — Am. J. Sports. Med., **26**, 1998, 540-543.
3. Bhargava, A, D. A. Ferrari. Posterior medial meniscus-femoral insertion into the anterior cruciate ligament. A case report. — Clin. Orthop., **348**, 1998, 176-179.
4. Fukuta, S, K. Masaki, F. Korai. Prevalence of abnormal findings in magnetic resonance images of asymptomatic knees. — J. Orthop. Sci., **7**, 2002, 287-291.
5. Goldman, A, T. R. Waugh. The menisci of the knee. — Orthop. Rev., **14**, 1985, 67-76.
6. Jung, Y B, J. K. Yum, Y. J. Bae, K. S. Song. Anomalous insertion of the medial menisci. — Arthoscopy, **14**, 1998, 505-507.
7. Kim, S. J., D. W. K I m, B. H. M I n. Discoid lateral meniscus associated with anomalous insertion of the medial meniscus. — Clin. Orthop., **315**, 1995, 234-237.
8. Ohkoshi, Y, T. Takeuchi, C. Inoue, T. Hashimoto, K. Shigehobu, S. Yamane. Arthroscopic studies of variants of the anterior horn of the medial meniscus. — Arthroscopy, **13**, 1997, 725-730.
9. Pagnani, M. J, D. E. Copper, R. F. Warren. Extrusion of medial meniscus. — Arthroscopy, **7**, 1991, 297-300.
10. Papadopoulou, Th. The role of intermediate zone between articular cartilage and synovial membrane during the process of elimination of the components of haemarthrosis. — B. J. Ort. Traum., **35**, 1999, No 4, 263-268.
11. Rainio, P., J. Sarimo, J. Rantanen, J. Alanen, S. Orava. Observation of anomalous insertion of the medial meniscus on the anterior cruciate ligament. — Arthroscopy, **18**, 2002, No 2, E9.
12. Vidinov, N., A. Djerov. Ultrasructural changes in the transitional zone between articular cartilage and synovial membrane during the development of experimental ostreoarthrosis. — International orthopedics, **26**, 2002, 137-140.
13. Yain, E. H, I. Gallo, R. E. Hughes, J. E. Kuhn. The relationship between Parson's tubercle and the insertion of the anterior horn of the medial meniscus. — Arthroscopy, **17**, 2001, No 7, 737-740.

Institute of Experimental Morphology and Anthropology

Acta morphologica et anthropologica, 10
Sofia•2005

Morphology of the Valve Sinus Wall in Essential Varicosity of the Great Saphenous Vein — TEM and SEM Investigations

M. Minkov, R. Guidoin***

* *Department of Anatomy, Histology and Embryology, Medical University Varna*
** *Department of Surgery, Laval University and Quebec Biomaterial Institute, Quebec, Canada*

Venous hypertension alters the morphology of the valve sinus wall by damaging the specific arrangement model of endothelial cells, smooth muscle cells (SMC), elastic and collagen fibres as well. Besides the specificity of the structural modifications in SMC there is a process of transformation from a contractile into a synthetic-secretory phenotype. This explains in part the important functional changes observed in the SMC. The progression of the venous hypertension acts on the valvular cusp and the valvular complex and increases the development of the varicosis process.

Key words: vein, valves, varicosis, SEM, TEM.

Introduction

Nowadays the development of venous varicosity is explained by a series of hypotheses [1, 2, 3, 4, 6, 9]. According to the hemodynamic hypothesis, this development is due to the venous hypertension and venous stasis acting not only on the venous wall but also on the components of the valvular complex. The morphological changes occurring in the valve sinus wall during the progression of the varicosis process were observed in both transmission and scanning electron microscopy (TEM and SEM, respectively)

Material and Methods

The valve sinus wall of the great saphenous vein harvested from 28 patients was analyzed. They were operated on because of venous varicosity. The selected specimens were fixed in 4% glutaraldehyde in phosphate buffer at pH 7,4, post-fixed in 1% OsO_4, and dehydrated in ethanol of graded concentrations. The material for TEM was embedded in Durcupan. Semithin and ultrathin sections were prepared. The material for SEM was soaked in hexamethyldisilazane for 5 min and then air-dried. The preparations were gold-palladium coated and examined in a Jeol JSM-35 CF scanning electron microscope.

Results

The investigation of the sectional surface of the valve sinus wall by means of SEM demonstrates that the proximal part of the wall is cross-striated due to densely located transversal invaginations of the endothelial surface and the distal part possesses an undulating relief (Fig. 1). As observed in TEM examination the endothelial cell (EC) of morphologically inadequate valves sharply expresses congestion of the cellular matrix, changes in the micropinocytic vesiculation, enlargement of the vacuoles and increased number of Weibel-Palade bodies. In the tunica media, SMC are clearly individualized from the collagen of the connective tissue and can be assembled to form bundles. The transformation of the smooth muscle cells (SMC) from a contractile into a synthetic-secretory phenotype is demonstrated in the veins after progression of the varicosis process (Fig. 2). Ultrastructurally, the enlarged number of the cellular organelles designed for performance of an active synthetic-secretory function was well evidenced. In the morphologically inadequate valves one can observe not only a great variety of the fibrillar diameters but also an increased number of the atypical forms of the fibrils. The presence of atypical, giant fibrils is confirmed, too. Some of these fibrils are spirally screwy, however, the characteristic cross striation along the whole fibril remains intact. In some single fibrils the so-called 'crease-like' deformities as a sign of fibrillar overstretching can occur, too.

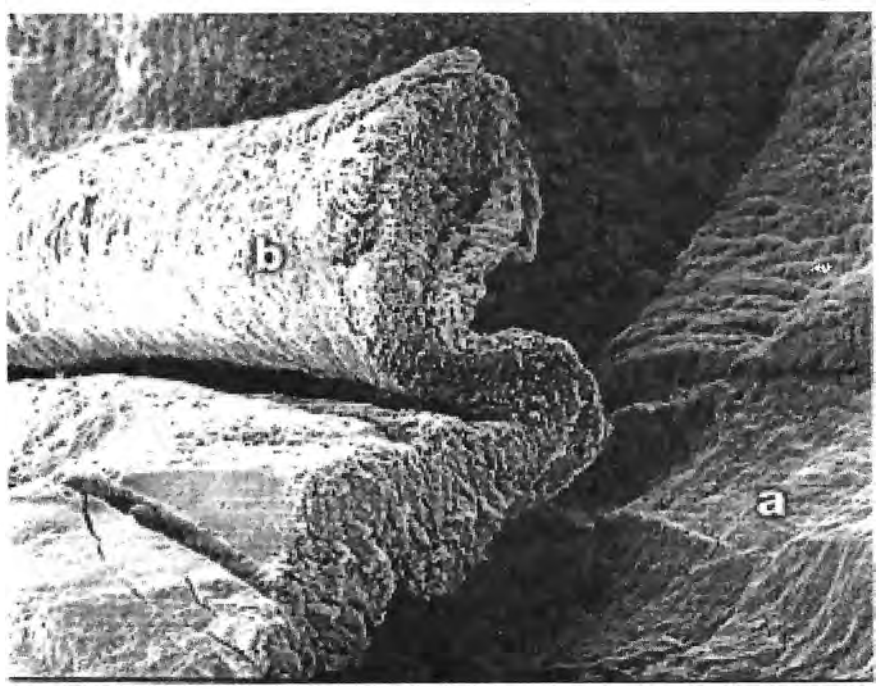

Fig. 1. Valve complex of a morphologically inadequate valve
a — valve sinus wall; b — valvular cusp (SEM, Magn. × 200)

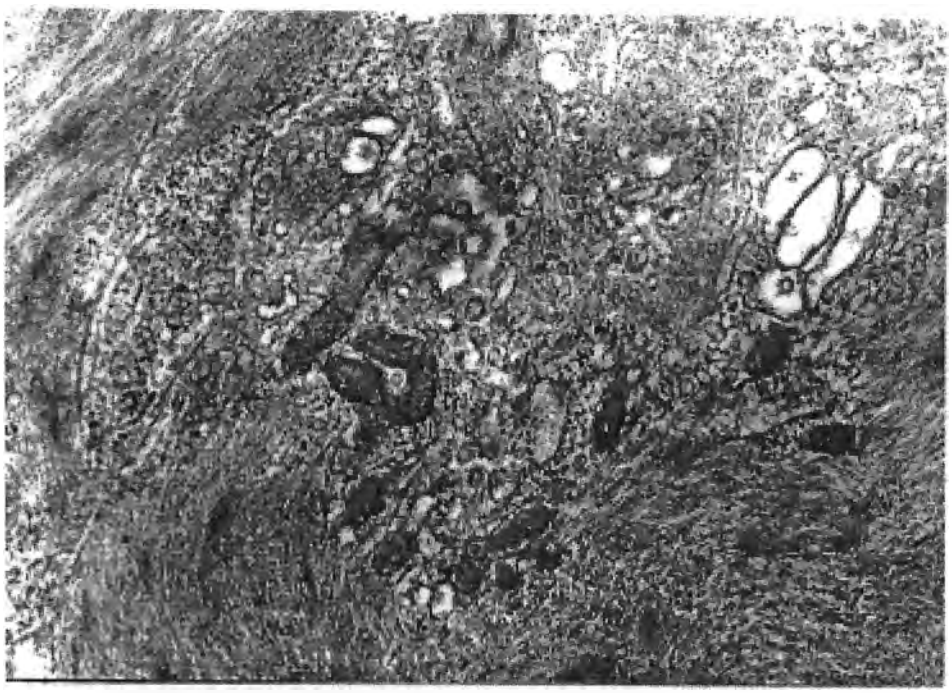

Fig. 2. Smooth muscle cells from the valve sinus wall of a morphologically inadequate valve (TEM, Magn. × 20 000)

Discussion

The presence of SMC of a synthetic-secretory phenotype is the first response of the wall to the venous hypertension. Remodelling of the wall is the next time-dependent process during its adaptation to the new conditions. The fibrosing of the wall and the presence of destructive changes in the SMC and extracellular matrix testify not only to the duration of the varicose process but also to the exhausted adaptation capacities towards the venous hypertension and hypoxia. Besides this investigation demonstrates that the established electron microscopic changes in the valve sinus wall correlate with our previous data [5, 7, 8] dealing with the morphological alterations occurring in the valve complex during the development of the varicose process.

References

1. Butterworth, D. M. et al. Light microscopy, immunohistochemistry and electron microscopy of the valves of the lower limb veins and jugular veins. — Phlebology, 7, 1992, 27-30.
2. Gottlob, R., R. May. Venous valves. Morphology, function, radiology, surgery. With an electron-optical chapter by S. Geleff. Wien and New York, Springer Verlag, 1986. 227 p.
3. Kosugi, I. et al. Matrix metalloproteinase-9 and urokinase-type plasminogen activator in varicose veins. — Ann. Vasc. Surg., **17**, 2003, 234-238.
4. Marinov, G., V. Vancov. Early changes of the smooth muscle cells (SMC) and extracellular matrix in the wall of the varicose veins. — Verh. Anat. Ges., Anat. Anz., **84**, 1991, Suppl. 168, 99-100.

5. Marinov, G., M. Minkov, V. Knyazhev. Spécificités ultrastructurelles des cellules endothéliales valvulaires de la veine saphène interne variqueuse et non-variqueuse. — Phlébologie, 47, 1994, 145-150.
6. Mashiah, A., S. S. Rose, I. Hod. The scanning electron microscope in the pathology of varicose veins. — Isr. J. Med. Sci., 27, 1991, 202-206.
7. Minkov, M. Valve sinus wall morphology in varicose and nonvaricose saphenous magna vein. — Anatomical Collection, 2003, 62-63.
8. Minkov, M. et al. Surface morphology of the endothelium in varicosis of the great saphenous vein — scanning — and transmission electron microscopy study. — Acta Morphol. Anthropol., 7, 2002, 48-55.
9. Ванков, В. Морфология на вените. С., Медицина и физкултура, 1989. 208 с.

Institute of Experimental Morphology and Anthropology

Acta morphologica et anthropologica, 10
Sofia • 2005

Comparative Ultrastructural Analysis of the Articular Cartilage in Overloading and in Big Temperature Deviations

N. Vidinov, K. Vidinov, M. Kalniev, D. Krastev, N. Krastev

Department of Anatomy, Medical University, Sofia

We had compared the results from our experiments on Wistar rats undergoing overloading on the tredbahn and experiments on other Wistar rats whose limbs had been subsequently put into cold water- 1-2 degrees and then into hot water 60 degrees. We played special attention to the articular cartilage as this is a particular structure with a specific metabolism and the chondrocytes comprising it are not connected with a vascular system. From the results of the light and electron microscopy of the two animal groups it becomes clear that the wave-like undulating bordering line between the articular cartilage and the bone — the so called tide mark, is significantly thinner, the proteoglycans in the territorial matrix were significantly and evidently different from those in the interteritorial matrix. The computer analysis of the globular subunits in the extracellular matrix of the articular cartilage of the first group showed that in cases of overloading an increase of the big subunits in contrast to the small and average once was found. The same thing was observed with the globular subunits in the extracellular matrix of the articular cartilage in animals converged to sharp temperature changes.

Key words: articular cartilage, ultrastructure, proteoglycans, globular subunit, computer analysis.

Introduction

The state of the articular cartilage in different conditions, such as overloading [7, 8] is always expressed by variety of symptoms such as: stiffness, limited mobility and pains. These symptoms are also seen in some individuals during rapid temperature changes, which make these individuals believe that they have a certain meteorological abilities in predicting the whether. Previous research on the structure of the cartilage in these conditions shows that it is an extremely sensitive structure, giving quick changes evident on the electron microscopical examinations [1, 6, 8]. It was our aim to compare the results from our experiments on Wistar rats undergoing overloading on the tredbahn and experiments on other Wistar rats which limbs had been subsequently put into cold water- 1-2 degrees and then into hot water 60 degrees. We paid special attention to the articular cartilage as this is a particular structure with a specific metabolism and the chondrocytes comprising it are not connected with a vascular system.

Material and Methods

Material taken from 36 "Wistar" rats aged 8-12 months were employed. The 1st group of animals was investigated under the condition of intensive movement (animals were put in the tredbahn for 1 hour every 10 days), and the 2nd group were investigated under the condition of high temperature differences (their right legs were put in the water with temperature 1 degrees C and 60 degrees C). Material for investigation from intensive zone of articular cartilage was taken. Light microscopical investigations were performed after the methods of Masson. Electron microscope study was performed also for demonstrating proteoglycan complexes of the intercellular cartilage matrix after the method of Shepard and Mitchel (1976 (5), using Safranin O for the purpose.

Results

Comparing the results from the light microscopy of the two animal groups it becomes clear that the wave-like undulating bordering line between the articular cartilage and the bone — the so called tide mark — is significantly thinner. It is easily distinguished as well stained band, which outer border is relatively flat and the inner one is largely indented. Looking closely and investigating specifically this structure we found out that it is comprised mainly of chondroblasts with hypertrophy and have an oval shape and relatively big size (Fig.1). In the extracellular matrix a fine network

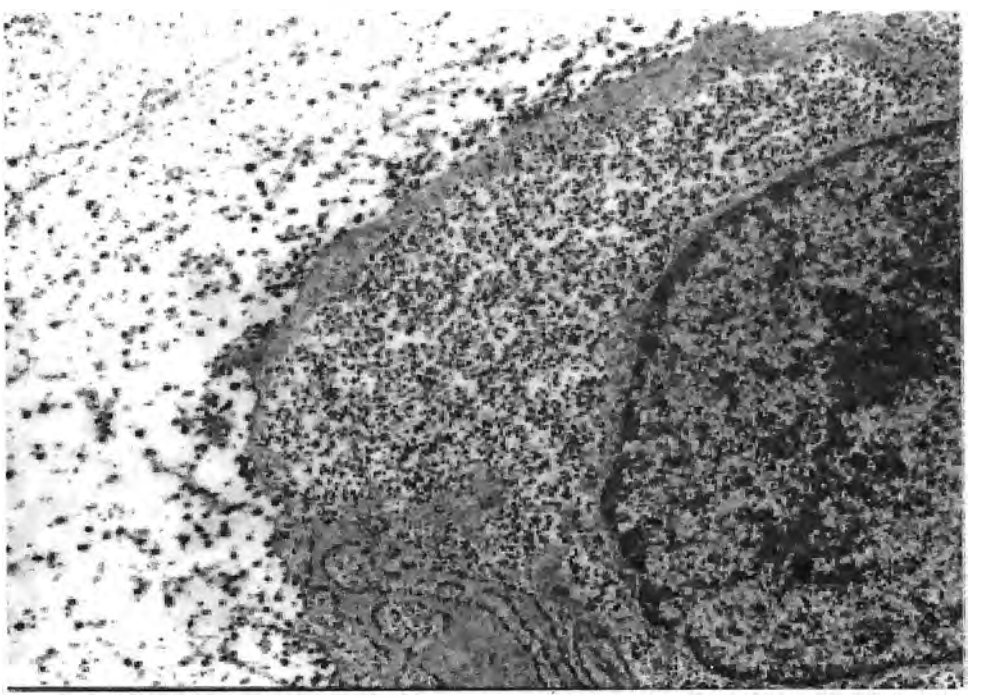

Fig.1. We found out that the tide mark is comprised mainly of chondroblasts with hypertrophy and have an oval shape and relatively big size (× 18 000)

of collagen bundles and proteoglycan complexes, equally distributed in the territorial and interterritorial matrix was observed. When examining the chemical structure of the proteoglycan complexes more closely, we established that it is composed of one core protein in the center, connecting proteins and glucosaminoglican chains. During prolongated and intensive overloading (10 days with 1 hour each day) on the tredbahn changes in the surface layer of the articular cartilage were detected. Indentations and roughness of the articular cartilage as well as disappearance of Lamina splendes were also found. In the tide mark changes in the carbohydrates metabolism are observed both during overloading and in drastic temperature changes. At first we depicted glycogen deposition in the chondroblasts and in the same time increase of the proteoglycan concentration in the territorial matrix of the cells. The intensity of the staining and the structure of the proteoglycans in the territorial matrix were significantly and evidently different from those in the interteritorial matrix. The computer analysis of the globular subunits in the extracellular matrix of the articular cartilage of the first group showed that in cases of overloading an increase of the big subunits in contrast to the small and average once was found. The same thing was observed with the globular subunits in the extracellular matrix of the articular cartilage in animals converged to sharp temperature changes. In those case a bigger clustering of the proteoglycan complexes was also typical (Fig. 2). When staining the slides for collagen and proteoglycans we see a fine network in which the proteoglycans serve as bridge structures between the collagen fibers, keeping them in a certain distance from one another (Fig. 3). As a result of the overloading and the temperature abnormalities this particular network is slightly damaged and disturbed, causing the proteoglycan bridges to disappear and then the collagen fibers stick to one another.

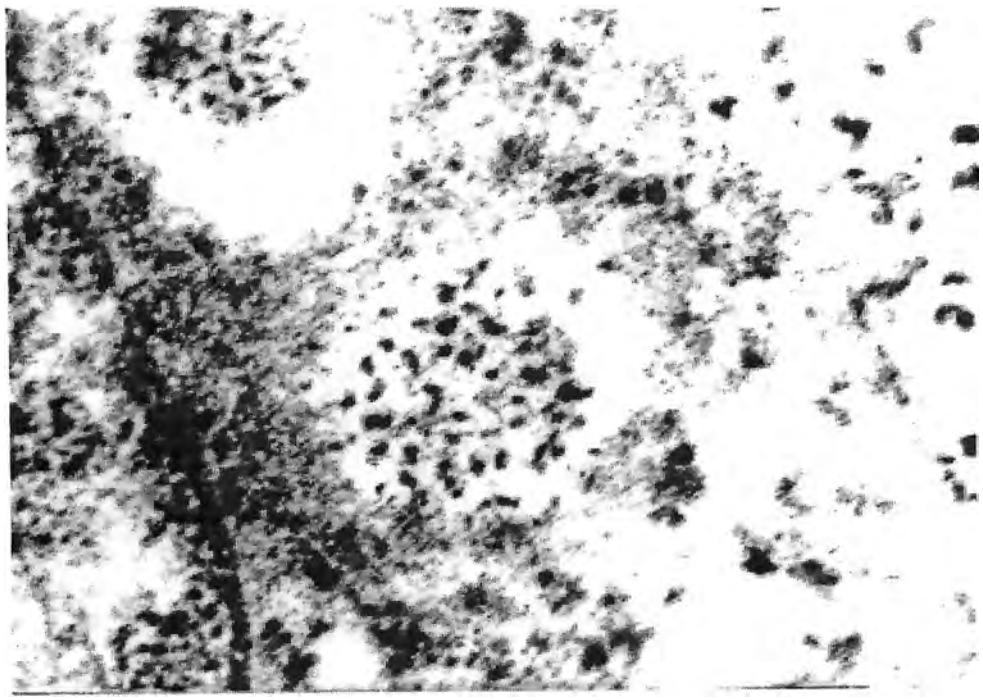

Fig. 2. In thise case a bigger clustering of the proteoglycan complexes was also typical (× 23 000)

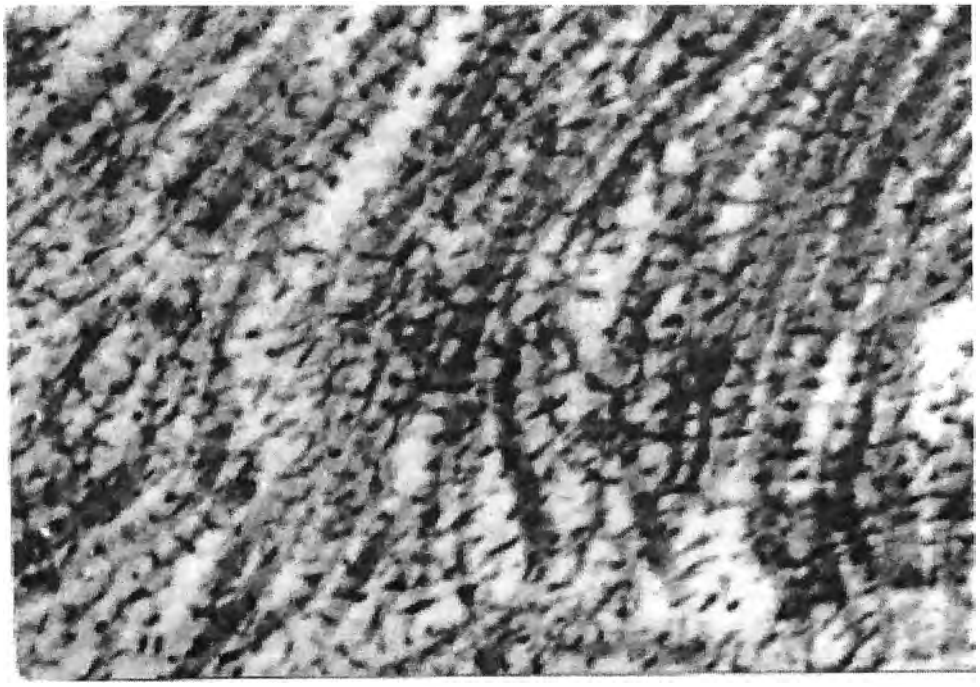

Fig. 3. Staining for collagen and proteoglycans shows a fine network in which the proteoglycans serve as bridge structures between the collagen fibers, keeping them in a certain distance from one another (× 48000)

Discussion

The results from the comparative analysis show that there are similarities in the fine changes in the matrix of the articular cartilage in sharp temperature changes and overloading of the articular apparatus. They are mainly expressed in the processes of increased anaerobe glycolisis in the transitional zone cartilage-bone called tide mark [9]. Morphologically that is visualized by glycogen deposition in the chondroblasts and increase of the proteoglycan synthesis [4]. At the same time we established that the produced proteoglycans are composed of bigger globular subunits and tend to merge with one another. Alterations in the character of the collagenogenesis also take place. It can be assumed that the alterations in the cartilage metabolism lead to the hindered elimination of the waste products by the synovial membrane and to the clinical signs of articular discomfort. With the same mechanism we can explain the changes in the cartilage due to sharp change of the climate and mainly sharp temperature changes.

References

1. D a v i e s, D. et al. Electron microscopy of articular cartilage in the young adult rabbit. — Annals of the Rheumatic Diseases, **21**, 1962, 11-21.

2. Garcia, F., D. Mitrovic. Joint reaction to polyethylene implantation: a method for inducing osteoarthrotic changes and osteophyte formation in the rabbit knee joint. — Annals of Anatomy, **182**, 1998, 145-167.
3. Moskowitz, R. et al. Experimentally induced corticosteroid arthropathy. — Arth. and Rheum, **13**, 1970, 236-244.
4. Papadopoulou, Th. The role of intermediate zone between articular cartilage and synovial membrane during the process of elimination of the components of haemartrosis. — B. J. Ort. Traum., **35**, No 4, 1999,263-268.
5. Shepard, N., N. Mitchell. The localization of proteoglycan by light and electron microscopy using Safranin O. — J. Ultrastruct. Res., **54**, 1976, 451-460.
6. Telhag, H., L. Linberg. A method for inducing osteoarthritic changes in rat,s knees. — Clinical Orthopeadics and Related Research., **86**, 1972, 214-223.
7. Vasilev, V., H. J. Merker, N. Vidinov. Ultrastructural changes in the synovial membrane in experimental induced osteoarthrosis of rabbit knee joint. — Histol.Histopathol., **7**, 1992, 119-127.
8. Vidinov, N. Histochemical and computer analysis of aggrecan complex distribution in the deep layer matrix of the articular cartilage. — Annals of Anatomy, **179**, 1997, 177-200.
9. Vidinov, N., A. Djerov. Ultrasructural changes in the transitional zone between articular cartilage and synovial membrane during the development of experimental osteoarthrosis. — International orthopedics, **26**, 2002, 137-140.

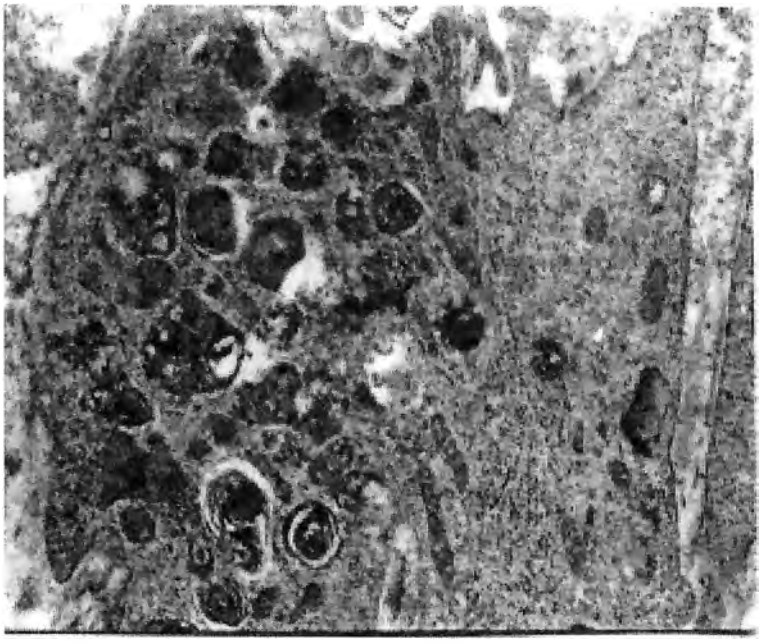

Fig. 4. A synovial cell after five intraarticular injections of hydrocortisone. In the cytoplasm, numerous phagolysosomes with heterogeneous structure are seen (× 18 000)

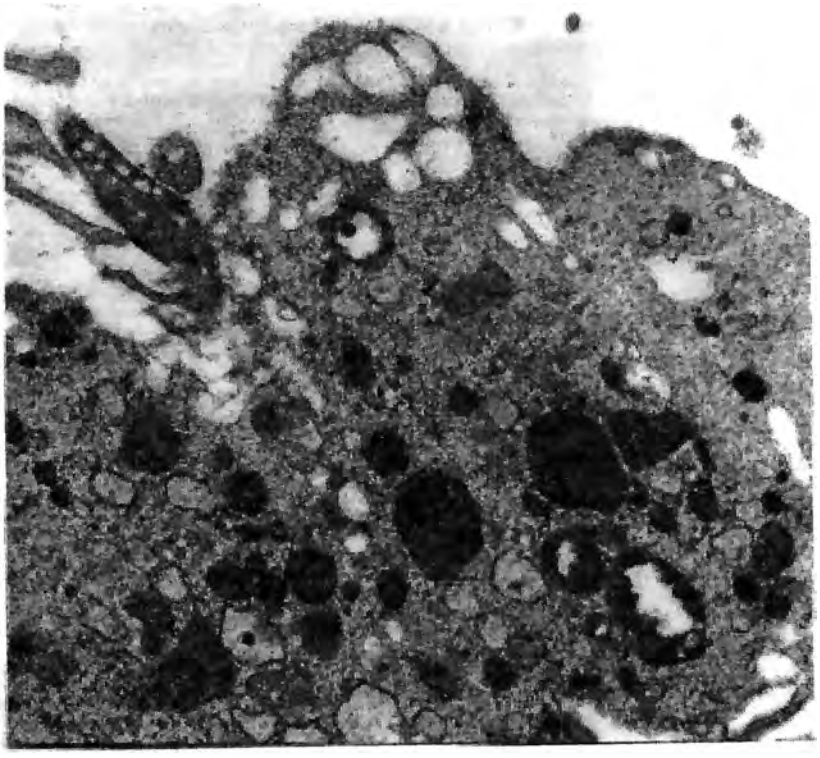

Fig. 5. A synovial macrophage with erythrocyte particles 10 days after experimental hemarthrosis (× 23 000)

mice (mice with amputated forelimbs) were used, in order to mould the influence of the enhanced axial pressure on the lumbar segments [6]. Lumbar backbones of the experimental animals, taken at different stages (up to 12 months) after the amputation were examined light-microscopically. The X-ray controls revealed the presence of changes in the backbone configuration — enhancement of the cervical lordosis and of the thoracic kyphosis, and occurrence of lumbar lordosis. Changes in the intervertebral segment — disorganization of the terminal plates, alterations of the network of chordal cells in the nucleus pulposus, occurrence of blood vessels at the insertion of the collagen lamellas of annulus fibrosus, were also established (Fig. 1). At the later stages of the experiment, partial ruptures of the fibrous annulus and single prolapses of the nucleus pulposus (disc chernias) were observed. The conclusion is that the increased mechanical pressure could be a reason for structural alterations in the intervertebral segment.

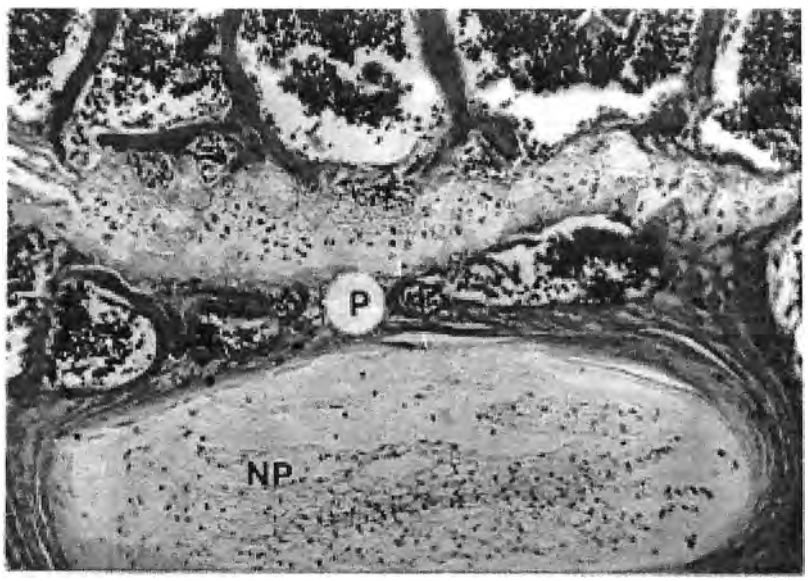

Fig. 1. Intervertebral segment of a bipedal mouse one year after the experiment. Disorganization of the terminal cartilage plate (P) and of the nucleus pulposus (NP) (× 160)

Changes in the ultrastructure of skeletal muscles after tenotomy

Tenotomy (experimental transection of muscle tendons) is a good model of tendon ruptures. The aim of the study was to examine the ultrastructural changes occurring in tenotomized skeletal muscles. Soleus and plantaris muscles of adult Wistar rats with partially or completely transected Achilles tendon were examined with the routine electron microscopic technique. In the experimental muscles, destructive changes were first observed — disorientation, disintegration and loss of myofilaments, fragmentation, streaming and occurrence of rod-like bodies of the Z-lines (Fig. 2), looser structure and, in sites, separation of the basal lamina of muscle fibers from the sarcolemma, and partial destruction of the mitochondrial crists. From the second week after the tendon transection on, morphological signs of regeneration

were available, i.e. an increased number of myosatellite cells rich in organelles, frequent nucleoli in the nuclei, and enhanced amount of ribosomes and polysomes in the sarcoplasm. The results indicate that the destructive process in tenotomized muscles is relatively soon replaced by a process of regeneration [1] and is therefore reversible.

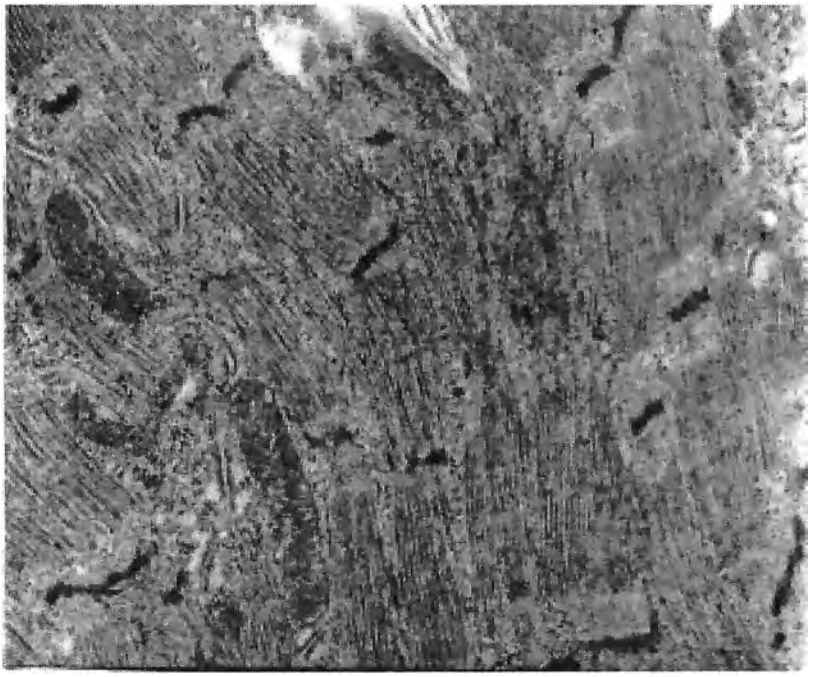

Fig. 2. Muscle fiber one week after tenotomy. Disorganization of the myofilaments, streaming and fragmentation of the Z-lines (× 23 000)

Regeneration of the synovial membrane

Synovioectomy is applied for treatment of many inflammatory and degenerative joint diseases. The aim of the study was to determine as to whether the removed synovial membrane of the joint capsule is replaced by new one. Experimental model were domestic rabbits with aseptic open subtotal synovioectomy of one of the knee joints. The regenerating tissue of the joint capsule was examined light- and electron microscopically at different stages after the experiment. The results revealed lack of boundary cell layer of the capsule during the first week [4]. The fibrosblasts of the fibrous layer of the capsule showed signs of an increased functional activity. At the second week, on the surface of this layer elongated fibroblasts, thin collagen fibers and blood vessels were observed. Gradually, a synovial intima was found to appear, in which, during the third week, the two types of synoviocytes could be identified — synovial fibroblasts (the predominating type) and synovial macrophages (Fig. 3). The conclusion from the experiment is that the synovial membrane does regenerate.

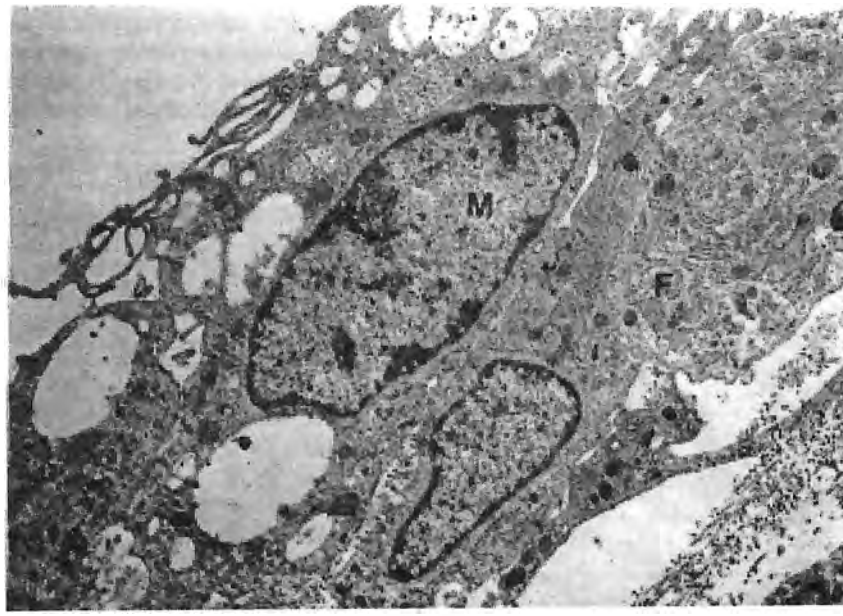

Fig. 3. Regenerated synovial intima six months after synovioectomy. A synovial macrophage (M) with multiple vacuoles, and a synovial fibroblast (F) with prominent endoplasmic reticulum (× 10 000)

Changes in the synovial membrane after intraarticular administration of hydrocortisone

Corticosteroids are widely applied for treatment of the joint diseases. However, data are also available to show that their local application may cause destructions of the joint structures. The aim of the study was to examine the alterations in the synovial membrane after intraarticular administration of high doses of hydrocortisone. The experimental model represented domestic rabbits in one of the knee joints of which different doses of hydrocortisone were injected. The synovial membrane was examined light- and electron microscopically at different stages of the experiment [2]. The results revealed first occurrence of hyperemy in the synovial membrane, with multiplication of the blood vessels. The boundary cell layer was thickened, and predominating in it were the synovial macrophages. Later, in their cytoplasm osmiofillic bodies with variable morphology were found to occur and, after six injections, in many of the synoviocytes giant phagolysosomes were observed (Fig. 4). The conclusion is that high doses of locally administered hydrocortisones could lead to destructive alterations in the synovial membrane, as a result of which the homeostasis of the joint is disturbed and a secondary injury of the joint cartilage occurs.

Changes in the synovial membrane after traumatic hemarthrosis

Hemarthrosis accompanies most of the joint traumas. Subsequently, the blood is eliminated from the joint cavity. The aim of the study was to examine the changes in the synovial membrane during the blood elimination. The experimental model rep-

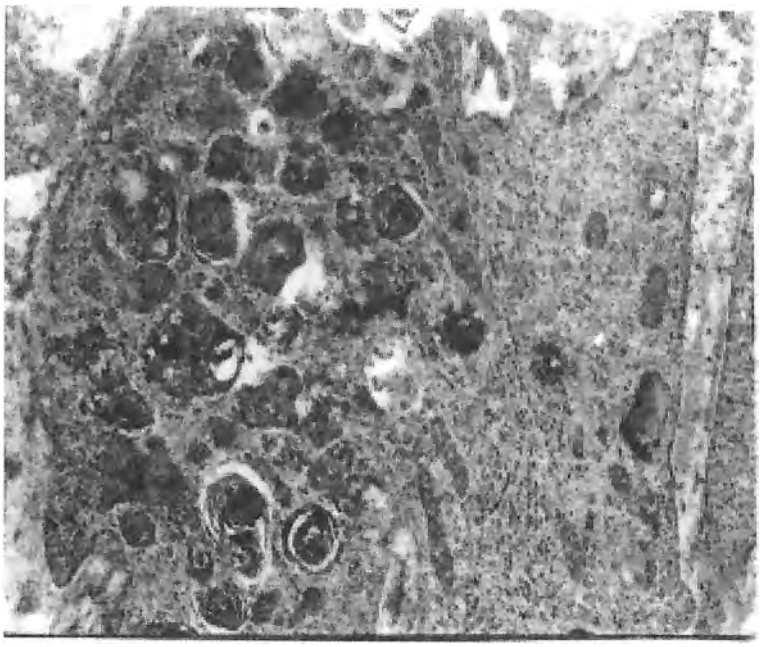

Fig. 4. A synovial cell after five intraarticular injections of hydrocortisone. In the cytoplasm, numerous phagolysosomes with heterogeneous structure are seen (× 18 000)

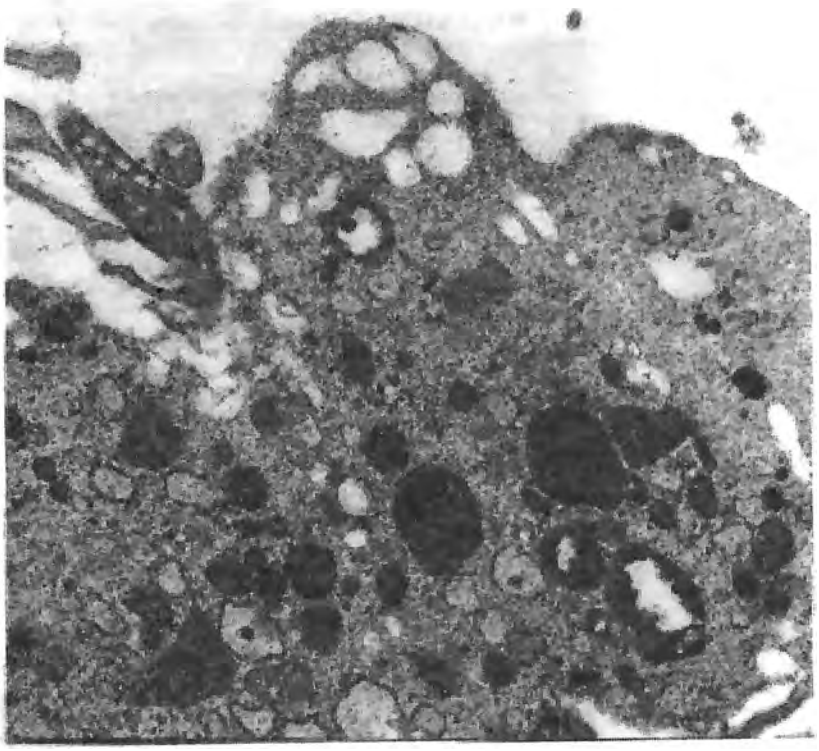

Fig. 5. A synovial macrophage with erythrocyte particles 10 days after experimental hemarthrosis (× 23 000)

resented domestic rabbits with intraarticular fracture of the femoral condyles in one of the knee joints. Synovial membrane from the experimental joints was examined with light and electron microscopy at different terms after the fracture [3]. The destruction of the released erythrocytes was found to start with fragmentation, taking place extracellularly. Together with this the synovial macrophages were activated and, after the third day, observed in them were phagolysosomes containing erythrocyte particles — erythrophagosomes (Fig. 5). The end products of the erythrocyte destruction represented haemosyderin granules packed in syderosomes. The conclusion is that the synovial membrane takes active part in the resorption of free blood from the joint cavity. Erythrocytes are fragmented extracellularly, by the enzymes of the joint fluid, and the brake down of the fragments takes place in the cytoplasm of the synovial macrophages under the influence of the lysosomal enzymes.

The examples quoted above illustrate the importance of the experimental morphological investigations to the clarification of questions from the practical medicine [5]. These examples contain our experience as morphologists and, on the other hand, keep up our self-confidence as physicians. They require, however, a good preparation on the problem investigated. The student knowledge is not sufficient for this purpose. Such preparation could be acquired only by working of the anatomists in the relevant clinic — a practice which did existed in the past and deserves to be stimulated also nowadays.

References

1. Andreev, D., W. Wassilev, K. Chakalsky. Ultrastructural changes in the terminal portion of the striated muscle fibers after tenotomy. — Verh. Anat. Ges. (Suppl. Anat. Anz), **80**, 1980, 483-484.
2. Vasilev, V. A. Changes in the ultrastructure of the synovial membrane under the effect of hydrocortisone. — Acta. Inst. Sup. Med. Sofia, **50**, 1971, 25-30.
3. Vasilev, V. A. Comparative assessment of articular cartilage and synovial membrane in experimental hemarthrosis. — Acta. Biol. Acad. Sci. Hung., **35**, 1984, 305-314.
4. Wassilev, W. A. Über die Ultrastructur der regenerierten Synovialmembran beim Menschen. — Arch. orthop. Unfall-Chir., **69**, 1971, 197-204.
5. Wassilev, W. A. Funktionelle Struktur der Synovialmembran. — Verh. Anat. Ges. (Suppl. Anat. Anz), **75**, 1981, 221-234.
6. Wassilev, W. A., R. Dimova. Der Einfluss der mechanischen Faktoren auf die Struktur der Zwischenwirbelscheiben. — Arch. orthop. Unfall-Chir., **68**, 1970, 273-281.

Institute of Experimental Morphology and Anthropology

Acta morphologica et anthropologica, 10
Sofia • 2005

Distribution and Morphometric Characteristics of Mast Cells in the Kidney of Domestic Swine

*A. Vodenicharov**, *M. Gulubova***, *T. Vlaykova****, *G. Kostadinov**

* *Department of Veterinary Anatomy, Histology and Embryology, Faculty of Veterinary Medicine, Trakia University, Stara Zagora (TUSZ)*
** *Department of General and Clinical Pathology, Faculty of Medicine, TUSZ*
*** *Department of Chemistry and Biochemistry, Faculty of Medicine, TUSZ*

The distribution and morphometric characteristics of mast cells in pig kidney were studied using the histochemical staining with toluidine blue (TB) and alcian blue/safranin (AS). It is found that the mast cells are located in all part of the kidney, and their number per mm^2 in the cortex is significantly smaller than that in the medulla of the kidney independently of the methods of staining ($p<0.0001$, ANOVA test). However, the mast cells in the medulla have significantly smaller length compared to the cells in the cortex, independently of staining procedure ($p=0.005$, ANOVA test), whereas the width are commensurable. In addition, the comparative analyses show that the staining with AS detects significantly more mast cells than that with TB ($p<0.0001$, Paired t-test), and the values of the length of the mast cells stained with AS are significantly bigger than the values obtained after TB staining ($p<0.0005$ ANOVA test). The values of the width are comparable. The results of our current investigation are in the line of those in similar studies on domestic pig and other animals. On the basis of our findings we discuss the role of the mast cells in the kidney of domestic pig.

Key words: Mast cells, kidney, domestic pig, localization, morphometry.

Introduction

Although the mast cells are extensively studied in human and experimental animals, there is only very limited information about them in domestic animals as the data for mast cells in pigs are extremely scanty. Such data are reported in the studies of some investigators [1, 18] which concern the characteristics of mast cells in intestine mucose of pigs after helminth invasion. X u et. al., [24] observed variable density and distinct difference in number and size of mast cells in some organs of pigs with different age. Earlier we reported data for the presence of mast cells in the media of kidney artery and vein and in its valves [20, 21, 25], as well as in the wall of proximal tubule of kidney in pigs [22].

The presence of mast cells in the kidney of mammals is also very poorly investigated. In the studies on heart and kidney of guinea-pig and man, it was shown that the mast cells have similar localizations in kidney of the both species. They were found in intersticium of the cortex and in the outer medulla, in perivascular connec-

tive tissue of proximal and distal tubules, as well as in vicinity of the Bowman's capsule [9]. According to the authors, the mast cells observed in heart and kidney of the both species showed certain resemblance, however, they were morphologically and histochemically distinct from peritoneal mast cells of rats.

For quantitative measurements of the density of mast cells, it has been ascertained that in addition to the fixative, some influence is exerted by the staining method. The results of quite a number of research groups have shown that the observed cells are more numerous when the Carnoy's liquid is used compared to the fixation with neutral formalin [6, 7, 8, 14, 15, 16, 17]. Moreover, after comparative staining with alcian blue/safranin (AS) and toluidine blue (TB), the number of mast cells labelled with AS was higher [2, 10, 12, 24].

The insufficiency of data for the localization, number and morphometrical characteristics of mast cells in kidney of domestic pig motivated us to carry out the current study. The aim of this investigation is to clear up the type and organ specificity of mast cells in domestic swine.

Material and Methods

Tissue materials was obtained from 12 pigs of both genders (6 castrated male, 2 noncastrated male, and 4 castrated female), with age from 8 to 10 months. The pigs were slaughtered in town's abattoir, Stara Zagora. The kidneys were obtained immediately after slaughtering of the animals and small pieces — 5 mm^3 from different areas of the cortex and medulla — were fixed in Carnoy's liquid. Six of the kidneys were preliminary perfused with Carnoy's liquid, after which the tissue samples were fixed with the same fixative. Fixation was performed for 2 to 4 hours depending on the size of the specimens, followed by routine process for paraffin-embedding: rinsing in water, dehydration in grading ethanol chain, clearing in xylene and embedding in paraffin. The 5-7 μm sections were made and were stained either with 0.1% solution of toluidine blue in McIlvane buffer (pH 3) [19] or with a solution of alcian blue/safranin, pH 1.42 [5].

The mast cells were counted in the cortex and medulla of the kidney using the light microscope Zièss with an ocular-micrometer and the results were presented as mast cells/mm^2. Morphometrical measurements of the mast cells (length/width) were carried out only on well outlined cells with nuclei using an ocular-micrometer as well. There were studied 200 fields with 1360 mast cells. 779 of them were stained with alcian blue and 581 with toluidine blue.

The data were statistically analysed using the StatView™ package for Windows, v.4.43 (Abacus Concepts. Berkeley CA, USA). Basic descriptive statistics were used to calculate mean values and the standard deviations (SD). The ANOVA test was utilized to evaluate the significance of differences of data between two independent groups of specimens, whereas Paired *t*-test was applied for analyzing the differences between the data of dependent groups. When $p<0.05$, the differences were considered to be statistically significant.

Results

The light microscopic observations showed that mast cells in examined structures were distributed unequally: the density of mast cells in the medulla of kidney was significantly higher than in cortex independently of staining procedure ($p<0.0001$, ANOVA test) (Fig. 1).

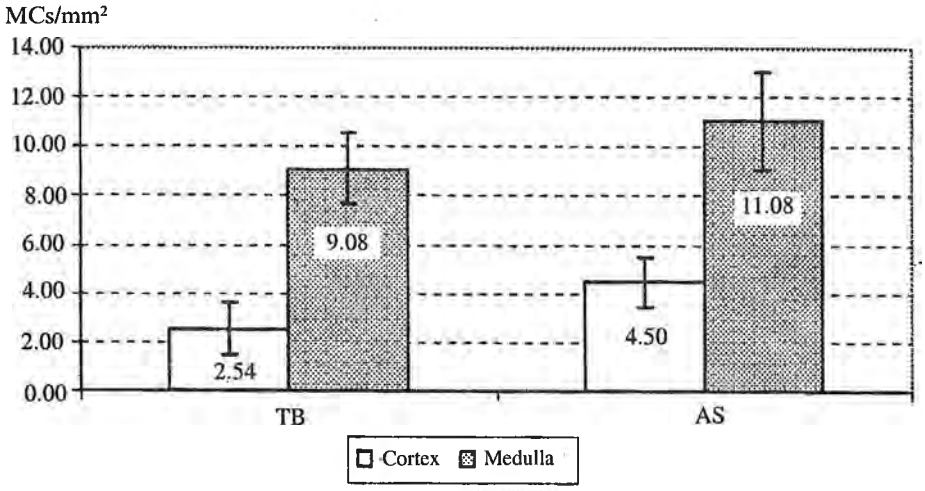

Fig. 1. The density of mast cells in cortex and medulla of pig kidney stained with alcian blue/ safranin (AS) and toluidine blue (TB). The data are presented as mean of MCs/mm² ± SD

The mast cells in cortex stained with the both methods were observed in perivascular connective tissue, between the tubules of nephron and the collective tubules, as well as in vicinity of their basal membrane. Single mast cells were also seen between the epithelial cells of the tubules and inside of the glomerules. The latter localization was detected predominantly in glomerules of the juxtamedullary nephrons (Fig. 2).

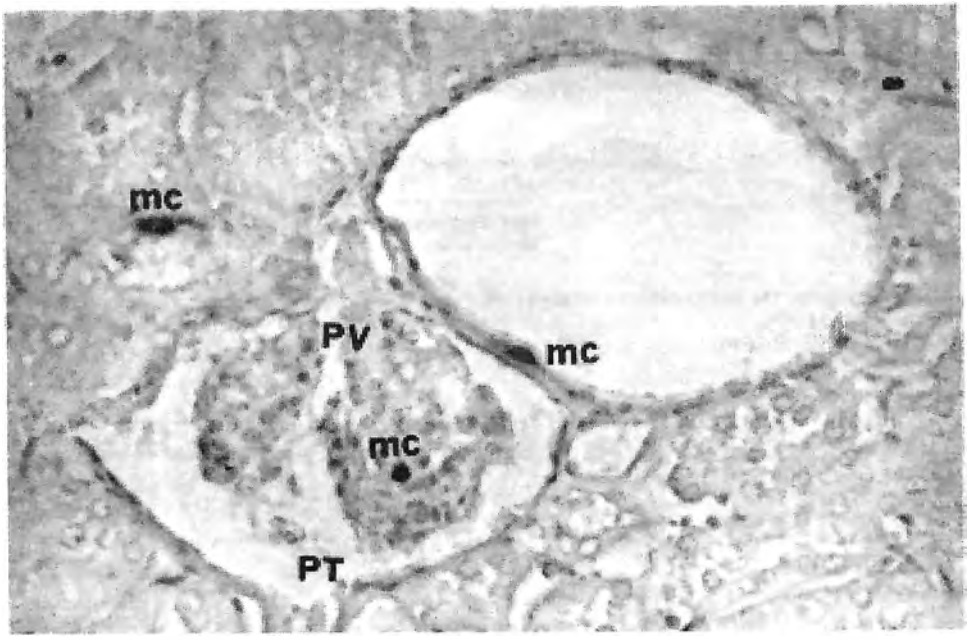

Fig. 2. Mast cells (mc) in the juxtamedullar glomerul, wall of venula and proximal tubule: PV — Polus vascularis and Polus tubularis of the glomerulus. Under PT the beginning part of proximal tubule is seen (× 100)

In the medulla, the mast cells had no predilection localization, although there was also a tendency for an uneven distribution. Mast cells were observed around all structures of kidney medulla. As it was in the cortex, mast cells were found in propinquity to the basal membrane of epithelial cells of the tubules and in close proximity to the wall of straight vessels.

Mast cells seen both in the cortex and in medulla showed positive reaction for biogenic amine when they were stained with AS and well-expressed g-metachromasia when stained with TB. All other cells were orthochromatic. The shape of prevalent part of the observed mast cells was mainly ovoid. Rarely the cells were with cylindrical (cigarette-like) and spindly shape. The latter two types of cells were found predominantly near to the adventitia of blood vessels.

The morphometric analyses showed that the mast cells in the cortex were with significantly bigger length of the sections compared to the cells in the medulla, independently of the staining procedure ($p<0.0001$ for TB staining, and $p=0.005$ for AS staining, ANOVA test) (Fig. 3). However, the width was commensurable, independently on the staining type ($p=0.638$ for TB, and $p=0.727$ for AS, ANOVA test) (Fig. 3).

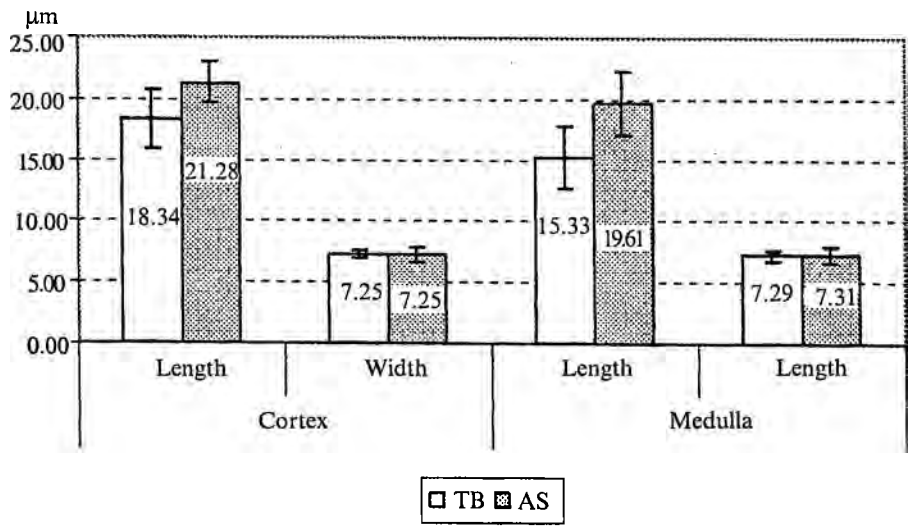

Fig. 3. Results of the morphometric analyses on the length and width of the mast cells sections located in the cortex or in the medulla of the kidney and stained with either alcian blue/safranin (AS) or with toluidine blue (TB). The data are presented as mean values in mm ± SD

The comparative analyses of the both staining procedures showed that the staining with AS detected significantly more mast cells than the other type of procedure, with TB ($p<0.0001$, Paired t-test) (Fig. 1). The mean number of TB-labelled mast cells per mm^2 in the cortex was 2.54 ± 1.073, whereas this was 4.5 ± 1.074 when mast cells were stained with AS ($p<0.0001$, Paired t-test). Analogous results were obtained for the medulla: 9.08 ± 1.426 TB-stained mast cells/mm^2 vs. 11.08 ± 1.978 AS-stained mast cells/mm^2 $p<0.0001$, Paired t-test).

The size of the mast cells (length and width of the sections) also presented higher values after AS staining compared that after TB staining (Fig. 3). In the cortex, the mean of the length of AS-stained mast cells was significantly higher (21.28 ±

1.7 μm) than TB-stained cells (18.0 ± 2.5 μm, $p<0.0001$, ANOVA test). The width of the cells with both days were commensurable (7.25 ± 0.6 μm for AS and 7.25 ± 0.3 μm for TB, $p=0.957$, ANOVA test). Respectively, the mean value of the length of AS-labeled mast cells in the medulla was 19.61 ± 2.6 μm, which was significantly higher in comparison to the mean value of 15.33 ± 2.6 μm corresponding to the length of TB-stained mast cells ($p<0.0001$, ANOVA test). The width of the cells in the medulla stained with the both types of procedure was again comparable (7.31 ± 0.7 μm for AS and и 7.29 ±0.4 μm for TB, $p=0.927$, ANOVA test).

Discussion

The results of the current study showed that the mast cells in kidney of pigs are localized unequally. Analogous unequal distribution was earlier reported in the ureter's wall of domestic pig [23], but the number of mast cells of mm^2 in the present study was less in comparison to that found in the ureter. Moreover, in the porcine kidney it was found out that number of the mast cells stained with AS is higher than that of the cells stained with TB, as the difference was statistically significant. Our data confirmed those reported by other research groups [2, 10, 12, 14, 24], which were focused on the study of other domestic and experimental animals. The difference of staining quality may depend on variable maturity of mast cells, by the influence of tissue surrounding these cells [3], and the presence of different proteoglycans in the mast cells granules [2, 11, 12, 13].

An interesting observation is the difference in the size between the mast cells localized in the cortex and in the medulla. It makes impression that after staining with AS, the length of the cells has statistically higher values than that of cells stained with TB. Differently, the width of the cells with the both types of staining was commeasurable, and no significant differences were obtained. Similar results were reported for cattle mast cells [4] and mast cells in mucosal and submucosal layer in porcine intestine [24]. Recently, we also observed similar differences in the size of mast cells in porcine ureter, where the biggest cell were found in the middle shell [23]. That bigger size of mast cells stained with AS may explain with a large content of biogenic amines and better capacity of Carnoy's liquide to fix mast cell granules and their contents, respectively. In the other part, the size of mast cells may also depend on their function [10].

In conclusion, the presence of mast cells in porcine kidney suggest that they may take an important role in physiological and pathological conditions of that organ. Further immunocytochemical investigation allow more knowledge about detailed function of porcine renal mast cells.

References

1. Ashraf, M., J. Urban, T. Lee. Characterization of isolated porcine intestinal mucosal mast cells following infection with *Ascaria suum*. — Veterinary Parasitology, **29**, 1988, 143-158.
2. Barret, K., F. Pearce. Heterogeneity of mast cells. — In: Histamine and Histamine Antagonist, Vol. 97 (Ed. B. Uvnäs), Berlin, Springer-Verlag, Berlin-Heidelberg, 1991, p. 93-116.
3. Beil, W., M. Schulz, U. Wefelmeyer. Mast cell granule composition and tissue location — a close correlation. — Histology and Histopathology, **15**, 2000, 937-946.
4. Chen, W., M. Alley, B. Mankteлow, P. Slack. Mast cells in bovine lower respiratory tract: morphology, density and distribution. — British Veterinary Journal, **146**, 1990, 425-436.
5. Csaba, G. Alcian blue — Safranin method for mast cells. — In: Theory and Practice of Histological Techniques, (Eds. Y. D. Bancroft, A. Steven), New York Livingstone, 1990, p. 639.

6. Enerbäck, L. Mast cells in rat gastrointestinal mucosa. 1. Effect of fixation. — Acta pathologica et Microbiologica Scandinavica, **66**, 1966a, 289-302.
7. Enerbäck, L. Mast cells in rat gastrointestinal mucosa. 2. Dyebinding and metachromatic propertirs. — Acta pathologica et Microbiologica Scandinavica, **66**, 1966b, 303-312.
8. Frangogiannis, N., A. Burns, L. Michael, M. Entman. Histochemical and morphological characteristics of canine cardiac mast cells. — Histochemistry Journal, **31**, 1999, 221-229.
9. Ghanem, N., E. Assem, K. Leung, F. Pearce. Cardiac and renal mast cells: morphology, distribution, fixation and staining properties in guinea pig and preliminary comparison with human. — Agents and Action, **23**, 1988, 223-226.
10. Harris, W., J. Marshal, S. Yamashiro, N. Shaku. Mast cells in the bovine trachea: Staining characteristics, dispersion techniques and response to secretagogues. — Canadian Journal of Veterinary Research, **63**, 1999, 5-12.
11. Hill, P., R. Martin. A review of mast cell biology. — Veterinary Dermatology, **9**, 1998, 145-166.
12 Hunt, T., A. Campbell, C. Robinson, S. Holgate. Structural and secretory characteristics of bovine lung and skin mast cells: evidence for the existence of heterogeneity. — Clinical and Experimental Allergy, **21**, 1991, 173-182.
13. Jolly, S., J. Detilleux, F. Coignoul, D. Desmecht. Enzyme-histochemical detection of a chymase-like proteinase within bovine mucosal and connective tissue mast cells. — Journal of Comparative Pathology, **122**, 2000, 155-162.
14. Küther, K., L. Audige, P. Kube, M. Welle. Bovine mast cells — distribution, density, heterogeneity, and influence of fixation techniques. — Cell and Tissue Research, **293**, 1998, 111-119.
15. Kube, P., L. Audigé, K. Küther, M. Welle. Distribution, density and heterogeneity of canine mast cells anf influence of fixation techniques. — Histochemistry and Cell Biology, **110**, 2, 1998, 129-135.
16. Marshall, J., G. Ford, E. Bell. Formalin sensivity and differential staining of mast cells in human dermis. — British Journal of Dermatology, **117**, 1987, 29-36.
17. Michaloudi, H., G. Papadopoulus. Mast cells in the sheep, hedgehog and rat forebrain. — Journal of Anatomy, **195**, 1999, 577-586.
18. Pabst, P., B. Beil. Mast cell heterogeneity in the small intestine of normal, gnotobiotic and parasitized pigs. — International Archive Allergology, **88**, 1988, 363-366.
19. Pearce, A. Histochemistry, 2nd ed., London, J. & A. Churchill, Ltd., 1960, p. 692.
20. Vodenicharov, A., P. Cinuchanov. Morphological studies of the valves of the kidney vein in domestic swine. — Anatomia, Histologia, Embryologia, **24**, 1995,a 159-163.
21. Vodenicharov, A., P. Cinuchanov. Microscopic and ultrastructural studies of the renal artery in domestic swine. — Anatomia, Histologia, Embryologia, **24**, 1995b, 237-240.
22. Vodenicharov, A., Ch. Chouchkov. Morphological study of mast cells localization in the wall of the proximal tubule in the domestic swine kidney. — Anatomia, Histologia, Embryologia, **28**, 1999, 85-88.
23. Vodenicharov, A., R. Leiser, M. Gulubova, T. Vlaykova. Morphological and immunocytochemical investigations on mast cells in porcine ureter. — Anatomia, Histologia and Embryologia, 2004, (in press).
24. Xu, L., M. Carr, A. Bland, A. Hall. Histochemistry and morphology of porcine mast cells. — Histochemistry Journal, **25**, 1993, 516-522.
25. Воденичаров, А. Върху структурата на бъбречната вена при домашната свиня. — Ветеринарна медицина, 1, Suppl., 1995, 12-15.

Institute of Experimental Morphology and Anthropology

Acta morphologica et anthropologica, 10
Sofia • 2005

Hormonal Estimation of Serum Levels of Gonadothropic Hormones (FSH and LH) and Testosterone in Infertile Men

*B. Nanova**, *A, Russinova***

* *Department of Anatomy,Histology and Embryology,Medical University of Varna, Bulgarian Academy of Sciences*
** *Institute of Experimental Morphology and Anthropology, Sofia*

Some of the proved reasons for male infertility are the congenital and acquired diseases of male reproductive system. They pass with changes in sperm analysis expressed with different levels of oligoastenozoospermy (II, III dg. or azoospermy) and are accompanied with alterations in hormonal statute-the level of reproductive hormones,which are characteristic for the definite clinical forms of hypogonadism. The aim of the present hormonal study is to differentiate certain types of hypogonadism in patients with fertile disorders. For the goal of the study hormonal esimation of 58 infertile men is carried out and serum levels of FSH, LH and Testosteron are determinated.Results obtained from the study showed 39 patients are with normogonadothropic hypogonadism, 14 — with hypergonadothropic hypogonadism and only 5 — with hypogonadothropic hypogonadism. On the basis of obtained results we can define the reasons for the certain type of hypogonadism and give trends in choice of therapeutical approach.

Key words: FSH, LH, Testosterone male infertility.

Some of the proved reasons for male infertility are congenital and acquired diseases of male reproductive system [6]. They pass with changes in sperm analysis,expressed with different levels of oligoastenozoospermy (II, III dg. or azoospermy) and are accompanied with alterations in hormonal statute-the level of reproductive hormones, which are characteristic for the definite clinical forms of hypogonadism. Hormonal regulation through hypothalamic-pituitary-testis axis is functionally conditioned and coordinated during all periods of sexual development in men — embryonal, fetal and postnatal periods, puberty, fertile age till andropause [1, 4, 5]. That's why hormonal problems in adults are of great importance.They are expressed with fertile disorders or sexual problems such as decreased erection, premature ejaculation or both [8]. Having in mind that infertility in men in 5 to 8 % is hormonally determinated it is necessary paralelly with estimation of spermal indices to carry out basical hormonal profile with estimation of gonadothropic hormones (FSH and LH) and Testosterone as a main androgen in men.

The aim of the present hormonal study is to differentiate certain types of hypogonadism in patients with fertile disorders and after that to point out the reasons for this kind of infertility and to recommend exact therapeutical approach.

Material and Methods

For the goal of the current study hormonal estimation of 58 infertile men is carried out and serum levels of gonadothropic hormones — FSH, LH and Testosteron are determinated. Examinations are carried out in specialized hormonal laboratory. Serum levels of gonadothropic hormones are detected using immunofluorescent methods (MEIA) in "IMX" apparatus-Firm Abbott, USA. Normal values are:
FSH: 1,00-12,00 mlU/ml
LH: 2,00-12,00 mlU/ml

Testosterone: 2,50-10,50*Testosterone is estimated using immunophotometric method on "Serosim" apparatus-Firm Serono, USA.

Results

From 220 examined men (for the whole period of time-2003 year), 160 are with fertile disorders, 60 are fertile [4]. From 160 infertile men, 58 are with deviations in hormonal statute, but 102 are without any alterations in hormonal statute. From 58 infertile men with hormonal disorders the data received from semen analysis showed changes in normal semen indices.

P. Kolarov (1968) and L. J. Rodrigues-Rigau (1983) proposed following classification of hypogonadism:

— Primary testicular insufficiency leading to hypergonadothropic hypogonadism;

— Secondary testicular insufficiency leading to hypogonadpthropic hypogonadism;

— Tubular testicular insufficiency leading to normogonadothropic hypogonadism.

According to this classification from 58 infertile men with hormonal deviations: 39 were with normogonadothropic hypogonadism, 14 — with hypergonadothropic hypogonadism and in 5 patients—hypogonadothropic hypogonadism was observed. In the group with normogonadothropic hypogonadism,consisted of 39 patients, the data received from semen analysis showed in 5 patients—azoospermy, 10 men — with oligoastenozoospermy III dg, in 16—oligoastenozoospermy II dg and 8 men were with low levels of Testosterone. The reasons for infertility are: oligoastenozoospermic syndrome, idiopathic varicocele, inflammatory diseases such as Hlamidia Trahomatis and Gonorrhoea, and noxious professional hormone-replacement therapy.

In the group of patients with hypergonadothropic hypogonadism (n=14) the data received from semen analysis showed in 5 of them azoospermy and in 9 patients-oligoastenozoospermy III dg. Results received from hormonal study showed increasing serum levels of FSH and LH, leading by itself to structural and functional alterations. The most common reasons are cryptorchidism and pseudocryptorchidism, trauma and torsio testis. The therapeutical approach is hormone-stimulating and hormone-replacement therapy and in cases with trauma and torsio testis — surgical interference, as well.

Only in 5 patients hypogonadothropic hypogonadism was observed and in all of them the results from semen analysis showed azoospermy and severe testicular

lesions affected seminiferous tubules expressed with suppressed and arrested spermatogenesis, affected peritubular tissue and process of peritubular fibrosis. All these alterations are based on secondary testicular insufficiency and therapeutical approach is hormone-stimulating and androgen therapy.

Discussion

The first group is consisted by most of the patients. The reason for infertility is the oligoastenozoospermic syndrome on the basis of tubular insufficiency, professional noxious and having inflammatory diseases —orchitis, orchiepididimytis as a reason for *Gonorrhoea, Chlamidia tracomatis* etc [1, 2]. Therapeutical approach is hormonostimulative and hormone-replacement therapy.

Changes in hormonal statute in second group with hypergonadotropic hypogonadism are based on primary testicular insufficiency expressed with structural and functional alterations based on bilateral pseudocryptorchidism, retractile testes and single cases with torsio and trauma testes [9, 10]. Therapeutical approach is surgery or hormonostimulative and hormone-replacement therapy.

In third group the reasons for hormonal changed statute is secondary testicular insufficiency expressed with absence of secondary sex signs, hypothalamic lesions, tubular insufficiency because of estrogenic disbalance, interstitial tubular insufficiency and therapeutical approach is hormonostimulative and androgen therapy [3, 5, 6, 7, 11].

Having in mind received data we can define the reasons for the type of hypogonadism as the trends in choice of therapeutical approach as well.

References

1. Bartke, A. et al. Relationship of the length of exposure to short photoperiod to the effect of prolactin on pituitary and testicular function in golden hamster. — J. Reprod. Fertil., **69**, 1983, 587-95.
2. Eliasson, R. Clinical examination of infertile men. — In: Human Semen and Fertility Regulation in Men. (Ed. E.S.E. Hafez), St. Louis, Mosby, 1976, 321-331.
3. Garcia, Diez, L. et al. Enzyme and hormonal markers in the differential diagnosis of human azoospermia. — Arch. Androl., **28**, 1992, 181-184.
4. Negro-Vilar, A., M. D. Lumkin. Inhibin: central and peripheral effects to regulate follicle-stimulating hormone secretion. — In: Male Reproduction and Fertility (Ed. A. Negro-Vilar), New York, Raven Press, 1983, 159.
5. Rodriguez-Rigau, L. J., K. D. Smith, E. Steinberger. A possible relation between elevated FSH levels and Leydig cell dysfunction in azoospermic and oligospermic men. — J. Androl., **1**, 1980, 127-132.
6. Tzvetkov, D., P. Tzvetkova, L. Kanchev. Congenital anarchism: diagnostic and therapeutic aspects. — Arch. Androl., **2**, 1994, 243-249.
7. Villapando, S., L. Mondragon, C. Baron. Role of testosterone and dihydrotestosterone in spontaneous gynecomastia of adolescents. — Arch. Androl., **28**, 1992, 171-176.
8. Кацаров, М., В. Хаджидеков, М. Тодорова. Метод за диагностика на еректилната импотенция-спонгиография. — Андрология, **3**, 1994, 13—18.
9. Мартинова, Й., Л. Кънчева, Д. Цветков. Ултраструктура на тестис у човек при норма и крипторхизъм. — Хирургия, **1**, 1985, 17—23.
10. Протич, М. et al. Крипторхизъм и фертилитет. — Акуш. и гинекол., **1**, 1982, 62—66.
11. Цветкова,П., Д. Цветков, Л. Кънчев. Хормонални аспекти при първичен идиопатичен хипогонадизъм и инфертилитет. — Андрология, **2**, 1993, 11—17.

Institute of Experimental Morphology and Anthropology

Acta morphologica et anthropologica, 10
Sofia • 2005

Femoral Vein Wall Remodelling in Chronic Arterial Insufficiency of the Lower Limb

*D. Stavrev**, *G. Marinov**, *V. Kniazhev***

* *Department of Anatomy, Histology and Embryology, Medical University, Varna*
** *Clinic of Vascular Surgery, Medical University, Varna*

The remodelled FV wall in CHAILL preserves the basic principles of its structure. From this point of view, it does not yield to the remodelled GSV as a possible autograft.

Key words: femoral vein, lower limb, remodelling.

Introduction

Usage of great saphenous vein (GSV) as an autograft during reconstructive operations of arterial vessels is limited in a considerable number of patients that requires the introduction of alternative autografts [3, 4]. Femoral vein (FV) offer such an opportunity [6, 9]. The objective of the present study is to investigate the remodelling of the wall of FV in patients with chronic arterial insufficiency of the lower limb (CHAILL) with a view to assess the possibilities for its application as an autograft.

Material and Methods

One FV taken intraoperatively from 4 amputated limbs in the Clinic of Vascular Surgery, Medical University of Varna, was fixed in 10% formalin and embedded in paraffin or Histowax. Five μm-thick sections were stained with hematoxylin-eosin (HE), orcein, AZAN and by the methods of Van-Gieson and of Mallory and then examined with OLYMPUS BX-50 microscope. Representative areas from sections filmed using video-camera were quantitatively examined by means of Image Tool 3.00 software (The University of Texas Health Science Center in San Antonio, TX, USA).

Results

No fresh fibrin coatings and thrombotic masses are observed on FV luminal surface. The greater part of tunica intima is covered by endothelial cells. The thicknesses of the tunica intima, tunica media and tunica adventitia vary according to the circumference of FV not only in one and the same patients but also in single patients. The ratio between the thicknesses of the media to that of the intima is variable, too (Fig. 1) as the differences in the thickness of the media are considerably less ex-

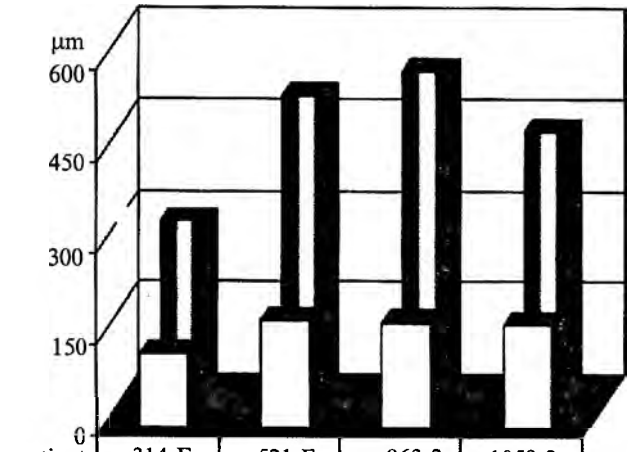

patient	314-Г	521-Б	963-2	1059-2
intima	118.96	174.43	171.73	168.13
media	285.53	492.36	531.83	435

Fig. 1 Average size of the thikness of femoral vein

pressed. The smooth muscle cells (SMC) are longitudinally oriented. Their amount is greater subendothelially and in the proximity of the media. Single and even numerous SMC presenting with differently manifested vacuolization of the cytoplasm are observed at various places, more commonly subendothelially, in the intima which does not involve all the cells (Fig. 2). Elastic structures form a network as at the borderline to the media an internal elastic membrane is created. At certain places a subendothelial membrane-like accumulation of elastic fibres is observed, too. In some areas there is a reduction of the elastic fibres due to the incorporation of an old organized thrombus (Fig. 3). The collagen fibres form a spatial network that is densest close to the media.

SMC in the media build-up circular layers. Vacuolized SMC are absent. Between SMC bundles, single or grouped thick elastic fibers and bundles of collagen fibers are located. Vasa vasorum are of relatively small size and reach up to the middle part of the media. In one case there is a scanty inflammatory cell infiltration in the media located to the adventitia.

SMC in the adventitia form longitudinal bundles of different thickness. Single or small groups of SMC amounting only up to 20-30% of their total number are vacuolized (Fig. 4). The bundles of elastic and collagen fibres are of different thickness and direction.

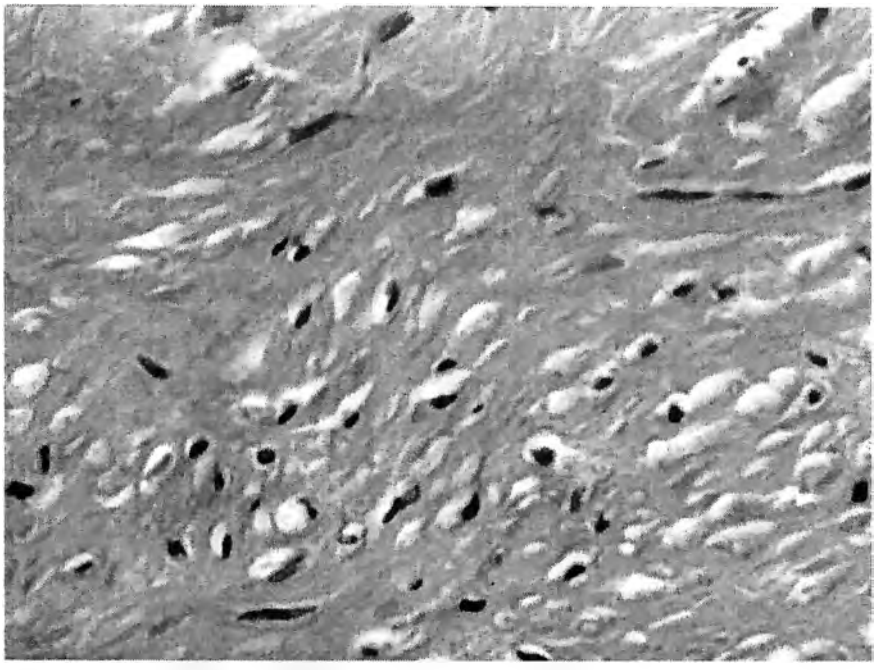

Fig. 2. FV. HE stain. Microphotograh (40×20)

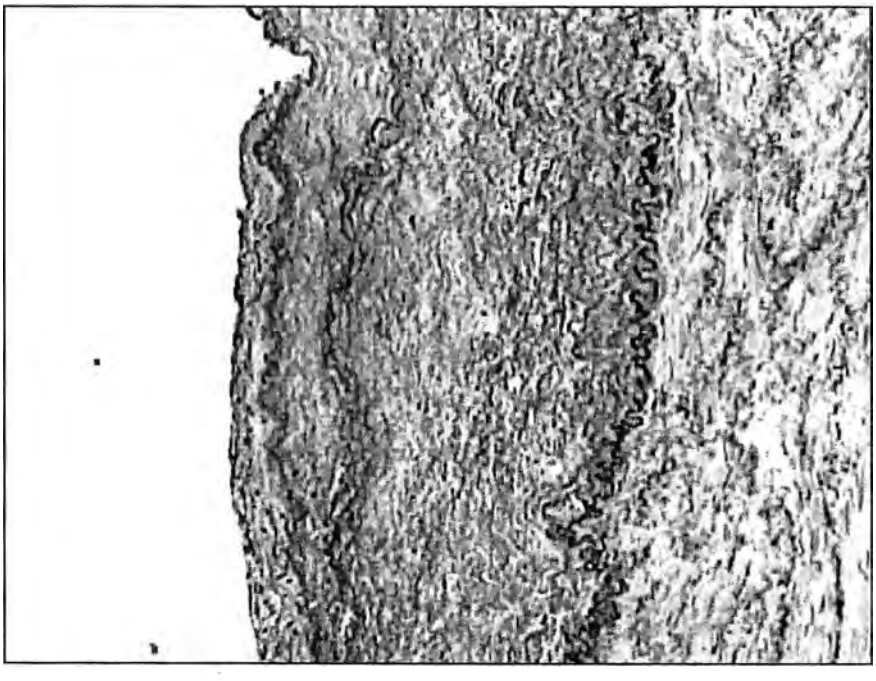

Fig. 3. FV. Orcein stain. Microphotograph (20×10)

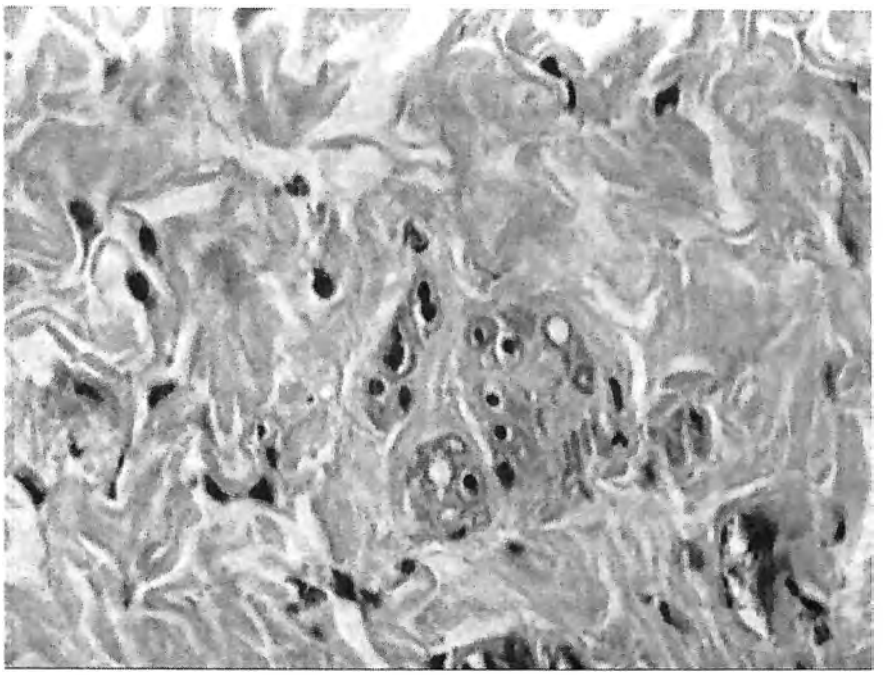

Fig. 4. FV. HE stain. Microphotograh (40×20)

Discussion

This first systemic investigation of FV wall remodelling in CHAILL presents important data about the assessment of the risk when using this vein as an autograft. During the development of CHAILL, FV wall undergoes a remodelling: changes occur in the thicknesses of the intima and media, in the ratio between them and in the arrangement of the elastic and collagen fibres. There is a reduction of the diameter of the vasa vasorum in the media and of the elastic fibres in some areas of the intima. SMC with differently manifested vacuolization of the cytoplasm are observed in the intima and adventitia as well. As the intracellular hypercytolipidemia compromises the cytoarchitecture of the cellular compartments [1] the lipid accumulation in the venous wall requires further research to clarify its significance for venous grafts' survival [2, 5, 7, 8]. Basic characteristics of the good venous autograft have been shown in our previous work [10]. The remodelled FV preserves a lot of these characteristics. Its diameter is sufficient and its lumen is free and partially well-endothelized. The intima, media and adventitia are sufficiently well-developed to maintain FV primary mechanical properties. The elastic skeleton is very well preserved and, probably, keeps FV elastic properties to a great extent. The collagen skeleton is well preserved, too, and likely ensures the necessary strength of the wall during its maximal stretching.

Conclusion

The remodelled FV wall in CHAILL preserves the basic principles of its structure. From this point of view, it does not yield to the remodelled GSV as a possible autograft. Taking into consideration the risk, the problem with the abundant SMC vacuolization in the intima and, to a lesser extent, in the adventitia of both veins remains insufficiently clarified yet. From a hemodynamic viewpoint, however, FV leading away from the venous circulation results in more significant circulatory disturbances than GSV one.

References

1. Garris, D. R., B. L. Garris. Genomic modulation of diabetes *(db/db)* and obese *(ob/ob)* mutation-induced hypercytolipidemia: cytochemical basis of female reproductive tract involution. — Cell Tiss. Res., **316**, 2004, 233-241.
2. Marinov, G. R. Lipid droplets in the myocytes of the venous vessel wall in arterial occlusive lower limb disease. — Anat. Anz. (Verh. Anat. Ges.), **80**, 1986, (Suppl.), 605-606.
3. Merrell, G. A., R. J. Gusberg. Infrainguinal bypass conduit: Autogenous or synthetic - A national perspective. — Vasc. Endovasc. Surg., **36**, 2002, 247-262.
4. Nasr, M. K. et al. Infrainguinal bypass graft patency and limb salvage rates in critical limb ischemia: Influence of the mode of presentation. — Ann. Vasc. Surg., **17**, 2003 Mar. 192-197.
5. Petruzzo, P. et al. Lipid metabolism and molecular changes in normal and atherosclerotic vessels. — Eur. J. Vasc. Endovasc. Surg., **22**, 2001, 31-36.
6. Schulman, M. L., L. G. Schulman, A. M. Lledo-Perez. Unusual Autogenous Vein Grafts. — Vasc. Surg., **26**, 1992, 257-264.
7. Shi, Y. et al. Oxidative stress and lipid retention in vascular grafts: Comparison between venous and arterial conduits. — Circulation, **10**, 2001, 2408-2413.
8. Renò, F. et al. Fourier Transform Infrared Spectroscopy Application to Vascular Biology: Comparative Analysis of Human Internal Mammary Artery and Saphenous Vein Wall. — Cell Tiss. Org., **175**, 2003, 186-191.
9. Yukizane, T. et al. Isotopic study of the effects of platelets on development of intimal thickening in autologous vein grafts in dogs. — Br. J. Surg., **78**, 1991, 297-302.
10. Ставрев, Д., Г. Маринов, В. Княжев. Ремоделиране на стената на Vena Saphena Magna при облитерираща атеросклероза на долния крайник. — Ангиология и съдова хирургия, **IV**, 2003, 30—39.

Institute of Experimental Morphology and Anthropology

Acta morphologica et anthropologica, 10
Sofia•2005

Androgen Receptor in Rat Adrenal Gland after Treatment with Anabolic Androgenic Steroids and Submaximal Training

E. Petrova, Y. Koeva*, P. Atanassova*, S. Delchev*, K.Georgieva**, L. Popova**

* *Department of Anatomy, Histology and Embryology, Medical University, Plovdiv*
** *Deparment of Physiology, Medical University, Plovdiv*

The anabolic androgen steroids (AAS) find wide application in contemporary medicine and in sport. Their influence on the morphology and function of the adrenal gland are target of numerous studies. There is no information on the combined influence of AAS and continuous endurance training on different organs. The purpose of the present study is to follow the influence of AAS and submaximal training on the function of the adrenal gland by immunohistochemical expression of the androgen receptors in the adrenal cells. Male white Wistar rats divided into two groups are used. One of the groups exercised on treadmill with sub maximal loading (65-70%VO_2max) 5 day/wk for 8 weeks and was simultaneously treated with 10mg/kg Nandrolone Decanoate (ND) i.m. The other group did not exercise and were treated with Placebo (Pl) i.m. After eight weeks the animals were decapitated and the adrenal glands were extracted for further study. The androgen receptors were proven immunohistochemically by the avidin-biotin-peroxidase complex (ABC) method was applied using Vectastain® *Elite* ABC kit (Vector, USA). Immunopositive nuclei were observed in the cortex cells of both groups of animals, but without positive reaction in the medulla cells. In the animals of the T+ND group a significant decrease of the intensity of the immunocytochemical reaction was observed. Consequently the simultaneous application of AAS and endurance training apparently results in decreasing of the AR immonohistochemical activity.

Key words: rat adrenal cortex, androgen receptor, anabolic androgenic steroids, submaximal training.

Introduction

The use of androgenic anabolic steroids (AAS) by sportsmen and non-athletes is increasing. The continuous acceptance of high doses AAS combined with physical training results in psychiatric and physiologic changes in the organism. A lot of authors study the effects of AAS on hypothalamic-pituitary-adrenal axis function and more accurately on the morphology and function of the adrenal cortex cells [13]. The changes in the steroidogenesis in the adrenal cortex of rats after a prolonged treatment with AAS are histochemicaly proven in our previous studies [11]. The influence of androgens on growth, differentiation and function of different mamma-

lian tissues is realized by a specific intracellular receptor and modification of gene expression [10]. Androgen receptor (AR) has been identified in the adrenal cortex of immature and adult Rhesus monkeys by immunocytochemistry [9] and in adrenocortical tissue of adult rat by immunoblot assay [1]. Such data has been reported in other steroidproducing cells like the Leydig cells of rat testis [6, 7]. On the other hand, a lot of authors reported functional changes in the adrenal gland, predominantly in the adrenal medulla under different physical exercises and stress conditions [5] but there are less studies on the cortex cells.

Our study is a part of a project for investigation of the influence of AAS on endurance performance in different tissues and organs. The aim of the present work was to investigate the immunohistochemical expression of androgen receptors in rat adrenal cortex after simultaneous treatment with anabolic androgenic steroids and submaximal training.

Material and Methods

Male Wistar rats were distributed into 2 groups. One of them exercised on treadmill with submaximal loading (65-70% VO_2 max) 5 day/wk for 8 weeks. After 2 weeks all of the trained and sedentary rats received weekly either 10 mg/kg — Nandrolone Decanoate (ND) or Placebo (P) i.m. for 6 weeks. Day after the last exercises all the groups: 1. sedentary + Pl (S+P) and 2. trained + ND (T+ND) were decapitated. Adrenal cortex fragments were fixed in Bouin's fluid for 24 hours and embedded in paraffin. For the antigen detection the avidin-biotin-peroxidase complex (ABC) method was applied using Vectastain® *Elite* ABC kit (Vector, USA) using primary polyclonal rabbit anti-androgen receptor antibody (Alpha Diagnostics; 1:100). The peroxidase activity was then developed by means of the Peroxidase Substrate kit (DAB), (Vector, USA). *As controls*, sections were used in which the primary or secondary antibodies were replaced by phosphate-buffered saline (PBS) or only the peroxidase activity was visualized.

Results

Our results demonstrated that there was positive immnohistochemical expression of AR in the rat adrenal gland of both examined groups. In the animals of the S+P group immunocytochemistry revealed that the staining for AR was located in the cell nuclei. AR reaction was more prominent in the cells of zona fasciculata and zona reticularis compared with the zona glomerulosa. No positive signals were detected in the medulla cells (Fig.1). In the animals of the T+ND group a significant decrease of the intensity of the immunocytochemical reaction was observed with the same nuclear localization of AR. The staining was again lower in the cells of the zona glomerulosa than both other zones of adrenal cortex (Fig. 2).

Discussion

AR is a member of the steroid-thyroid hormone-retinoic acid family of transcription regulatory factors [14]. Understanding the regulation of the expression of these receptors is fundamental for elucidating the mechanism of various hormones' action. It is a well-documented fact that AR was also localized in the nuclei of the adrenal cortical cells [4]. It is known that adrenal androgens are secreted by zona

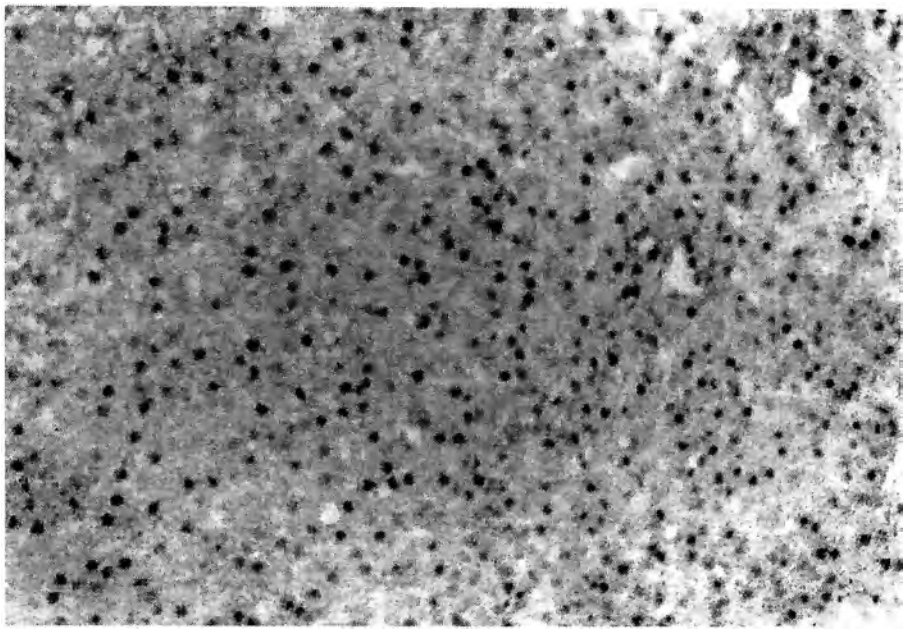

Fig. 1 Immunohistochemical expression of AR in adrenal cortex cells — S+P group (× 100)

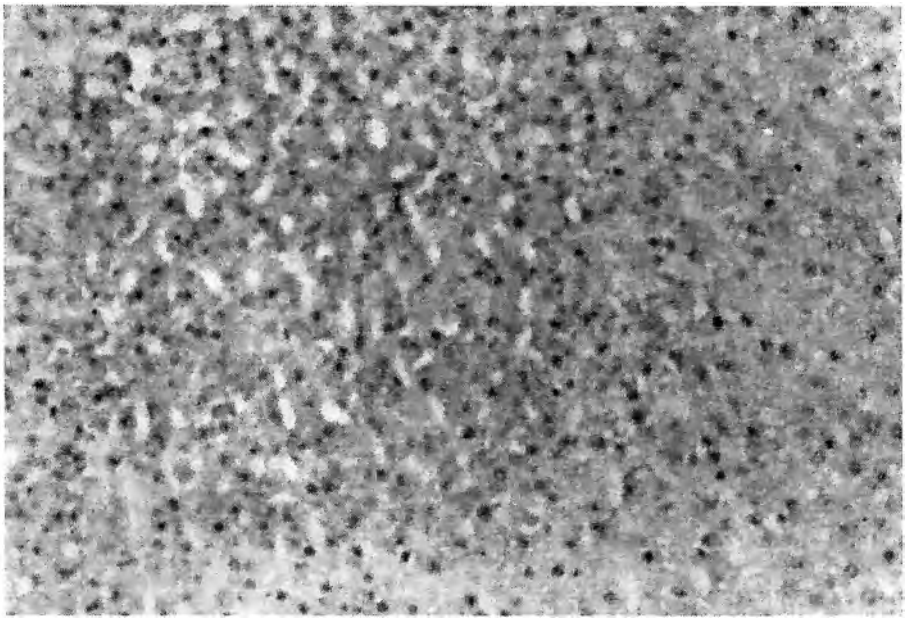

Fig. 2 Immunohistochemical expression of AR in adrenal cortex cells — T+ND group (× 100)

reticularis. The presence of staining of cell nuclei of the three zones suggests that AR may be involved in the autocrine function. The weaker AR expression in the T+ND group of our study suggest that adrenal cortex function is decreased, which is connected to the continuous treatment with ND combined with submaximal training. These facts show that AAS has influence on the functional activity of the adrenal cortex [9]. Long-term administration of AAS leads to adrenal insufficiency [2]. The changes in the functional activity of the adrenal cortex cells under physical exercises are very disputable. They depend on the continuation as well as on the load of the physical training. Changes in the secretion of cortisol and adrenocorticotropin hormone are found out [3]. There are no data about the effect of endurance training on the adrenal cortex morphology as well as the combination of endurance training and AAS. Our previous results showed changes in the immunohistochemical expression of AR in other steroidproducing cells like the rat Leydig cells following AAS administration and endurance training [8].

In conclusion, the combination of both factors — long-term AAS treatment and submaximal training apparently results in decreasing of the AR immonohistochemical activity in adrenal cortex cells. This might be one of the modes of action of AAS and physical training on the functional activity of the rat adrenal cortex.

References

1. Bentvelsen, F. M. et al. Regulation of immunoreactive androgen receptor in the adrenal gland of the adult rat. — Endocrinology., **137**, 1996, 2659-2663.
2. Dowling, P. M., M. A. Williams, T. P. Clark. Adrenal insufficiency associated with long-term anabolic steroid administration in a horse. — J. Am. Vet. Med. Assoc., **204**, 1994, 329-30.
3. Duclos, M. et al. Trained versus untrained men: different immediate post-exercise responses of pituitary adrenal axis. A preliminary study. — Eur. J. Appl. Physiol. Occup. Physiol., **75**, 1997, 343-50.
4. Kimura, N. et al. Immunocytochemical localization of androgen receptor with polyclonal antibody in paraffin-embedded human tissues. — J. Histochem. Cytochem., **41**, 1993, 671-678.
5. Kjaer, M. Adrenal medulla and exercise training. — Eur. J. Appl. Physiol. Occup. Physiol., **77**, 1998, 195-199.
6. Koeva, Y, M. Bakalska, M. Davidoff. Developmental pattern of androgen receptor in Leydig cell repopulation and changes in levels of luteinizing hormone and testosterone following ethane 1, 2- dimethane sulphonate treatment of rats. In: Congress of European Association of Clinical Anatomy, Montpellier (France) 2001, Abstracts; 245.
7. Koeva, Y. Morphofunctional characteristics of regenerating Leydig cells following ethane-dimethanesuphonate (EDS) treatment of rats. — Annals of Anatomy, **184**, 2002, Suppl. 1, 93-94.
8. Koeva ,Y. et al. Androgen receptor expression in rat testis following anabolic androgenic steroids administration and endurance training. — Anatomical Collection, 2003, 47-48.
9. Hirst, J. J., N. B. West, R. M. Brenner, M. J. Novy. Steroid hormone receptors in the adrenal glands of fetal and adult rhesus monkeys. — J. Clin. Endocrinol. Metab., **75**, 1992, 308-314.
10. Mooradian, A. D., J. E. Morley, S. G. Korenman. Biological actions of androgens. — Endocrine Revue, **8**, 1987, 1-28.
11. Petrova-Souvandjieva, E. et al. Histochemical chenges in the adrenal cortex of rats after tretment with anabolic androgenic steroids. — Scripta sientifica medica, **34**, suppl. 1, 2002, 88.
12. Schmidt, K. N., L. E. Gosselin, W. C. Stanley. Endurance exercise training causes adrenal medullary hypertrophy in young and old Fischer 344 rats. — Horm. Metab. Res., **24**, 1992, 511-515.
13. Schlussman, S. D. et al. Effects of the androgenic anabolic steroid, nandrolone decanoate, on adrenocorticotropin hormone, corticosterone and proopiomelanocortin, corticotropin releasing factor (CRF) and CRF receptor1 mRNA levels in the hypothalamus, pituitary and amygdala of the rat. — Neurosci. Lett., **284**, 2000, 190-194.
14. Tsai, M. J., B. W. O'Malley. Molecular mechanisms of steroid/thyroid receptor super family members. — Annu. Rev. Biochem., **63**, 1994, 451-486.

Institute of Experimental Morphology and Anthropology

Acta morphologica et anthropologica, 10
Sofia • 2005

Mammal Histological Tissues According to Recent Knowledge

K. Kovachev, E. Sapundzhiev

Faculty of Veterinary Medicine, University of Forestry, Sofia

The aspiration for a more accurate classification of the diversity of cell communities in the organism is aimed at a better study of their structural and functional specification. It is underlying the attempt for their precise classification as every such effort reflects the level of scientific knowledge of the time in which it has been attempted.

The tissue classification of Leidig (1853) — Kölliker (1863) of 4 main tissues forming the organism — epithelial, connective, muscle and nervous tissues — quite rightly gives rise to dissatisfaction among a number of scientists both in Bulgaria and abroad. Current multiple research micromorphology methods and techniques show a number of discrepancies, incompleteness and groundless claims for the pertinence of certain tissues to some of the basic tissues, as was stated in it. Such tissues are genital tissue, blood tissue, cartilage tissue and bone tissue.

Looking back to Haeckel (1885) but applying contemporary argumentation and rationalization, Krustev [10, 12] substantiates the existence of 7 basic tissues of the organism — epithelial, genital, connective, blood, adminiculo-mechanical, muscle and nervous. Sharing his classification in present study we determine also these forming tissues and their subdivisions.

A classification of the basic tissues is presented in this research. It is also specified all the divisions, subdivisions, varieties and types of tissues where we came across such like.

Mammal tissue diversity is a fact which needs to be reflected in a present classification. It will help to improve the concept of the organ structure and to understand how the interrelations of the tissues in them, as a whole, form the integrity of the body. A well grounded, detailed tissue classification is necessary for pathology and clinic. It will also make the study and teaching of morphology more precise for future human and veterinarian medics.

Key words: mammals, tissue, classification.

The aspiration for a more accurate classification of the diversity of cell communities in the organism is aimed at a better study of their structural and functional characteristics and is underlying the attempts for their precise classification as every such effort reflects the level of achievement of scientific knowledge of the time it has been attempted. Retrospection on this matter confirms that.

After anatomist Bichat (1801 — who gives 28 basic tissues) and Mayer (1819 — respectively 19), the morphologists Leydig [3] and Kölliker [2] reduced them and present arguments for the real existence of 4 basic tissues — epithelial, connective, muscle and nervous. This classification has survived until the present time almost 150 years. During that time research techniques and methods in the field of micro-

morphology developed greatly and this revealed a number of discrepancies, incompletenesses and ill-grounded reasoning of the pertinence of certain tissues to some of the basic tissues.

After Leydig and Kölliker a number of authors grounded classification charts in their efforts to determine the existence of other basic tissues and have indicated them.

Haeckel [1] advanced and defended the existence of 8 basic histological tissues in the organism — embryonic, covering, glandular, adminiculo-mechanicus, filling, blood, muscle, nervous. After him a number of scientists abroad expressed satisfaction from Leydig and Kölliker's classification. These authors [2, 6, 8, 24] did not list the genital tissue, on the one hand, and the blood, cartilage and bone tissues, on the other hand, under the epithelial tissue and respectively to the connective tissue. The accumulated structural and functional data had given sufficient and conclusive grounds for their opinion.

Similar dissatisfaction was shared by Bulgarian morphologists who substantiate the treatment of genital and blood tissues as a basic classified tissues [7, 9, 13, 14, 16, 17, 19, 20, 21, 22, 23, 25, 26].

Krustev [10, 11, 12] advanced extensive and conclusive arguments for the objective existence of 7 basic tissues — epithelial, connective, blood, adminiculo-mechanicus, muscule, nervous, genital. This is reverting to Haeckel but with contemporary arguments and reasons. He pointed out that even with the current achievement and knowledge as to the tissue characteristics we could hardly correct substantially his classification. The only change that can be made is for Haeckel's glandular tissue, which now could be classified as a kind tissue belonging to the epithelial tissue.

We accept the existence of 7 basic tissues as advanced and argued by Krustev. The aim of the current article is an attempt to exemplify the tissues (Table 1) under each basic category in more detail in accordance with accepted Latin terminology as per Nomina histologica [5]. The different kinds of tissues belonging to a basic tissue differentiate from one another having their own specific functional and structural features, at the same time keeping the specific characteristics of the basic tissue.

The genital tissue is presented by characteristic cell communities. These are generations of genital cells with unique qualities, on the one hand, and community of satellite cells which function, as a tropho-metabolic mediator and have protective and supportive function, on the other hand. Their epithelial-like arrangement is by no means grounds for affiliation to epithelial tissue.

Grounds for treating blood tissue as a separate basic tissue have existed quite objectively since Haeckel, Hadzhiolov, Villee, Krustev, what is more they have been enriched over the years.

The cartilage and bone tissue are related to the adminiculo-mechanicus tissue. These are avascular, philogenetically connected with a dominating extracellular matrix and specific cell composition which are natural for each one of them. They both take part in the building of the skeleton, the limbs and the shaping of the body. In some parts of the body where there is mobility the cartilage tissue is present. Both tissues have clear structural and functional specific features.

Tissue variety in the organism is a fact and we need an up-to-date classification to reflect it. This will help to improve the picture of organ structure and it will enable us to understand their integrity in the organism. This classification is necessary and can also come to the aid of pathological and clinical subjects. In addition it will make the teaching and study of morphology science more precise for the future human and veterinarian medics.

Tissue classification **Table 1**

Basic tissue	Kind tissue	Subdivision tissue	Variety tissue	Type tissue
1.	1.1.	1.1.1.	1.1.1.1.	1.1.1.1.1.

1. TEXTUS EPITHELIALIS (EPITHELIUM)
- **1.1. Epithelium superficiale**
  - ***1.1.1. Epithelium simplex***
    - 1.1.1.1. Epithelium simplex squamosum
      - *1.1.1.1.1. Endothelium*
      - *1.1.1.1.2. Mesothelium*
      - *1.1.1.1.3. Epithelium respiratorium*
    - 1.1.1.2. Epithelium simplex cuboideum
    - 1.1.1.3. Epithelium simplex columnare
    - 1.1.1.4. Epithelium pseudostratificatum
  - ***1.1.2. Epithelium stratificatum***
    - 1.1.2.1. Epithelium stratificatum squamosum
      - *1.1.2.1.1. Epithelium stratificatum squamosum noncornificatum*
      - *1.1.2.1.2. Epithelium stratificatum squamosum cornificatum*
    - 1.1.2.2. Epithelium stratificatum cuboideum
    - 1.1.2.3. Epithelium stratificatum columnare
    - 1.1.2.4. Epithelium transitionale (Urothelium)
- **1.2. Epithelium glandulare**
- **1.3. Epithelium sensorium**
- **1.4. Epithelium pigmentosum**

2. TEXTUS CONNECTIVUS
- **2.1. Textus connectivus embryonalis**
  - ***2.1.1. Mesenchyma***
  - ***2.1.2. Textus connectivus mucosus***
- **2.2. Textus connectivus fibrosus**
  - ***2.2.1. Textus connectivus collagenosus laxus***
  - ***2.2.2. Textus connectivus fibrosus compactus***
    - 2.2.2.1. Textus connectivus collagenosus compactus irregularis
    - 2.2.2.2. Textus connectivus collagenosus compactus regularis
    - 2.2.2.3. Textus connectivus compactus elasticus
- **2.3. Textus connectivus reticularis**
- **2.4. Textus adiposus**
  - ***2.4.1. Textus adiposus albus***
  - ***2.4.2. Textus adiposus fuscus***
- **2.5. Textus connectivus pigmentosus**

3. TEXTUS ADMINICULO-MECHANICUS
- **3.1. Textus cartilagineus**
  - ***3.1.1. Textus cartilagineus hyalinus***
  - ***3.1.2. Textus cartilagineus elasticus***
  - ***3.1.3. Textus cartilagineus collagenosus***
- **3.2. Textus osseus**
  - ***3.2.1. Textus osseus reticulofibrosus***
  - ***3.2.2. Textus osseus lamellaris***

4. TEXTUS SANGUINIS

5. TEXTUS MUSCULARIS
- **5.1. Textus muscularis nonstriatus**
- **5.2. Textus muscularis striatus**
  - ***5.2.1. Textus muscularis striatus skeletalis***
  - ***5.2.2. Textus muscularis striatus cardiacus***

6. TEXTUS NERVOSUS

7. TEXTUS GENITALIS
- **7.1. Textus genitalis masculinum**
- **7.2. Textus genitalis femininum**

References

1. Haeckel, E. Ursprung und Entwicklung der Tierischen Gewebe. — Jen. Zschr. Naturwiss. ,1885, **18**, 216-275.
2. Kölliker, A. Handbuch der Gewebelehre des Menschen. Leipzig, 1889.
3. Leydig, H. Lehrbuch der Histologie des Menschen und Tiere. Frankfurt, 1867.
4. Motta, P. Antlante fotografico a colori di anatomia mikroskopica. Milano, Vallardi, 1972.
5. Nomina histologica. International Committee on Veterinary Histological Nomenclature. Gent, 1992.
6. Вилли, К. Биология. М., Мир, 1964, 56.
7. Георгиев, И. Експериментални приноси към реактивността на кръвната тъкан. Дисерт. труд, Пловдив, 1959.
8. Заварзин, А. Основы сравнительной гистологии. Ленинград, Ленингр. унив., 1985.
9. Йорданов, Ж. Експериментални (хистокултурални) изследвания върху диференциацията на ембрионалните гонади при пилето с оглед теорията на половата тъкан и тъканно-органоидното устройство на гонадите. — В: Проблеми на сравнителната и експерименталната морфология и ембриология. С., БАН, 1977, 156—171.
10. Кръстев, Х. Върху учението за тъканите и тъканната класификация от биологично и философско гледище. — Вет. мед. науки, **8**, 1977, 13—17.
11. Кръстев, Х. Върху учението за клетката и тъканите и тяхната ултраструктурна реактивност от биологично и методологично гледище. Дисерт. труд, 1977.
12. Кръстев, Х. Философски проблеми на клетъчната тъканната и теоретичната биология. С., БАН, 1988.
13. Петков, П. Цитология и обща хистология. С., Медиц. и физк., 1974.
14. Петков, П., И. Георгиев, В. Доков. Обща хистология и ембриология. С., Медиц. и физк., 1986.
15. Такева, Ц. и др. Специална хистология, ч. I. С. 1997.
16. Хаджиолов, А. И. Приноси към теоретичната хистология. I. За половата и кръвната тъкан. — Год. СУ, Медиц. фак., **II**, 1931/1932.
17. Хаджиолов, А. И. Кръв и кръвообразуване. С., СУ, 1935.
18. Хаджиолов, А. И. Приноси към теоретичната хистология. II. Историко-теоретично разглеждане на кръвната тъкан. — Год. СУ, Медиц. фак., **XXI**, 1941/1942.
19. Хаджиолов, А. И. Учебник по хистология. Ч. I. С., СУ, 1946.
20. Хаджиолов, А. И. Основи на хематологията. С., СУ, 1950.
21. Хаджиолов, А. И. Приноси към теоретичната хистология. III. Методологично значение на тъканната и органна биология. — Изв. Инст. по морфология, БАН, **V**, 1960.
22. Хаджиолов, А. И. Приноси към теоретичната хистология. IV. Моноцитите и макрофагите от гледището на кръвната тъкан и система. — Изв. Инст. по морфология, БАН, **VI**, 1962.
23. Хаджиолов, А. И. Хистология и ембриология. С., Медицина и физкултура, 1973.
24. Хлопин, Н. Г. Общебиологические и экспериментальные основы гистологии. М., АМН, 1946.
25. Чакъров, Е., Ч. Начев. Атлас (клетка и тъкани). С., Народна просвета, 1984.
26. Чакъров, Е. Тъканна принадлежност, биологична организация и фотокинезиграфска характеристика на сперматозоидите. Дисерт. труд. С., 1985.

Institute of Experimental Morphology and Anthropology

Acta morphologica et anthropologica, 10
Sofia•2005

Apoptosis, Degeneration and Regeneration in Seminiferous Epithelium of Adult Rats after Treatment with EDS

*M. Bakalska**, *N. Atanassova**, *Y. Koeva***, *C. McKinnell****, *B. Nikolov**, *M. Davidoff*****

* *Institute of Experimental Morphology & Anthropology, Bulgarian Academy of Sciences, Sofia, Bulgaria*
** *Department of Anatomy and Histology, Higher Medical Institute, Plovdiv*
*** *MRC, Human Reproductive Sciences Unit, Edinburgh, UK*
**** *Institute of Anatomy, University of Hamburg, Germany*

We aimed to carry out a detailed quantitative analysis of male germ cell apoptosis in seminiferous epithelium in a long period after EDS administration. The apoptosis in adult rat testes was induced by EDS and was assessed by TUNEL method. First signs of seminiferous epithelium regression were manifested by marked increase in number of apoptotic cells on 3rd day after EDS treatment. The maximal value of germ cell apoptosis was established on 7th day post EDS that coincided with lowest T levels. Quantitative patterns of germ cell death after testosterone deprivation reveal in advance the kinetic of germ cell depletion and regeneration in a long period after EDS.

Key words: EDS, apoptosis, spermatogenesis, rat.

Introduction

Apoptosis is considered as a mechanism by which the testicular germ cells are removed during normal and various pathological conditions [3]. Manipulation of spermatogenesis by deprivation of survival factors provides a basis for detailed study on the regulatory mechanisms of germ call death. Male germ cell apoptosis in response of androgen withdrawal due to elimination of Leydig cells (LCs) by ethane dimethanesulfonate (EDS) was studied in detail in a short time-window post EDS when LCs were completely missing from the testis [2, 5, 9]. Kinetics of apoptotic events was not examined in a long period after EDS treatment when new LC population developed in the testis. In this respect we aimed to study kinetics of male germ cell apoptosis in seminiferous epithelium after EDS administration and to extend our previous results on kinetics of germ cell death in the testis [1].

Material and Methods

The apoptosis in adult rat testes was induced by a single, i.p. injection of EDS at a dose of 75 mg/kg body weight. The TUNEL assay for in situ detection of apoptosis [6] and quantitation of apoptotic germ cells [9] were performed on testicular sections on 1, 3, 7 14, 21 and 35 day after EDS.

Results

First signs of seminiferous epithelium regression were manifested by marked increase in frequency of apoptotic germ cells in comparison with control rat testis (Fig. 1). Germ cell apoptosis was accompanied with depletion of elongating spermatids from the seminiuferous tubules first in late and then in early stages of the spermatogenic cycle. The germ cells undergoing apoptosis were mostly pachytene spermatocytes and round spermatids in stages I—VIII. Three day after EDS the germ cell apoptotic index was dramatically increased and 7 days post EDS the parameter was 10-fold higher than control, afterwards decreased but remained still significantly higher compared to control (Fig. 2). The highest values of germ cell apoptosis found by 7 day after EDS corresponded to the lowest plasma level of testosterone (T) (< 0.1 ng/ml in comparison to 2.14 ± 0.39 ng/ml in the control). Elevated germ cell apoptosis decreased after 14 days EDS that coincided with significant rise of T levels on day 14^{th} (0.51 ± 0.25 ng/ml) and 21^{th} (1.27 ± 0.3 ng/ml) even they remained lower than controls.

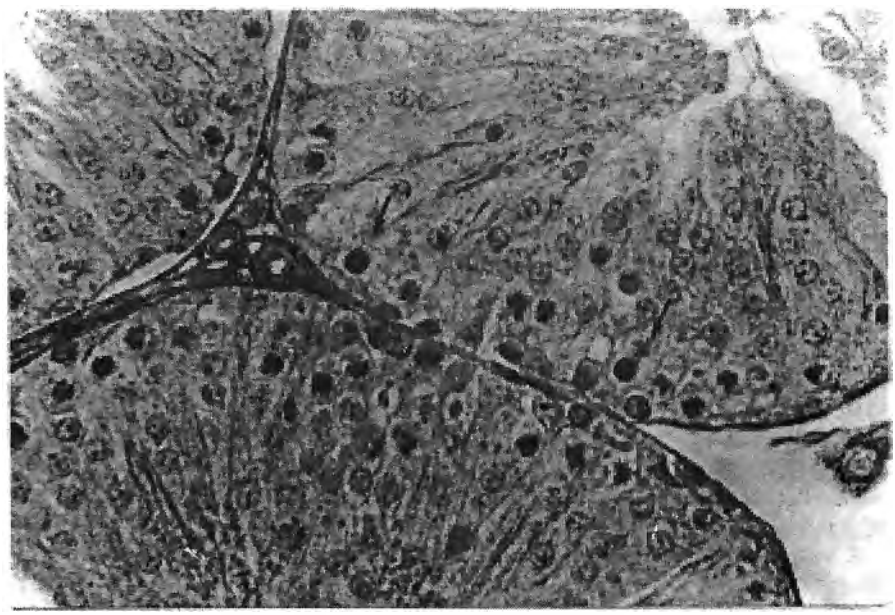

Fig. 1. Testicular cross section of rat at 7^{th} day after EDS administration. Apoptotic germ cells — spermatocytes (arrows) are seen in seminiferous tubules in early stages of the cycle (× 400)

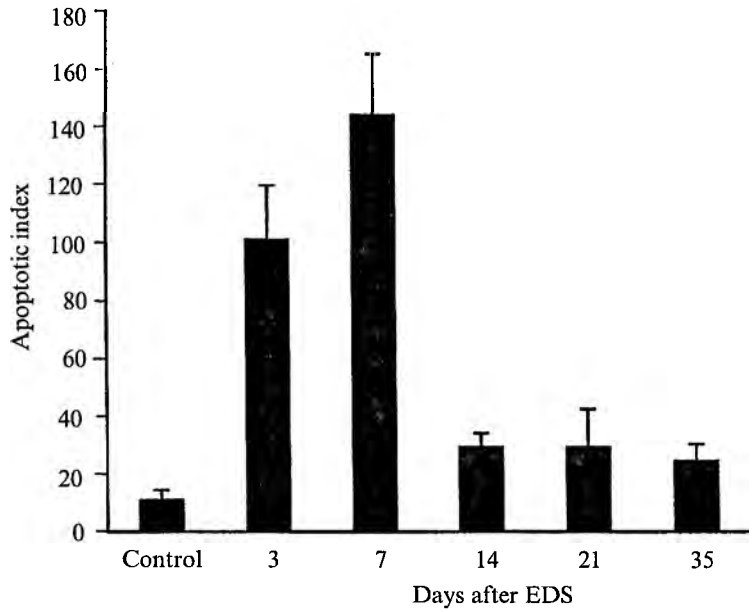

Fig. 2. Temporal changes in apoptotic index following EDS administration. The values of apoptotic index were calculated by multiplying the percentage of tubules containing apoptotic cells by the number of apoptotic germ cells per tubule. Each point represents the mean ± SD (n=4), p<0.001

Discussion

Our observation in the present study showed that germ cell death caused by testosterone withdrawal in adult EDS treated rats is mediated by apoptosis. We have demonstrated by detailed quantitative analysis profound time-dependent increase in germ cell apoptosis in seminiferous epithelium after testosterone deprivation by EDS administration. The highest values of germ cell apoptosis we established by day 7th after EDS coincided with the lowest plasma testosterone levels and complete absence of Leydig cells. The induced germ cell death could be interpreted as an "echo" of preceding Leydig cell apoptosis latter documented by M o r r i s et al. [4]. A growing body of evidence has demonstrated that the withdrawal of androgens in adult rats results in the acceleration of germ cell apoptosis at specific stages of the spermatogenic cycle [2, 7]. Our data showed that predominant germ cell types undergoing apoptosis as a result of androgen ablation include pachytene spermatocytes and round spermatids in early (I—VI) and middle stages (VII—VIII) from the spermatogenic cycle. The preferential cell death was reported to occur in androgen dependent stages VII—VIII after testosterone withdrawal [5]. The similar relationship between germ cell apoptosis and T deprivation was reported in adult rats treated with GnRH-antagonist that were also deficient in androgens [8].

Quantitative analysis of time and cell specificity of germ cell apoptosis in the present study develops our previous data [1] that testosterone withdrawal caused stage-dependent loss of haploid germ cells (spermatids) due to differential sensitiveness of different germ cell populations. The time-dependent changes in germ cell

apoptosis after EDS administration, we found in the present study, precedes the specific total loss of elongating spermatids and disappearance of pachytene spermatocytes from the seminiferous epithelium. In conclusion our results indicate that quantitative pattern of germ cell death after testosterone deprivation reveal in advance the kinetic of germ cell depletion and regeneration in a long period after EDS. These new findings bring additional support to the concept that germ cell apoptosis is a hormonally regulated process.

References

1. Bakalska, M. et al. Degeneration and restoration of spermatogenesis in relation to the changes in Leydig cell population following ethane dimethanesulfonate treatment in adult rats. — Endocrine Regul., **35**, 2001, 211-215.
2. Henriksen, K., H. Hakovirta, M. Parvinen. Testosterone inhibits and induces apoptosis in rat seminiferous tubules in a stage-specific manner: in situ quantification in squash preparations after administration of ethane dimethanesulfonate. — Endocrinology, **136**, 1995, 3285-3291.
3. Henriksen, K., M. Parvinen. Stage-specific apoptosis of male germ cells in the rat: mechanisms of cell death studied by supravital squash preparations. — Tissue & Cell Res., **30**, 1998, 692-701.
4. Moris, A. J., M. F. Taylor, I. D. Moris. Leydig cell apoptosis in response to ethane dimethane sulfonate after both in vivo and in vitro treatment. — J. Androl., **18**, 1997, 274-280.
5. Sharpe, R. M. Regulation of spermatogenesis. — In: The physiology of reproduction. (Eds. E. Knobil & JD Neill). New York, Raven Press, 1994, 1394-1434.
6. Sharpe, R. M. et al. Abnormalities in functional develpoment of the Sertoli cells in rats treated neonatally with diethylstilbestrol: A possible role for estrogens in Sertoli cell development. — Biol. Reprod., **59**, 1998, 1084-1094.
7. Sinha Hikim, A. P. et al. Significance of apoptosis in the temporal and stage-specific loss of germ cells in the adult rat after gonadotropin deprivation. — Biol. Reprod., **57**, 1997 1193-1201.
8. Sinha Hikim, A. P., R. S. Swerdloff. Hormonal and genetic control of germ cell apoptosis in the testis. — Reviews of Reproduction., **4**, 1999, 38-47.
9. Woolveridge, I. et al. Apoptosis in the rat spermatogenic epithelium following androgen withdrawal: Changes in apoptosis-related genes. — Biol. Reprod., **60**, 1999, 461-470.

Institute of Experimental Morphology and Anthropology

Acta morphologica et anthropologica, 10
Sofia•2005

Local Regulation of Granulosa Cell Steroidogenic Function and Apoptosis in Human Ovary

*R. Denkova**, V. Bourneva**, E. Zvetkova**, K. Baleva**, E. Yaneva**, B. Nikolov**, I. Ivanov***, K. Simeonov***, T. Timeva****

* *Institute of Experimental Morphology and Anthropology, Bulgarian Academy of Sciences, Sofia*
** *Institute of Experimental Pathology and Parasitology, Bulgarian Academy of Sciences, Sofia*
*** *Institute of Sterility and Assisted Reproductive Technologies, Sofia*

The present study was undertaken to demonstrate the in vitro effects of Inhibin A on apoptotic cell death and steroidogenesis in ovarian granulosa cells of women with different hormonal status. The immunoexpression of apoptotic marker (M30, caspase-3), pro- and antiapoptotic proteins (Bcl-2, Bc-xl, Bak), proliferation marker (Ki67) and steroid production were investigated. Inhibin A inhibits apoptosis rate in GCs and stimulate estradiol production. The results suggest a potential role of Inhibin in the processes of apoptosis, proliferation and steroidogenesis.

Key words: granulosa cells, inhibin, apoptosis, steroid production.

The processes of follicular growth, differentiation and cell death are hormonally regulated processes, depending on peptide and steroid hormones. Even though ovarian steroid hormones are essential for follicular development, steroidogenic functions and degeneration, it has become increasingly apparent that intraovarian locally produced soluble factors may also play an imporant role in the processes that occur in the ovarian granulosa cells (GCs). Recently we have reported that some intraovarian substances (oxytocin, endothelin, relaxin) in physiological doses affected GC differentiation. To clarify the in vitro effects of the locally produced growth factor Inhibin A (I) on steroidogenesis and apoptotic cell death and its mechanisms in ovarian GCs the production of estradiol (E2) and progesterone (P) and the immunoexpression of early and late apoptosis markers (M30; caspase-3), pro- and anti-apoptotic proteins (Bcl-2, Bcl-xl, Bak) and proliferation marker (Ki-67) were evaluated in GCs of ovaries obtained from women of different hormonal status.

Material and Methods

Granulosa cells were isolated from ovarian antral follicles of [1] women participating in an in vitro fertilization (IVF); [2] young (Y) normally cycling, hormonally nontreated women and [3] premenopausal (PrM) women (without any hormonal therapy for at least one year). GCs were cultured in DMEM (Sigma) in the presence of 10% fetal calf serum (FCS, Sigma) either with or without Inhibin A (Sigma, 10 ng/ml) for 72 hours. The steroid levels were estimated by means of of radioimmunoassay (RIA). The cell monolayers were incubated overnight at 4°C with one of the primary monoclonal antibodies: M30 CellDeath; Caspase 3, Bcl-2, Bcl-xL, Bak, Ki-67. To calculate the percentage of immunopositive cells by light microscopy at 400 × magnification, labelled nuclei/labeled cells were counted in 450 randomly selected granulosa cells from three slides per marker studied and per patient.

Results

Apoptotic cells were found in GC cultures of IVF women as is seen by the detected activity of caspase-3 and M30 in the GC cytoplasm (tabl.1). The apoptotic cells were numerous in GC cultures of Y patients, non hormonally treated and were even more abundant in GCs of PrM women. The majority of the nuclei of IVF patient GCs was staining, indicating expression of the Ki67 (Table 1). Percentages of proliferation rate, seen in GCs of Y patients were weakly expressed and diminished in GCs of PrM women. Bak (pro-apoptotic factor) is slightly immunohistochemically detected in GC cytoplasm of IVF patients, enhanced in GCs of Y patients and is markedly increased in GCs of PrM patients. In contrast pro-oncogene Bcl-2 expression is well represented and similar in both groups of Y patients and relatively lower in PrM women. Bcl-xl is well immunoexpressed in GC cytoplasm of IVF patients, slightly weaker in GCs of young patients and almost 2 fold decreased in GC cultures of PrM women. In ovarian GCs from the three experimental groups inhibin A exposition enhanced the nuclear staining with Ki67 and reduced the activation of caspase-3 enzyme and M30 as compared with controls /without I in the culture medium/ (Table 1). Inhibin treatment slightly increased the immunoexpression of pro-oncogenes Bcl-2 and Bcl-xl in all groups. After I addition in the culture medium scattered ovarian

Table. 1. Percentage of caspase-3, M30, Ki67, Bak, Bcl-2, Bcl-xl immunopositive ovarian granulosa cells from young (Y), in vitro fertilized (IVF) and premenopausal (PrM) women (control and after inhibin treatment). Values are mean ± SE of 11 cultures from 2 experiments

Markers	Control (%)			Inhibin (%)		
	IVF	Y	PrM	IVF	Y	PrM
Caspase-3	6.9	15.8	26.6	5.0	11.1	24.5
M30	5.3	12.0	22.4	3.9	9.7	21.6
Ki67	41.3	34.0	28.2	46.2	41.0	31.3
Bak	8.0	11.0	16.0	3.0	4.0	12.0
Bcl-2	24.0	23.0	16.0	27.0	26.0	15.0
Bcl-xl	26.0	25.0	14.0	28.0	27.0	15.0

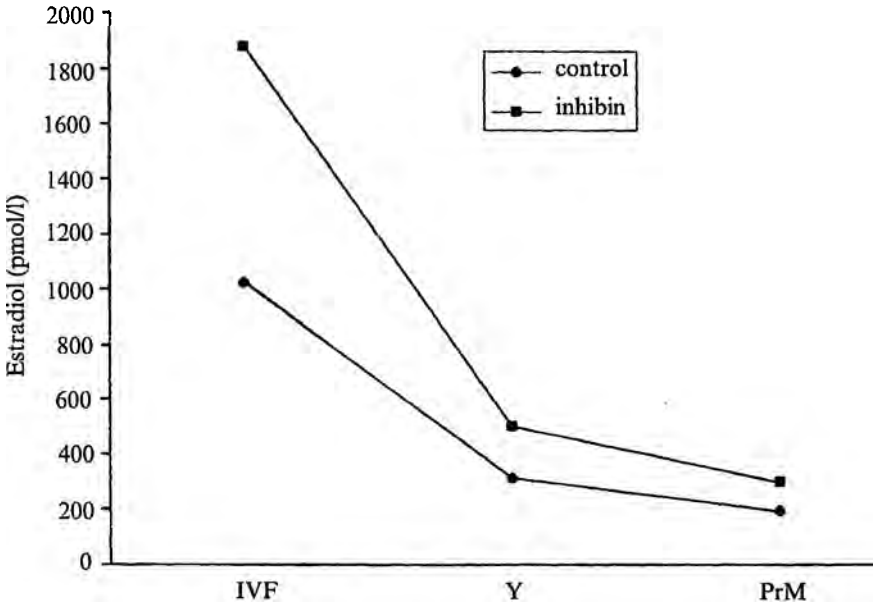

Fig. 1. Inhibin A effect on estradiol production by cultured human ovarian granulosa cells. Values are mean ±SD of 12 cultures from 3 experiments

GCs of Y and IVF patients are with Bak activation, whereas in GCs of PrM patients the expression of apoptosis promoter Bak is better detected. In vitro treatment with inhibin did not change the basal P secretion of GCs from women of the three experimental groups, whereas the E2 production is stimulated especially in GC conditoned media of patients with IVF (Fig. 1).

Discussion

The present data pointed out that the in vitro treatment of GCs from ovaries of women with different hormonal status with inhibin A enhanced estradiol secretion especially in patient with IVF, whereas the progesterone secretion was not affected. Granulosa cell death in "in-vitro" cultures was shown to be apoptotic by the detection of M30 and caspase-3 enzyme activity and by the immunoexpression of pro- and anti-apoptotic proteins respectively. The investigations of several authors [2, 4, 5, 7] have also shown apoptosis in animal and human GCs to be regulated by caspases and Bcl-2 gene family members. The enhancement of GC apoptosis is paralleled by enhanced expression of proapoptotic protein Bak and decreased expression of anti-apoptotic Bcl-2 and Bcl-xl proteins. Estrogen is known to modulate in vitro apoptosis in cultured human GCs [1, 6]. Our results pointed out parallel changes of the stimulated estradiol production after inhibin treatment, supressed apoptosis rate and less pronounced pro-apoptotic proteins. These data are in agreement with the analyses of Campbell and Baird [1] and are contrary to the results of Jimenez et al. [3].

The decrease in the immunoexpression of apoptosis markers and pro-apototic protein (Bak) and the augmentation of Ki76, Bcl-2 and Bcl-xl in GCs from women with different hormonal status after inhibin exposure suggest the involvement of the growth factor I in the processes of proliferation and apoptosis.

References

1. Campbell, B. K, D. T. Baird. Inhibin A is a follicle stimulating hormone-responsive marker of granulosa cell differentiation, which has both autocrine and paracrine actions in sheep. — J. Endocr., **169**, 2001,333-345.
2. Catz, S. D., J. L. Johnson. Bcl-2 in prostate cancer. — Apoptosis, **8**, 2002,29-37.
3. Jimenez-Krassel, F. et al. Evidence for a negative intrafollicular role for inhibin in regulation of estradiol production by granulosa cells. — Endocrinlogy, **144**, 2003,1876-1886.
4. Khan, S. M., L. M. Dauffenbach, J. Yeh. Mitochondria and caspases in induced apoptosis in human luteinizing granulosa cells. — Biochem. Biophys. Res. Commun., **269**, 2000, 542-545.
5. Otala, M., K. Erkkile, T. Tuuri. Cell death and its suppression in human ovarian tissue culture. — Mol. Hum. Reprod., **8**, 2002, 228-236.
6. Song, R., R. J. Santen. Apoptotic action of estrogen. — Apoptosis., **1**, 2000, 55-60.
7. Vaskivuo, T. E. et al. Role of apoptosis, apotosis-related factors and 17 beta-hydroxysteroid dehydrogenases in human corpus luteum regression. — Endocrinology, **194**, 2002,191-200.

Institute of Experimental Morphology and Anthropology

Acta morphologica et anthropologica, 10
Sofia•2005

Ultrasonographic Features of Prostate Gland in the Cat

*R. Dimitrov**, *P. Yonkova**, *P. Georgiev***

* *Department of Veterinary Anatomy, Histology and Embryology, Faculty of Veterinary Medicine, Thracian University, Stara Zagora*
** *Department of Obstetrics, Gynaecology and Andrology, Faculty of Veterinary Medicine, Thracian University, Stara Zagora*

Twelve sexually mature, clinically healthy male European shorthair cats at the age of 1-2 years were studied. Following anaesthesia, the urinary bladders of 10 cats were catheterized and filled with physiological saline. A transabdominal prepubic sonographic approach was used. The study was performed with Aloka SSD 500 Micrus equipment and a 5 MHz linear transducer. The prostate gland was observed in three views. The prepubic ultrasonography with a distended urinary bladder was found to be a good method for visualization of feline prostate in transverse and longitudinal sections up to the transverse plane through the caudal border of the gland. The glandular stroma was visualized as a hyperechoic structure compared to parenchyma and was equally well seen on transverse and longitudinal sonograms. The dorsal median sulcus between both glandular lobes was seen only on transverse sections. The lumen of prostatic urethra was observed as a hypoechoic ventromedial finding on transverse sections whereas the hyperechoic urethral wall was better visualized on longitudinal sections. The considerable difference between the transverse and the craniocaudal sizes (1 cm) evidenced the ovoid shape of the gland.

Key words: prostate, ultrasonography, anatomy, cat.

Introduction

In male cats, the urinary bladder neck passes caudally into a relatively long preprostatic urethra located under the rectum, craniocaudally to the pelvic brim. The prostate is a bilobed symmetrical organ located dorsolaterally to the prostatic urethra, behind the cranial border of the pelvic symphisis. Caudally, the pelvic (membranous) urethra goes up to the bulbourethral glands [7].

According to Barsanti [3], feline prostate is less developed compared to that in dogs and the prostatic urethra is respectively shorter. The gland do not encircle ventrally the urethra in cats as it is observed in dogs.

Souza et al. [9], having done a rectal examination of 32 clinically healthy dogs, reported that there was not a significant correlation between age, prostate location, shape, length and height.

Atalan et al. [1] reported a correlation between the weight and volume of the gland with both body weight and age.

It is well known that ultrasonography is a popular safe, non-invasive method for evaluation and investigation of the prostate gland [2]. In humans, the transrectal ultrasonography permits an excellent visualization of the gland whereas in small animals it is used only for experimental purposes [10].

Ultrasonographically, three views are recommended for estimation of human prostate: sagittal, transverse and dorsal, its position being dependent on urinary bladder distention.

In animals, the gland is examined for dimensions, shape and symmetry, echogenicity and cystic formations. The caudal border could be hidden by ossa pubis [2]. In the dog prior to puberty the prostate encircles the urethra, it is small with scarcely visible lobes and is uniformly hypoechoic [4, 8]. The adult prostate is symmetrically homogenous and echoic. After castration, the gland involutes and its lobes are hardly distinguishable [2].

The data about the ultrasonographic particularities of the prostate gland in cats motivated the present study of its sonographic morphological features, compared to both dogs and humans.

Material and Methods

Twelve sexually mature, clinically healthy male European shorthair cats at the age of 1-2 years were ultrasonographically studied. The animals were anaesthetized with 0.03 mg/kg atropine sulfate s.c.(Atropinum sulfuricum, Sopharma), followed by 2 mg/kg xylazine i.m. (Alfazan) after 15 min and 15 mg/kg ketamine (Alfazan) i.m. after another 15 min [6]. The urinary bladder of 10 cats was catheterized and physiological saline (Natrii chloridum 0.9%, Balkanpharma) was applied. The manipulation was not performed in the other 2 animals. The distended urinary bladder, going along the ventral abdominal wall up to the umbilicus (frequently with a right flexion) was used as acoustic window. The study was performed with Aloka SSD 500 Micrus ultrasonic equipment, a 5 MHz linear transducer and front length of 56 mm. The findings were documented on a Mitsubishi P91E printing device. Prior to the examination, the hair of the observation field was clipped from the transverse umbilical line to the transverse line through pecten ossi pubis and laterally, to plicae lateralis.The gland was visualized by means of a contact gel (Eko-gel, Lessa, Spain). For the transverse visualization of the prostate, the transducer was directed obliquely caudally, having been placed transversely on the ventral abdominal wall paralelly to the pelvic brim. Afterwards, the transducer was moved sagittally and the prostate was longitudinally viewed. Thus, the three prostatic dimensions were determined: width (transverse size), thickness (dorsoventral size) and height (craniocaudal size). The gland was observed in 3 views: transverse, longitudinal and oblique (45° vs the median plane). The sonographic approach was transabdominal, prepubic.

Results and Discussion

Ultrasonographically, the prostate is visualized as a solid homogenous structure with a relatively high echogenecity. The capsula and the stroma were more echoic than the parenchyma. The gland was ovoid and well defined. In its middle part, lin-

ear hyperechoic findings could be seen, differing from the weaker ultrasonic intensity of parenchyma (Fig. 1 and 2). The echographic intensity of the parenchyma in the dog was lower.

The caudal border of the gland was hardly visible because of the adjacent pelvic bones and its position deeply behind the pelvic brim. The normal prostate surrounded the urethra dorsoventrally whereas ventrally, the hypo- or anechoic urethra was seen. The dorsoventral diameter of the gland in the cat was smaller than canine one [3]. It wall also shown that the wall of the urethra was also with higher echogenicity than the urethral lumen, i.e. the periurethral area was hyperechoic and uniform (Fig. 3). This feature is similar to those observed in dogs and humans [2, 5].

On the transverse general view, a hyperechoic gland located dorsolaterally to a hypoechoic ventromedial centre (the prostatic urethra) was visualized (Fig. 1).

Ultrasonographically, a transverse ovoid shape of feline prostate was found out because of he average values of the craniocaudal and the transverse sizes of the gland (1.2 and 2.2 cm respectively). The average prostatic circumference was 5.5 cm and the average area — 2.2 cm^2 (Fig. 1).

On the sagittal view (Fig. 2), the echostructure of the glandular lobe was visible through indication of the urethra with a catheter. The echoic features of the parenchyma were not species-specific.

The dorsal median sulcus between both glandular lobes was observed only on the transverse view (Fig. 3), similarly to that in dogs [2] although in cats the sulcus was less deep.

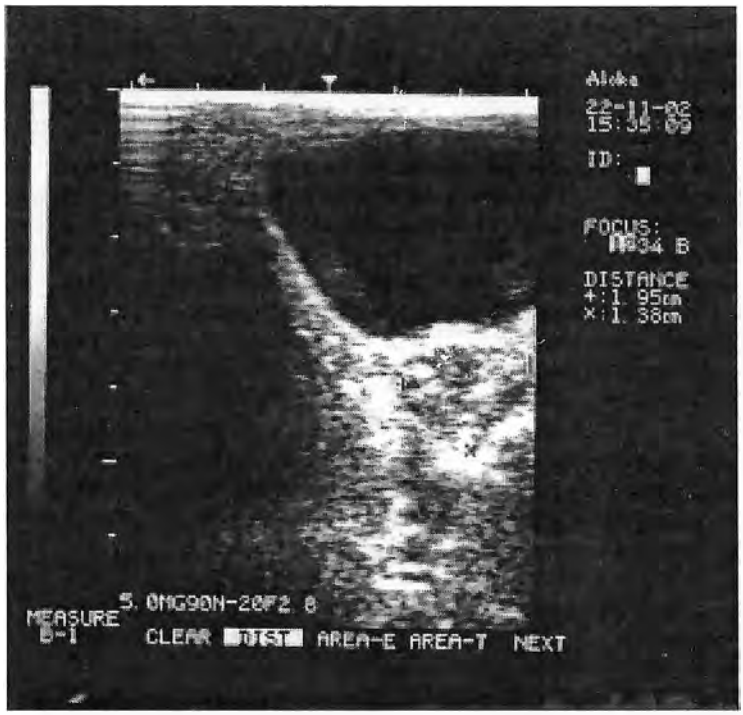

Fig. 1. Ultrasonographic photo of cat prostate — general view

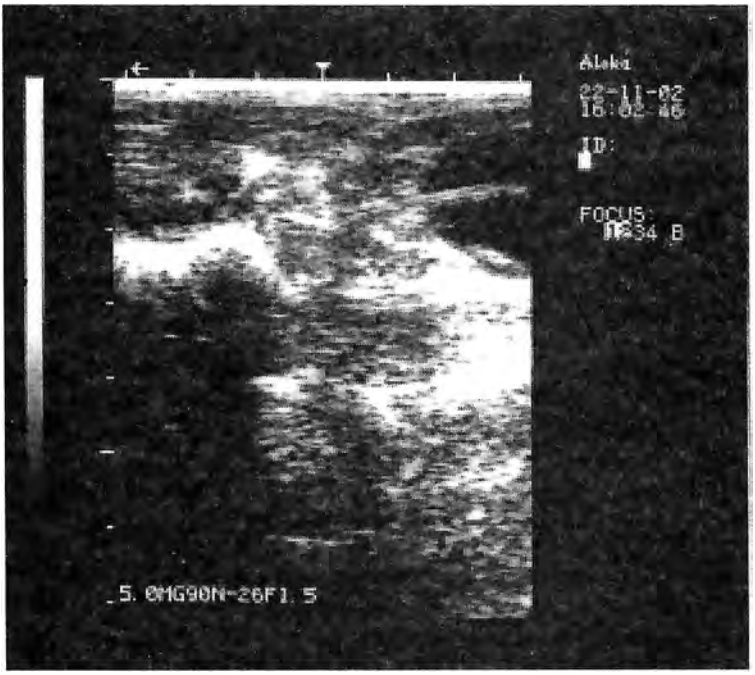

Fig. 2. Ultrasonographic photo of cat prostate — sagittal view

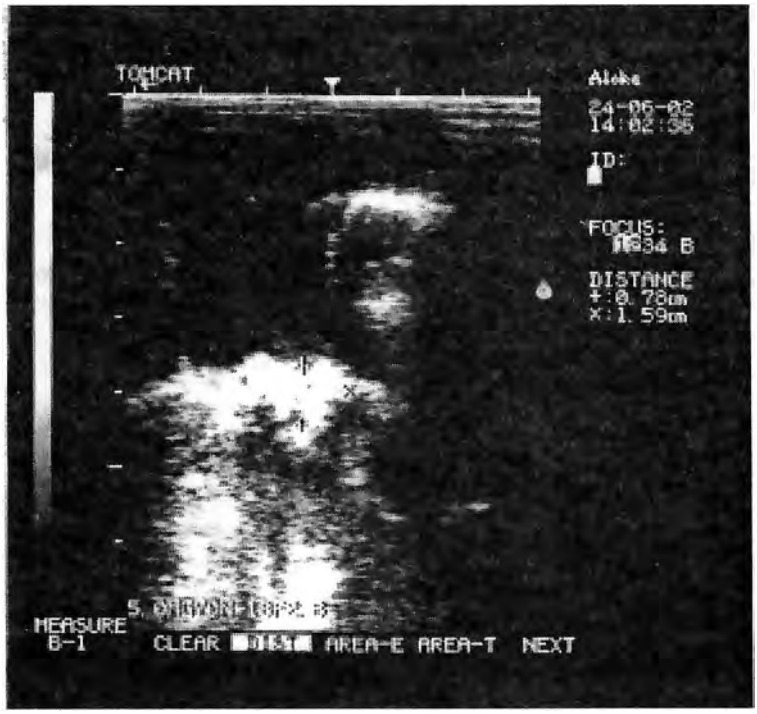

Fig. 3. Ultrasonographic photo of cat prostate — transversal view

Our results allowed to recommend the application of the prepubic ultrasonography over a distended urinary bladder as a good means for visualization of feline prostate in both transverse and longitudinal sections up to the level of the transition between gland and membranous urethra. The caudal border of the gland is distinctly observed via transrectal ultrasonograph, generally in men and dogs [10]. In male cats however, it is hardly applicable. For this approach, the urinary bladder should be empty and it is applied for evaluation of small intraglandular structures. Because of the small rectal lumen in male cats, the cranioventral abdominal position of the distended urinary bladder and the well developed pars externa prostate, we, similarly to Selcer [8] and Basinger [4], assumed that the prepubic transabdominal sonographic approach was sufficient for evaluation of the shape and size of the normal feline prostate.

In the course of our studies we confirmed that the distended urinary bladder was the only acoustic window for observation of the gland [2] and that its stroma is well visualized as a hyperechoic structure vs the parenchyma, uniformly in transverse and longitudinal views.

The lumen of the prostatic urethra was seen as a hypoechoic ventromedian finding on a transverse sonogram whereas the hyperechoic urethral wall was better visualized on longitudinal sonograms in catetherized urinary bladders.

In our opinion, the transversely ovoid shape of the gland could be evidenced via ultrasonography. The significant difference (1 cm) between the transverse and the craniocaudal dimensions is a reliable proof in this connection.

References

1. Atalan, G. et al. Ultrasonographic estimation of prostatic size in canine cadavers. — Res. in Veterinary Science, **67**, 1999, 17-15.
2. Barr, F. Ultrasound diagnostics of diseases in dogs and cats. Akvarium Ltd ed., (translation from the Blackwell Science Ltd edition, 1990), 1997, 76-85.
3. Barsanti, J. Diseases of the Prostate Gland. — In: Canine and feline nephrology and urology. Philadelphia, Williams & Wilkins, 1995, 726-755.
4. Basinger, R. et al. The Prostate. — In: Small Animal Surgery. Philadelphia, WB Saundres, 1997, 2, 1349-1367.
5. Chakarski, V. et al. Atlas of Abdominal Ultrasonography. Sofia, 1996, 207-217.
6. Dinev, D., B. Aminkov. Veterinary anaesthesiology. Stara Zagora, 1999, 117.
7. McClure, R., M. Dallman, Ph. Garrett. The Genital System. — In: Cat Anatomy: an atlas, text and dissection guide. Philadelphia, Lea & Febiger, 1973, 158-162.
8. Selcer, B. The Reproductive System. — In: Practical Veterinary Ultrasound. Philadelphia, Williams & Wilkins, 1995, 252-258.
9. Souza, F., G. Toniollo, L. Trinca. Canine prostatic size evaluation by ultrasonography. — Ars Veterinaria, **18**, 2002, 3, 204-209.
10. Zohil, A., M. Castellano. Prepubic and transrectal ultrasonography of the canine prostate, a comparative study. — Vet. Radiology & Ultrasound, **36**, 1995, 393-396.

Institute of Experimental Morphology and Anthropology

Acta morphologica et anthropologica, 10
Sofia•2005

Fiber Type Distribution in Soleus Muscle of Trained Rats with and without Anabolic Steroid Supplementaion

S. Delchev, K. Georgieva**, P. Atanassova*, Y. Koeva**

* *Department of Anatomy, Histology and Embryology, Medical University, Plovdiv*
** *Department of Physiology, Medical University, Plovdiv*

The aim of the study was to investigate the combined effect of anabolic androgenic steroid (AAS) treatment and endurance training on fiber type distribution in soleus muscle of male rats. Wistar rats were allocated into three groups: one was sedentary and two groups were trained on treadmill for 8 weeks. One of the trained groups received weekly 10 mg.kg^{-1} Nandrolone Decanoate (T+ND), and the sedentary (S) and the other trained group (T) received placebo for the last 6 weeks of the trail. At the end of experiment, on serial cryostat cross sections from soleus muscle, reactions for myofibrillar ATPase activity after alkaline and acid preincubations were carried out. Muscle fiber types were determined as I, IIc, IIa и IId/x. The results didn't show significant difference in relative percentage of the fiber types between groups.

Key words: rat, soleus muscle, submaximal training, Nandrolone Decanoate, fiber type.

Endurance training induces a variety of physiological and morphological adaptations in skeletal muscles and increases aerobic working capacity [5]. Endurance training promotes fast-to-slow shift in fiber type distribution and myosin heavy chains (MHC) expression (4, 8). The extend of the fiber type transition depends on of the muscle type and the duration of the training [3].

Anabolic androgenic steroids (AAS), synthetic derivatives of testosterone, are used by participants in endurance sports but little is known about their effects on endurance performance and fiber type distribution [9]. Data about the effects of AAS treatment on fiber type distribution (MHC expression) in untrained rats are contradictory [1, 6]. To our knowledge only one study investigates these effects on treadmill trained rats, but because of the design of the experiment it is not clear whether the reported changes in m. soleus are due to the combined influences of training and AAS treatment or to the training alone [6]. The interaction between submaximal training and AAS treatment on fiber type distribution in typically red muscle as soleus is not well defined.

The aim of our experiment was to determine the effects of AAS treatment on muscle fiber type distribution in soleus muscle of submaximal trained male rats.

Material and Methods

Male Wistar rats were distributed into 3 groups (n=7). One was sedentary (S) and two groups were trained on treadmill with submaximal loading (about 70-75% VO_{2max}) 5 day.wk^{-1} for 8 weeks. After 2nd week, when the training session reached 40 min.d^{-1}, one of the trained groups received weekly 10 mg.kg^{-1} Nandrolone Decanoate (ND; Retabolil, Gedeon Richter, Hungary) and the other trained group and sedentary rats received placebo (Pl) i.m. for the last 6 weeks of the trial. The experiment was approved by the Ethic Committee at the Medical University of Plovdiv.

All the groups: sedentary + Pl (S); trained + Pl (T) and trained + ND (T+ND) were subjected on running endurance test at the beginning and the end of the experiment. At the end of the trial each animal was decapitated and entire soleus muscles were collected in liquid nitrogen and stored at —70°C until analysis. On serial cryostat cross sections (10 μm) enzymohistochemical reactions for myofibrillar ATPase activity after alkaline (10.55 pH) and acid preincubations (4.5, 4.6, 4.7 pH) were carried out according the technique of S a n t'a n a P e r e i r a et al. [7]. Muscle fibers were classified as type I, IIa, IId/x or IIb on the base of histochemical staining. In addition to the four "pure" fiber types intermediate hybrid fibers (type IIc) were also evident in all groups. Type IIc fibers contain both MHC type I and type IIa [2]. Fiber typing was done using computer image-processing system. The proportion of fiber types was determined from a sample of 200-300 fibers across the entire section of each muscle. Data were expressed as mean ± SEM and were analyzed by one-way ANOVA.

Results and Discussion

Soleus muscle is slow-twitch skeletal muscle and predominantly contains slow type I fibers (about 75-85%). In rat soleus muscle there is a lack of the fastest fiber type IIb (2). Histochemical reactions in rat soleus muscle of the experimental groups are presented in Fig. 1.

Mean fiber type percentage values for soleus muscle are presented in Fig. 2.

Our results about fiber type distribution in the soleus muscle of the control group correspond to those reported by other anthors [2, 3].

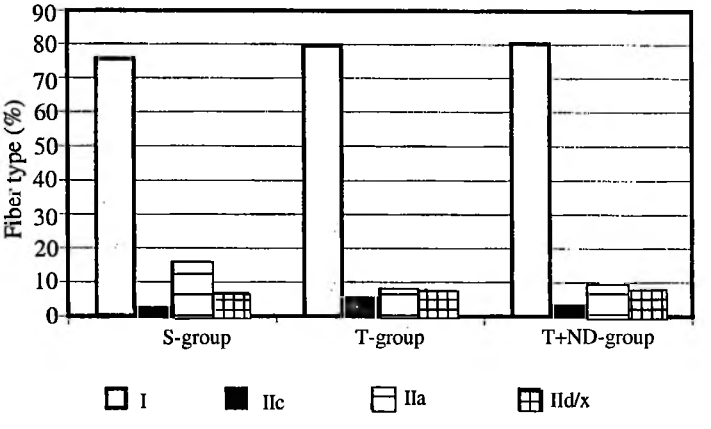

Fig. 2. Fiber type distribution (%) in soleus muscle of the studied groups at the end of the experiment

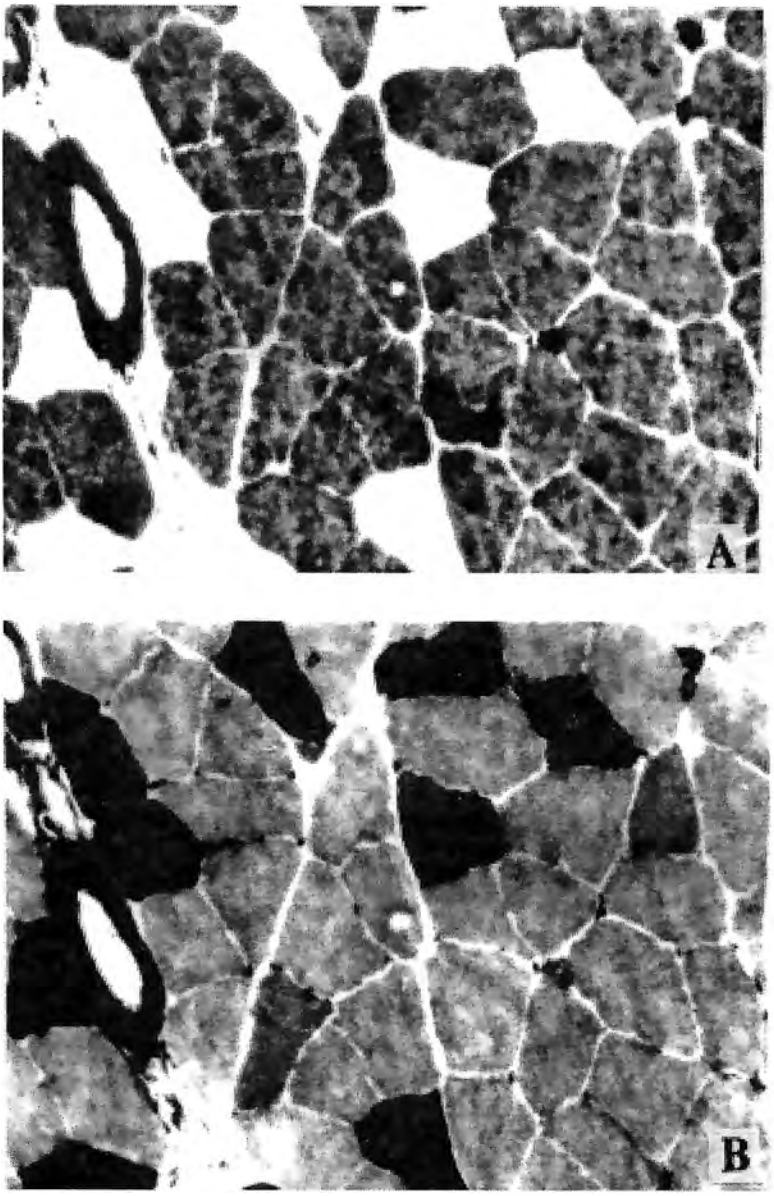

Fig. 1. Myofibrillar ATPase histochemistry of serial cross-sections of rat soleus muscle from group S (**A, B**), from group T (**C, D**) and from group T+ND (**E, F**), after acid preincubation at pH 4.6 (**A, C, E**) and alkaline preincubation at pH 10.55 (**B, D, F**) (× 200)

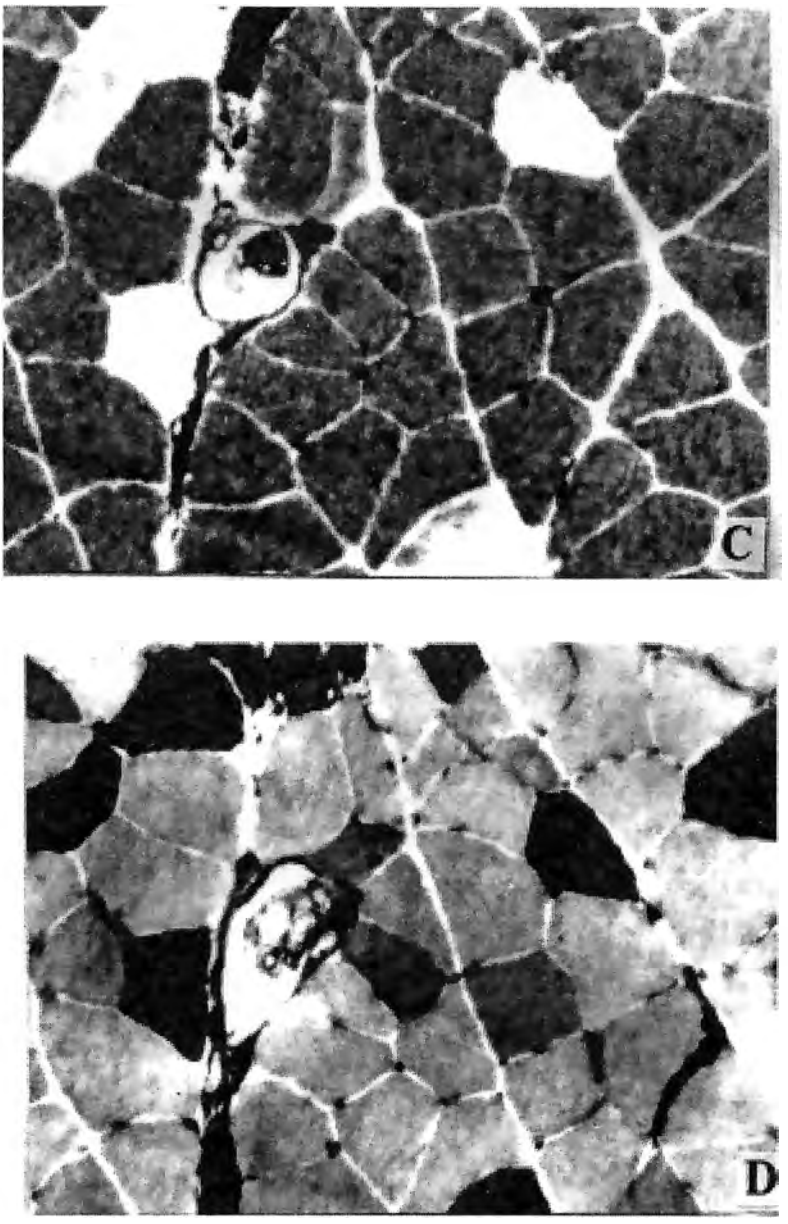

Fig. 1. Myofibrillar ATPase histochemistry of serial cross-sections of rat soleus muscle from group S (**A, B**), from group T (**C, D**) and from group T+ND (**E, F**), after acid preincubation at pH 4.6 (**A, C, E**) and alkaline preincubation at pH 10.55 (**B, D, F**) (× 200)

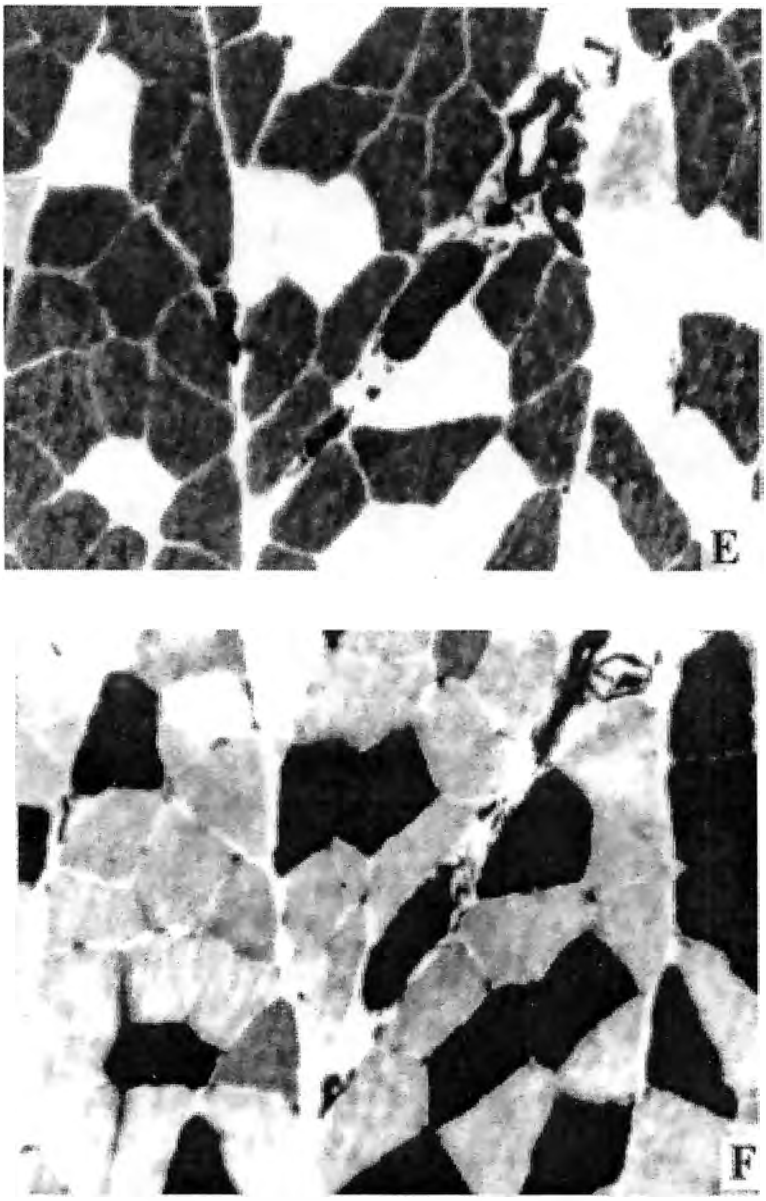

Fig. 1. Myofibrillar ATPase histochemistry of serial cross-sections of rat soleus muscle from group S (**A**, **B**), from group T (**C**, **D**) and from group T+ND (**E**, **F**), after acid preincubation at pH 4.6 (**A**, **C**, **E**) and alkaline preincubation at pH 10.55 (**B**, **D**, **F**) (× 200)

The statistical analysis of the data didn't show significant difference in relative percentage of I, IIc, IIa and IId/x fiber types between the studied groups ($P>0.05$). In both trained groups (with or without Nandrolone Decanoate) there was a tendency endurance training to increase the percentage of I type and to decrease type IIa myofibers in comparison with the control group, but the differences did not reach statistical significance.

The fiber type distribution in the different muscles is predominantly genetically determined. MHC isoforms differ in their ATPase activity — MHC-IIb has highest and MHC-I has lowest one — and this is resulted in the differences of the contracting velocity. It is clear from many experimental studies that fibers are capable to change their phenotype characteristics. Physical activity (training or detraining) and some hormones (thyroid) lead to changes in fiber type distribution. The transformation of the myofiber types has an obligatory pathway in this order: I ⇔ IIc ⇔ IIa ⇔ IId/x ⇔ IIb [3, 8]. In rats endurance training promotes fast-to-slow shift in fast fiber subtypes (IIa, IId/x and IIb) in fast and mixed muscles but have no effect in slow-twitch m. soleus [3, 4, 8].

Our results demonstrate that the combined influence of submaximal training and AAS treatment have no effect on the fiber type distribution in slow-twitch m. soleus compared with sedentary and endurance trained male rats. In contrast with these results, our previous study on mixed gastrocnemius muscle of the same animals showed well-expressed fast-to-slow shift (i.e., from IIb to type IId/x to type IIa) in T+ND compared with the S and T rats [10]. The summarized data of these studies showed that probably the combine effect of submaximal training and AAS treatment on fiber type distribution depends on the type of the muscle.

References

1. Bricout, V. A. et al. Effects of hind limb suspension and androgen treatment on testosterone receptors in rat skeletal muscles. — Eur. J. Appl. Physiol., 1999, 79, 443-448.
2. Delp, M. D., C. Duan. Composition and size of type I, IIA, IID/X, and IIB fibers and citrate synthase activity of rat muscle. — J. Appl. Physiol., 1996, 80, 261-270.
3. Demirel, H. A. et al. Exercise induced alterations in skeletal muscle myosin heavy chain phenotype: dose-response relationship. — J. Appl. Physiol., 1999, 86, 1002-1008.
4. Diaz-Herrera, P. et al. Effect of endurance running on cardiac and skeletal muscle in rats. — Histol. Histopathol., 2001, 16, 29-35.
5. Jones, A. M., H. Carter. The effect of endurance training on parameters of aerobic fitness. — Sports Med., 2000, 29, 373-386.
6. Noirez, P., A. Ferry. Effects of anabolic/androgenic steroids on myosin heavy chain expression in hindlimb muscles of male rats. — Eur. J. Appl. Physiol., 2000, 81, 202-208.
7. Sant'ana Pereira, J. A. et al. The mATPase histochemical profile of rat type IIX fibers: correlation with myosin heavy chain immunolabelling. — Histochem. J., 1995, 27, 715-722.
8. Sullivan, V. K. et al. Myosin heavy chain composition in young and old rat skeletal muscle: effects endurance exercise. — J. Appl. Physiol., 1995, 78, 2115-2120.
9. Van Zyl, C. G., T. D. Noakes, M. I. Lambert. Anabolic-androgenic steroid increases running endurance in rats. — Med. Sci. Sports. Exerc., 1995, 27, 1385-1389.
10. Георгиева, К. и др. Кандролон деканоат повишава субмаксималната издръжливост и променя съотношението на мускулните влакна при тренировани плъхове. Спорт & Наука, 2004, 4 (под печат).

Institute of Experimental Morphology and Anthropology

Acta morphologica et anthropologica, 10
Sofia•2005

Prenatal Morphogenesis and Remodelling of the Wall of the Main Arteries of the Leg and Foot

S. Pavlov, G. Marinov

Department of Anatomy, Histology and Embryology, Medical University, Varna

The age-related remodelling of the walls of the main leg and foot arteries during the prenatal ontogenesis is accomplished according to a common plan. In some arterial wall areas there is an anticipating intimal development.

Key words: leg and foot arteries, fetuses, structure, remodelling.

Introduction

The structure of the walls of lower-limb arteries represents an interest because of the variety and severity of their diseases [6]. However, the age-related remodelling of the arterial wall is very difficult to distinguish from pathological alterations of this wall [2, 3, 8, 10]. The objective of the present work is to study the remodelling of the main leg and foot arteries during prenatal ontogenesis.

Material and Methods

The study covers histo-topographical sections of the leg and foot from 20 lower limbs of 135-388-mm-long fetuses and histological sections at the middle of the main leg and foot arteries from 12 lower limbs of mature stillborn fetuses. The sections were stained with hematoxylin-eosin, orcein, Weigert-Mallori and Van Gieson methods. They were examined on Olympus BX 50 microscope and pictures were taken with Ikegami ICD-840P digital camera.

Results

A. tibialis posterior (ATP), a. tibialis anterior (ATA), a. peronea (AP) and *a. dorsalis pedis (ADP)* are built-up according to a common plan. In 130-140-mm-long fetuses the thin intima is composed by endothelium and homogenous internal elastic membrane (IEM). Endothelium looks relatively higher in the nuclear region than in

adult individuals while the cell nuclei are located closer to each other. The thin media is formed by 2-3 loose rows of smooth muscle cells (SMC). Single elastic fibres (EFs) can be observed in the external half of the media. Spindle-shaped fibroblasts, are located in the adventitia.

With fetus' elongation the arterial structure changes, and diameter and the thickness of the wall increase. Short lamellae entering the internal media region break away in single IEM areas in 256-310-mm-long fetuses (Fig. 1). SMC number in the media increases. The media is clearly distinguished from the adventitia because of the changes of SMC appearance such as elongated, light, with corkscrew-like undulated nuclei that are of larger volume than the nuclei in adults (Fig. 2). Some EFs in the outer media layers are grouped into small lamellae. Initial stages of an external longitudinal fibroelastic layer (FEL) can be observed in the inner adventitial layers. The breaking-away of the short IEM-related lamellae as well as the formation of lamellae in the inner media develops most intensively in the distal third of the leg arteries and in *ADP*, as it is less expressed in their proximal and weakest — in their middle third.

In 365-395-mm-long fetuses, IEM thickens and even doubles in some areas, and some intima parts develop more intensively. Media thickness increases on the account of SMC number. The borderline between the media and adventitia is sharper as SMC nuclei are darker, more flattened and more elongated than these of the adventitial cell populations. The EFs in the internal and middle third of the media disappear. The EFs of the FEL thicken and arrange in denser groups (Fig. 3). The priority development of the above described alterations persists in the distal third of the leg arteries and in *ADP* along with their weaker development in their proximal third and the weakest one in their middle third.

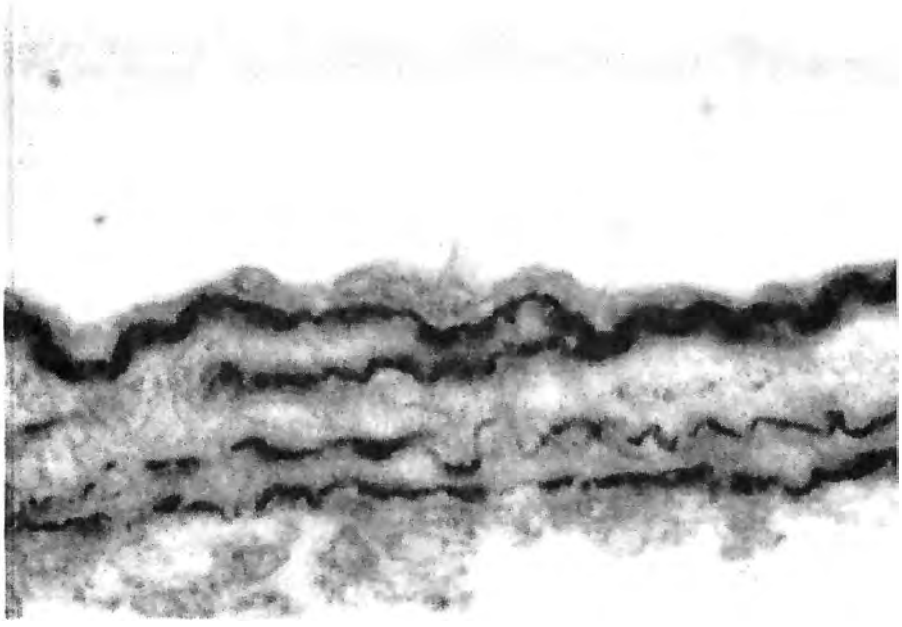

Fig. 1. Transversal section of peroneal artery at the distal third. 257 mm fetus. Orcein. Microphotograph (× 1000)

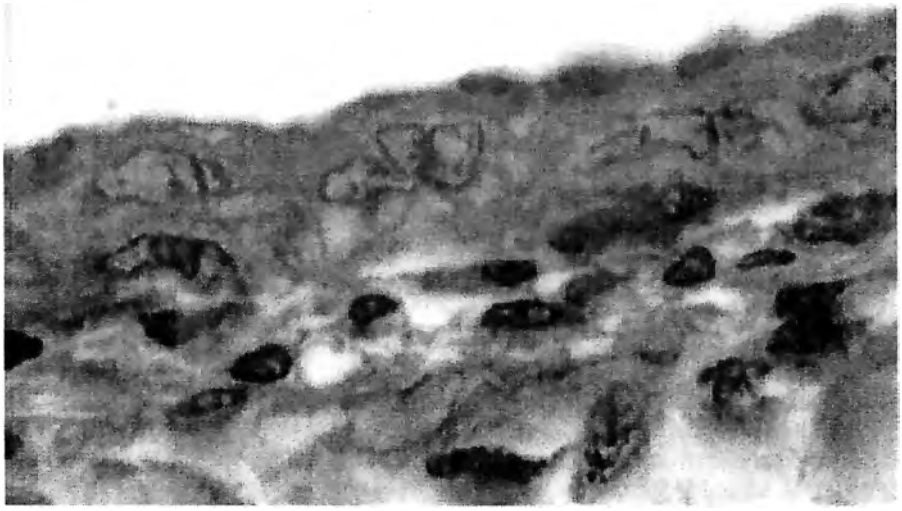

Fig. 2. Transversal section of peroneal artery at the distal third. 257 mm fetus. Hematoixilin-Eosin stain. Microphotograph (× 1000)

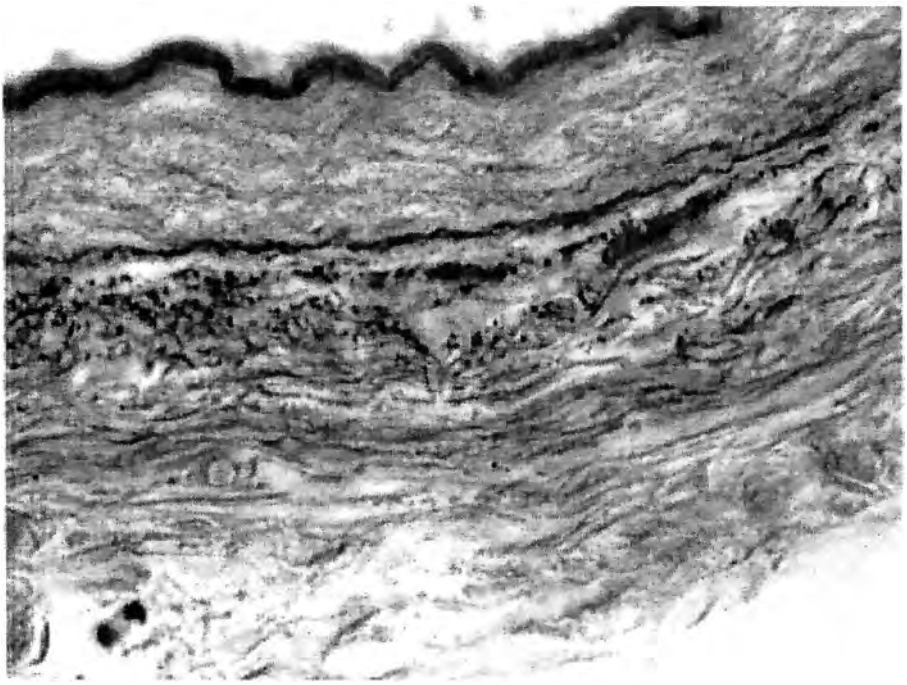

Fig. 3. Transversal section of posterior tibial artery at the middle third. 388 mm fetus. Orcein. Microphotograph (×1000)

In stillborn, IEM is homogenous, dense and thickened. The media muscular layer is thicker and compact. Single circularly oriented EFs are located in its outer half. In the adventitia are clearly differentiated an inner FEL and an outer connective tissue layer rich in collagen fibres. In some areas a continuing anticipating intimal development was established. In certain areas IEM doubles within a small region and a connective tissue layer between both sheets is formed. In these regions intimal thickness reaches up to 8 μm and their extent on the vascular circumference reaches up to 70 μm. In other regions there is incomplete IEM reduplication as from it some lamellae break away and direct themselves either to the endothelium, or to the media.

Discussion

The most essential element of the established in some arterial parts anticipating wall development is the development of a thin subendothelial layer and IEM duplication only in single small fields of the intima. These forms of development can be related to the mechanism of intimal development through migration of cellular elements from the media that has been described in the literature [7]. This process is most intensive in the distal third of the leg arteries and of *ADP*, less expressed in their proximal third and weakest in their middle third. The structural peculiarities of the distal parts of the leg arteries and of *ADP* can be related to the dynamic change of the geometry of these vessels caused by the movements in the knee and leg joints which are, in principle, one of the basic factors for vascular bed remodelling [4]. The possible role of these regions for the earlier started pathogenesis of the atherosclerotic process remains a task of further purposeful research [1, 5, 9].

References

1. Ishizu, T. et al. Effect of age on carotid arterial intima-media thickness in childhood. — Heart Vessels, **19**, 2004, 189-195.
2. Kent, K. C., B. Liu. Intimal Hyperplasia—Still Here after All These Years! — Ann. Vasc. Surg., **18**, 2004, 135-137.
3. Marinov, G. R., T. Tabakov. Medial and medio-intimal thickening and atherosclerosis. A light microscopical study on the lower limb arteries. — Verh. Anat. Ges., **76**, 1982, 291-292.
4. Marinov, G., Tz. Tzvetkova. Age related differentiation in the local peculiarities of the terminal vascular bed of the lower limb skin. — Verh. Anat. Ges., **71**, 1977, 689-695.
5. Taute, B.-M. et al. Common carotid intima-media thickness in peripheral arterial disease. — Int. J. Angiol., **13**, 2004, 27-30.
6. Toursarkissian, B. et al. Outcomes following distal bypass graft occlusion in diabetics. — Ann. Vasc. Surg., **17**, 2003, 670-675.
7. Vancov, V., Sp. Nikolov, G. Chaldakov. Zur ontogenese der Wand der großen Blutgefäße beim Kaninchen. Eine elektronenmikroskopische Untersuchung. — Verh. Anat. Ges., Jena **69**, 1975, 163-170.
8. Маринов, Г. Възрастови особености в структурата на стената на магистралните артерии на долния крайник. — Медико-биологични проблеми, V, 1977, 49—57.
9. Маринов, Г. Ранни задебеления на артериалната стена — класификация и роля в развитието на артеросклеротичния процес. — В: X Юбилейна сесия на ВМИ—Варна (31.X. 1981, Варна), 1982, 31—34.
10. Маринов, Г, Т. Табаков. Структура и локализация на ранните интимални разрастванията в стените на магистралните артерии на долния крайник в пренаталната онтогенеза. — Медико-биологични проблеми, VIII, 1980, 42—50.

Institute of Experimental Morphology and Anthropology

Acta morphologica et anthropologica, 10
Sofia•2005

The Impact of Human Recombinant Interferon-γ on the Capacity of the Human CD 34+ Hematopoietic Progenitor Cells to Differentiate *in vitro* into Mature Bone Marrow Macrophages

Y. Gluhcheva, K. Schroecksnadel**, B. Wirleitner**, E. Bichkidjieva*, I. Ilieva*, E. Zvetkova*, G. Konwalinka**, D. Fuchs***

* *Institute of Experimental Morphology and Anthropology, Bulgarian Academy of Sciences, Sofia*
** *Medical University, Innsbruck, Austria*

Interferon-gamma (IFN-γ) stimulated the formation of granulocyte/macrophage- and pure macrophage colonies when added to the culturing medium. The stimulatory effect was better observed when the purified and enriched human CD34+ hematopoietic progenitor cells were cultured in Agarleucocyte conditioned medium (Agar-LCM).

Key words: CD34+ hematopoietic progenitor cells; IFN-γ; granulocyte/macrophage-(CFU-GM) and macrophage-(CFU-M) colonies.

Introduction

Hematopoiesis depends on continuous proliferation, expansion and differentiation of hematopoietic stem cells and their immediate progeny — hematopoietic progenitor cells. The two subsets of cells express CD 34 antigen — regulator of hematopoietic cell adhesion to stromal cells in the bone marrow [5]. CD34+ cell population comprise approximately 1% of the cells present in the bone marrow. Progenitor cells are also called colony forming cells (CFC) because of their ability to form colonies or clusters (bursts) during proliferation and differentiation when cultured in semi-solid medium [3]. In order to proliferate and differentiate into mature blood cells the progenitor cells require specific growth factors [10, 5]. It is a large group of proteins known as hematopoietic cytokines. According to Ogawa [12] the hematopoietic growth factors can be divided into 3 groups based on the stage of cell development which they affect: **late-acting, lineage-specific factors** — G-CSF, Epo, IL-5, IL-6; **intermediate-acting, lineage non-specific** — IL-3, IL-4, GM-CSF and **factors which affect the kinetics of cell cycle dormant primitive progenitors** — SCF, IL-6, IL-11, IL-12, G-CSF. Based on the effect of the cytokines - stimulatory or

inhibitory of the processes of cell proliferation and differentiation, the hematopoietic growth factors can be further divided into two groups: *stimulators* and *inhibitors* [12]. The most widely used cytokines known to stimulate hematopiesis *in vitro* are: stem cell factor (SCF), erythropoietin (Epo), different colony-stimulating factors (CSF). TNF-alpha, TGF-beta and IFN-γ act primarily as inhibitors.

IFN-γ is an inflammatory cytokine produced by activated T-lymphocytes, macrophages and *natural killer cells*. There are data [1, 2, 3, 13] showing its inhibitory effect on *in vitro* hematopoietic colony formation, and its ability to synergize with SCF. On the other hand, IFN-γ stimulates formation and maturation of granulocyte/macrophage- and macrophage colonies [4, 8, 9, 11]. It is suggested that the effects of this inflammatory cytokine depend on its dose, duration of time, the other factors present in the medium and the stage of maturity of the cells cultured [14].

Material and Methods

Cell cultures

Purified (density of 2.5×10^3/well) and enriched (density of 0.4×10^5/well) human CD34+ hematopoietic progenitor cells were cultured in semi-solid agar cultures. Two experimental systems were developed: IMDM was supplemented with SCF, IL-3 (called *recombinant cocktail - RC*), Epo or with Agar-stimulated leukocyte conditioned medium (*Agar-LCM*). IFN-gamma was added at 5000 U/ml once or at 200 U/ml or 400 U/ml — every second day. The cell cultures were incubated for 14 days at 37°C in humidified air of 5% CO_2. After incubation the colonies were scored and observed by light microscopy after staining with May-Grünwald-Giemsa.

Results

In the *semi-solid agar cultures* can be observed:
— *CFU-E* — smallest and most rapidly maturing erythroid colonies, consisting of 1 or 2 clusters and containing maximum 100-200 erythroblasts.

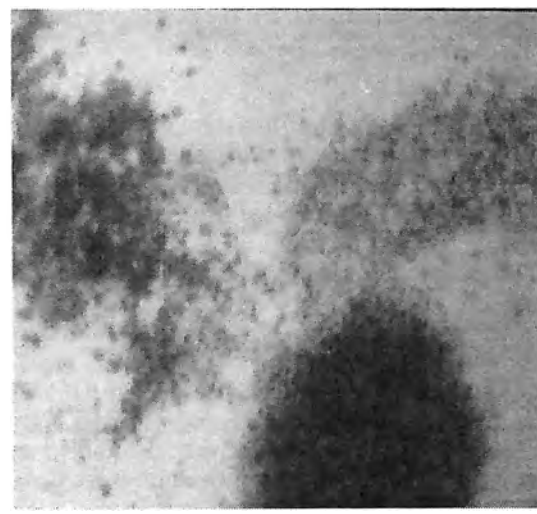

Fig. 1. IFN-γ induced three types of hematopoietic colonies: macrophage (M-); erythroid — (BFU-E); mixed granulocyte/macrophage — (GM-); May-Grünwald-Giemsa staining (× 160)

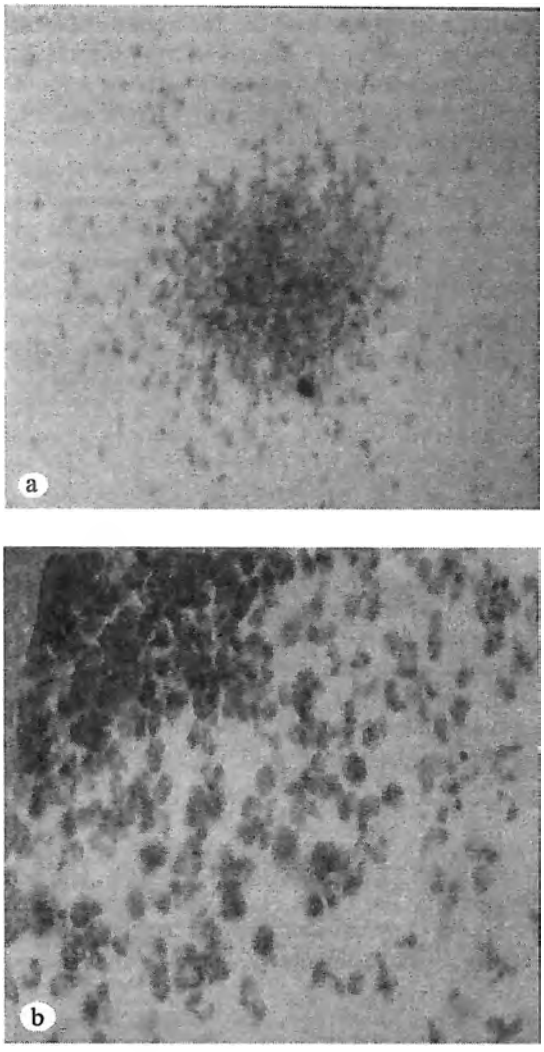

Fig. 2. **a)** Immature granulocyte/macrophage colony **(a)** and a part of the same colony containing granulocytes and macrophages in different stages of maturity **(b)**; Part of the same colony; granulocytes and macrophage can be seen; May-Grünwald-Giemsa staining (× 160; × 400)

— *BFU-E* — more primitive than CFU-E, give rise to larger, multi-clustered erythroid colonies which consist of 1 large or 3 small clusters (**Fig. 1**). *BFU-E* can be further divided into *mature* and *primitive BFU-E.*

— *CFU-GM* — with concentrated central core surrounded by a less dense halo of cells.

In all cases where *IFN-γ* was added a *stimulatory effect* only *on BFU-E and CFU-GM* formation was observed; no such effect was registered for the CFU-E colonies [6].

IFN-γ - added to cultured *in vitro* human CD34+ hematopoietic progenitor cells, *stimulated* (in a dose-dependent manner) *proliferation* and *differentiation* of *CFU-GM* and *CFU-M*. IFN-γ induced macrophage differentiation in the pure macrophage- (M-) and mixed — granulocyte/macrophage (GM-) colonies: a large number of mature, well-differentiated macrophages with vacuolated cytoplasm, more than one nucleus and dispersed (active) nuclear chromatin were observed (**Fig. 1c; 2a, b; 3a, b**).

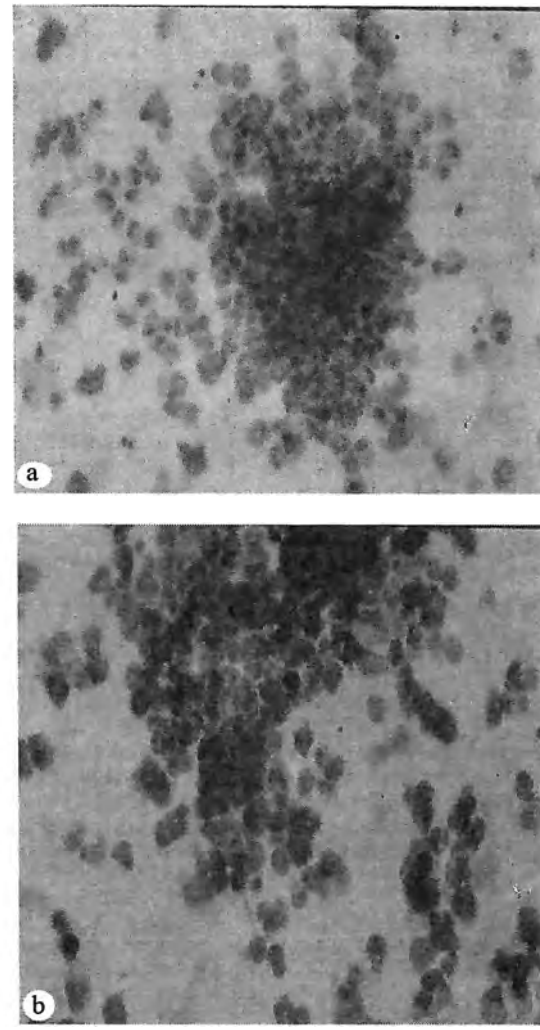

Fig. 3. Mature granulocyte/macrophage colony (a) and a part of the same colony (b) May-Grünwald-Giemsa staining (× 160, × 400)

Discussion

It was found that IFN-γ potentiates the proliferative effects of IL-3 and GM-CSF on CD34+ hematopoietic progenitor cells purified from cord blood and bone marrow [2]. Additionally, cell analysis showed that this effect of the cytokine is directly mediated on its target cells: day 14 colony assays showed that IFN-γ strongly potentiates both monocytic and granulocytic series, as it affects the erythroid lineage.

The results of the present study are in agreement with these of Caux et al. [2], Kawano et al. [7] and clearly show that this inflammatory cytokine appears to potentiate early myelopoiesis and the development of mature CFU-GM. The observed by us *in vitro* differences in the regulated by IFN-γ bone marrow macrophage development and maturation may contribute to the understanding of the macrophageal functional heterogeneity *in vivo* [8].

Conclusions

IFN-γ stimulated (in a dose-dependent manner) *proliferation* of *CFU-GM* and *CFU-M* when added to cultured *in vitro* human CD34+ hematopoietic progenitor cells. The better observed stimulatory effect of IFN-γ on cells cultured in *Agar-LCM* was likely due to the presence of *colony stimulating factors* (*CSFs*) in the conditioned medium used. The IFN-γ-induced *macrophage differentiation* (*GM-* and *M-colonies in different stages of maturity*) possibly contributes to the morphological and functional heterogeneity of these cells in the human bone marrow.

References

1. Broxmeyer, H. E. et al. Comparative analysis of the influences of human γ, α and β interferons on human multipotential (CFU-GEMM), erythroid (BFU), and granulocyte-macrophage (CFU-GM) progenitor cells. — J. Immunol., **131**, 1983, No 3, 1300-1305.
2. Caux, C. et al. Interferon-γ enhances factor-dependent myeloid proliferation of human CD 34+ hematopoietic progenitor cells. — Blood, **79**, 1992, No 10, 2628-2635.
3. Coutinho, L. H., N. G. Testa, T. M. Dexter. The myelosuppressive effect of recombinant interferon γ in short-term and long-term marrow cultures. — Br. J. Haematol, **63**, 1986, 517-524.
4. Delneste, Y. et al. Interferon-γ switches monocyte differentiation from dendritic cells to macrophages. — Blood, **101**, 2003, No 1, 143-150.
5. Flores-Guzman, P., M. Gutierrez-Rodriguez, H. Mayani. *In vitro* proliferation, expansion, and differentiation of a CD34+ cell-enriched hematopoietic cell population from human umbilical cord blood in response to recombinant cytokines. — Arch. Med. Res., **33**, 2002, No 2, 107-114.
6. Gluhcheva, Y. et al. Influence of interferon-gamma on human CD34+ hematopoietic progenitor cells. — Pteridines, **15**, 2004, No 2, 50-51.
7. Kawano, Y. et al. Synergistic effect of recombinant interferon-γ and interleukin-3 on the growth of immature human hematopoietic progenitors. — Blood, **77**, 1991, No 10, 2118-2121.
8. Lucas, D. M. et al. Analysis of the IFN-γ-signalling pathway in macrophages at different stages of development. — J. Immunol., **160**, 1998, 4337-4342.
9. McDowell, M. A. et al. Different utilization of IFN-γ responsive elements in two maturationally distinct MP cell lines. — J. Immunol., **155**, 1995, No 10, 4933-4938.
10. Metcalf, D. Hematopoietic regulators: redundancy or subtlety? — Blood, **82**, 1993, 3515-3523.
11. Nicolet, C. M., D. M. Paulnock. Promoter analysis of an interferon-inducible gene associated with MP activation. — J. Immunol., **152**, 1994, No 1, 153-163.
12. Ogawa, M. Differentiation and proliferation of hematopoietic stem cells. — Blood, **81**, 1993, 2844-2853.
13. Shiohara, M., K. Koike, T. Nakahata. Synergism of interferon- γ and stem cell factor on the development of murine hematopoietic progenitors in serum-free culture. — Blood, **81**, 1993, No 6, 1435-1441.
14. Tsanev, R., I. Ivanov. Immune Interferon — properties and clinical applications. Boca Raton, CRC Press LLC, 2002.

Institute of Experimental Morphology and Anthropology

Acta morphologica et anthropologica, 10
Sofia•2005

In vivo Effect of Heavy Metals Cd, Pb, Cu and Zn on Mice Spermatogenic Cells and Chromosome Reactivity

Y. Martinova, M. Topashka-Ancheva**, S. Petkova**

* *Institute of Experimental Morphology and Anthropology, Bulgarian Academy of Sciences, Sofia*
** *Institute of Zoology, Bulgarian Academy of Sciences, Sofia*

ICR mice were given a diet enriched of heavy metals Cd, Pb, Cu and Zn for 15, 40, 60 and 90 days. The ultrastructural alterations in male germ cells and chromosome reactivity were studied. Spermatogonia and spermatocytes were found the most sensitive cells. The disturbances were seen predominantly in the cytoplasm and nuclei of the spermatocytes with dilatation of the endoplasmic reticulum cisternae and chromatin condensation. The tripartite structure of synaptonemal complexes have shown significant persistence. Chromosome aberrations of chromatide and isochromatide type, Robertsonian translocations and changes in chromosome spiralization were significantly increased in all experimental groups. There was no direct correlation between duration of the treatment and the percentage of aberrant mitoses. The presence of metaphases with altered coiling and "C-banding" effect related with changes in chromatin spiralization were confirmed by ultrastructural observation on spermatogenic cells.

Key words: heavy metals, spermatogenesis, chromosomes.

Introduction

The drastic increase in number of toxic chemicals in environment results irreversible adverse effects in animals and human beings. Reproductive system is very sensitive to different environmental factors and could be used as a useful tocl to solve many ecological problems. Due to complexity and long duration of the spermatogenic process, the testes of mammals are highly sensitive to damage produced by environmental expose to chemicals [5]. The polymetallic industrial dust as a waste product in lead-zinc factory near Assenovgrad (Bulgaria) is very rich in heavy metals Cd, Cu, Pb and Zn. In our previous article we have published the bioaccumulation of the above heavy metals in liver, kidney, spleen and bones in mice [6] and the effect on body weight, blood, oxygen consumption, mitotic index etc. [7]. In the present study we focus on the in vivo effect of Cd, Cu, Pb and Zn on subcellular structure of spermatogenic cells and chromosome reactivity in mice under ecologo-toxicological experiment.

Material and Methods

Male and female 10 weeks old ICR mice were given a diet summarized in Table 1. Polymetallic industrial dust from electrofilters of the lead-zinc rafinery near Assenovgrad (Bulgaria) was mixed mechanically at 1% ratio from conventional animal food. Samples were taken at 15, 40, 60 and 90 day of treatment. Two hours before sacrification mice were given C-methyl 3H-thymidine (NEW Products, Boston, MA)(spec act. 20mCi/mmol) in a dose of 2 μCi/g of body weight. Pieces of testes were proceeded for routine histological, autoradiographic and ultrastuctural study. Chromosome preparations "slides" were obtained from colchicine blocked bone marrow cells (2-4 g/kg b.w.) according to a routine protocol [4]. Air dried slides were stained with 5% Giemsa solution.

Table 1. Quantity of heavy metals (mg/kg) in the diet of mice

Group	n	Cadmium	Lead	Cooper	Zinc
Experimental	5	64.1± 10.5	784± 244	20.9 ±7.3	1945±429
Control	5	3.5 ±1.9	61.8± 20.9	1.3 ±1.1	90.9± 25.9

Results and Discussion

Histological assessment did not show significant differences between the testes of control and experimental animals. On the autoradiographs the percentage of labelled spermatogonia in control mice was 42±3 without significant difference between control and experimental groups with exception of day 40—20±2% labelled spermatogonia.

At the ultrastructural level in the experimental groups different alterations were visible. Spermatogonia and spermatocytes were the most affected germ cells and could be seen in different degree of destruction. In some of them the cytoplasm was highly vacuolized and the chromatin was condensed in amorphous heterochromatin accumulations. Fully destructed spermatocytes were obvious. The tripartite structure of synaptonemal complexes (SC)was well preserved even in completely degenerated pachytene spermatocytes. The higher resistence of SC was observed after in vivo x-ray irradiation due to a high degree of chromatin condensation and the strength of DNA-protein complexes [3] The cytoplasm of some Sertoli cells was rich in lysosomes as an expression of increased phagocytic activity.The higher bioaccumulation of heavy metals in liver, kidney and bones at 40, 60 and 90 day [6] coincides with the above described ultrastructural alterations of spermatogenic cells. Obviously the excess exposure of the organism to heavy metals disturbs the whole homeostasis including reproductive system. More studies are required to follow the effect of interactions between several heavy metals like Cd/Zn, Cd/Cu, Pb/Cu on the process of spermatogenesis.

Analysis of the metaphases preparations including structural and numerical changes was carried out both on control and treated mice. Chromosome aberrations were of chromatide (breaks and fragments) or isochromatide type — the first prevailing. The presence of ring chromosomes and Robertsonian translocations was also noticed. The analysis of characteristics of the chromosome aberrations suggests they are the results of clastogenic effect of Pb++ as a basic component of applied industrial dust [1, 2]. Metaphase analysis has shown a lack of direct correlation

between duration of the treatment and the total percentage of aberrant metaphases. The constancy in harvested aberrations in rapidly proliferating bone marrow cells could be explained with an equilibrium between the process of induction of observed aberration by the mutagens and the elimination of the aberrant cells in the course of mitotic division.

More than 5% of analysed metaphases in the treated animals have shown changes in the spiralization of chromosomes and clear "c-banding" effects most probably related with changes in the chromatin spiralization. The highest percentage of metaphases with altered spiralization and "C-banding" effects at 15th day of treatment indicates an adverse influence of the heavy metals on chromatin structure, confirmed by ultrastructural observations on spermatogenic cells.

References

1. Dhir, H., A. K. Roy, A. Sharma, G. Talukder. Modification of clastogenicity of lead and aluminium in mouse bone marrow cells by dietary injection of Phyllanthus emblica fruitextract. — Mutat. Res., **242**, 1990, 305-312.
2. Gerber, H., A. Leonard, P. Jacqet. Toxicity, mutagenicity and teratogenicity of lead. — Mutat. Res., **76**, 1980, 115-141.
3. Martinova, Y., L. Kancheva, A. Hadjioloff. Electron microscopic study of the radiation damages in mouse spermatocytes. — C. R. Acad. Bulg. Sci., **36**, 1983, 253-256.
4. Preston, R. J. et al. Mammalian in vivo cytogenetic assays: analysis of chromosome aberrations in bone marrow cells. — Mutat. Res., **189**, 1987, 159-165.
5. Russell, L. D. Normal testicular structure and methods of evaluations under experimental and disruptive conditions. — In: Reproductive and developmental toxicity of metals (Eds. T. W. Clarkson, G. F. Nordberg and P. R. Sager). Plenum Publishing Co., New York, USA, 1983, 227-252.
6. Teodorova, S., R. Metcheva, M. Topashka-Ancheva. Bioaccumulation and damaging action of polymetal industrial dust on laboratory mice Mus musculus alba. I. Analysis of Zn, Cu, Pb and Cd disposition and mathematical model for Zn and Cd bioaccumulations. — Environmental Res., **91**, 2003, 85-94.
7. Topashka-Ancheva, M., R. Metcheva, S. Teodorova. Bioaccumulation and damaging action of polymetal industrial dust on laboratory mice Mus musculus alba. II. Genetic cell and metabolic disturbances. — Environmental Res., **92**, 2003, 152-160.

Institute of Experimental Morphology and Anthropology

Acta morphologica et anthropologica, 10
Sofia•2005

Developmental Study of Murine Gut Mucosa by Scanning Electron Microscopy

D. Dimitrova, B. Alexieva, M. Cholakova, M. Bratanov, L. Petrov, E. Nikolova

Institute of Experimental Morphology and Anthropology, Bulgarian Academy of Sciences, Sofia

The morphology of mucosa of terminal ileum during postnatal development of mice has been investigated using scanning electron microscopy. The age-related changes in small intestinal mucosa in mice of different age (newborn, 5, 15, 25 and 29 days old) were shown and analyzed. The results demonstrated marked differences in morphological parameters as height and shape of small intestinal villi between investigated periods. This study is the first detailed SEM examination of morphology of developing murine gut and is a part of work aimed to elucidate the role of mother's milk in maturation of the gastrointestinal tract of the offspring in mammals.

Key words: development, mucosa, small intestine, ileum, villi, scanning electron microscopy.

Introduction

The development of mammalian gut after birth is an important physiological phenomenon that is determined and modulated by a complex of factors: genetic developmental programming factors, suckling, weaning, food composition, microbial flora, hormones and growth factors [1]. Despite of many experimental data concerning the postnatal gut development in mammals, knowledge about this process regarding morphological changes in the small intestinal architecture during ontogenesis is still controversial and incomplete.

This study was designed to examine the maturational changes of small intestinal mucosa during the first 30 days of postnatal life in mice using scanning electron microscopy.

Material and Methods

Balb/c mice aged 0,/newborn/, 5, 15, 25 and 29 days were used. Tissue sections (1cm) were taken 0,5 cm proximal the ileocaecal junction. Tissue preparation for SEM was performed by the method reported by P o t t e r et al. [4] with some modifications.

Briefly, the tissue specimens were fixed with 2% glutaraldehyde in 0,05M phosphate buffer (pH 7,4) for 48h at 4°C, followed by postfixation (1% OsO_4 in 0,1M phosphate buffer with added 0,15M sucrose) for 45 min at 4°C. They were subsequently dehydrated, dried in a critical point drier and coated with gold. The specimens were examined with scanning electron microscope (JEOL, JEM-35) under five magnifications: × 100, × 360, × 860, × 4000 and × 10 000.

Results and Discussion

We found significant changes in the morphology of small intestinal mucosa during the postnatal development of murine gut. A gradual increase in villous height was observed between the investigated postnatal periods up to day15. (Fig. 1 — *A*, *B*, *C* and *D*). Using higher magnification of the same objects, the morphologic features of the luminal surface of small intestine, mentioned above, could be more clearly demonstrated (Fig. 2 — *A* and *B*). Our findings confirmed the previous results obtained by other morphological methods that there is an increase of villous length during the first 3 weeks of postnatal life in mice [2], and also that the major changes of gut morphology are associated with the weaning of mammals [1].

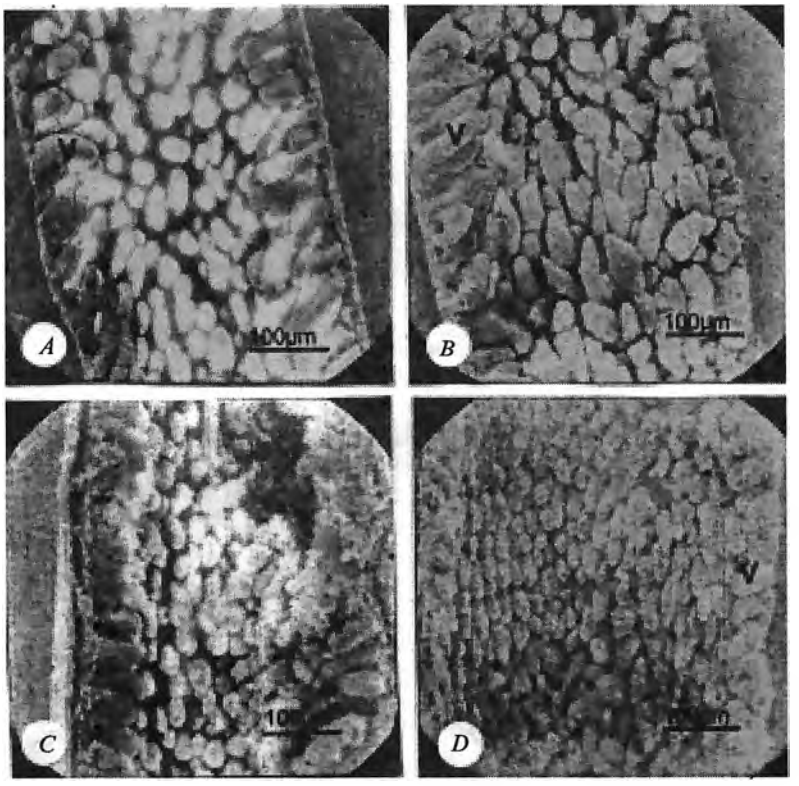

Fig. 1. Scanning electron micrographs of ileal small intestinal mucosa of mice of different age: newborn (A), 5-day-old(B), 15-day-old(C) and 25-day-old(D) mice. V — villi. Orginal magnification ×100, bar 100µm

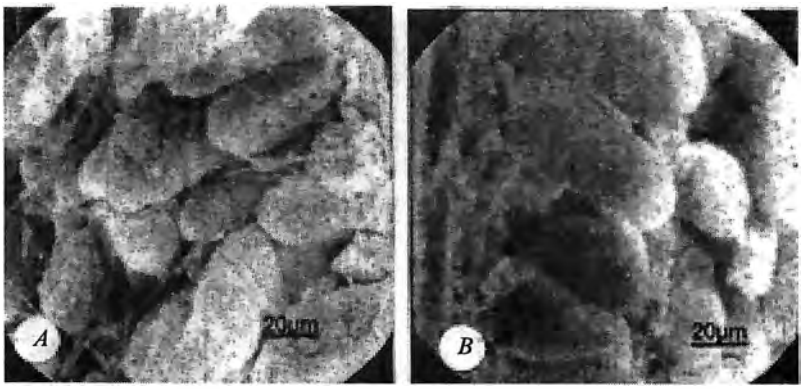

Fig. 2. Scanning electron micrographs of the same tissue samples from 5(A) and 15-day-old(B) mice at highermagnification. Orginal magnification ×360, bar 20μm

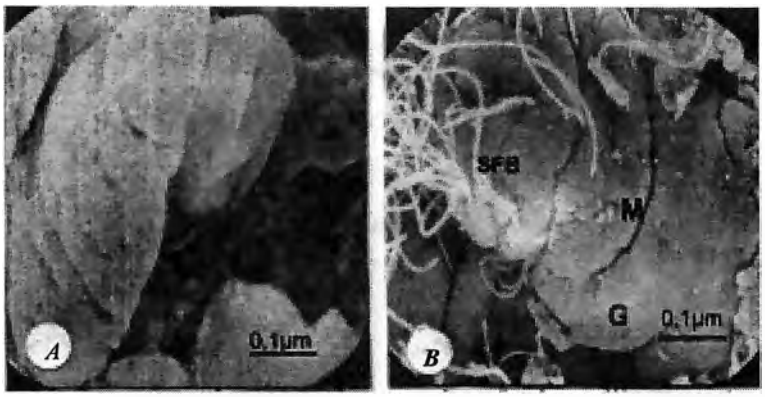

Fig. 3. Scanning electron micrographs represent morphological details of villous surface. A: 5-day-old; B: 29-day-old mice. Orginal magnification ×860, bar 0,1μm. G — goblet cell orifices, M —mucus

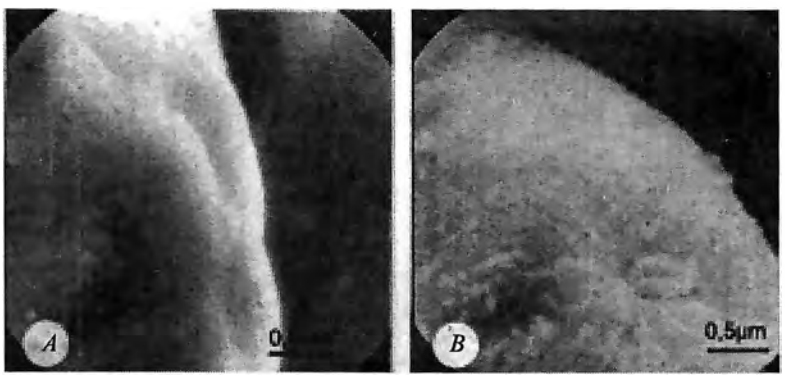

Fig. 4. Scanning electron micrographs of microvillous surfaces of newborn (A) and 15-day-old (B) mice. Orginal magnification ×4000, bar 0,5μm

Another aspect of villous morphology was the dynamics of villous shape. As shown in figures, at birth the villi are predominantly finger-like (Fig. 1 — *A*]. In the next age periods investigated leaf- and ridge-shaped villi dominated (Fig. 1 — *B*, *C* and *D*). We suggest that the shape of the villi could be utilized as a marker for maturational stage of gut mucosa.

An interesting finding was the difference in villi pattern among the investigated periods. At birth (day 0) the villi of the small intestinal mucosa had irregular pattern (Fig. 1 — *A*). Villi either with normal shape and size (high and thin/or smaller villi short and thick), could be distinguished. Our findings illustrated an early stage of maturation of the small intestinal mucosa which is characterised morphologically with irregular villous development: smaller villi were not enough developed as spatial structure. By day 5 villi became more uniformed (Fig. 1 — *B*) and at day 15 villi reached their maximum uniformity in height (Fig. 1 — *C*). This gradual change from irregularity to uniformity in villi height was the major feature of the morphology of developing mouse ileum.

Discrete details of villous morphology could be revealed under higher magnifications [3]. The results demonstrated that the corrugations of the villous surface were obvious in all investigated age periods. The orifices of Goblet cells without or with mucous secretions were well visible (Fig. 3 — *A* and *B*). Presence of segmented filamentous bacteria (SFB) in small intestine of 29-day-old animal (Fig. 3 — *B*) was an interesting finding. Finally, at instrumental magnification ×4000 the apical surfaces of enterocytes building villi could be observed (Fig. 4). In newborn mice microvillous surface was not well developed (Fig. 1 — *A*). The well differentiated microvillous surface were present on day15 and progressively developed up to day29 of age (data not shown).

The results presented here demonstrate marked age related dynamics of morphology of small intestinal mucosa in Balb/c mice. Information gained in this study will help to better understand the process of gut mucosa development during postnatal life.

References

1. Cummins, A. G., F. M. Thompson. Effects of breast milk feeding and weaning on epithelial growth of the small intestine in humans. — Gut, **51**, 2002, 748-754.
2. Falk, P. G. et al. Creating and maintaining the gastrointestinal ecosystem: what we know and need to know from gnotobiology. — MMBR, **62**, 1998, 1157-1170.
3. Marsh, M. N., J. A. Swift. A study of small intestinal mucosa using the scanning electron microscope. — Gut, **10**, 1996, 940-949.
4. Potter, U. J., A. J. Collins. Recovery and preparation of small bowel biopsies taken by enteroscopy for SEM. — Microscopy and Analysis, **5**, 1999, 25-27.

Institute of Experimental Morphology and Anthropology

Acta morphologica et anthropologica, 10
Sofia • 2005

Changes in A 549 Cells Morphology in Response to the Toxic Effect of Halothane

R. Valtcheva, E. Stephanova*, Z. Lalchev**, G. Altankov***, R. Pankov*, S. Kalenderova*****

* *Department of Cytology, Histology and Embryology, Faculty of Biology, Sofia University "St. Kliment Ohridski", Sofia*
** *Department of Biochemistry, Faculty of Biology, Sofia University "St. Kliment Ohridski", Sofia*
*** *Institute of Biophisics, Bulgarian Academy of Sciences, Sofia*
**** *Department of Chemistry and Biochemistry, Medical University–Sofia*

Cell adhesion, motility and cellular response to different external stimuli are regulated by the dynamic interaction of the cytoskeletal elements. The integrins are transmembrane receptors that interact with actin cytoskeleton and with the extracellular matrix proteins. This interaction induces clustering of signal proteins, forming focal and fibrilar adhesions.
The goal of the present study was to determine the influence of the volatile anaesthetic halothane on actin cytoskeleton and focal adhesion contacts in A 549 cells. The results from immunofluorescence staining with RITC-phalloidin, revealed that the F-actin is disrupted by 1.5 and 2 mM halothane. Indirect immunofluorescence staining of paxillin in the focal adhesion complexes, showed the same effects of anaesthetic. These changes were absent when cells were treated with the non-toxic halothane concentration of 0.9 mM, although cell spreading was delayed.

Key words: A 549 cells, focal adhesions, cytoskeleton, anaesthetics.

Introduction

The structural organization of eukaryotic cells depends on the dynamic interactions among the cytoskeletal elements. The cytoskeletal systems induce changes in cell morphology and motility in response to external stimuli [1, 2]. Actin cytoskeleton interacts with the transmembrane receptors called integrins, which are responsible for the cell adhesive properties and signal transduction between cellular interior and the extracellular matrix [3-5]. The interactions between integrins and their ligands (extracellular matrix proteins, such as fibronectin, laminin, collagen etc.) induce clustering of a various signal transduction proteins and result in the formation of focal and fibrilar adhesions complexes [6, 7].

In our study we used lung cell line A 549 as a model system, which possesses the typical property of type II pneumocytes, to synthesize and release some of the

alveolar surfactant components [8]. Lung tissue is the first one, that interacts with inhaled agents, such as anaesthetics. The anaesthetics could induce immunosuppression, due to the reduction of the activity of NK cells and macrophages [9]. There are also data, demonstrating that the volatile halogenated hydrocarbones could directly interact with the components of the alveolar surfactant, leading to its dysfunction [10]. All these negative effects of the anaesthetics result in metabolic, cardiovascular and respiratory problems in the post-operative period. These anaesthetic agents interact with the phospholipid bilayer, which results in an increased fluidity and changes in the activity of the ion-channels [10, 11]. There are data, showing that the anaesthetics influence the organization MHC molecules on the cell surface and the cell surface receptors, responsible for cell adhesion [12, 13, 14].

The goal of the present study was to determine whether the volatile anaesthetic halothane, applied in concentrations that induce membrane damages, causes also disorganization of the actin cytoskeleton and changes in the focal adhesion contacts in A 549 cells. The results from direct immunofluorescence analyses (staining with RITC-phalloidin), revealed that the F-actin is disrupted by 1.5 and 2 mM halothane. Indirect immunofluorescence staining of paxillin in the focal adhesion complexes, showed the same negative effects of the halothane doses mentioned above. These morphological changes were absent when cells were treated with the non-toxic halothane concentration of 0.9 mM, although cell spreading was delayed.

Material and Methods

Cell culture: The human lung carcinoma cell line A 549 (ATCC No CCL-185) was grown in DMEM supplemented with 10 % fetal bovine serum (FBS) and antibiotic mixture Ampicilline/Streptomycine/Fungizone. Cells were cultured at 37°C in the presence of 5 % CO_2 and were subcultured 24 hours before each experiment.

Halothane dilution and treatment: The culture medium DMEM, supplemented with FBS was saturated with halothane to the final concentration of the anaesthetic agent of 3mM [13].

Immunofluorescence. For visualization of F-actin cytoskeleton and the focal adhesion complexes, A 549 were cultured for 5 hours on pre-coated cover slips with 10 μg/ml collagen IV, until most of the cells adhere, then cells were treated with indicated halothane concentrations for 2 hours [13]. After treatment, cells were fixted in 4 % paraphormaldehyde and stained for 30 minutes at 37°C with 20 U/ml phalloidin conjugated with the fluorochrome RITC, or with mouse monoclonal anti-human paxilline antibody and secondary anti-mouse antibody, conjugated with CY3™.

Results and Discussion

Our previous studies on the effect of halothane on A 549 cells showed, that these cells reach maximal adhesion after 5 hours of culturing. The adhesive properties of the cells were reduced after treatment with halothane concentrations equal or higher than 2.1 mM. The present study revealed that the lower halothane dose of 1.5 mM destroyed F-actin in some of the cells (Fig. 1. — *C*), and after 2 hours of treatment with concentration of 2 mM there were a complete disorganization of the actin cytoskeleton (Fig. 1. — *D*). Similar results were observed in the focal adhesion complexes (Fig. 2). Paxillin level has decreased evidently as a result of the treatment with anaesthetic, applied at concentration of 1.5 mM (Fig. 2. — *C*) and there was a com-

plete loss of the focal adhesions in cells affected by 2.1 mM (Fig. 2. — *D*). Although the treatment with the non-toxic dose of 0.9 mM halothane didn't seem to influence F-actin and the morphology of the focal adhesion complexes, it's clear from Fig. 2. — *A* and *B* that A 549, treated with non-toxic halothane concentration spread two times slower, than non-treated cells. These results show that the non-toxic halothane doses, however affect cell morphology, resulting in delayed and/or inhibited cellular spreading.

We could summarized that the volatile anaesthetics belonging to the halogenated hydrocarbon family negatively influenced the A549 lung cells. The doses, we used for cell treatment correspond to the clinically relevant concentrations cited in the literature [15]. Our results, concerning whole cell morphology, cytoskeleton and the focal adhesions, showed that the cell line A 549 could be used as a useful in vitro model system for studying the dose-dependent effect of the volatile anaesthetics on the cellular level.

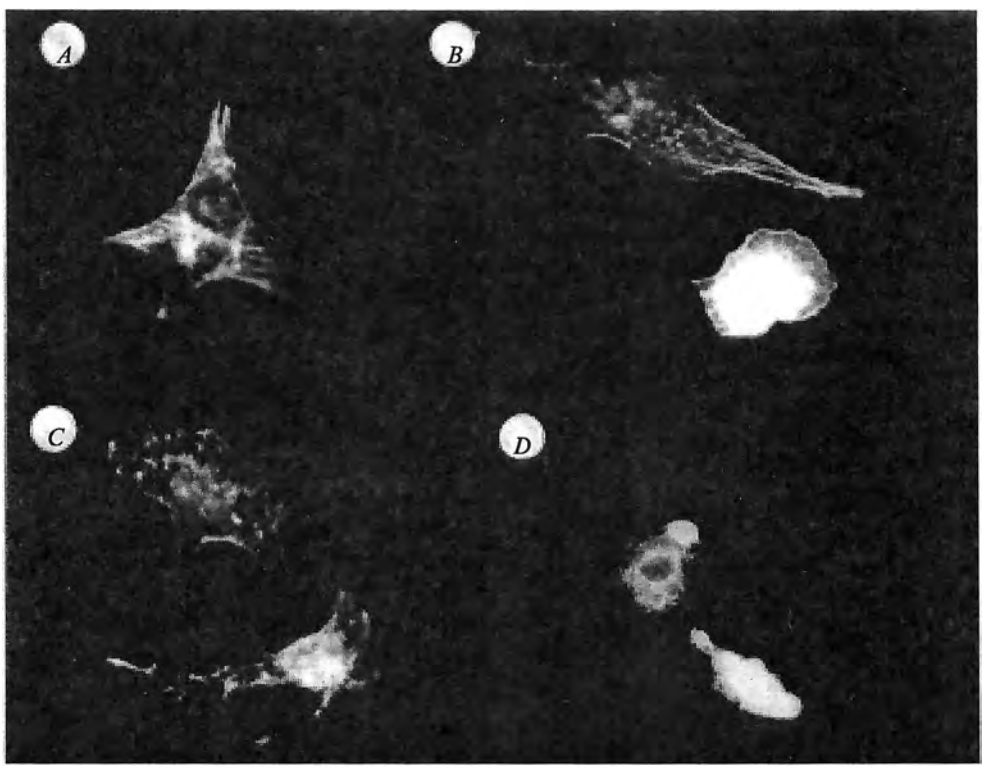

Fig. 1. Direct immunofluorescence staining with RITC-phalloidin. F-actin in A 549 cells is visualized, after 5 hours culturing on collagen IV covered glasses.
A — non-treated cells; *B* — cell treaed 2 hours with 0.9 mM halothane; *C* — cell treaed 2 hours with 1.5 mM halothane; *B* — cell treated 2 hours with 2.1 mM halothane (all photos were taken at magnification 100×)

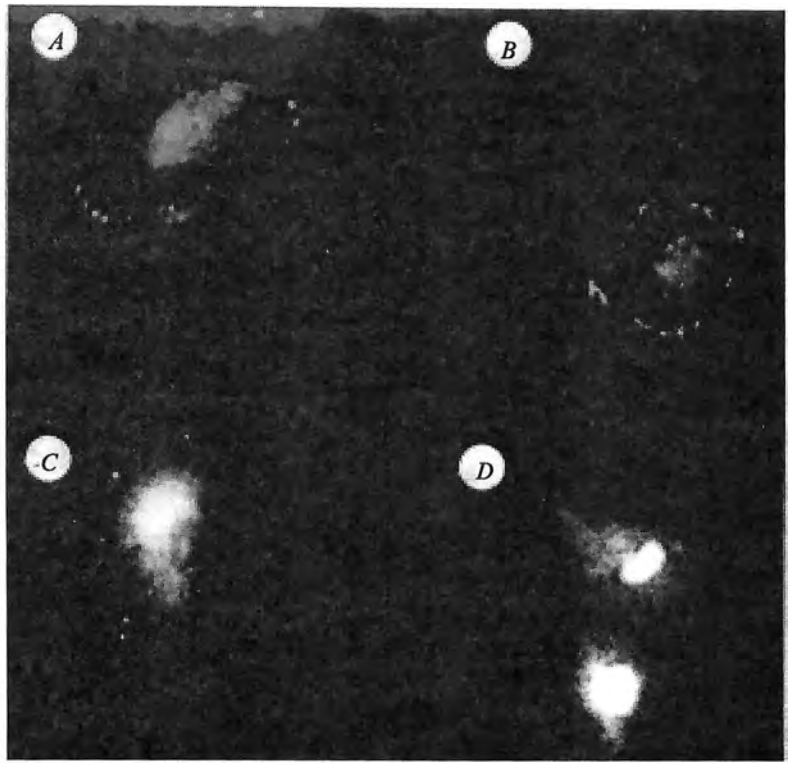

Fig. 2. Indirect immunofluorescence staining with mouse monoclonal anti-human paxillin antibody and CY2™ conjugated secondary anti-mouse antibody. The focal adhesions are visualized after 5 hours culturing on collagen IV covered glasses. *A* — non-treated cells; *B* — cell treated 2 hours with 0.9 mM halothane; *C* — cell treated 2 hours with 1.5 mM halothane; *B* — cell treated 2 hours with 2.1 mM halothane (all photos were taken at magnification 100×)

Acknowledgements: This work was supported by Ministry of Education and Sciences of Bulgaria (Grant MU-K 1301/03 — 2375) and by Medical University, Sofia.

References

1. Chang, L., R. D. Goldman. Intermediate filaments mediate cytoskeletal crosstalk. — Nature, **5**, 2004, 601-613.
2. Revenu, C. et al. The co-workers of actin filaments: from cell structures to signals. — Nature, **5**, 2004, 635-646.
3. Kinbara, K. et al. Ras GTPases: Integrins' friends or foes? — Nature, **10**, 2003, 767-776.
4. Hass, T.-A, E. Pox. Integrin-ligand interactions: a year in review. — Curr. Opin. Cell. Biol, **6**, 1994, 656-662.
5. Liu, S., D. A. Calderwood, M. H. Grinsberg. Integrin cytoplasmic domain-binding proteins. — J. Cell. Sci, **113**, 2000, 3563-3571.
6. Tran, H. et al. Integrin clustering induces kinectin accumulation. — J. Cell. Sci., **115**, 2002, 2031-2040.
7. Geiger, B., A. Bershadsky, R. Pankov, K.Yamada. Transmembrane cross-talk between the extracellular matrix and the cytoskeleton. — Nat. Rev. Mol. Cell. Biol, 2, 2001, 793-805.
8. Lieber, M. et al. A continuous tumor-cell line from a human lung carcionma with properties of type II alveolar epithelial cells. — Int. J. Cancer, **17**, 1976, 62-70.

9. T o n n e s e n, E. Immunological aspects of anaesthesia and surgery. — Dan. Med. Bull., 36, 1989, 263-281.
10. L a l c h e v, Z. et al. Alterations of biochemical and physicochemical quantities of pulmonary lavages attending halothane and penthrane treatment in rats. — Applied Cardiopulmonary Pathophysiology, 4, 1992, 315-322.
11. F r a n k s, N., W. L i e b. Molecular and cellular mechanisms of general anesthesia. — Nature, 333, 1994, 662-664.
12. D z o l j i c, M. et al. Ethanol and halothane differently modulate the HLA class I and class II oligomerization. A new look at the mode of action of anesthetic agents through fluorescence spectroscopy. — J. Photochem. Photobiol. B, 56, 2000, 48-52.
13. V a l t c h e v a, R. et al. Effect of Halothane on human lung carcinoma cells A 549. — Chem. Biol. Interact, 146, 2003, 191-200.
14. B a t a i, I., M. K e r e n y i. Halothane decreases bacterial adherence in vitro. — Acta Anaesthesiol. Scand., 43, 1999, 760-763.
15. B a z i l, C. W. et al. Equilibration of halothane with brain tissue in vitro: comparison to concentration during anaesthesia. — J. Neurochem, 49, 1987, 952-958.

Institute of Experimental Morphology and Anthropology

Acta morphologica et anthropologica, 10
Sofia • 2005

Effect of Inhalation Anesthetics on the Mitochondrial Structure and Secretory Activity of Human Alveolar Cells

T. Topouzova-Hristova, V. Moskova, E. Stephanova

Department of Cytology, Histology and Embryology, Faculty of Biology, Sofia University "St. Kliment Ohridsky"

During administration, anaesthetics can affect physiology of the lung and can provoke oxidative injury applied even in a small concentration. This may cause post-operative disturbances and inflammation and as a consequence programmed cell death. Our previous investigations on the impact of inhalation anesthetics halothane and penthrane on human bronchial and alveolar epithelial cell lines showed strong *in vitro* cyto- and genotoxic effect, after treatment with concentrations close to clinically relevant.

In this study we focused our attention on changes in structure and distribution of mitochondria and in organization of lamellar bodies after treatment of A549 cells with inhalation anesthetics halothane and penthrane. The experiments were performed with a lung-derived human carcinoma cell line A549. Specific *in vivo* staining with Yanus green B was used to assess cytoplasmic localization of mitochondria. Analysis of ultrastructural changes was performed with electron microscopy observations.

Key words: halothane, penthrane, A549 cells, stress-induced apoptosis, necrosis.

Introduction

Recently inhalation anesthesia is widely used in medical practice. During adminisration, anesthetics can affect physiology of the lung applied even in small concentrations and can provoke oxidative damage [1]. This may cause post-operative disturbances and inflammation and as a consequence programmed cell death. Many severe lung diseases, such as adult respiratory distress syndrome and idiopathic pulmonary fibrosis, are associated with increased apoptotic characteristics in pneumocytes type II [2]. This process is accompanied with changes in surfactant production as well [3]. The alveolar surfactant is a phospholypide-protein complex, which prevents alveolar collapse during breath and has protective and antioxidant effect [4]. It is produced by alveolar pneumocytes type II in the form of special organelles — lamellar bodies. Considering the surfactant production, these cells are progenitor for alveoli and have central role in tissue turnover and repair.

Our previous investigations on the impact of inhalation anesthetics halothane and penthrane on human bronchial and alveolar epithelial cell lines (16HBE14o-

and A549, respectively) showed strong *in vitro* cyto- and genotoxic effect after treatment with concentrations close to clinically relevant [5, 6]. We found time- and dose-dependent genotoxic effect of halothane expressed as fragmentation of nuclear DNA and chromosome aberrations [7]. Furthermore we observed changes in nuclear morphology, nuclear and cellular fragmentation during post-treatment period [8].

In accordance with the degree of injury, cells can avoid or undergo cell death (stress-induced apoptosis). The mitochondria considered to be the structures participating in regulation of apoptosis. Signals of pro-apoptotic proteins can activate caspases and hence to induce apoptosis released cytochrom c as a result of injury. All these data focused our attention regarding alterations of mitochondrial structure and distribution in A549 cells and changes in organization of lamellar bodies after treatment with inhalation anesthetics halothane and penthrane.

Material and Methods

Cell culture

The experiments were performed with A549 cells, a lung-derived human carcinoma cell line, which maintains many of the morphological and biochemical characteristics of pneumocytes type II [9] (kindly provided by Anna Segerman, Umeå University, Sweden). Cells were grown in DMEM, supplied with 10 % FBS (HiBond), at 37°C, 5 % CO_2 until they reached 80 % confluence.

Cells were treated for 4 hours in a culture medium, pre-saturated with 3 mM halothane (Narcotane, Leciva) [10] or 0.5 % penthrane (Abbott, USA) at 37 °C. After treatment the cells were washed with phosphate buffer saline (PBS), pH 7.4, the medium was changed and the cells were maintained up to 3 days at optimal conditions without anesthetic.

Analysis of redistribution of mitochondria by light microscopy observations

Specific *in vivo* staining with Yanus green B was used to assess cytoplasmic distribution of mitochondria. The cells were grown on sterile cover slides. One to four days after treatment, cells were washed with PBS, pH 7.4 and incubated with 0.0025 % stain solution for 5-10 min, at 37°C. Redistribution of mitochondria was assessed under the Fluoval light microscope.

Analysis of ultrastructural changes by electron microscopy observations

On the first and third day after treatment, the cells were washed twice with PBS, pH 7.4 and fixed with 1.6 % glutaraldehide in 0.1 M cacodilate buffer (CB), for 1 hour at 4°C in darkness. The dishes were washed threefold with 0.1M CB (each 5 min) and monolayers were detached by scraping, transferred in Eppendorf tubes and pelleted by centrifugation. Post-fixation with 1 % osmium tetraoxide in 0.1 M CB for 1 hour at 4°C (in darkness) was performed. Cells were repeatedly washed with 0.1 M CB, dehydrated following a standard procedure and counterstained with uranyl acetate. The samples were embedded in Epon 812. Ultrathin sections were obtained by Reichert-Jung Ultracut E ultramicrotome and observed under the transmission electron microscope EM "Hitachi H-500".

Results and Discussion

In the control untreated cells generally mitochondria are localized into cytoplasm and after staining they form network-like structure (Fig. 1. — *A*). When the cells undergo apoptosis, mitochondria are accumulated around the nucleus, which probably due to the disturbances of cytoskeletal structures and kinesin-mediated transport [11]. We detected significant mitochondrial displacement after treatment of A 549 cells with 1.5 mM and 2.1 mM halothane. They are gathered in the central part of cytoplasm, mainly around the nucleus (Fig. 1. — *B*). Mitochondrial redistribution maintained to the end of studied period and this may serve as indication of apoptosis induction. If the anaesthetics caused reversible damages in the cells, mitochondrial redistribution could persist only in earlier stages of post-treatment period. Observed mitochondrial behaviour suggested irreversible injury in the A549 cells.

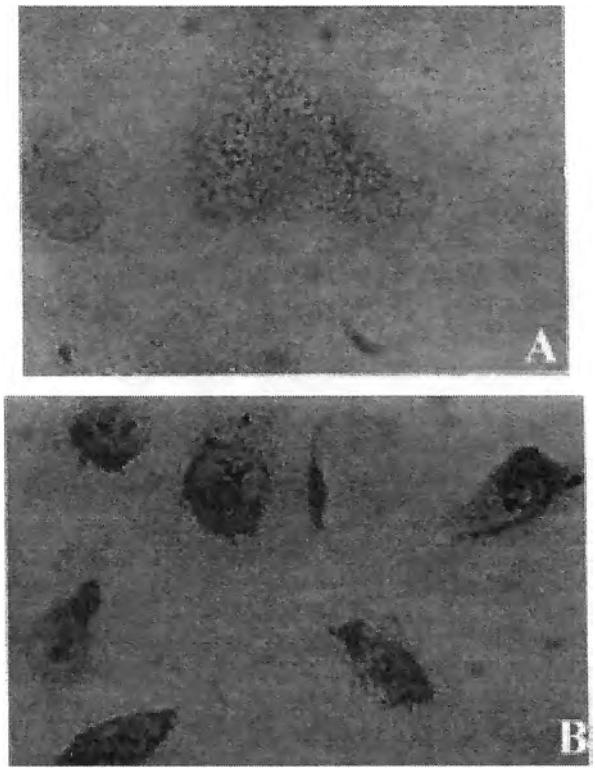

Fig. 1. Redistribution of mitochondria in A 549 cells after 2 hours treatment with 1.5 mM halothane
A — Localization of mitochondria in control (untreated) cell; *B* — Cells on the second day after treatment. In vivo staining with Yanus Green B, original magnification (×400)

The alterations mentioned above were confirmed on the ultrastructural level by electron microscopy observations. Normally A 549 cells have well structured cytoplasm with the typical membrane organelles such as endoplasmic reticulum, Golgi apparatus and lysosomes; moderate number of mitochondria; a large nucleus with small amount of heterochromatin component and one or two nucleoli. Specific organelles for pneumocytes type II as well as for A549 cells are lamellar bodies, which are storage structures for alveolar surfactant (Fig. 2. — *A*).

After treatment with halothane we established significant injuries of mitochondria, which related with swelling, lightening of mitochondrial matrix and kristae de-

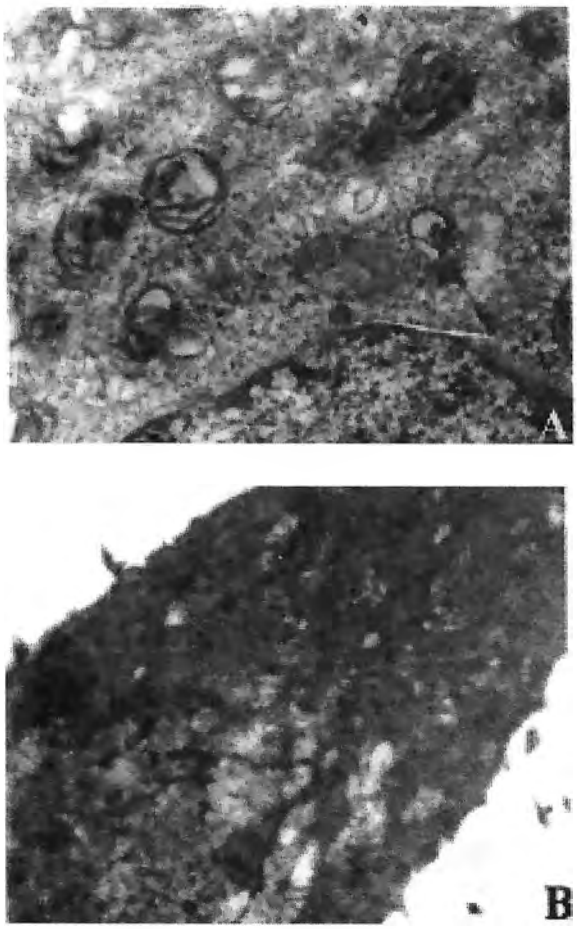

Fig. 2. Ultrastructural changes in mitochondria after halothane treatment. *A* — Ultrastructure of an untreated A 549 cell. Note the lamellar bodies in cytoplasm (×15 000); *B* — On the third day after treatment highly damaged mitochondria are localized around the nucleus and lamellar bodies are disappeared (×12 000)

struction (Fig. 2. — *B*). These changes continued during all studied period. At the same time we observed redistribution of mitochondria around the nucleus; often they form dense clumps close to the outer nuclear membrane. Cells in all samples were with smooth periphery and without lamellar bodies in cytoplasm which indicated inhibition of surfactant synthesis (Fig. 2. — *B*).

Treatment with penthrane caused necrosis in a part of cells (not shown), while other part managed to adapt and possessed relatively preserved morphology (Fig. 3). The cytoplasm was well structured, with many lamellar bodies, endoplasmic reticulum and mitochondria (Fig. 3. — *A*). The cell periphery was relatively smooth but we do not observed secretion (Fig. 3. — *B*). Some mitochondria look dense and with reduced volume.

Conclusions

The ultrastructural changes observed after treatment with 3 mM halothane allowed us to suggest induction of apoptosis-like cell death. The halothane applied at this concentration completely suppressed surfactant production and mitochondria are

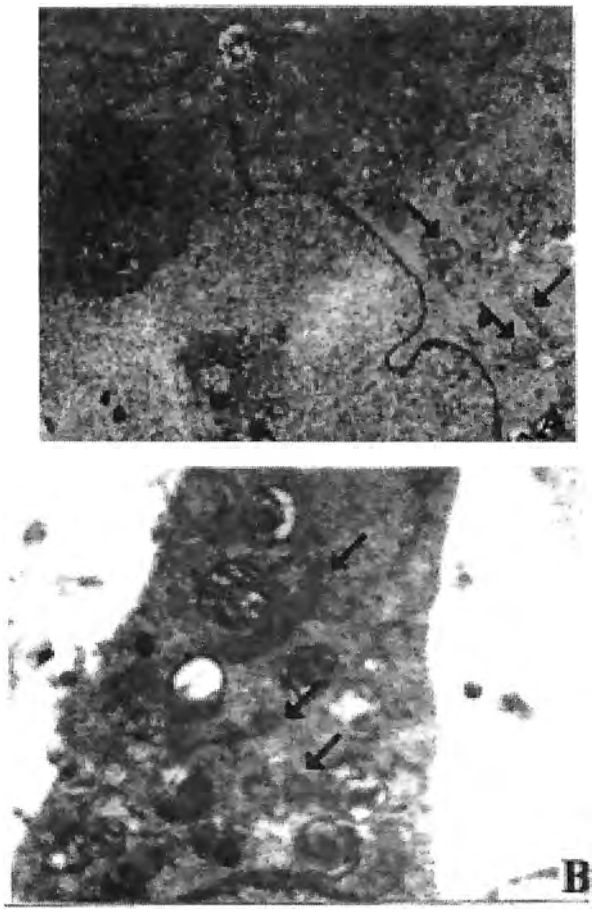

Fig. 3. Survived A 549 cells after treatment with penthrane
A — A 549 cell on the first day after treatment. Large nucleus with two nucleoli and many membrane structures in cytoplasm are seen (×6 400); *B* — A 549 cell on the third day after treatment. The lamellar bodies still persist but cell periphery is relatively smooth (×12 000). Some mitochondria look dense and with reduced volume (marked with arrows)

subjected to ultrastructural injuries, which were observed up to the third day after treatment. We established two groups of cell populations in dependence of the susceptibility to penthrane — more sensitive, which undergo necrosis, and more resistant, which preserve the morphology relatively unchanged.

Acknowledgements. The authors are very grateful to Prof. D. Markov from IMB, BAS and Prof. Bozilova-Pastirova from Medical University, Sofia. The authors are thankful to R. G. Stephanov for the technical assistance. This work was supported by a Grant from the Ministry of Education and Science (Grant MU-K-1307).

References

1. Lalchev, Z. et al. Alterations of biochemical and physiological quantities of pulmonary lavages attending halothane and penthrane treatment in rats. — Appl. Cardiopul. Pathophys., 4, 1992, 315-322.
2. Albertine, K. H. et al. Fas and Fas ligand are up-regulated in pulmonary edema fluid and lung tissue of patients with acute lung injury and the acute respiratory distress syndrome. — Am. J. Pathol., **161**, 2002, No 5, 1783-1796.

3. Morrison, R. J., A. Bidani. Acute respiratory distress syndrome epidemiology and pathophysiology. — Chest. Surg. Clin. N. Am., **12**, 2002, No 2, 301-323.
4. Lalchev, Z. Surface Properties of Lipids and Proteins at Bio-Interfaces. — In: Handbook of Surface and Colloid Chemistry (Ed. K. S.Birdi). CRC Press, Boca Raton, New York, 1997, 660-666,
5. Topouzova, T. et al. Cytotocic effect of inhalation anesthetics on human lung cells. — Ann. Univ. Sofia, **95**, 2003, No 4, 53-58.
6. Topouzova, T. et al. Assessment of genotoxicity of volatile anesthetic penthrane to human lung cells. — Ann. Univ. Sofia, **95**, 2003, No 4, 47-52.
7. Moskova, V., M. Pesheva, E. Stephanova. Preliminary studies for cytogenetic effect of halothane on human A549 cells and yeast *Saccharomyces cerevisiae*. — Ann. Univ. Sofia, **96**, (in press).
8. Topouzova, T. et al. Volatile anesthetic halothane causes DNA damage in A549 cells. — Cell Biol. Toxicol. (submitted).
9. Lieber, M. et al. A continuous tumor-cell line from a human lung carcinoma with properties of type II alveolar epithelial cells. — Int. J. Cancer, **17**, 1976, 62-70.
10. Valtcheva, R. et al. Effect of halothane on lung carcinoma cells A 549. — Chem.-Biol. Interact., **146**, 2003, 191-200
11. Desagher, S., J.-C. Martinou. Mitochondria as the central control point in apoptosis. — Trends in Cell Biol., **10**, 2000, 369-377.

Institute of Experimental Morphology and Anthropology

Acta morphologica et anthropologica, 10
Sofia • 2005

Presence and Distribution of *NGF* and *BDNF* Immunopositive Cells in Human Hyperplastic Thymus

*Ts. Marinova**, *K. Velikova***, *D. Petrov****, *G. Chaldakov*****, *L. Manni******, *L. Aloe******

* *Departments of Medical Biology, Medical University, Sofia*
** *Departments of General and Clinical Pathology, Medical University, Sofia*
*** *Departments of Surgery, Medical University, Sofia*
**** *Division of Cell Biology, Department of Forensic Medicine, Medical University, Varna*
***** *Institute of Neurobiology and Molecular Medicine, Rome*

We investigated, both at light and electron microscopic levels, the cellular distribution of immunoreactivity for *NGF (Nerve Growth Factor) and BDNF (Brain-Derived Neurotrophic Factor)* in myasthenic thymus. NGF and BDNF were expressed in human thymus and their expression was enhanced in the thymus of patients affected by Myasthenia gravis (histopathological findings-thymic hyperplasia), compared to the control subjects. The increased distribution of NGF and BDNF immunopositive cells correlated with thymocyte microenvironment alterations during myasthenic thymic transformation.

Key words: NGF, BDNF, thymus, hyperplasia, microscopy.

Introduction

Recent evidence indicates that some thymic cells produce NGF and BDNF, and express their low- and high-affinity receptors (p75, TrkA and TrkB) under both normal and pathological conditions, including autoimmune diseases [1, 2, 4, 7]. The present study was focused on: (i) cellular distribution of NGF and BDNF immunoreactivity, and (ii) structural alterations in the thymocyte microenvironment of human hyperplastic myasthenic thymus at both light and electron microscopic level.

Material and Methods

Thymus specimens from healthy subjects (n=7) and patients affected by Myasthenia gravis (MG), (histopathological findings-thymic hyperplasia, n=16, age range, 22 to 53 years) were obtained from surgery cases and used for histological and immunohistochemical analysis. Some kinds of antibodies (Ab), namely: Anti-NGF Ab (r)-(NGF H-20, sc-548), Anti-BDNF Ab (m)-(C-9, sc-8042), Anti-TrkA Ab (m)-(p-

TrkA E-6, sc-8058), Anti-TrkB Ab (r)-(794, sc-12) and Anti-Pan cytokeratin (m)-(C 1801), as well as ABC Staining System (r), ABC Staining System (m), Anti-rabbit IgG- and Anti-mouse IgG (whole molecule, 5nm or 10 nm gold granules) were used. Routine light microscopy, indirect immunoperoxidase method, transmission electron microscopy, immunoelectron microscopy, and immunogold-silver staining procedure were performed according to the standard protocols that we have previously described [3, 5]. Staining specificity was assessed by control tests. Labomikroscop Axioskop 20 (Fb Carl Zeiss Opton) and electron microscope Hitachi H500 were used.

Results

All types of medullary epithelial cells and some cortical epithelial cells displayed NGF and BDNF immunoreactivity in both pathological and normal thymuses. Strong immunoreactivity for NGF and BDNF was found in the medullary, subcapsular/subseptal epithelial cells, as well as in some mast cells, macrophages, and interdigitating reticulum cells in the thymus of subjects with hyperplasia-associated myasthenia gravis. The increased distribution of NGF and BDNF cortical immunopositive epithelial cells, forming islands or streaks, correlated with a spectrum of epithelial microenvironment structural alterations such as giant Hassall's corpuscles with atypical localization, lympho-epithelial cell complex formations and accumulated in large intrathymic areas intermediate filaments (Fig. 1). Numerous Hassall's bodies of MG subjects displayed elevated NGF- and BDNF-positivity

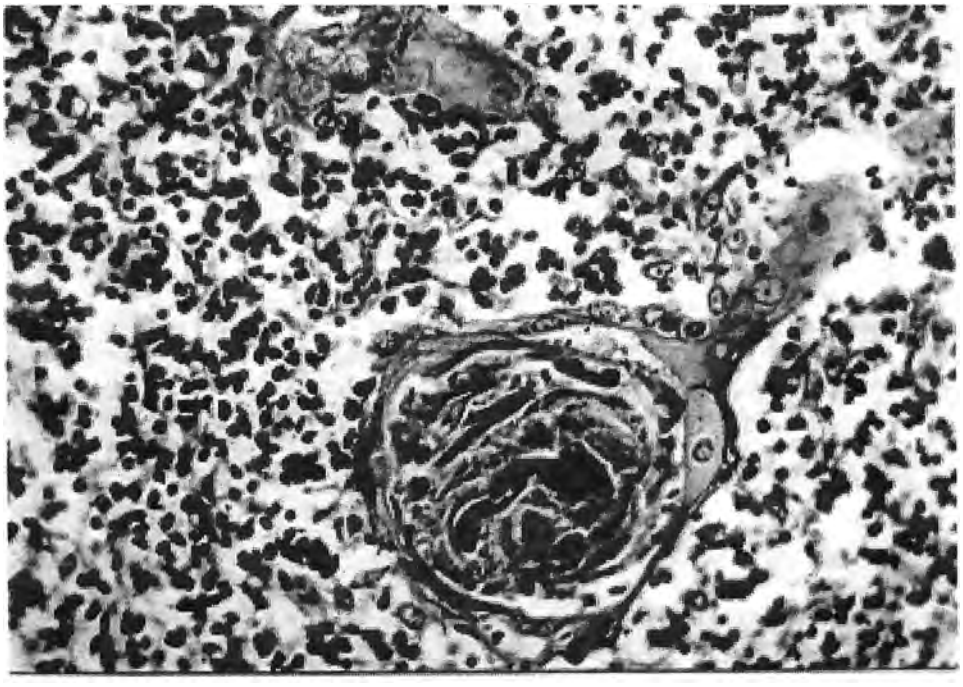

Fig. 1. Section showing a giant Hassall's corpuscle in the medullary region of hyperplastic myasthenic thymus (Magnification × 200)

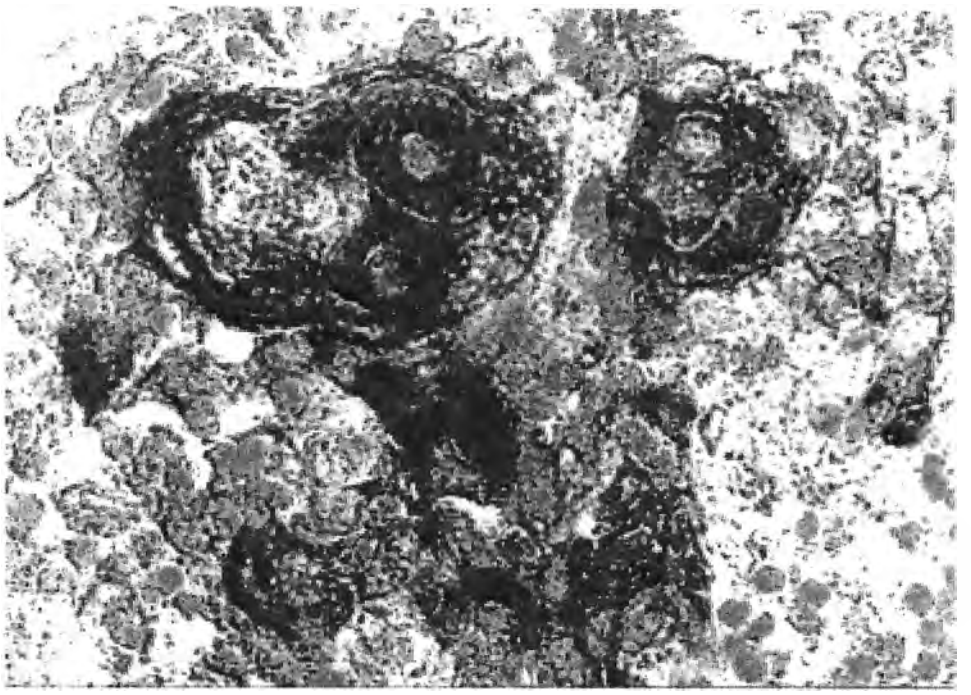

Fig. 2. Light micrograph demonstrating a strong NGF immunopositivity in the thymic medullary region, including in Hassall's corpuscles of myasthenic thymus (Magnification × 1000)

as compared to the Hassall's bodies in control thymus (Fig. 2). NGF- and BDNF-immunoreactivity was also found in the lympho-epithelial complexes of the myasthenic thymus, which were mainly localized in the cortical area.

Discussion

MG is a human autoimmune disease often leading to pathological manifestation in the thymus and in the nervous system [1, 6]. We have recently shown that the thymus of patients affected by MG expresses elevated levels of NGF suggesting a role of this neuroimmune mediator in the pathobiology of MG [5]. In the present study we detected that the thymocyte microenvironment undergoes reorganization during myasthenic hyperplasia, which includes essential regional and intracellular (structural and immunocytochemical) peculiarities. The increased expression of NGF and BDNF in thymic stromal cells suggests that these factors might be part of epithelial microenvironmental molecules implicated in thymic cell function and/or in the pathophysiology of MG. Our data raise the question of NGF and BDNF role in the local auto- and/or paracrine regulatory processes, and in the thymocyte microenvironment plasticity during myasthenic transformation.

References

1. Aloe, L. et al. Nerve growth factor and autoimmune diseases. — Autoimmunity, **19**, 1994, 141-150.
2. Aloe, L. Nerve growth factor and neuroimmune responses: basic and clinical observations. — Arch. Physiol. Biochem., **109**, 2001, 354-356.
3. Marinova, T. et al. Cellular localization of NGF and NGF receptors in aged human thymus. — Folia Biol. (Praha), **49**, 2003, 160-164.
4. Parrens, M. et al. Expression of NGF receptors in normal and pathological human thymus. — J. Neuroimmunol., **85**, 1998, 11-21.
5. Stampachiacchiere, B. et al. Altered levels of nerve growth factor in the thymus of subjects with myasthenia gravis. — J. Neuroimmunol., **146**, 2004, 199-202.
6. Turrini, P., M. L. Saccaria, L. Aloe. Presence and possible functional role of nerve growth factor in the thymus. — Cell. Mol. Biol., **47**, 2001, 55-64.
7. Vega, J. A. et al. Neurotrophins and the immune system. — J. Anat., **203**, 2003, 1-19.

Institute of Experimental Morphology and Anthropology

Acta morphologica et anthropologica, 10
Sofia•2005

Anthropology

Body Proportionality during the Growing up Period

A. Nacheva, L. Yordanova, E. Lazarova

Institute of Experimental Morphology and Anthropology, Bulgarian Academy of Sciences, Sofia

The aim of the present study is to characterize the formation of the specific for both sexes body proportionality during childhood and youth in boys and girls throughout 7 and 17 years of age. The data in the present work are a part of complex anthropological investigation (1993-2001) of 7-17 years old schoolchildren from Sofia city (1778 boys and 1824 girls). The bio-statistical characteristics of 5 basic body proportions and 5 relations in the growing up aged 7, 9, 11, 13, 15, and 17 years are analyzed and assessed. The results show that in 17 years old boys and girls, body structure is still far removed from those in 30-40 years old men and women. The 17 years old girls, lag more markedly in the formation of breadth body and extremity proportions, while the 17 years old boys lag in the formation of lower extremity length proportion, and its interrelation with the length of upper body segment.

Key words: body configuration, anthropometrical proportions and relations, childhood, youth.

Introduction

The proportionality of different body parts vary from birth till body maturation and reflect the conformity between the individual development stage and proportionality of separate body parts [1, 2, 3, 4]. The **aim** of the present study is to characterize the formation of the specific for both sexes body proportionality during childhood and youth in boys and girls throughout 7 and 17 years of age.

Material and Methods

The data in the present study are a part from complex anthropological investigation (1993-2001) of 7-17 years old schoolchildren from Sofia (1778 boys and 1824 girls). The bio-statistical characteristics of 5 basic body proportions and 5 relations in the 7, 9, 11, 13, 15, and 17 years old growing up schoolchildren are analyzed and assessed. The features' names are marked in the table.

Results about differences between male and female growing up individuals

Torso. During the period 7-17 years of age, the torso length proportion is relatively near for both sexes, as the relative length is bigger in the 7 years old children. At 13 years boys and girls have equal proportions, then the relative torso length in boys increases more sensible, and in girls more unnoticeable.

Chest. During the entire period of study, girls have relatively deeper chest, and boys have wider chest. In both sexes the chest proportions are bigger at 13 years.

Shoulders. Between 7 and 17 years, boys have relatively wider shoulders compared with girls, such as the sexual differences in adults are. Between 7 and 13 years, the relative shoulders' breadth decreases for both sexes, because of the more intensive stature growth in this period probably. In 13 years old boys and girls, the shoulders are relatively narrowest after what the relative shoulder breadth increases more markedly in boys.

Pelvis. After 7 years girls have wider pelvis consecutively than boys what are the sexual differences for adults. At 9 years of age for both sexes the bicristal breadth proportion is bigger. After 9 years this proportion decreases consecutively and at 17 the relative bicristal breadth is least for the studied period. The little relative pelvis width in 15 and 17 years old boys and girls compared with adults reflects the more intensive stature growth during this ontogenetic period. It is important to be mentioned the considerably smaller sexual difference for the 17 years old individuals (0,2 Index Units /IU/) compared with adults (1,3 IU). It shows that for both sexes after 17 years the pelvis' configuration will continue its formation until gathering the final pelvis' proportions type for 30-40 years old males and females.

Acromiocristal index. The correlation between bicristal and biacromial breadth distinctly characterized the sexual body configuration differences. Between 7-17 years girls have consequently higher values for this index, i.e. they are with wider relative pelvis measurements. At 9 years for both sexes, pelvis is with widest breadth proportion assigned to the acromion one, and at 17 years pelvis is with narrowest breadth.

Upper extremities. During the whole period 7 — 17 years, girls have smaller upper extremity length proportion than boys, what is the sexual difference in adults, as well. The data about breadth-length hand index show that at 7 years, girls have more gracile hands than boys have. These sexual differences maintain till 17 years of age. For both sexes, hand is most massive at 13 years.

Lower extremities. At 9 years boys and girls are with better-expressed makroskely. At 13 years the sexual differences are bigger, when the puberty in girls is already finished. After 13 years, the formation of the final lower extremity length proportion accelerates with more intensive rate.

The correlation of both foot measurements in adults shows a little bigger foot breadth proportion in females, probably because of the flatfootness, which occur more frequently in them. Opposite to the adults throughout the period 7 and 17 years, girls have more gracile feet (relatively narrower) compared with boys. The intersexual differences are significant till 11 years, and after this age they diminish. Between 13 and 17 years for both sexes the foot configuration didn't alter.

Inter-extremities index. The proportionality between upper and lower extremities length is important characteristics of human body configuration and bears specific information about sexual differences. In the 30-40 years old individuals, the upper extremity length assigned to the lower extremity length is longer in males compared with females. The same is the tendency of sexual differences throughout the period 7-17 ages. These differences are least between 11 and 13 years of age.

Table 1. Investigated features and their statistical data

Sex	Features	7 years n=182		9 years n=189		11 years n=182		13 years n=165		15 years n=124		17 years n=118		**Adults n=2427**
		X	SD	X	SD	X	SD	X	SD	X	SD	X	SD	X
Boys	Torso length proportion	29.5	1.8	28.4	1.4	27.3	1.2	26.7	1.4	28.1	1.2	28.3	1.6	**31.0**
	Thoracal index	71.2	4.6	72.6	4.8	71.9	5.0	72.8	5.2	72.4	6.7	72.0	7.0	**72.0**
	Biacromial breadth proportion	21.9	0.8	21.8	0.8	21.7	0.8	21.7	0.8	22.3	0.9	22.6	1.1	**23.7**
	Bicristal breadth proportion	15.2	0.8	15.4	0.9	15.3	1.0	15.1	1.1	14.9	1.1	14.9	1.0	**17.6**
	Acromiocristal index	69.8	4.5	70.9	3.9	70.6	4.2	69.5	4.9	66.7	4.3	65.9	4.1	**74.3**
	Upper extremity length proportion	45.8	1.6	45.5	1.4	45.3	1.2	45.1	1.3	44.7	1.2	44.6	1.4	**44.6**
	Hand breadth-length index	39.6	3.1	40.9	2.9	41.0	2.3	42.1	2.6	41.2	2.8	41.0	2.9	**43.1**
	Lower extremity length proportion	57.6	1.6	59.6	1.3	58.3	1.5	59.1	1.3	58.2	1.2	57.7	1.3	**56.8**
	Foot breadth-length index	37.2	1.8	37.0	1.8	37.0	1.7	37.9	1.9	37.8	2.0	37.9	2.0	**38.7**
	Interextremity index	79.7	3.2	76.3	2.8	77.7	2.7	76.4	2.4	76.9	2.4	77.3	2.6	**78.5**
Number		n=178		n=183		n=205		n=184		n=137		n=135		**n=2847**
Girls	Torso length proportion	28.9	1.4	28.1	1.3	27.3	1.1	26.9	1.2	27.3	1.6	27.5	1.3	**31.4**
	Thoracal index	71.9	5.1	73.1	5.3	72.2	6.0	73.9	5.8	73.8	6.3	73.0	6.0	**72.0**
	Biacromial breadth proportion	21.5	0.8	21.5	0.8	21.4	1.0	21.4	1.0	21.7	1.0	21.8	0.9	**23.3**
	Bicristal breadth proportion	15.0	0.9	15.5	1.0	15.3	1.1	15.3	1.2	15.1	1.0	15.1	0.9	**18.9**
	Acromiocristal index	69.7	3.7	72.2	4.3	71.7	4.6	71.4	4.8	69.6	4.4	69.0	4.1	**81.3**
	Upper extremity length proportion	45.2	1.5	44.8	1.3	45.0	1.2	44.3	1.3	43.9	1.3	43.8	1.3	**44.0**
	Hand breadth-length index	39.0	3.6	40.2	2.9	40.2	2.5	40.9	3.0	40.6	3.2	40.7	2.5	**42.0**
	Lower extremity length proportion	57.7	1.4	59.6	1.2	58.0	1.3	58.1	1.3	57.6	1.3	57.3	1.2	**57.2**
	Foot breadth-length index	36.3	1.9	36.0	1.8	36.5	1.6	37.5	1.8	37.5	2.0	37.6	1.7	**39.1**
	Interextremity index	78.3	2.8	75.3	2.1	77.5	2.4	76.3	2.2	76.2	2.4	76.4	2.4	**77.0**

Differences between the 17 years old individuals and the adults aged 30-40 years.

At 17 years the **torso length proportion** for both sexes is considerably lower than those for adults / boys (—2,7 IU); girls (—3,9 IU)/, as in the 17 years old girls the relative trunk length will continue to grow up more intensive than in boys. The **chest form** in boys aged 17 years is already the same as it is in adult males, while the 17 years old girls have still more childish chest configuration. At 17 years the **relative shoulder width** for both sexes have lower values than those in adults /boys (—1,1 IU); girls (—1,5 IU).

The **pelvis proportionality** at 17 for both sexes is far from its configuration for adults /boys (—2,7 IU); girls (—3,8 IU)/. The data about acromiocristal index show that during puberty and post puberty ages the formation of body breadth configuration drop behind body height configuration because of the more intensive stature growth in them probably. At 17 years the slow-down is more strongly expressed in girls /boys (—8,4 IU), girls (—12,3 IU)/. The sexual difference in the 17 years old individuals is 3,1 IU in favour of the female ones, and in the 30-40 years old females it is more than two times higher — 7,0 IU. The **upper extremity length proportion** for both sexes show that at 17, the corresponding linear configuration for adults is already shaped up. The formation of the hand massiveness, however, is still forthcoming /boys (—2,1 IU), girls (—1,3 IU)/. The **lower extremity length proportion** shows that in girls at 17 the formation of the corresponding linear configuration is already finished. The boys at 17 are still with relatively longer lower extremities than the males at 30-40. The **proportionality between upper and lower extremities length** in the 17 years old girls are closer to the respective ones in adults (—0,6 IU), while in the 17 years old boys this difference is (—1,2 IU), i.e. for them the formation of the final proportion between upper and lower extremities length is forthcoming.

Conclusion

The body configuration of the 17 years old boys and girls is still far from the body configuration of the 30-40 years old men and women.

The backward of the 17 years old girls is more well expressed in the formation of the proportionality of body and extremity breadth measurements, and of the 17 years old boys in the formation of the proportionality of lower extremity length and its correlation to the upper extremity length.

References

1. Growth and Ontogenetic Development in Man IV. — In: Pross. of the Symp., Humpolec, 1989. (Ed. K. Hajnis), 123-136; 175-184.
2. Human Growth. A comprehensive treatise, sec. Edition. T. 3. (Ed. Falkner Fr., J. Tanner), 1987, 331p.
3. K o m e n d a, S., J. K l e m e n t a. Proportion of Body Dimensions in Children and Youth. Praha, 1978, 270p.
4. Physical Status: The Use and Interpretation of Anthropometry. — In: Report of a WHO Expert Committee. Techn. Rep. Series, **854**, 1995, 4-33.

Institute of Experimental Morphology and Anthropology

Acta morphologica et anthropologica, 10
Sofia•2005

Height and Some of the Body Proportions by the Vision of Artistic Anatomy

A. Yilmaz, S. Cikmaz, M. E. Cicek

Trakya Universty, Faculty of Medicine, Department of Anatomy, Edirne, Turkey

In this study, we tried to examine the body proportions of Turkish woman according to artistic anatomy and how the change of length values of the parts that form the body effect the body height.

541 male students who had no orthopaedic and physical defect and educating in Trakya University Medical Faculty took place in our study. The Harpender anthropometer was used in measurements. The measurement distances, mean values, standard deviations, proportions to body height and correlation coefficients in our study are like this respectively: **1) Basion-vertex (body height):** 173,67 ± 5,34 **2) Basion-gnathion:** 149,40 ± 4,94, %86,01, 0,31, **3) Basion-acromion:** 143,36 ± 5,8 %82,54, 0,84, **4) Basion-suprasternale:** 141,50 ± 4,76, %81,25, 0,60, **5) Basion-thelion:** 127,27 ± 4,33, %73,29, 0,88, **6) Basion-omphalion:** 104,44 ± 3,95, %60,13, 0,87, 7) **Basion-iliospinale:** 98,49 ± 3,92, %56,19, 0,83, **8) Basion-trochanterion:** 90,39 ± 3,87, %51,34, 0,78, **9) Basion-symphysis:** 88,40 ± 3,34, %50,70, 0,79, **10) Basion-gluteale:** 79,40 ± 3,45, %45,71, 0,81, **11) Basion-dactylion:** 64,64 ± 3,48, %37,21, 0,68, **12) Basion-tibiale:** 46,14 ± 2,81, %26,28, 0,58, **13) Basion-sphyrion:** 8,35 ± 0,55, %4,80, 0,22.
As a result, we could say that:Thigh length has much important effects on forming the body length, than the leg length. These results are compared with the data available in the literature.

Key words: Artistic anatomy, anthropology, proportion.

Introduction

For 5 thousand of years, the human body had been studied continually by artists and scientists. The artists, who use the human body as a narration symbol, had investigated the human anatomy by the vision of artistic anatomy thoroughly. They had accepted: Their work of arts like their pictures and statues have some proportions on human body. And they had used these proportions in their lots of evidence [1, 2].

The proportions between the different parts of the human body had been called CANON. And the unit measure of every canon had been defined as MODULE [1, 4, 6]. Artists had used different modules like foot length, hand length, head height and third finger length in different canons [8, 9].

The oldest canon which is in Egypt, accepts the foot length as module. From their graves and not-ended pictures in pyramids, we understand that the height of the human body is equal to six times of the foot length. However, some artists had accepted the foot length 1:7 of the body height. But on the new Egyptian Canon, the module is the third

finger length of the hand. As humanity history develops, lots of artists had defined different canons in their own cultural and social comprehension [5, 10].

In 19th Century, whith the Schmidt-Fritsch Rule, which was planned by Schmidt and developed by Fritsch, anthropometric methods were used. This rule explains the anatomical structure of human body with mathematical expressions. According to the rule, from a portion of the human body, the other parts could be determined. The proportions between the portions of human anatomy was scientifically defined by Dr. Paul Richer for the first time [1, 2, 4, 8].

With this study, we purposed to examine some of the human body proportions on Turkish male adults by artistic anatomy. We searched the orientation points mentioned in canons, the levels according to body height of a man figure standing up right, commission parts from the base line. And the most important thing, that we consider, is how much effects portions that constitute the human body on the body height.

Material and Methods

We made this study on 541 male students of Trakya University Medicine Faculty. Our subjects have not any physical or orthopedic defects. We did not care race, lineage and religion. Only, representing Turkish male was sufficiently for us. We used Harpender anthropometer for our measurements. Findings were recorded to the view that we made at first. Arithmetic average, standard deviation and correlation analysis were checked.

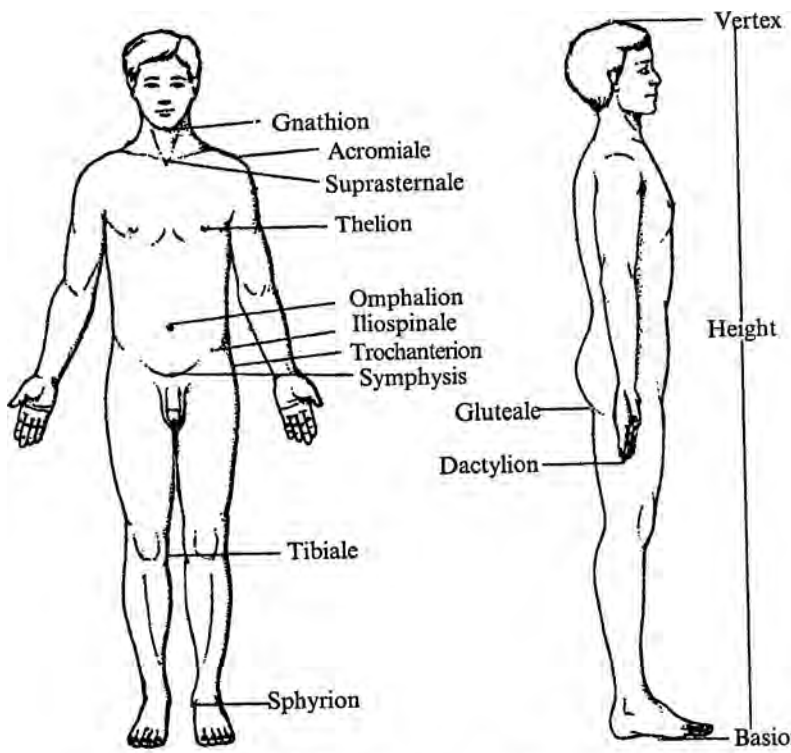

Fig. 1. Anthropological points

The aim of our research is not the averages of body height of subjects or metric values of some of the body portions. Our aim is to create the correlation between height and the proportions that constitute the height. We got benefit from classical known anthropological locations for a standard measurement. And we added some superficial locations which didn't use anthropometry but are preferred in plastic anatomy [7, 11].

On normal anatomical position, the distance between anthropological spots and sole was compared (Fig. 1). 1-Vertex 2-Gnathion 3-Acromion 4-Suprasternale 5-Thelion 6-Omphalion 7-Iliospinale 8-Trochanterion 9-Symphisis 10-Gluteale 11-Dactylion 12-Tibiale 13-Sphyrion [11].

Findings

The average values and determined ratios of our study on young Turkish men are shown in table 1 by using per cent.

And the correlation analysis between our subjects' height and proportions that constitute the height is shown in a shape of diagram (Table 2).

Table 1. The average values and determined ratios of our findings

Features	min	max	mean	SD(±)
Boy	148.00	194.00	173.67	5.34
B-Gn	129.50	168.00	149.40	4.94
(B-Gn/body height)*100	79.94	86.60	86.01	0.33
B-Acr	100.00	180.00	143.36	5.08
(B-Acr/ body height)*100	67.57	92.78	82.54	0.60
B-St	119.00	160.00	141.10	4.76
(B-St/ body height)*100	80.41	82.47	81.25	3.68
B-Ma	107.00	145.00	127.27	4.33
(B-Mam/ body height)*100	74.66	74.74	73.29	3.32
B-Um	85.00	124.00	104.44	3.95
(B-Um/ body height)*100	57.43	63.92	60.13	0.48
B-Sp	80.00	112.00	98.49	3.92
(B-Sp/ body height)*100	54.05	58.95	56.19	5.73
B-Tro	74.00	104.00	90.39	3.87
(B-Tro/ body height)*100	50.00	54.88	51.34	6.23
B-Sy	72.00	100.00	88.40	3.34
(B-SY/ body height)*100	48.65	51.81	50.70	3.27
B-Gul	64.00	93.00	79.40	3.45
(B-Gul/ body height)*100	43.24	47.94	45.71	0.60
B-Acm	50.50	78.00	64.64	3.48
(B-Acm/ body height)*100	34.12	40.21	37.21	0.90
B-Tib	37.00	57.00	46.14	2.81
(B-Tib/ body height)*100	25.00	29.38	26.28	2.80
B-Sph	5.50	15.00	8.35	1.15
(B-Sph/ body height)*100	3.50	7.73	4.80	0.55

Table 2. Correlation analysis between our subjects' height and proportions that constitute the height and the comparison of our findings with the literature data

Leonardo, Dürer	Paul Richer	Our Study	Correlation	Vertex	
100	100	100			
				Gnathion	
87,5	86,7	86,01	0,31	**B-Gn**	0,31
				Acromiale	
****	****	82,54	0,84	**B-Acr**	0,84
				Suprasternale	
83,0	****	81,25	0,60	**B-St**	0,60
				Thelion	
75,0	73,4	73,29	0,86	**B-Th**	0,86
				Omphalion	
****	60,1	60,13	0,87	**B-Omp**	0,87
				Ɔliospinale	
****	****	56,19	0,83	**B-Sp**	0,83
				Trochanterion	
****	****	51,34	0,78	**B-Tro**	0,78
				Symphysion	
50,0	****	50,7	0,79	**B-Sy**	0,79
				Gluteale	
****	46,8	45,71	0,81	**B-Glu**	0,81
				Dactylion	
****	****	37,21	0,68	**B-Dac**	0,68
				Tibiale	
25,0	26,7	26,28	0,58	**B-Tib**	0,58
				Sphyrion	
****	****	4,8	0,22	**B-Sph**	0,2

Discussion

Body height of the human beings and the proportions of their body parts change according to the geographical region that they live in, their race and nourishment styles [3, 5].

Today artists, but also a lot of scientists make studies on human body. At the same time, esthetics and forensic medicine have progressed on the term.

Our subjects' average height is: 173.67 cm. And height changes according to the changes in social and economic conditions. However, proportions could be changed. Our proportions are harmonius with those of Paul Richer (1920), who has studied contemporary Europeans, rather than the archaic epoch (Polykleitos) and Renaissance Period (Leonardo, Dürer). Besides, the olden famous artists had had a search of ideal artistic models. But Paul Richer preferred to evaluate a real, alive average European type by scientific methods [1].

The most important point of our view is the effects of the parameters that form the body length. We searched the correlation between the average values of the body portions and the average height. And as a result, the most important parts that effect the height are mamillar, umblical, gluteal, symphysis, trochanterion, spinale and acromion heights.

4.80% of average body height made of Sphyrion height and 86.01% of average body height made of Gnathion height haven't any correlation with body height. We

could explain this with the augmentation of the head heights of Turkish men. The upper and lower points (sphyrion, gnathion) haven't a direct correlation with the body length. Because of that, it's impossible to evaluate the foot height and head height with the height of human beings. Tibiale and suprasternale that are close to these points, have not a strong relation too. But the middle parts of the body height (omphalion, thelion), which are soft tissues, have the best relation. Acromiale, that joins the upper extremity and iliospinale that joins the lower extremity, may be safe criterions. Dactylion which shows the length of upper exremity and Trochanterion which is about lower extremity have a poor relation index. In the past, Gluteale, which had been determined by Paul Richer, is rather a safe point, and it has a good relation with the body height.

As a result, we could say that: Thigh length has much important effects on forming the body height, than the leg height.

References

1. Cokanov, K. Plasticna Anatomia. Sofia, Nauka i Izkustuo, 1974, 360-390.
2. Dere, F., O. Oguz. Artistik Anatomi. Adana, Nobel Kitabevi, 1996, 11-20.
3. Inan, A.Türkiye halkının Antropolojik karakterleri ve Türkiye tarihi; Türk Tarih Kurumu Basımevi. Ankara, 1947, 54-72.
4. Kahraman, G.Yetiskin Turk Kadin ve Erkeklerinde Ust ekstremite Olcumleri ve Oranları. Uzmanlık Tezi, Istanbul, 1988.
5. Kahraman, G. et al. Turk Kadinlarinda Ust Ekstremite'ye Ait Bazi Olcum ve Oranlar. — T.U.Tip Fakultesi Dergisi, **12**, 1995, No 1, 60-71.
6. Lumley, Jhon, S. P. Surface Anatomy, The Anatomical Basis Of Clinical Examination, International Student Edition (Second Edition). — Edinburgh, London, Churchill-Livingstone, 1966, 55-81.
7. Mesut, R., M. Yildirim. İnsan Vucudunda antropolojik ve Yuzeyel Bulus Noktaları. — Istanbul, Beta Basim Yayim Dagitim A.S., 1989, 50-58.
8. Muftuoglu, A.Yetiskin Turk Erkeklerinde Bazi Vucut Olcumleri ve Aralarindaki Oranlar. — Uzmanlık Tezi, Istanbul, 1981.
9. Taskınalp, O., R. Mesut. "Boy-Beden" Iliskisine Esas Bazı Antropometrik Orantilar.-T.U.Tip Fakultesi Dergisi, **8, 9, 10** (Bilesik sayı), 1991, 1-8.
10. Yildirim, M., O. Taskinalp, G. Kahraman. Yetiskin Turk Erkeklerinde Boy ile bazi El ve Ayak Olculeri Arasında Somatometrik Iliıokiler. — T.U.Tıp Fakultesi Dergisi, **5**, 1988, No 1, 75-81.
11. Yordanov, Y. Naritchnik po antropologiya. Sofia, Universitetsko İzdatelstvo "Sv. Kliment Ohridski", 1997, 150-159.

Institute of Experimental Morphology and Anthropology

Acta morphologica et anthropologica, 10
Sofia • 2005

The Variations of Auricular Tubercle in Turkish People

H. Gurbuz, F. Karaman, R. Mesut

Members of Trakya University, Medical Faculty, Department of Anatomy, Edirne, Turkey

In this study, 202 ears of 44 male and 57 female volunteer students were examined in order to classify the variations of auricular tubercle of Darwin in a Turkish population. Ears were classified into five subtypes according to the existence and significance of Darwin's Tubercle. The relation of birth order and gender to the variation of auricular tubercle were also investigated in this study. No difference was found related to gender but birth order was found to affect the variations.

Key words: Darwin's tubercle, helix, auricle, variation, classification.

Introduction

Ear, our hearing and balance organ, has three components: outer ear, middle ear and inner ear. Auricle (outer ear) is formed by auricle and external acoustic mea. Middle ear is a pneumatic space in the petrose part of temporal bone. Inner ear contains the components that are related to hearing and balance [12].

At the embryological development state, the inner ear develops from the ectoderm, the middle and the outer ear develop from the branchial system. Auricle (outer ear) appears as six mesenchymal bulges on the 1st and 2nd pharyngeal arcs. These bulges, the half of which are located at both sides of external ear passage, then unite to form the permanent earlap [1, 11, 13].

The characteristics of auricle comes from the cartilage of the ear. The prominent rim of the auricle is called the helix. Helix begins from the point where the skin of ear is connected to the head and developes upwards and downwards. Where the helix turns downward behind, a small tubercle, the auricular tubercle of Darwin, is frequently seen in Fig. 2-6 [6]. In some people where the Darwin's tubercle is located the helix is not curled but bare and tense. This broads the upper part of the ear and causes it to be similar to that of some adult monkeys'. In some rare cases this curled part does not exist, with being broad and pressed down to backwards which causes it to look as if the margin has been cut. Also sometimes the upper part of the helix is sharply pointed, this is called apex auricle (Darwin) [10, 15, 17] (Fig. 1). As we can understand from this, Darwin's tubercle exist in many different types. This formation is similar to that of some sharp-eared mam-

mals [8]. This feature is called Darwin's tubercle, even though it was first described by Woolner, a sculptor. A diagram of this landmark appears in Darwin's The Descent of Man (1871) [3-http://www.gpnotebook.co.uk- http://uic.edu].

The fusion of earlap bulges is a complex process, for this reason frequently developmental abnormalities can be seen. Many of recessions, processes, channels, cavities exist on the external side of auricle. Darwin's tubercle is assumed by evolutionary biologists to be a "residual" of quadrupeds which had various shapes of ears and it has been carried to humans. This tubercle is very evident about the sixth month of fetal life when the whole auricle has a close resemblance to that of some adult monkeys, after that it becomes smaller [2, 15].

Auricular tubercle can be described as one of the relatively common simple traits found in humans and it's widely used as a landmark in many studies [5, 9, 14].

Aims

The tubercle is inherited as a dominant, but the expression (size) is quite variable (http://www.faculty.fairfield.edu). Its absence is inherited as a ressesive. Some induviduals may have it only on one ear (http://uic.edu). The aim of our study was to classify the variations of auricular tubercle in five subtypes and investigate their relations to gender and birth order in a Turkish population.

Material and Methods

The ears of forty-four male and fifty-seven female students of Trakya University Medical Faculty were examined in this study. Students were randomly chosen and they were asked about their ages and birth orders. Afterwards Darwin's tubercle in both ears were recorded as one of the subtypes and a single sample of each subtype was monitorized with a digital camera. These subtypes include:

1 =Undeveloped Darwin's Tubercle
2 =Semi-developed Darwin's Tubercle
3 =Fully-developed Darwin's Tubercle
4 =Very significant Darwin's Tubercle
5 =Multiple Darwin's Tubercle

Subtype 1 = Undeveloped Darwin's Tubercle:
In this type no Darwin's tubercle was seen on the helix.

Subtype 2 = Semi-developed Darwin's Tubercle
There was a semi-developed sized Darwin's tubercle in this subtype but still it was not easily seen.

Subtype 3 = Fully-developed Darwin's Tubercle
In this subtype Darwin's tubercle was easily found on helix but was not so clear as to be seen from half a meter away.

Subtype 4 = Very significant Darwin's Tubercle
Darwin's tubercle was very significant and even from a meter away it could easily be seen.

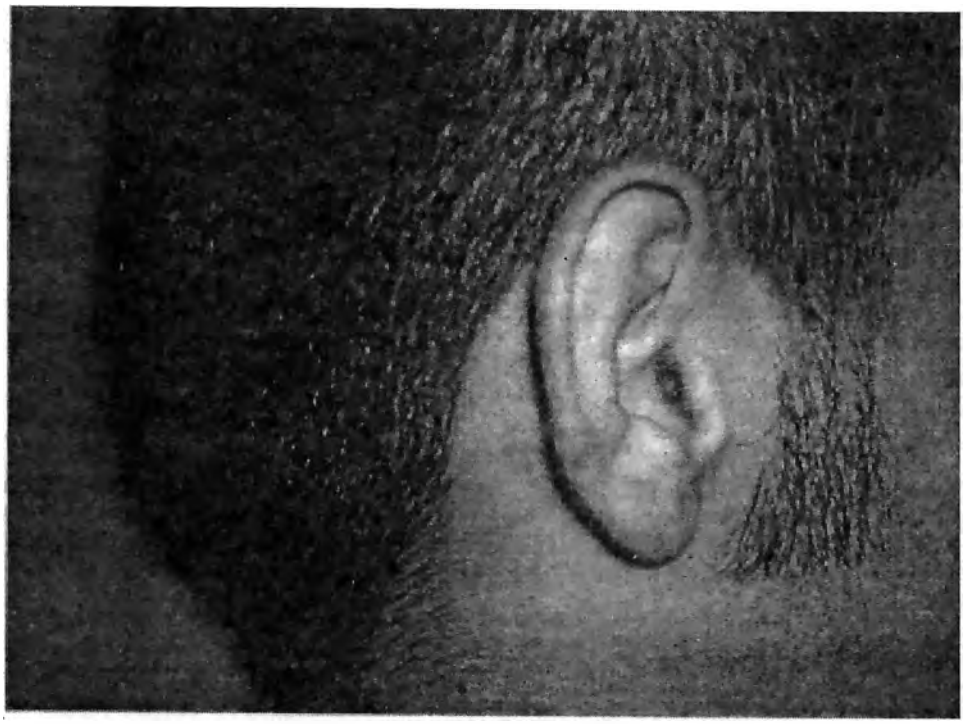

Fig. 1. Undeveloped Darwin's Tubercle

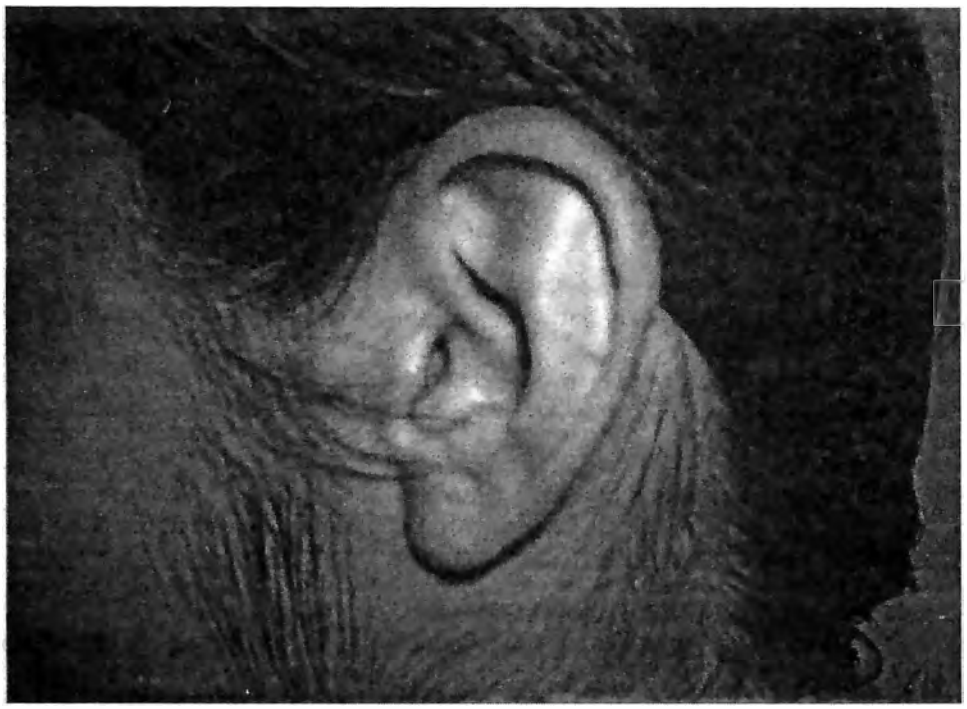

Fig. 2. Semi-developed Darwin's Tubercle

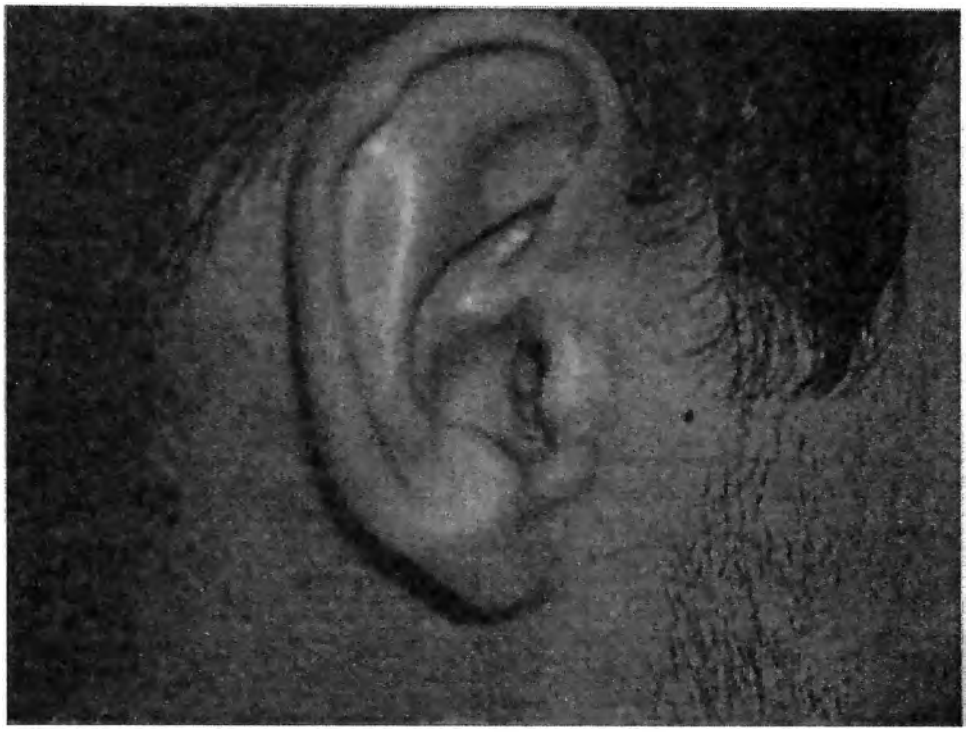

Fig. 3. Fully-developed Darwin's Tubercle

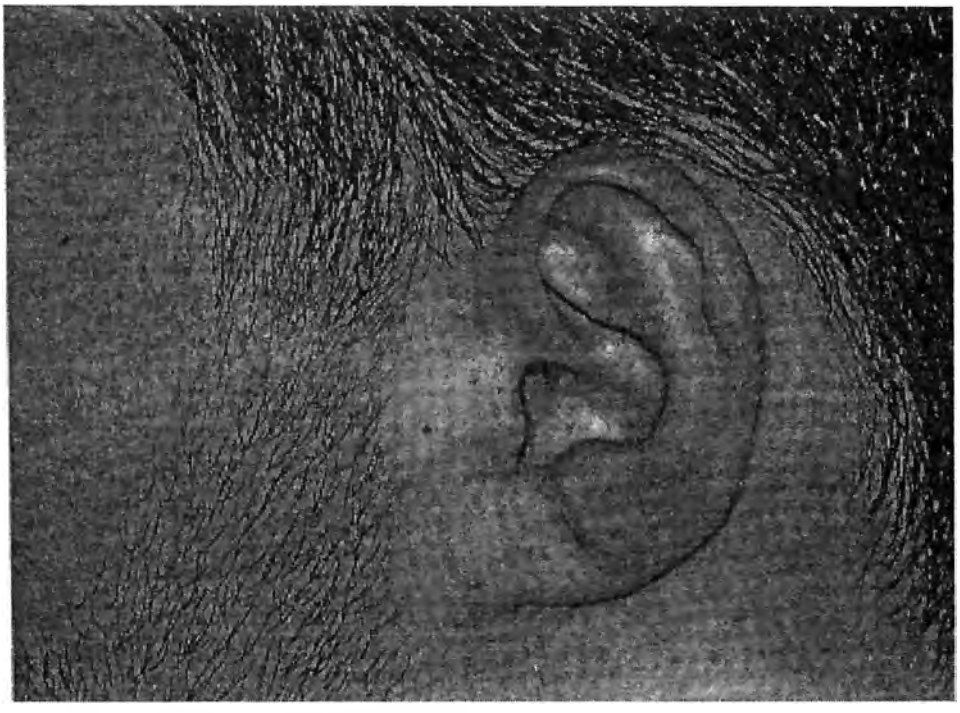

Fig. 4. Very significant Darwin's Tubercle

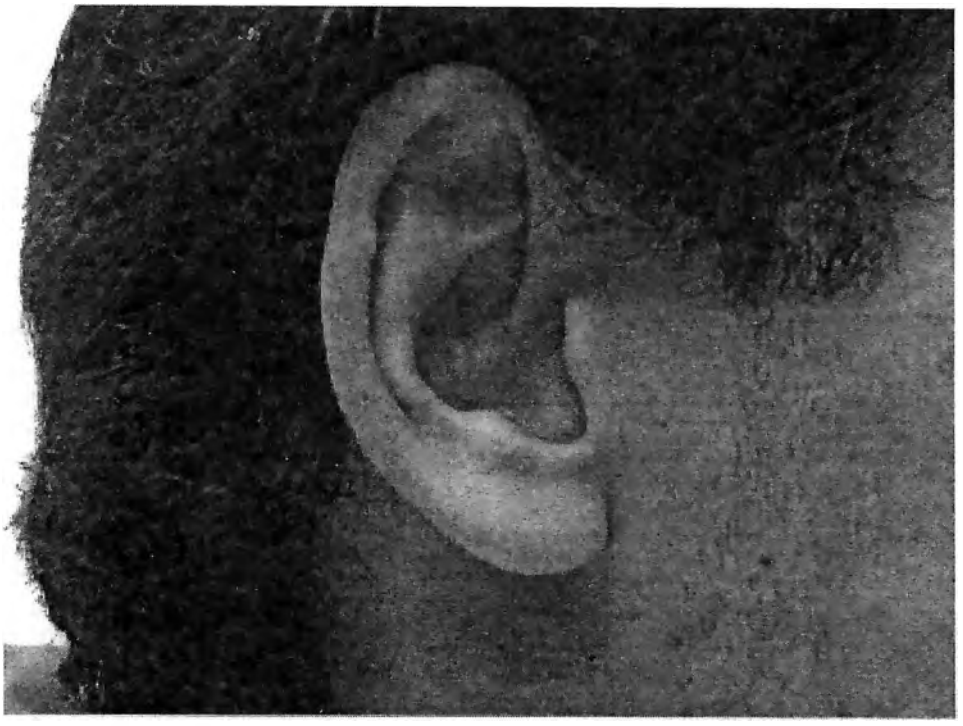

Fig. 5. Multiple Darwin's Tubercle

Fig. 6. Apexauricle. spg

Subtype 5 = Multiple Darwin's Tubercle
In this subtype more than one Darwin's tubercles were seen.

Statistical analysis was performed with SPSS 10.0 for Windows, $p<0.05$ was considered statistically different. Spearman's sho correlation test was used to perform the statistics.

Findings

There was no significant difference related to birth order in variation of right auricular tubercle ($p>0.05$). Significance occurred in left auricular tubercle ($p<0.05$). No Darwin's tubercle was the most frequent in first children. Undeveloped Darwin's tubercle was the secondly most frequent. The third, fourth, and fifth parameters were mostly frequent in first children also. There were fifty-three first children and the being first child was the most frequent. In second children the first parameter was significantly more frequent, others did not have any significance in the existence of auricular tubercle. Neither right ($p>0.05$) nor left ear had any difference related to gender. On both sides it was homogene and had no difference related to birth order. In both genders there was positive relation in left and right auricle and increase in one auricle affected the other which caused the tubercle of the opposite one to increase too.

Discussion

In our study we investigated the existence of auricular tubercle in a Turkish population. We subtyped the existence according to our findings.

Cephaloscopy, a technique used for classification of the head according to proper points [16].

In an animal study about the role of excessive doses of vitamin A during pregnancy, it was found that the primary target for retinol-induced dysmorphogenesis was the craniofacial region. In the same study six of the eight malformed fetuses exhibited unilateral or bilateral ear defects which consisted of hypoplasia of some areas of ear derived from the first pharyngeal arch (helix, crus of helix) or second pharyngeal arch (auricular tubercle, crura of antihelix, lobule, and antitragus). Although we did not study its effects, this data lead us to think besides the genetic affects the variation of auricular tubercle might be a result of the variable vitamin A consumption during pregnancy [7]. But we believe that further studies on this topic are still needed and for further studies on this topic our classification of the variations of auricular tubercle is going to be helpful.

With this study we wished the classification of auricular tubercle to be a premiss both to clinical anatomy and to anthropology.

References

1. Altuğ, H., F Senocak, O. Sunar. Autolaryngologia. Istanbul, Hilal Press, 1983, 4-5.
2. Arıncı, K., A. Elhan. Anatomy. Ankara, Gunes Press, 1995, 466 p.
3. Cankur, S. Dictionary of morphological eponyms. Istanbul, Nobel Medical Press, 2002, 151.
4. Çokanov, K. 1974. Plasticnaya anatomia, Sofia, Nauka i Izkustvo, 167 p.

5. Dharap, A. S., M. Than. Five anthroposcopic traits of the ear in a Malaysian Population. — Anthropol. Anz., 5, 1995, No 4, 359-363.
6. Grant Boileau, J. C. Atlas of Human Anatomy (Ed. O.Kuran). — Istanbul, Guven Press, 1977, 469 p.
7. Hendrickx, A. G. et al. Vitamin A teratogenicity and risk assessment in the macaque retinoid model. — Reprod. Toxicol., 14, 2000, No 4, 311-323.
8. Kadanov, D., 1957. Anatomia Na Nervnata sistema i na setivnite organi, Sofia, Meditsina i Fizkultura, 379 p.
9. Kino, K. et al. Reconsideration of the bilaminar zone in the retrodiscal connective tissue of the TMJ. 2. Fibrosus structure of the retrodiscal connective tissue and relation between those fibers and the disk. — Nihon Ago Kansetsu Gakkai Zasshi., 1, 1998, No 2, 43-54.
10. Kuran, O. Systematic Anatomy. Istanbul, Filiz Press, 1983, 760 p.
11. Moore, K. L., T. V. N. Persaud. Human Embryology (Ed. M. Yıldırım M). Istanbul, Nobel Medical Press, 2002, 507 p.
12. Sadler, T. W. Medical Embryology (Ed. AC. Basaklar). Ankara, Ozkan press, 1996, 338-341.
13. Snell, R. S. Clinical Anatomy (Ed. M. Yıldırım). Istanbul, Nobel Medical Press, 1998, 725-726.
14. Tolleth, H. Artistic Anatomy,dimensions, and proportions of the external ear. — Clin. Plast. Surg., 5, 1978, No 3, 337-345.
15. Williams, P. L. et al. Gray's Anatomy. New York, 1995, 1367 p.
16. Yordanov, Y. Naritchnik po antropologia. Sofia, Universitetsko Izdetelstvo, 1977, 139 p.
17. Zren, Z. Human Anatomy. Istanbul, Celiker Press, 1971, 620 p.

http://www.faculty.fairfield.edu , Building A Hardy-Weinberg Database:Extracting Genotypic Information fom Phenotypic Traits, adapted from Harti; 1985.
http://www.gpnotebook.co.uk ,General Practice Book-a UK medical, encyclopedia on the world wide web.
http://uic.edu , 5.3 Simple Human Non-Metric Traits/II.Darwin's Tubercle.

Institute of Experimental Morphology and Anthropology

Acta morphologica et anthropologica, 10
Sofia • 2005

Basic Body Diameters and Their Proportions of Newborns in Sofia during 2001

I. Yankova

Institute of Experimental Morphology and Anthropology, Bulgarian Academy of Sciences, Sofia

In the present study data about basic body diameters and their proportions in newborns are analyzed and the sexual differences are estimated as well. During the period of April — May 2001 a total of 219 full-term (38 — 42 G.W.) and healthy newborns (110 boys and 109 girls) are studied in the first 24 hours after birth. Seven body diameters are measured by the standard method and their proportions are calculated. The metrical data show that boys have bigger sizes of biacromial and pelvis diameters and proportional wider shoulders and pelvis than girls. The newborn boys and girls didn't differ significantly according to the two chest diameters, although the girls have wider chest and boys have deeper chest.

Key words: newborns, body diameters, proportions of body diameters.

Introduction

Body diameters are a group of anthropometrical features characterizing body development and massiveness of different body parts: shoulders, chest, and pelvis. The body proportions give general notion about body physical type and its growth changes.

The aim of the present study is to analyze the basic body diameters and their proportions of newborns in Sofia at the beginning of the 21st century.

Material and Methods

The present data are a part of detailed anthropological investigation, carried out during April-May 2001. The study includes 219 full-term and healthy newborns (110 boys and 109 girls). Thirty-eight anthropometrical features are measured in the first 24 hours after birth by Martin-Saller's classical method [1]. Data about seven diameters and their proportions are presented below.

The sexual differences are assessed by the Student's t-test ($P<0,05$) and by the Index of sexual differences (ISD = $X_{♀} \times 100 / X_{♂}$).

For the estimation of secular changes of body structure in newborns during the past century are used the data of S l a n c h e v et al. [2] and T z i r o v s k i [3].

The statistical analysis of the data is made by SPSS program.

Results and Discussion

The results obtained by the variation-statistical analysis are presented in Table 1 and Fig. 1.

Table 1. Basic body diameters of newborns in Sofia

Anthropometrical features	Boys (n = 110)		Girls (n = 109)		t ♂/♀	ISD (%)
	mean	SD	mean	SD		
Biacromial breadth	11.99	0.70	11.80	0.63	2.1*	98.42
Chest breadth	9.41	0.58	9.48	0.57	0.88	100.74
Chest depth	8.96	0.50	8.90	0.46	1.0	99.33
Waist breadth	10.55	0.73	10.53	0.67	0.21	99.81
Bicristal breadth	8.88	0.53	8.76	0.54	1.5	98.65
Bispinal breadth	7.98	0.54	7.85	0.43	1.91	98.37
Bitrochanterian breadth	9.37	0.57	9.30	0.46	0.94	99.25

* Statistically significant differences (P<0.05)

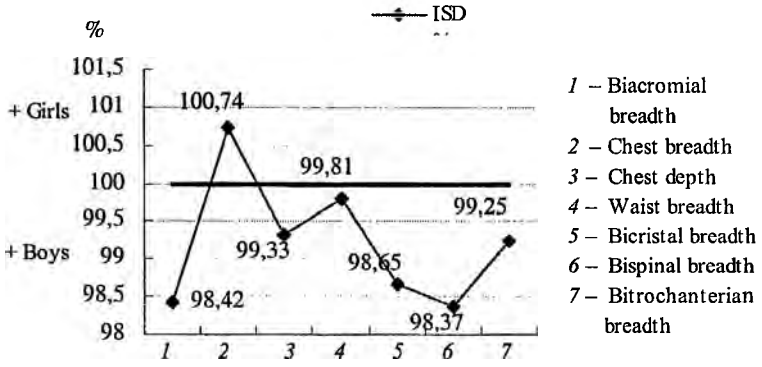

Fig. 1. Sexual differences in the basic diameters of newborns, according to the ISD data

The data of biacromial diameter give information about structure and massiveness of shoulders. The newborn boys have significantly wider shoulders with 0.19 cm or 1.58 % than the newborn girls.

The newborn boys and girls have approximately equal mean values of the two chest diameters (chest breadth and chest depth), that define child configuration of the chest typical for this period of postnatal ontogenesis. Nevertheless, the newborn girls have wider chest with 0.07 cm than the newborn boys, who have, however, deeper chest with 0.06 cm. The newborn boys and girls didn't differ significantly, as well in regard to the rate of waist breadth, although the boys have wider waist with 0.19 %, according to the ISD data.

The data about bicristal, bispinal and bitrochanterian diameters characterize the massiveness of pelvis and show presence of sexual dimorphism even at birth. The sizes of bicristal and bispinal diameters in newborn boys are bigger with 0.12 cm and 0.13 cm, respectively. According to the ISD data, the boys' pelvis is wider than the girls' one with 1.35 % (bicristal area) and 1.63 % (bispinal area). The bitrochanterian diameter is the widest from the external pelvis diameters. The newborns from both sexes have approximately equal sizes of this diameter, as difference between them is only 0.75 %.

The body proportions show the ratios between absolute values of every anthropometrical feature and stature. They characterize the proportionality in body structure.

The data about biacromial breadth proportions show that the newborn boys have relatively wider shoulders with 0.17 index units (IU) (ISD = 0.72 %) than the newborn girls, but the sexual differences are not statistically significant. According to the Brugsch' categorization [1], more than a half of boys (69.06 %) and girls (81.65 %) fall into category of individuals with wide shoulders. In regard to proportion of chest breadth, the girls have relatively ($P < 0.05$) wider chest than boys with 0.30 IU, or with 1.61 % according to the ISD (Table 2, Fig. 2).

Regarding the rest four proportions the sexual differences are not significant. The chest depth and waist breadth are relatively bigger with 0.04 IU and 0.14 IU in the newborn girls, while the newborn boys have relatively wider pelvis approximately with 0.11 IU. According to the Brugsch' categorization [1] about bicristal diameter is established that 46.36 % of boys fall into the category "wide pelvis", 44.55 % — into the category "middle pelvis" and only 8.18 % — into the category "narrow pelvis". From the girls 54.13 % fall into the category "narrow pelvis", 30.28 % — into the category "middle pelvis", and 15.60 % — into the category "wide pelvis". In regard to the bitrochanterian diameter the girls have priority with 0.11 % (Table 2, Fig. 2).

Table 2. Proportions of body diameters of newborns in Sofia

Body proportions of	Boys (n = 110)		Girls (n = 109)		t ♂/♀	ISD (%)
	mean	SD	mean	SD		
Biacromial breadth	23.73	1.20	23.56	1.21	1.06	99.28
Chest breadth	18.61	1.01	18.91	1.02	2.21*	101.61
Chest depth	17.72	0.89	17.76	0.84	0.30	100.23
Waist breadth	20.86	1.31	21.00	1.17	0.84	100.67
Bicristal breadth	17.57	0.88	17.47	0.96	0.82	99.43
Bispinal breadth	15.78	0.93	15.67	0.80	0.96	99.30
Bitrochanterian breadth	18.54	0.91	18.56	0.87	0.21	100.11

* Statistically significant differences (P<0.05)

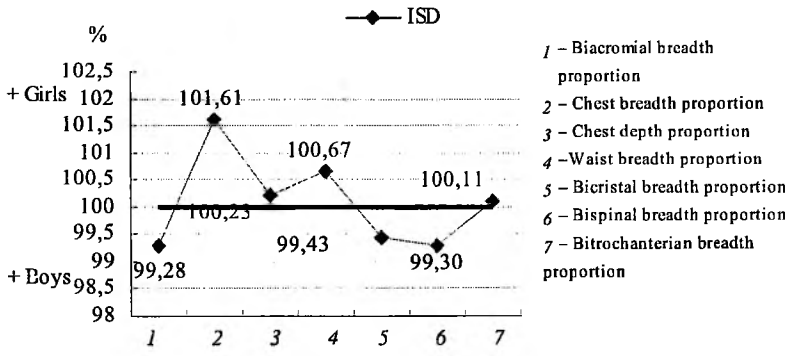

Fig. 2. Sexual differences in the proportions of basic diameters of newborns, according to the ISD data

The data about secular changes of the sizes of diameters and their proportions in the newborns show that boys and girls born in 2001 have significantly narrower chest and bitrochanterian breadths, and relatively wider biacromial diameter than the generation born during the period 1980-1982 [2]. The newborns in 2001 have significantly bigger sizes of chest, pelvis and shoulders compared to the newborns from Plovdiv during the period 1968-1986 [3].

Conclusions

The results obtained show that even at birth exist sexual differences in body dimensions and structure of newborns similar to those in adults.

- The newborn boys have bigger sizes of biacromial and pelvis diameters and proportional wider shoulders and pelvis than girls.
- The newborn boys and girls didn't differ significantly according to the two chest diameters, although the girls have wider chest and the boys have deeper chest.
- The boys and girls born in 2001 have narrower chest and pelvis and relatively wider biacromial diameter compared to the boys and girls born in Sofia dur ing the period 1980-1982 and wider chest, pelvis and shoulders compared to the generation born during the period 1968-1986.

References

1. Martin,R., K. Saller. Lehrbuch der Anthropologie in sistematischer Darstellung. T. I. Stuttgart, Gustav Fischer Verlag, 1957, 273-385.
2. Слънчев, П. и др. Физическо развитие, физическа дееспособност и нервно-психическа реактивност на населението на България (1980—1982). С., Национална спортна академия, 1992, 43—44, 211—212, 242—244.
3. Цировски, М. Медико-антропологично изследване на деца от периодите кърмачество и ранно детство. Дисерт. труд (Пловдив), 1987, 1—298.

Institute of Experimental Morphology and Anthropology

Acta morphologica et anthropologica, 10
Sofia • 2005

Relation between the Indicators of Lung Function and the Anthropometric Features of the Chest in Adults

M. Koleva, A. Nacheva***

* *Department of Hygiene, Medical Ecology and Nutrition, Medical University, Sofia*
** *Institute of Experimental Morphology and Anthropology, Bulgarian Academy of Sciences, Sofia*

During prophylactic examinations, the question of whether the anthropometric measurements and the indicators of lung function are interchangeable arises. The purpose of this research was to study the state of the lung function and the correlation between the anthropometric characteristics of the chest and the indicators of lung function in men and women, between 20 and 60 years of age. The subjects were 556 men and women, ethnic Bulgarians, divided into two groups. Some of the subjects were exposed to ammonia and carbon disulfide at their work place. The results of this study confirm our hypothesis about the effects of smoking, obesity, and contact with ammonia. The sex difference in some of the anthropometric indicators, the fluctuating physiometric changes, and the correlation coefficients, as well as the existing difference in the frequency of the disturbances of external breathing are in unison with the model of professional and nonprofessional behavior among men. The complex approach of this study is most successful in revealing the changes in the ventilation function of the lungs, and it makes the evaluation of the involved health risks easier.

Key words: lung function, ventilation capacity, lung volume and flow, anthropometric features.

Introduction

The anthropometric measurements of the chest are a component of the physical development evaluation. There is a correlation between the morphometric characteristics of the chest and the indicators of lung function (ventilation capacity, volume, and flows). Regardless of that, during prophylactic examinations, the question of whether they are interchangeable arises.

The primary purpose of this research was to study the state of the lung function and the correlation between the anthropometric characteristics of the chest and the indicators of lung function in men and women, between 20 and 60 years of age.

Material and Methods

The subjects in this cross-sectional epidemiologic study were 556 men and women, ethnic Bulgarians, divided into two groups, according to age: 20-40 years old and 40-60 years old. Some of the subjects were exposed to proven irritants (ammonia and

carbon disulfide) at their work place, while the rest of the subjects did not come in contact with chemical substances.

We measured and calculated the following factors: chest circumference — pause; chest circumference — inspiration; chest circumference — expiration; and average chest circumference; as well as the differences between these. We also studied factors of evaluation of external breathing: inspiratory vital capacity (IVC); forced vital capacity (FVC); forced expiratory volume in one second (FV_1); Tifno Index (FV_1/VC); peak expiratory flow (PEF); forced expiratory flows (FEF_{25}, FEF_{50}, and FEF_{75}); representing respectively 0.25%, 0.50%, and 0.75% of the fluctuation of the forced vital capacity.

We analyzed the individual results of every subject and, according to the registered changes of their external breathing we determined the type of ventilation insufficiency: **restrictive** ventilation insufficiency, **obstructive** ventilation insufficiency, or **mixed** ventilation insufficiency.

The statistical processing (variational and correlational analyses) was performed using a SPSS package. The Student-Fisher's *t*-criterion a level of significance $p<0,05$ was used as correction markers. All the results were statistically systematized at the same level of reliability ($p<0.05$) by means of the "Epi-Info" program for assessment of the relative risk and odds ratio.

Results

Our attempts to establish a correlation between the disturbances in the external breathing of our subjects and their occupations did not yield statistically significant results, neither for men, nor for women. It was found that the frequency of disturbances in the external breathing of obstructive, restrictive, or mixed type and the obstruction of the small respiratory tracts is on average 10%, with an existing gender difference: 3.7% for women and 13.2% for men.

We established statistically significant age-related changes in the anthropometric indicators — chest circumferences at inspiration, expiration, and pause, as well as the average chest circumferences for men and women. The age-related differences for men vary between 29.9 mm and 31.4 mm. These are significantly more pronounced for women, varying between 49.8 mm to 55.0 mm. The differences between the measured chest circumferences, related to the elasticity of the chest wall and the breathing capacity of the lungs, do not significantly change with age. In subjects over 40 years of age two of them decrease, which is more noticeable in women than in men (—5.2 versus —3.3 and —4.8 versus —0.8).

The analysis of the statistical and dynamic ventilation indicators (volume and flow) did not show statistically significant differences in the age subgroups, with the exception of the inspiratory vital capacity (IVC) in men over 40 years old (Table 1 and 2). There is a slightly noticeable linear correlation between the anthropometric and physiometric indicators (Table 3).

By using a single-variable models of risk analysis, we established that smokers have a high risk of external breathing disturbances (OR=3.96 in 95%, CI=1.59 — 10.49). Exposure to ammonia in the work place causes moderate risk of external breathing disturbances (OR=1.68 in 95%, CI=1.00 — 3.00).

Table 1. Basic statistics of anthropometrical and functional characteristics of male

Anthropometric and functional characteristics	Male up to 40 y $n = 179$	Male over 40 y $n = 158$	p
Chest circumference — pause (mm)	969.5 ± 94.5	1000.9 ± 80.2	0.001
Chest circumference — inspiration (mm)	1015.3 ± 90.8	1044.3 ± 76.9	0.05
Chest circumference — expiration (mm)	941.6 ± 94.7	971.7 ± 78.4	0.05
Average chest circumference (mm)	978.3 ± 92.5	1008.1 ± 77.3	0.05
Difference (Chest circ. inspiration — pause) (mm)	45.6 ± 15.2	42.3 ± 14.3	
Difference (Chest circ. pause — expiration) (mm)	27.6 ± 13.1	29.1 ± 14.8	
Difference (Chest circ. inspiration — expiration) (mm)	73.2 ± 19.0	72.4 ± 17.9	
IVC (%)	91.3 ±13.2	96.3 ± 15.5	0.001
FVC (%)	99.2 ± 12.1	97.5 ± 12.6	
FV_1(%)	94.0 ± 18.8	96.0 ± 17.9	
FV_1/ VC (%)	101.7 ± 21.6	99.7 ± 18.2	
PF (%)	72.7 ± 29.0	71.4 ± 25.1	
MF_{75}(%)	74.9 ± 31.5	73.6 ± 28.1	
MF_{50}(%)	87.1 ± 30.8	91.2 ± 33.6	
MF_{25}(%)	100.5 ± 37.2	101.4 ± 43.3	

Table 2. Basic statistics of anthropometrical and functional characteristics of female

Anthropometric and functional characteristics	Female up to 40 y $n = 45$	Female over 40 y $n = 63$	p
Chest circumference — pause (mm)	823.0 ± 107.1	878.0 ± 80.9	0.05
Chest circumference — inspiration (mm)	860.3 ± 100.7	910.1 ± 76.3	0.05
Chest circumference — expiration (mm)	801.7 ± 104.0	856.3 ± 82.5	0.05
Average chest circumference (mm)	831.0 ± 102.1	883.2 ± 78.9	0.05
Difference (Chest circ. inspiration — pause) (mm)	37.3 ± 15.9	32.1 ± 13.3	
Difference (Chest circ. pause — expiration) (mm)	21.3 ± 10.5	21.7 ± 10.6	
Difference (Chest circ. inspiration — expiration) (mm)	58.6 ± 15.1	53.8 ± 17.3	
IVC (%)	99.1 ± 32.9	93.6 ± 17.0	
FVC (%)	100.3 ± 10.3	99.6 ± 15.6	
FV_1(%)	95.3 ± 14.3	96.3 ± 18.6	
FV_1/ VC (%)	104.5 ± 23.2	107.4 ± 16.9	
PF (%)	65.9 ± 18.4	69.2 ± 22.6	
MF_{75}(%)	69.0 ± 19.9	71.4 ± 21.3	
MF_{50}(%)	79.6 ± 24.3	80.6 ± 23.0	
MF_{25}(%)	92.1 ± 28.0	86.4 ± 34.8	

Discussion

We found that among the examined subjects, both men and women, there are many external occupational and non-occupational factors, which significantly affect the components of the respiratory system — upper respiratory tracts, lungs, lung circulation of the blood, central nervous system, and chest wall.

The most significant factor is the occupational exposure to ammonia and carbon disulfide — industrial poisons with a proven irritating effect.

A high concentration of ammonia has been proven to be a serious health hazard. Ammonia was one of the first extremely hazardous substances (EHS's) to be addressed by NAC (National Advisory Committee) AEGL (acute exposure guideline levels), and is of great concern both to companies and communities.

Ammonia in concentration levels above 3500mg/m^3 results in immediate death, caused by seizures, inflammation, and oedema of the larynx [5]. The clinical picture of acute ammonia poisoning is characterized by the "curare" effect of ammonia and the sharp disturbances of the breathing and blood circulation. Post mortem, there are signs of chemical burns to the eyes and the upper respiratory tracts [13].

High concentrations of ammonia cause heavy eye lacrimation and pain, accompanied by a sharp decrease of the lung ventilation and acute emphysema [13, 4]. Most frequently described, clinically insignificant, reversible toxic effects of ammonia harm the eyes and the upper respiratory tracts. There are noticeable irritation of the eyes, lacrimation, and changes in breathing [12]. CS_2 has an even more pronounced irritating effect on the skin and the mucous membranes, causing second and third degree burns at contact with the skin [13]. Decreased vital volume and dyspnoea can be observed after exposure to CS_2 in its gas state [10, 3]. Vanhoorne et al. (1995) have produced reliable evidence of pain that is more frequent, burning, and photophobia after exposure to CS_2. It is accepted that CS_2 is primarily a neurotropic poison [1, 2, 8, 7].

The effect that ammonia and carbon disulfide have on the CNS disturbs the muscle activity of the chest wall, which could lead to disturbances in external breathing.

After analyzing the registered individual dynamic and static ventilation indicators, our results show that 10% of the studied subjects, on average, experience ventilation insufficiency, with a noticeable difference in the frequency between males and females. Much more frequently, ventilation insufficiency is experienced by men, who represent half of the machine operators and most of the maintenance staff, often working with high concentrations of ammonia and carbon disulfide.

Table 3. Correlation coefficients of selected functional variables with some anthropometrical featues

Variables	Male	Female
IVC / Difference (Chest circ. inspiration — pause)	0.182	0.252
IVC / Difference (Chest circ. inspiration — expiration)	0.213	0.251
FVC / Difference (Chest circ. inspiration — pause)	0.247	0.204
FVC / Difference (Chest circ. pause - expiration)	0.118	0.247
FVC / Difference (Chest circ. inspiration — expiration)	0.291	0.337
FV_1 / ГО Difference (Chest circ. inspiration — expiration)		0.196
FV_1/VC / Difference (Chest circ. inspiration — expiration)	- 0.112	

The muscles of the chest wall function as a "pump" of the respiratory system. The accumulation of subcutaneous fatty tissue (SFT) of the torso increases the thickness of the chest wall and impedes the proper functioning of this "pump." We found a statistically significant increase of the chest circumference at rest, without changes in the indicators of the ventilation function of the lungs during inhaling and exhaling. The statistically significant difference in the vital capacity of men of or above 40 years of age is within the physiological fluctuations of the method (± 20%). We are willing to accept that the increase in the anthropometric indicators is due to the accumulation of fatty tissue on chest cell wall. In previous studies, we have established significant difference in the quantity and location of SFT in women and men [14]. Obesity among the studied subjects, in combination with the chemical factor could disturb the normal connection and coordination between the regulator (CNS) and the "pump", changing the functioning of the respiratory system.

Smoking also affects the condition of the respiratory function, which is a harmful habit for 70% of the studied population. According to data by Roy [6], there is statistically reliable evidence that the indicators for evaluation of external breathing (FVC, FEV_1, $FEV_{0.7}$, and FEV%) are lower in men and women who smoke than in non-smokers. Our results completely support the role of smoking as one of the most significant risk factors for the observed disturbances of the ventilation function. The high risk of disturbances of the external breathing in smokers with OR = 3.96 with 95% CI = 1.59 — 10.49, realistically reflects the results of the combined effect of irritating gases, the increasing size of the wall cell caused by fatty tissue under the skin, and smoking for majority of the studied subjects. In support of this claim are the low correlation coefficients between the anthropometric and physiometric indicators, which we found both in men and in women (Table 3).

Conclusions

The results of this study confirm our working hypothesis about the effects of smoking, obesity, and contact with ammonia. The sex difference in some of the anthropometric indicators, the fluctuating physiometric changes, and the correlation coefficients, as well as the existing difference in the frequency of the disturbances of external breathing are in unison with the model of professional and nonprofessional behavior among men. The complex approach of this study is most successful in revealing the changes in the ventilation function of the lungs, and it makes the evaluation of the involved health risks easier.

References

1. Chrostek-Maj, J., B. Czeczotko. B The evaluation of the health state of the workers occupationally exposed to low concentration of carbon disulfide. Part two: The complex way of the examination of the central nervous system. — Przeglad Lekarski, **52**, 1995, No 5, 252-256.
2. Chu, C. C. et al. Polyneuropathy induced by carbon disulfide in viscose rayon workers. — Occup. Environ. Med., **52**, 1995, No 6, 404-407.
3. Kamat, S. R. Comparative medical impact study of viscose rayon workers and adjoining community in relation to accidental leak. — Chemical Engineering World., **29**, 1994, 107-111.
4. Markham, R. S. A review of damage from ammonia spills. In: Ammonia Plant Safety (and Related Facilities). Boston. MA: American Institute of Chemical Engineers, 1986, 137-149.
5. Michaels, R. A. Emergency Planning and the Acute Toxic Potency of Inhaled Ammonia. — Environmental Health Perspectives., **107**, 1999, No 8, 617-627.

6. R o y, S. K. Smoking status and its effect on cardiorespiratory system, body dimension and plucking performance of Oraon tea garden labourers. — Antrop. Anz., **56**, 1998, No 2, 151-162.
7. R u i j t e n, M. W., H. J. S a l l e, M. M. V e r b e r k. Verification of effects on the nervous system of low level occupational exposure to CS_2. — Br. J. Ind. Med., **50**, 1993, No 4, 301-307.
8. S i n c z u k-W a l c z a k, H. Certain diagnostic-certification problems in workers exposed chronically to carbon disulfide. — Med. Pr., **44**, 1993, No 5, 415-421.
9. S m i l, V. Global population and the nitrogen cycle. — Sci. Am., **277**, 1997, No 1, 76-81.
10. S p y k e r, D. A., A. G. G a l l n o s a, P. M. S u r a t t. Health effects of acute carbon disufide exposure. — J. Clin. Toxicol., **19**, 1982, 87-93.
11. V a n h o o r n e, M., A. d e R o u c k, D. D e B a c q u e r. Epidemiological study of eye irritation by hydrogen sulfide and/or carbon disulfide exposure in viscose rayon workers. — Ann. Occup. Hyg., **39**, 1995, No 3, 307-315.
12. V e r b e r k, M. M. Effects of ammonia in volunteers. — Int. Arch. Occup. Environ. Health., **39**, 1977, 73-81.
13. Вредные вещества в промышлености (под ред. Н. В. Лазарев, Н. В. Гадаскина). Ленинград, Химия, 1977, т. III.
14. Н а ч е в а, А., М. К о л е в а. Особености в количеството и разпределението на подкожна мастна тъкан при израснали. — J. Anthropol., **2**, 1999, 58-67.

Institute of Experimental Morphology and Anthropology

Acta morphologica et anthropologica, 10
Sofia • 2005

Some Nasofacial Indices in Turkish Men and Women

O. Taskinalp, N. Erden, Z. Yildiz

Trakya University, Faculty of Medicine, Department of Anatomy, Edirne, Turkey

We aimed to find some of the nasofacial indices in adult Turkish people studying 1038 person (495 women, 543 men) who were educated in the second class of the Medical Faculty of Trakya University between the years 1986 and 1993. The mean ages of the subjects were 19.4 (women) and 19.47 (men). Nose, face, mouth and orbita widths are taken as parameters in this study which were measured with a modified caliper compass. Nose width (women/men) 3.24+0.28/ 3.57+0.30 cm, face width 10.90+1.07/ 11.77+1.14 cm, mouth width 4.98+0.42/5.19+0.48 cm and orbita width 3.75+0.50/3.94+0.51 cm were found with the measurements. Nasofacial index (women/men) %29.72/ %530.33, nasooral index %65.06/ %68.78 and nasoorbital index % 86.40/7 %90.60 were found with the indices.

The results were compared with the literature and the difference between adult Turkish people and the other societies were determined.

Key words: Anthropometry, nasofacial index, nasoorbital index, nasooral index, Neoclassical Facial Canons.

Introduction

The studies on human body had begun before centuries and still go on. The aim was to know human body better in this studies which were continuing since the Hippoccrates time. The human body which has aroused the scientists' interest had the artists' interest then and this interest had been seen in their artworks. Especially with the renaissance this interest had got to the top, lots of artworks had been made which had had the human body as a subject [9, 3, 4, 6]. But the change in body measures was a subject which had been discussed for a long time. For this reason, a terminology named Anthropometria was developed for determining and grouping the measurement values scientifically [8]. The anthropometric studies on living human body is called somatometria. A division of somatometria includes head measurements and is called cephalometria. Measurements including only the skull were determined as craniometria [11]. The anthropological points are very important in anthropometric studies.

The first studies on this subject were made by Quetlet, the Belgian mathematician, in 1870 [8]. Also the studies have achieved ethnic specialties in 20th century. But, the measurements in ethnic studies on anthropology are at fenotype level, today. The anthropologists had attached importance to some points while they were classifying the mankind. The most important of these are the body measures and blood groups [7].

Head is the less differed part of human body. Lots of constant points are present on head which has the bones most in its anatomical structure. These are known as superficial finding points (Landmark) and anthropologic points. Most of the anthropological points had been described on head in human body. These characteristics provide that the studies about this region to be more easy and reliable [11].

The anthropometric measurements about face were constituting an important place, both in neoplasty in plastic and reconstructive surgery and in ideal face proportions. There is vertical and horizantal proportions in ideal face measurements. The harmony between the proportions depending on the nose which is at the middle of the face, is considered important in ideal face definition. And with this aim, we planned to investigate the values of some horizontal canons on face in Turkish people and compare them with the other ethnic groups.

Material and Methods

1038 persons (495 women, 543 men) who have educated in Medical Faculty of Trakya University and have had no deformity had taken place in our study. The mean ages of the subjects were 19.40 and 19.97 (women/men). The measurements were made with the same researcher, at the same time of the day (time: $14^{:00}$-$15^{:00}$) for reducing the error ratio. The measurements were repeated three times, the average values were taken for the study. A modified caliper compass suited to our aim was used in the study. The results were evaluated with the NCSS computer program, averages and standard deviations were calculated.

We can list the points which we used in our measurements like that [11, 5].

1. Nose width: The distance between the external points of ala nasi.
2. Face width: The distance between both zygions.
   Zygion: Lateral point of arcus zygomaticus.
3. Mouth width: The distance between the intersection points (comissura labiorum) of upper and lower lips while the mouth was closed.
4. Orbita width: The distance between the most protruding points of medial and lateral side of the basis of orbita.

We found some of the nasofacial indices by comparing the horizantal data with nose width. According to this:

a) Nasofacial index: The explanation of nose width/ face width by per cent.
b) Nasooral imdex: The explanation of nose width/ moth width by per cent.
c) Nasoorbital index: The explanation of nose width/ orbita width by per cent.

Results

The results that we found are shown in table 1. The indices we got from these results are shown in table 2. Though the proportions are in table 3.

Conclusions

We investigated some of the nasofacial indices in this study. But when literature were searched, it can be seen that there are results according to proportions of parameters to the number of subjects, not as an index, in this kind of studies. And this doesn't make complete comparison of the indices we found possible. But these studies give

Table 1. Statistical Data (mm)

Features	Women	Men
Nose width (mm)	32,4+2,8	35,7+3,0
Face width (mm)	109,0+10,9	117,7+11,4
Mouth width (mm)	49,8+4,2	51,9+4,8
Orbita width (mm)	37,5+5,0	39,4+5,1

Table 2. Data of Indices %

Features	Women		Men	
	ratio	%	ratio	%
Nasofacial index	1/3,36	29,72	1/3,29	30,33
Nasooral index	1/1,53	65,06	1/ 1,45	68,78
Nasoorbital index	1/1,15	86,40	1/ 1,10	90,60

Table 3. Proportions

Features	Women	Men
Face width/Nose width	3,36	3,30
Mouth width/Nose width	1,53	1,45
Orbita width/Nose width	1,15	1,10

us some information as well as it is not complete. Comparison of the data we got is with this limited information.

In our study, we found the nasofacial index %29.72 in woman and %30.33 in men. When we evaluate this proportions, it is seen that the nose width of Turkish people is less than 1/3 of their face width. However, Wang D. et al. had found the proportion of nose width to face width as %38.9 and %21.8 (less than 1/3) respectively in North American Indians and Chinese. In the same study, the proportion of nose width was found to be approximately equal to 1/3 of face width in %51.5 of Chinese and %36.9 of North American Indians [10]. We can think that these results had similarity with the study groups in the meaning of mathematics.

In our study the nasooral index was found %65.2 in women and %68.78 in men. In wide meaning, we can comment these proportions like that; mouth width is approximately less than 1.5 times of nose width in men (1.45 times) and approximately more than 1.5 times in women (1.53 times). Wang had found mouth width to nose width proportion less than 1.5 in %71.8 of Chinese in his study.

Though this proportion had been found %60.2 in North American Indians [10]. However, Bozkir et al. had found mouth width more than 1,5 times of nose width in %66.9 of women and %49.1 of men in a study which 272 women and 228 men had taken place [1]. Also in another study made by Borman et al. mouth width was found 1.5 times of nose width in %6 of women, wide mouth in a proportion of %53 and narrow mouth in %41 had been determined [2]. In another study made by Soyluoglu et al. this ratio had been found %67.23 in women and %70.85 in men too. The proportion of nose width to mouth width is less than 1.5 in both women and men in their study [8]. Less difference is seen when all proportions were evaluated. According to these data, mouth width is found to be equal to 1.5 times of nose width in Turkish people. However, the nose is wider in a ratio of ¾ than these proportions in Chinese people. The nose is more wide in %60 of North American Indians, too.

In the third part of our study we investigated the proportion of nose width to orbita width. This index is %86.4 in women, %90.6 in men in our study. In another definition, it is seen that, orbita width is 1.15 times of nose width in women and 1.1 times in men as well. This proportion shows us that the orbita width is wider in men than in women. But we could not find any data in literature to compare this proportion in ethnic aspect.

As a result, it is seen that the face width is approximately 3.3 times of nose width, mouth width is 1,5 times and orbita width is 1.15 times as well in adult Turkish women. However, these results are 3.3, 1.45 and 1.1 in men respectively.

References

1. Bozkir, M. G., P. Karakas, O. Oguz. Vertical and Horizontal Neoclassical Facial Canons in Turkish Young Adults. — In: Surgical Radiologic Anatomy, 2003, 19.
2. Borman, H., F. Ozgur, G. Gursu. Evaluation of Soft-Tissue Morphology of The Face in 1050 Young Adults. — Annal of Plastical Surgery, **42**, 1999, No 3, 280-288.
3. Cokanov, K. R. Plasticna Anatomia. Sofia, Navikai izkustvo, 1974, 370-396.
4. Kahraman, G. Yetişkin. Türk Kadın ve Erkeklerinde Üst Ekstremite Ölçümleri ve Oranları. — Uzmanlık Tezi., İstanbul. 1988.
5. Mesut, R., M. Yıldırım. İnsan Vücudunda Antropolojik ve Yüzeyel Buluş Noktaları. — İstanbul, Beta Basım Yayım Dağıtım A. Ş., 1989, 51-60.
6. Pestemalci, T., G, Kahraman. Türk Erkeklerinde Üst Ekstremiteye ait Bazı Ölçümler ve Oranlar. — Morfoloji Dergisi, **9**, 2001, No 2, 37-40.
7. Saran, N. Antropoloji. — Ankara, İnkilap Kitabevi, 1993, 72-75.
8. Soyluoğlu, A. I. et al. Erişkin Türk İnsanında Cranium'un Antropometrik İncelenmesi. — SBAD, **3**, 1992, 61-67.
9. Taskinalp, O. Yetişkin Türk Kadın ve Erkeklerinde Aksiyal Vücut Çapları ve Çevreleri. — Uzmanlık Tezi., Edirne. 1989.
10. Wang, D. et al. Differences in Horizontal, Neoclassical Facial Canons in Chinese (Han) and North American Caucasian Populations. Ï Aesthetic Plastical Surgery., **21**, 1997, N0 4, 265-9.
11. Yildirim, M., R. Mesut. Disseksiyona Yönelik Topografik Anatomi. T. 1. Baş-Boyun. — İstanbul, Beta Basım Yayım Dağıtım A. Ş., 1995, 10-26.

Institute of Experimental Morphology and Anthropology

Acta morphologica et anthropologica, 10
Sofia•2005

The Proportions of Upper Extremity in Turkish Men

O. Taskinalp, E. Ulucam, C. Bozer

Trakya University, Faculty of Medicine, Department of Anatomy, Edirne, Turkey

The aim of our study is to investigate the proportions of upper extremity in Turkish men. With this opinion, 532 male students who were studying in Medical Faculty of Trakya University between the years of 1986 and 1993 had taken place in this study. The lengths of total upper extremity, arm, forearm and hand were measured on subjects at an average age of 19.92 ± 1.33. The measurements were made with a millimetric segmented, not bending, wooden meter fixed on the wall.

We found the length of total upper extremity 78.68 ± 3.99 cm, the length of arm 34.82 ± 2.55 cm, the length of forearm 24.94 ± 2.16 cm and the length of hand 18.92 ± 1.50 cm. The proportions of the length of arm, forearm and hand to the upper extremity which they form are determined as % 44.25 ± 0.03, % 31.70 ± 0.02, % 24.04 ± 0.01 respectively as well. Also the proportions of the parts to each other are; hand length / arm length % 54.30 ± 0.05, hand length / forearm length % 75.80 ± 0.11 and forearm length / arm length % 71.60 ± 0.09.

In conclusion, it is determined that approximately, the arm length is 1/2, the forearm length is 1/3 and the hand length is 1/4 of the length of upper extremity in Turkish men. These results are compared with the literature.

Keywords: Anthropology, upper extremity, proportion.

Introduction

Since the time of Hippocrates, different studies had been made on human body. These studies which had started anatomically first were for learning the human body better. With the development of science and art, these studies had achieved an artistic and aesthetic way [1]. Especially with the period of Renaissance, many artists had appeared in arts like painting and sculpture and they had made work of arts which had had human as a subject. Artists like Polyclet, Lysipphus, Guyauma, Vitrivius, Michael Angelo and Paul Richer had measured some lengths of the human body and had found various proportions between them [1, 2, 3, 4]. This shows us that human body and art is in close relationship as well. Scientists had taken it in a different point of view and had standardized these findings. Then the anthropologists had taken part in the studies and named the results which they had found as "SCIENTIFIC RULE" [2, 4]. In 1895 Fritsch had developed these rules and found "FRITSCH RULE". Physical anthropologists had tried to understand and describe the origin of human, physical features, the causes of differences in different human groups, differences and similarities between physical features and evolution of these features too [6]. It

had been thought that some lengths of the human body were proportional [5]. Some constant proportions had been found with the assistance of the studies of the artists and scientists. These proportions had been named as "CANON" and the unit measure of each canon as "MODULE" [1, 2, 3, 4]. Hand, foot, head, third finger of the hand and metacarpophalangeal length had been used as module more often. French anatomist Paul Richer had determined some proportions on human body and used head height as a module [1, 2, 3, 4].

Material and Methods

Our study was made in the laboratory of anthropometry at the Department of Anatomy of Trakya University Medical Faculty. 532 male students who had educated in second class of our faculty between the years of 1986 and 1993 took part in this study. Measurements were made by the same researcher at the same time of the day and the measurements were made with a millimetric segmented, not bending, wooden meter fixed on the wall. The results were noted on forms those prepared before. The data collected were evaluated with the NCSS computer statistics program, the averages and standard deviations were calculated.

Upper extremities are the most active and flexible parts of the body and they are attached to each sides of the body with the shoulder joints. Although in anatomic nomenclature it is used "membrum" that means "limb" or "member", it is preferred to use "extremitas" that means "borderland" in medical terminology for upper extremities [7, 10]. The upper extremities are examined in three parts anatomically; arm, forearm and hand. These three parts are bound to each other with joints. And these joints were shoulder, elbow and wrist [9, 10, 11, 12].

While measuring the upper extremity, constant anthropological points and superficial anatomical formations were used. The anthropological points that have been used and the measurements that have been made in our study are respectively [5, 7, 11];

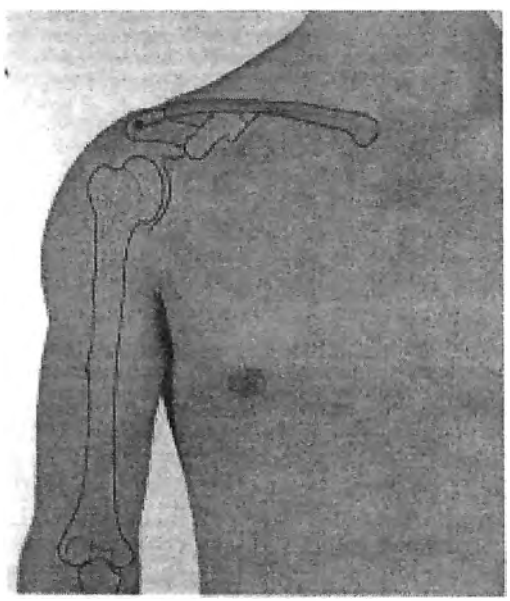

Fig. 1. Acromion (Acromiale)

Fig. 2. Radiale and Stylion

Total length of upper extremity: The distance between acromion and acromelion.
Acromion (Acromiale): The point at the superior and external border of the acromion process when the subject is standing erect with relaxed arms **(Figure 1).**
Acromelion (Onychion): The tip of of the middle finger which is the longest.
Arm length: The distance between acromion and radiale.
Radiale: The point at the upper and lateral border of the head of radius which is felt in fovea lateralis olecrani. **(Figure 2).**
Forearm length: The distance between radiale and stylion.
Stylion: The most distal point of the processus styloideus radii **(Figure 2).**
Hand length: The distance between stylion and acromelion.

Findings

In our study, the lengths of upper extremities were measured first (Table 1). Then the proportions between these results were discussed. The proportions of the parts of upper extremity were shown in table 2 and the proportions of the parts to each other in table 3.

Discussion and Results

We have searched the literature for the aim of comparison of the results that we had found. With this search we could not find any study that includes all the findings we got. However, we could find the possibility to compare some of our findings with some of the studies (Table 4).

Table 1. The lengths of upper extremity

Metric values	Average *n*-532
Upper Extremity Length	78.68 ± 3.99
Arm Length	34.82 ± 2.55
Forearm Length	24.94 ± 2.16
Hand Length	18.92 ± 1.50

Table 2. The proportions of the parts of upper extremity to upper extremity

Proportions	*n*	%
Arm / Upper Extremity Length	532	44.25 ± 0.03
Forearm/ Upper Extremity Length Length Length	532	31.70 ± 0.02
Hand / Upper Extremity Length	532	24.04 ± 0.01

Table 3. The proportions of the parts of upper extremity to each other

Proportions	*n*	%
Hand / Arm Length	532	54.30 ± 0.05
Hand/Forearm Length	532	75.80 ± 0.11
Forearm/Arm Length	532	71.60 ± 0.09

Table 4. The comparison of our findings with the literature

Features	Taskinalp	Kahraman	Muftuoglu	U.S.	Italian	French
Upper Extremity Length	78.68 ± 3.99	76.92	77.45		76	75.58
Arm Length	34.82 ± 2.55	32.21	32.48	28.20		
Forearm Length	24.94 ± 2.16	25.10	24.22	25.10		
Hand Length	18.92 ± 1.50	19.51	20.97	19		
Arm / Upper Extremity Length	%44.25 ± 0.03	%41.82	%41.9	%39		
Forearm / Upper Extremity Length	%31.70 ± 0.02	%32.78	%31.3	%34.7		
Hand /Upper Extremity Length	%24.04 ± 0.01	%25.38	%27	%26.3		
Hand / Arm Length	%54.30 ± 0.05					
Hand / Forearm Length	%75.80 ± 0.11					
Forearm Length / Arm Length	%71.60 ± 0.09					

We have measured total length of upper extremity as 76.68 cm in our study, also Kahraman had measured this length as 76.92 cm and Muftuoglu as 77.45 cm. This length is 76 cm in Italians and 75.58 cm in French people [3, 4, 8]. According to this, while our findings are nearly close to Muftuoglu's findings, they are different from the other researchers'.

In our study we have found the arm length 34.82 cm, forearm length 24.94 cm, and hand length 18.92 cm. While Kahraman has measured this length as 32.21 cm, 25.10 cm, 19.51 cm, Muftuoglu had measured 32.48 cm, 24.22 cm and 20.97 cm respectively. These findings were 28.20 cm, 25.10 cm and 19 cm respectively in a study which was made in the United States. According to this, our arm length finding is longer than Kahraman and Muftuoglu's findings, while the forearm lengths were near to eachother relatively. However, the hand length was found to be shorter than the other researchers' findings. While the arm length was longer than the American race's evidently, a nearness had been seen in forearm and hand lengths [3, 4, 8].

When we take a look at the proportions between the parts that form the upper extremity, we found arm (upper extremity proportion % 44.25, forearm / upper extremity proportion % 31.70 and hand) upper extremity proportion % 24.04 in our study. Kahraman had found the results as % 41.82, %32.78 and %25.38 and Muftuoglu had found as %41.90, % 31.30 and % 27 respectively as well. The nearnesses and differences are the same in proportions like it is in lengths. In our study, while the first proportion is higher, the second is near and the third is lower. These proportions were found as % 39, % 34.7 and %26.3 in a study made in the United States. When we make a racial comparison, it is seen that the first proportion was higher and the other proportions were lower in our study [3, 4, 8].

In the last part of our study we examined the proportions of the parts that form the upper extremity to each other. According to these we determined hand / arm length proportion as % 54.30, hand / forearm length proportion as % 75.80 and forearm / arm length proportion as % 71.60. We could not find any study that had been made before, to compare these results with.

As a result, according to the data of the studies, it can be seen that the upper extremity length of Turkish men had increased. This increase has resulted from the arm length. In spite of the little decrease in forearm and hand length, the increase in arm length compensates this decrease.

We hope that the results we found in this study may be useful in different parts of industry like clothing, furniture, body prosthesis, hand devices and making gloves.

References

1. Cokanov, K. Plasticna Anatomia. Sofia, Nauka i Izkustvo, 1974, 370-396.
2. Kahraman, G. Yetiskin Turk Kadin ve Erkeklerinde Ust Ekstremite Olcumleri ve Oranlari. — Uzmanlık Tezi, Istanbul, 1988.
3. Lumley, John, SP. Surface Anatomy. The Anatomical Basis Of Clinical Examination, International Student Edition (Second Edition). Edinburgh, London, Churchill — Livingstone, 1966, 55-84.
4. Mesut, R., M. Yildirim. Insan Vucudunda Antropolojik ve Yuzeyel Bulus Noktalari. Istanbul, Beta Basim Yayim Dagitim A. S., 1989, 51-60.
5. Mesut, R., M. Yildirim. Disseksiyona Yonelik Topografik Anatomi. T. 2. Ekstremiteler. Istanbul, Beta Basim Yayim Dagitim A. S., 1995, 11-23.
6. Muftuoglu, A. Yetiskin Turk Erkeklerinde Bazi Vucut Olcumleri ve Aralarindaki Oranlar. — Uzmanlik Tezi, Istanbul, 1981.
7. Ozer, K. Antropometri. Sporda Morfolojik Planlama. Istanbul, **38**, 1993, 44-46, 133 p.
8. Pestemalci, T., G. Kahraman. Turk Erkeklerinde Ust Ekstremiteye Ait Bazi Olcumler ve Oranlar. — Morfoloji Dergisi, **9**, 2001, No 2, 37-40.
9. Saran, N. Antropoloji. Istanbul, Inkilap Kitabevi, p. 22.
10. Sinnatomby, C. S. Lasts' Anatomy, Regioned and Applied (Tenth Edition). Edinburgh, London, Churchill — Livingstone, 1999, 35-36.
11. Taskinalp, O. Yetiskin Turk Kadin ve Erkeklerinde Aksiyal Vucut Caplari ve Cevreleri. — Uzmanlik Tezi. Edirne, 1989,
12. Zeren, Z., I. Eralp. Kisa Topografik Anatomi (4. Baski). Istanbul, Sermet Matbaasi, 1972, 248-249.

Institute of Experimental Morphology and Anthropology

Acta morphologica et anthropologica, 10
Sofia•2005

The Proportions of Upper Extremity in Turkish Women

O. Taskinalp, A. Yilmaz, C. Bozer

Trakya University, Faculty of Medicine, Department of Anatomy, Edirne, Turkey

The aim of our study is to investigate the lengths of upper extremity and their proportions to body height and to each other in adult Turkish women.

493 female students who have studied in Medical Faculty of Trakya University had taken place in our study. Body height, total upper extremity, arm, forearm and hand lengths were taken as parameters for the study. The proportions of these findings to body height and to each other were found.

The differences between the other populations and adult Turkish women were defined by comparing our results with the data from literature.

Key words: Anthropology, upper extremity, proportion.

Introduction

From the first human "Homo habilis" that had lived three million years ago on earth to the father of todays' human "Homo sapiens", the human body had changed continuously. Historians, artists and scientists had always been interested in this change [9].

All the civilizations in history had taken the human body up in their own cultural and social intelligence. Artists of the period had always used the human body as a way of telling. So, they had tried to understand the human anatomy. They had accepted the existence of some proportions in human body and used them in their studies [4]. The proportions between the parts of human body had been called as "canon" (Old Egypt, New Egypt, Greek Canons etc.). The unit measure of each canon had been named as "module". Hand, foot, head and length of third finger of the hand had been used as a module in various canons [3, 4, 7, 8, 11, 12].

In 19th century, the anatomic structure of human body had been explained with mathematical expressions by Schmidt and Fritsch. With this study which had made history as Schmidt-Fritsch Rule, the length of the parts could be defined from the length of another part. The proportions of human body had been defined scientifically by French anatomist Dr. Paul Richer first [7, 11, 12].

The men's body had been mostly examined as human body in social and cultural intelligence of its period. Albrecht Dürer was the first who had examined the

proportions of women body [12]. However, there are not enough and comprehensive studies on women anthropology in our country yet. We tried to fill this point with this study some.

Material and Methods

493 female students who studied in 2nd class of Trakya University Medical Faculty took place in our study. There was not any orthopaedical defect in our subjects. Measurements were made by the same researcher at the same times of the days in anthropometry laboratory. The results that measured with millimetric segmented, not bending, wooden meter fixed on the wall were recorded in the forms prepared before. The data collected were evaluated with the NCSS computer statistics program, the averages and standard deviations were calculated.

Constant anthropological points and superficial anatomical formations were used for our measurements to get standardization [3, 6, 10]. The anthropological points used and the measurements made in our study are respectively like that:

1-Total upper extremity length: The distance between acromion and dactylion in erect anatomical position.
2-Acromion (Acromiale) : The point that fits to angulus acromii.
3-Dactylion (Onychion) : The tip of of the middle finger which is the longest.
4-Arm length : The distance between acromion and radiale.

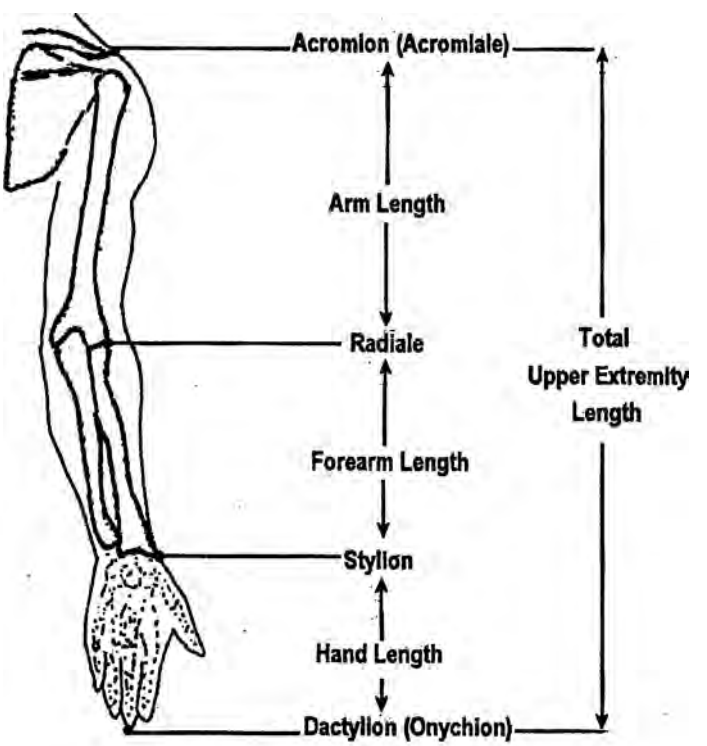

Fig. 1. Anthropological points and features

5-Radiale : The upper border of caput radii which is felt in fovea lateralis olecrani.
6-Forearm length : The distance between radiale and stylion.
7-Stylion : The point at the bottom of processus styloideus radii in carpal region.
8-Hand length : The distance between stylion and dactylion.

Findings

First, the lengths of upper extremities were measured on 493 female students whose mean age were 19,4 ± 1,1 (Table 1). Then the proportions of the parts of upper extremities to body height were calculated (Table 2). In Table 3 the proportions of the parts to upper extremity can be seen.

Table 1. The length of upper extremity

Features	Average (cm)
Upper Extremity Length	70.93±3.95
Arm Length	30.99±2.47
Forearm Length	22.74±1.98
Hand Length	17.21±1.56

Table 2. The proportions between upper extremity and body height (%)

Upper Extremity Length / Height	44.12
Arm Length / Height	19.28
Forearm Length / Height	14.14
Hand Length / Height	11.00

Table 3. The proportions between the parts and upper extremity (%)

Arm Length / Upper Extremity (%)	44
Forearm Length / Upper Extremity (%)	32
Hand Length / Upper Extremity (%)	24

Result and Conclusion

The studies are not much in number in the whole country which were made for the aim of defining the anthropometric measures of Turkish people. Studies about anthropometric measures of females are seen rarely as well. So that we could not come across a study in which all of our findings exist. But we could find the chance to compare some of our results with some studies.

We measured the body height of the subjects 160.73 ± 5.95 cm. At 1937 İnan, at 1960 Ciner, at 1999 Fellahoğlu, at 1995 Kahraman et al. and at 1999 Akın & Sağır had reported the body height 152.26 cm, 155.4 cm, 157.8 cm, 162.64 cm and 153.7 cm respectively [1, 2, 5, 6]. These values had been reported as 161,5 cm in Italians and 163,8 cm in Frenchs [6]. Our subjects' body heights are nearly close to Kahraman et al. and Italians' results but shorter than the Frenchs' and longer than the other reseaerchers' results as well.

We measured the total upper extremity length 70.93 cm in our study. This length had been measured 69.64 cm by Kahraman et al., 66.78 cm by Fellahoğlu, 66.66 cm by Akın & Sağır. Italians had measured 70,20 cm and Frenchs 74,93 cm as well [1, 6].

According to this, our findings are more likely with the findings of Italians and Kahraman et al. Noticeable differences can be seen with the other researchers' findings.

Arm, forearm and hand lengths are 30.99 cm, 22,74 cm and 17.21 cm respectively. Kahraman et al. had reported these as 28.42 cm, 22.82 cm and 18.40 cm [6]. In 1991 Fellahoğlu had measured arm length 31.33 cm and forearm length 24.20 cm, however Akın & Sağır had measured the same distances as 31.7 cm and 23.6 cm [1].

Our subjects' arm lengths are longer than the findings of K a h r a m a n et al., but likely with Akın and Fellahoğlu. And the forearm lengths are shorter than the findings of Fellahoğlu and Akın & Sağır in spite of the similarity with Kahraman's findings.

We could make a comparison only with Kahraman et al. in hand lengths. Kahraman et al. had measured 18,40 cm while we measured 17.21 cm in our subjects [6]. With the help of these results we can see that arm length plays the biggest role in the formation of upper extremity length.

The results we found by comparing each of our results with the body height are shown in Table 4. Approximately 2.25 times of total upper extremity length, 5 times of arm length, 7 times of forearm length and 9 times of hand length equals to body height. When we compare our results with the literature we could not find a noticeable difference.

T a b l e 4. The comparison of our findings with literature

Features	Our study	Kahraman (1995)	Italian	French	Çiner (1960)	Fellahoğlu (1991)	Akın (1999)	İnan (1937)
Height	160.73	162.64	161.50	163.83	155,40	157.80	153 70	152.26
Upper Extremity Length	70.93	69.64	70.20	74.93		66.78	66.6	
Arm Length	30.99	28.42				31.33	31.7	
Forearm Length	22.74	22.82				24.20	23.6	
Hand Length	17.21	18.40						
Upper Extremity/Height	44.12	42.80	44	45.73		42.34	43.31	
Arm Length/Height	19.28					19.85	20.62	
Forearm Length / Height	14.14					15.33	15.35	
Hand Length / Height	10.70	11.34						
Arm Length / Upper Extremity	43.69	26.42				46.91	47.7	
Forearm Length / Upper Extremity	32.05	32.75				36.23	35.43	
Hand Length / Upper Extremity	24.26	40.80						

If we have a look at the proportions between the parts that form the upper extremity, we find arm (upper extremity proportion 44 %, forearm / upper extremity proportion 32 % and hand) upper extremity proportion 24 % in our study. We could compare all of our findings only with Kahraman et al. Kahraman et al. reported these proportions as 40.8 %, 32.7 % and 26.42% respectively [6]. Fellahoğlu and Akın & Sağır had compared only the arm and forearm lengths with upper extremity length. Fellahoğlu reported as 46.91 %, 36.23 % and Akın & Sağır 47.7 % and 35.43 % as well respectively [1]. If we compare our results with K a h r a m a n et al. we see that our first proportion is higher, second is nearly close and third is

lower. We could compare only the proportions of arm and forearm lengths to upper extremity length with Fellahoplu and Akın & Sağır. Our findings are lower than their findings.

The anthropometric measurements of women, men and children from any country are different. Also by examining the studies made at various times, we can say that the anthropometric values can change with the time progression. Geography, genetics, nourishment style, habits, traditions and socioeconomic differences can cause differences in anthropometric measures of societies [1]. As a conclusion it is not true to evaluate the upper extremity length in Turkish women only. It must be evaluated together by accepting the existence of some proportions in human body.

We hope that the results we found in this study may be useful in different parts of industry like clothing, furniture, body prosthesis, hand devices and making gloves.

References

1. Akın, G., M. Sağır. Kırsal Kesimdeki Kadınların Bazı Antropometrik Ölçüleri. 7. Ulusal Ergonomi Kongresi, 14-16 Oct. 1999, Adana.
2.Ciner, R. Türk Kadınlarının Antropolojisi. — Ankara Üniversitesi Dil ve Tarih-Coğrafya Fakültesi Dergisi, **28**, 1960, No 3-4, 161-204.
3. Cokanov, K. R. Plasticna Anatomia. Sofia, Nauika i Izkustvo, 1974, 360-390.
4. Dere, F., O. Oguz. Artistik Anatomi. Adana, Nobel Kitabevi, 1996, 11-20.
5. İnan, A. Türkiye Halkının Antropolojik Karakterleri ve Türkiye Tarihi. Türk Tarih Kurumu Basımevi, Ankara, 1947.
6. Kahraman, G. et al. Türk Kadınlarında Üst Ekstremite'ye Ait Bazı Ölçüm ve Oranlar. — T.Ü.Tıp Fakültesi Dergisi, **12**, 1195, No 1, 60-71.
7. Kahraman, G. Yetişkin Türk Kadın ve Erkeklerinde Üst ekstremite Ölçümleri ve Oranları. Uzmanlık Tezi, İstanbul, 1988.
8. Lumley, Jhon, SP. Surface Anatomy. The Anatomical Basis Of Clinical Examination, International Student Edition (Second Edition). Edinburgh, London, Churchill-Livingstone, 1966, 55-81.
9. McHenry, H. M. How big were early hominids? — In: Evolutionary Anthropology, **1**, 1992, No 1, 15-25.
10. Mesut, R., M. Yıldırım. İnsan Vücudunda Antropolojik ve Yüzeyel Buluş Noktaları. — İstanbul, Beta Basım Yayım Dapıtım A.S., 1989, 50-58.
11. Taşkınalp, O., R. Mesut. "Boy-Beden" İlişkisine Esas Bazı Antropometrik Orantılar. T.U.Tıp Fakültesi Dergisi, 8, 9, 10 1991, (Bilesik sayı), 1-8.
12. Yordanov, Y. Narachnik po antropologiya. Sofia, Universitetsko İzdatelstvo "Sv. Kliment Ohridski", 1997, 150-159.

Institute of Experimental Morphology and Anthropology

Acta morphologica et anthropologica, 10
Sofia•2005

Comparison of the Anthropologial Studies of Metodi Popov in Bulgaria and Afet Inan in Turkey

R. Mesut, O. Taskinalp*, C. Algunes***

* *Trakya University, Faculty of Medicine, Department of Anatomy, Edirne Turkey*
** *Trakya University, Faculty of Medicine, Department of Medical Biology, Edirne Turkey*

The aim of this study is to shed light on the anthropological history of two neighbouring Balkan countries, Turkey and Bulgaria. Metodi Popov in Bulgaria and Afet Inan in Turkey unawarely performed widespread anthropological studies simultaneously (1937-1943). Metodi Popov measured 8.862 people (6.531 males and 2.331 females) and Afet Inan measured 59.728 people (39.465 males and 20.263 females). Although they used the same tools for measuring, only 10 metric values and 5 indexes related with these values can be compared partially because of differences in methodology. We wish to study on new anthropological research projects with anthropologists from Balkan Countries using the same methods in the future.

Key Words: History of Anthropology, Metodi Popov (Bulgaria), Afet Inan (Turkey).

During the first half of the 20th century, physical anthropology developed rapidly and anthropometric methods were used commonly. Scientists, who wanted to clarify ethnogenesis, found it appropriate to support historical, archeological and linguistic findings with anthropological data. The scientific world that set its hopes on 'Human Genome Project's today, relied on anthropological researches one hundred years ago. These studies had also been supported by National State Administrations. Almost all countries were performing anthropological profiles of their own citizens with widespread studies. This increasing trend was also spreading in Balkan countries. Towards the end of 1930's, two widespread anthroplogical studies that were performed both in Turkey and Bulgaria, are specifically noticable. After half a century of their publication, we would like to examine the differences and similarities of these studies that are parallel in terms of their time, method and aim.

Metodi Popov in Bulgaria and Afet Inan in Turkey were the scientific administrators of these studies. Let's introduce these famous scientist who are well known in their own countries.

Metodi Popov (1881-1954) was born in Shumen and graduated from Sofia University. He earned his PhD degree at Munich University in Germany. He became a professor in 1916 and a member of the Bulgarian Academy of Sciences in 1947. Metodi Popov, who was the rector of the University of Sofia and chairman of the Biology Institute, is accepted as the founder of modern Bulgarian Biology [7].

Between years 1938 and 1943, this famous scientist who was known for his studies on general biology, cytophysiology and microbiology, performed a widespread anthroplogical study with 8862 subjects, but could only publish his results as a book in 1959, 16 years later. *Antropolgiya na Bulgarskiya Narod, t.I.Fizitcheski oblik na Bulgarite(1959) BAN, Sofya [Anthropology of the Bulgarian People, c.I. Physical View of the Bulgarians* [11].

Afet Inan (1908-1985) was born in Doyran, country of Salonika, but after the Balkan War her family migrated to Turkey. Afet Inan, who graduated from the Bursa Teachers Training School, is one the first woman teachers of the Turkish Republic. Mustafa Kemal Atatürk, who visited her school in Izmir while she was a teacher there, because he knew Macedonian branch of her family, he took her under his protection and sent her abroad to be a scientist [8]. She studied first in Lausanne, then she attended Geneva University for history and sociology education. She became a student of prof. Eugène Pittard, who is a famous anthropolgist in the world, and performed an extraordinary widespread anthropological study on 64 000 people with his advice, in Turkey between years of 1937 —1938. She could published results of the study as a book 9 years later: *Türkiye Halkının Antropolojik Karakterleri ve Türkiye Tarihi (Anthrpological Characteristics of Turkish People and The History of Turkey)(1947), TTK Press, Ankara* [2]. Afet Inan, who became an associate professor in 1942 and a professor in 1950, worked as the president of the Turkish Historical Assembly and as a manager of the Turkish Institute of Reform History for many years. Between 1955-1979, she presented Turkey in UNESCO [9].

Because they represented over 1:1000 rate of the country population of that time, both of the studies have wide contents. Each of them had examined both of anthropometric and anthroposcopic (descriptive) parameters, and used the same tools for the metric measures such as anthropometer, compass, calliper. According to common view, both of the scientists search for racial and national features and interpreted in terms of ethnogenesis. However, none of them used expressions such as: superiority, racialism or chauvinism in any sentence. Both of them tried to increase number of female subjects as far as possible. Even though it is a Muslim country, 20.263 female subjects were measured in Turkey, due to the secular republic regimen that gives equal rights to women.

In order to examine 7.919 Bulgarian origin, 4.500 Pomak origin in Rhodope's region, 538 Macedonian origin in Vardar Macedonia, Metodi Popov divided Bulgaria into 3 geographical regions. Male/Female ratio was about 3:1.

In order to examine 39.465 male subject with 20.263 female subject, Afet Inan divided Turkey into 10 geographical regions. Statistical analyses were performed 59.728 subjects, after excluding unreadable cards. Male /female ratio was about 2:1. Afet Inan did not apply ethnic principles appropriate to that term ideologies and did not mention national minorities. Metodi Popov did not mention Turkish people and the other ethnic minorities either.

Afet Inan was greatly supported by the government: she was funded from the budget, was given the duty of organising the Ministry of Health and Social Aid by order from Atatürk, appointed pollsters and recieved great support from governors. Pollsters, who were pre-educated in Ankara, spread all over the country and completed the measurings in 1937. Unfortunately, 10% of measurings were lost. The statistical calculations were completed by about 30-40 civil servants from General Management of Statistics in 1938 [2]. In Bulgaria, Metodi Popov was complaning about the absence of government support, as he pointed out in his book which was completed in 5 years [11]. But it is a fact that the results were published by official academic corporations (BAS and TTK).

When he started his research, Metodi Popov was 57 years old and experienced. He earned his PhD degree in Germany and was following the German school. He applied Rudolph Martin's methodology in anthropology — definitions, terms, measuring methods and analysis were performed in accordance with Martin (1928) [4]: 31 metric measurings, 15 descriptive signs were calculated with 20 indexes.

Afet Inan was 30 years old when she started her study in anthropology. After she earned her PhD degree in Switzerland, she returned to Turkey and found the country in the distress of revolution. A few years before, she had performed a small scale anthropological study which was published internationally [1]. She was fluent in French and knew a lot about the culture. She had been the student of prof. E. Pittard and had been following French school in anthropology. Terms and analyses were performed in accordance with E. Pittard [5], but Turkish anthropologist Ş. A. Kansu prepared methodological guide [3]: 21 metric measurings, 6 descriptive signs were calculated with 28 indexes.

In terms of all parameters, it is not possible to compare the results of these two anthropological studies which were performed in different methods. The scientists were unaware of each other. Most of the measurings do not match and methodological differences are notable in the others. Only 10 metric measurings (height, length of open arms, head length, head width, frontal width, facial width, facial height, upper facial height, nasal length, nasal width), 5 indexes (ischelic index, open arms index, cranial index, facial index, nasal index) and 4 anthroposcopic marks are accepted identical in both of the studies but some of them rely on different methodologies (Table 1).

Table 1. Numerical results of M. Popov (1959) and A. Inan (1947)

Features	M. Popov (Bulgarian)		A. Inan (Turkish)	
	males (*n*-5759)	females (*n*-2160)	males (*n*-39465)	females (*n*-20263)
1. Height (mm)	1709.0	1603.8	1652.0	1522.0
2. Length of open arms (mm)	1756.2	1609.0	1714.0	1569.0
3. Head length(mm)	189.02	180.29	182.3	195.1
4. Head width (mm)	153.78	149.90	151.9	146.7
5. Frontal width (mm)	111.35	108.33	108.0	104.0
6. Facial width (mm)	139.63	132.43	139.0	130.6
7. Facial height (mm)	126.84[1]	118.52[1]	137.57[2]	129.49[2]
8. Upper facial height (mm)	79.28[3]	76.56[3]	90.10[4]	88.37[4]
9. Nasal length (mm)	58.25	56.53	52.00	48.40
10. Nasal width (mm)	33.72	31.34	34.00	31.00
1. Ischelic index (%)	53.32[5]	53.43[5]	93.91[6]	87.86[6]
2. Open arms index (%)	97.38[7]	99.79[7]	103.7[8]	103.6[8]
3. Cranial index (%)	81.30	83.23	83.33	83.78
4. Facial index (%)	90.81[1]	89.53[1]	102.32[2]	101.38[2]
5. Nasal index (%)	58.23	55.75	65.04	64.05

Explanations: 1- Nasion- Gnathion
2-Ophryon-Gnathion
3- Nasion — Stomion
4- Ophryon-Stomion
5- Sitting Height / Height
6- Height — Sitting Height / Sitting Height
7- Height / Length of open arms
8- Length of open arms / Height

Comparing anthroposcopic marks are very difficult, because criteria and categories used are different than others. Concave nasal profile ratio is 13.9% in Bulgarians, 7.64% in Turks, convex nasal profile ratio is 27.9% in Bulgarians, 61.19% in Turks (including beak shaped nose). Eye shaped epichantus frequency is 0.5% in Bulgarians and about 5% in Turks. Different scales used for eye color prevent comparison. For hair color, according to triple scale, dark-colored hair is found 41.17% in Bulgarians and 31.13% in Turks; brown hair is found 42.57% in Bulgarians and 60.27% in Turks; blonde hair is found 16.00% in Bulgarians and 8.61% in Turks.

In conclusion, the aim of this study is not to discuss the data of the two anthropological studies, that were performed 60 years ago, in detail. These studies, that were performed in two neighbouring countries simultaneously, relied on different methods and trends. But this is an interesting example of how two great anthropological schools (German and French), which do not compromise with each other, affect the developing Balkan anthropology. We want to express that both of these studies, which were performed simultaneously in Turkey and Bulgaria, are accepted as an important degree in anthropological history of the two countries [6, 10]. In the future, we would like to study on new anthropological researches with Turkish and Bulgarian anthropologists using same methods and principles.

References

1. Inan, A. Une étude anthropométrique sur 200 femmes turques en Turquie. Istanbul, 1937.
2. Inan, A. Türkiye Halkının Antopolojik Karakterleri ve Türkiye Tarihi. Ankara, TTK Basımevi, 1947.
3. Kansu, S. A. Antropometri Tetkikleri için Rehber. Ankara, Sağlık Bakanlığı Yayınları, 1937.
4. Martin, R. Lehrbuch der Anthropologie in systematischer Darstellung. Jena, Gustav Fischer Verlag, 1928.
5. Pittard, E. Les Peuples des Balkans. Paris, Georg &C^ie et Leroux.,1920. Pittard, E. Un Chef d'Etat, Animateur de l'anthropologie et de la préhistoire: Kemal Atatürk. Revue Anthropologique (Paris), 1939, p. 10.
7. http://www.evrika.org/Appendix3.htm
8. http://www.ataturk.net/ata/afet.html
9. http://www.humanity.ankara.edu.tr/fizikoantropoloji.html
10. Йорданов, Й. Наръчник по антропология. София, Унив. изд. „Св. Климент Охридски", 1997, 11—13.
11. Попов, П. Антропология на българския народ. Т. 1. Физически облик на българите. София, БАН, 1959.

Institute of Experimental Morphology and Anthropology

Acta morphologica et anthropologica, 10
Sofia•2005

Anthropological Characteristics in the Facial Morphology of Different Ethnicities

T. Petleshkova, S. Sivkov, I. Hristov, A. Baltadjiev, Y. Boukov, M. Daskalova

Department of Anatomy, Histology and Embryology, Medical University, Plovdiv

The present comparative cephalometric study of certain facial proportions of young men and women aims to enrich the knowledge of the head and face morphology in four ethnic populations from the Balkan Peninsula. The study includes 430 medical and dental students of four ethnicities at the Medical University of Plovdiv. The morphological height of the face (n-gn), maximal width of the face (zy-zy), height of the nose (n-sn), and width of the nose (al-al) were used to determine the morphological index of the face and height-width index of the nose. Excluding morphological facial index the data do not show statistically significant differences in the subcategory frequencies of both indices. The similarity in the facial characteristics of the examined ethnic groups could be due to genetic drift. The same racial identity, similar folk style and climatic conditions should also be borne in mind.

Key words: facial morphology, cephalometry, facial indices, ethnic groups.

Introduction

Morphological, quantitative and proportional differences between races and ethnic groups have been subject of numerous studies in the last century [1, 8]. The main traits that differentiate faces develop from adaptive mechanisms influenced by environmental factors and maintained during the evolution of man. Adaptation diversity has been considerably reduced during the period of human development. Significant differences within races become fewer and are caused mainly by microgenetic changes. These changes contribute to the differences between the racial subpopulations, termed prior anthropological types [2, 3].

As one of the most variable structures the craniofacial complex and especially the face appear of particular importance in the study of the human body morphology. Through its mimic the human face is an important means of communication and ensures the most direct contact with the surrounding world. The notion of attractive face can be briefly exposed as a face nice for the eye. The elaboration of objective criteria of attractive and unattractive face will provide valuable data for the esthetic and reconstructive surgery [4]. On the other hand, the head and face are often distorted by traumatic injuries or congenital malformations that require

reconstruction. Therefore, the knowledge of the craniofacial morphology, measurements and proportions is mandatory for reconstruction of the normal shape of the head and face [4, 5, 8]. The knowledge will be useful for artists, portraitists and facial illustrators.

The aim of the present comparative study of certain cephalometric proportions of young men and women is to enrich the knowledge of the morphology of the head and face in four ethnic populations from the Balkan Peninsula. The data will be useful for the needs of the craniofacial and reconstructive surgery as well as forensic identification.

Material and Methods

The study included 430 medical and dental students at the Medical University of Plovdiv. Of these 218 were Bulgarians, 63 Greeks, 77 Macedonians, and 72 Turks. Cephalometric measurements according to the rules of Martin-Saller were obtained

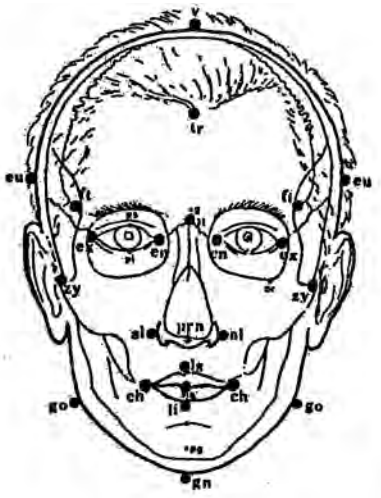

Fig. 1. Surface craniofacial landmarks used in cephalometric examinations

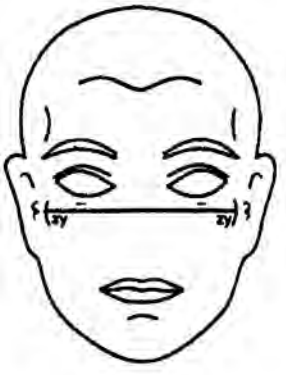

Fig. 2. Morphological height of the face (n-gn) and maximal width of the face (zy-zy)

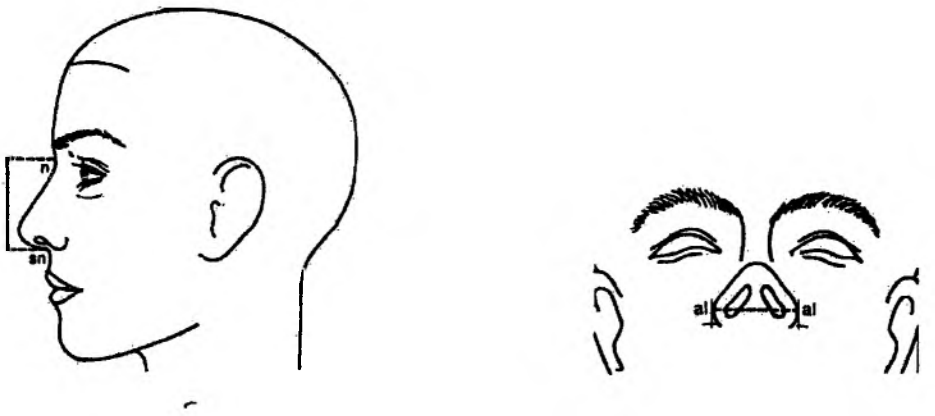

Fig. 3. Height of the nose (n-sn) and width of the nose (al-al)

from each subject [6]. Morphological height of the face (n-gn), maximal width of the face (zy-zy), height of the nose (n-sn), and width of the nose (al-al) were used to determine the morphological index of the face and height-width index of the nose [7].

The data obtained were analyzed by ANOVA analysis and Mann-Whitney U test at level of significance $p<0.05$.

Results

Height-width index of the nose

In the females of the four ethnic groups the height-width index varied between 50.9 and 60.7, i.e., they were leptorrhines with high and narrow nose (Table 1). Of the Bulgarian females 78% were leptorrhines, 16% were hyperleptorrhines, and 5.7% mesorrhines. The Turkish females presented with higher persentage of leptorrhines — 82.4%, smaller percentageage of hyperleptorrhines — 11.8% and similar percentage of mesorrhines compared with the Bulgarian females. The Macedonians presented mainly as leptorrhines — 71.7% but the percentage of hyperleptorrhines and mesorrhines was higher than in the Bulgarian and Turkish females (17.4% and 10.9%, respectively). The Greek females were leptorrhines in 68.8% and the hyperleptorrhines were of the highest percentage (21.9%) compared with the other

Table 1. Height-width index of the nose in the females of the four ethnic groups

	Bulgarians		Greeks		Macedonians		Turks		Statistical significance*	
Subcategory	Number	%	Number	%	Number	%	Number	%	F	*p*
									0.587	0.632
Hyperleptorrhine	17	16	7	21.9	8	17.4	4	11.8		
Leptorrhine	83	78.3	22	68.8	33	71.7	28	82.4		
Mesorrhine	6	5.7	3	9.4	5	10.9	2	5.9		
Hamerrhine	0	0	0	0	0	0	0	0		
Hyperhamerrhine	0	0	0	0	0	0	0	0		

*One-way ANOVA with Tukey's honesty significance (HSD) for multiple comparisons - <0.05

Table 2. Height-width index of the nose in the males of the four ethnic groups

Subcategory	Bulgarians		Greeks		Macedonians		Turks		Statistical significance*	
	Number	%	Number	%	Number	%	Number	%	F	*p*
									0.919	0.453
Hyperleptorrhine	8	7.1	1	3.2	2	6.5	4	10.5		
Leptorrhine	76	67.9	20	64.5	27	87.1	27	71.1		
Mesorrhine	27	24.1	10	32.3	2	6.5	7	18.4		
Hamerrhine	1	0.9	0	0	0	0	0	0		
Hyperhamerrhine	0	0	0	0	0	0	0	0		

*One-way ANOVA with Tukey's honesty significance (HSD) for multiple comparisons - <0.05

ethnic groups. Typical wide nose appearance — hamerrhine and hyperhamerrhine, was found in none of the females. There were no statistically significant difference in the subcategory frequency of the height-width index as a whole (ANOVA, F=0.587, p=0.632) and between single ethnic groups (p>0.05).

The males of the four ethnic groups presented as leptorrhines with index values between 63.0 and 65.0 (Table 2). The highest percentage of leptorrhines was found in the Macedonians (81.1%), followed by the Turks (71.1%), and almost equal percentage in the Bulgarians and Greeks (67.1% and 64.5%, respectively). The Turks showed the highest percentage of hyperleptorrhines (10.5%) and the Greeks the smallest (3.2%). Mesorrhines were most frequent in the Greeks and Bulgarians, 32.3% and 24.1%, respectively. The difference in frequency of the subcategories reached statistical significance neither as a whole (ANOVA, F=0.919, p=0.453) nor between single ethnic groups (p>0.05).

Morphological index of the face

In the females the morphological facial index varied between 87.2 and 87.7, i.e., leptoprosopes prevail in all ethnic groups (Table 3). The highest percentage of leptoprosopes showed the Turkish females (58.8%), followed by the Macedonians (39.1%) and Bulgarians (36.8%). The lowest percentage of leptoprosopes was in the Greek females (34.4%). The Greek and Bulgarian females presented with the highest percentage of hyperleptoprosopes (31.2% and 30.2%, respectively) and the lowest percent was found in the Turkish females (17.6%). High percentage of mesoprosopes was found in the Bugarian (24.5%), Greek (21.9%) and Macedonian (28.3%) females and much lower in the Turkish females (17.6%). Hypereuriprosopes were found in low percentage in the Bulgarian (3.8%) and Macedonian (4.3%) females and absent in the Greek and Turkish females. The last two groups presented with comparatively high percentage of euriprosopes — 12.5% in the Greek and 11.8% in the Turkish

Table 3. Morphological index of the face in the females of the four ethnic groups

Subcategory	Bulgarians		Greeks		Macedonians		Turks		Statistical significance*	
	Number	%	Number	%	Number	%	Number	%	F	*p*
									2.503	0.096
Hyperprosope	3	3.8	0	0	2	4.3	0	0		
Euriprosope	6	5.7	4	12.5	1	2.2	4	11.8		
Mesoprosope	26	24.5	7	21.9	13	28.3	4	11.8		
Leptoprosope	39	36.8	11	34.4	18	39.1	20	58.8		
Hyperleptoprosope	32	30.2	10	31.2	12	26.1	6	17.6		

*One-way ANOVA with Tukey's honesty significance (HSD) for multiple comparison s - <0.05

Table 4. Morphological index of the face in the males of the four ethnic groups

Subcategory	Bulgarians		Greeks		Macedonians		Turks		Statistical significance*	
	Number	%	Number	%	Number	%	Number	%	F	p
									5.087	0.012
Hyperprosope	6	5.4	0	0	1	3.2	1	2.6		
Euriprosope	21	18.8	3	9.7	2	6.5	7	18.4		
Mesoprosope	28	25.0	4	12.9	12	38.7	9	23.7		
Leptoprosope	40	35.7	13	41.9	10	32.3	16	42.1		
Hyperleptoprosope	17	15.2	11	35.5	6	19.4	5	13.2		

*One-way ANOVA with Tukey's honesty significance (HSD) for multiple comparisons - <0.05

females. The difference in frequency of the subcategories of the morphological facial index failed to reach statistical significance as a whole (ANOVA, F=2.503, p=0.096) and between single ethnic groups (p>0.05).

The males of the four ethnic groups were mainly leptoprosopes with index mean values varying between 88.0 and 91.3 (Table 4). Leptoprosopes were most numerous in the Turks (42.1%) and the Greeks were close (41.9%). In lower frequency leptoprosopes were found in the Bulgarians (35.7%) and Macedonians (32.3%). The highest percentage of hyperleptoprosopes was found in the Greeks (35.5%) and the lowest in the Turks (13.2%). Mesoprosopes were most frequent in the Macedonians (38.7%), and all but 12.9% in the Greeks. The highest percentage of euriprosopes was found in the Bulgarians (18.8%) and Turks (18.4%). Hypereuriprosopes were not present only in the Greeks. The analysis revealed statistically significant differences in the frequency of the subcategories of the morphological facial index as a whole (ANOVA, F=5.087, p=0.011). Statistically significant between-group differences were found between the Bulgarians and Greeks (U=22.5, p=0.03) and between the Bulgarians and Macedonians (U=23.00, p=0.03).

Conclusions

Like previous studies the present study data, together with the fact that the facial morphology is genetically determined, suggest that the similarity in the facial characteristics of the examined ethnic groups be due to mixture of the genetic background. Formation of the examined ethnic groups results from a long historical period and close coexistence. The same racial identity, similar folk style and climatic conditions should also be borne in mind.

References

1. Coon, C. S. The origin of races. New York, AA Knopf, 1962.
2. Chung, C. S., M. C. W. Kau, G. F. Walker. Racial variation of cephalometric measurements in Hawaii. — J. Craniofac. Genet. Dev. Biol., 2, 1982, 99-106.
3. Chunk, C. S. et al. Effects of interracial crosses on cephalometric measurements. — Am. J. Phys. Anthropol., 69, 1986, 465-472.
4. Farkas, L. G., J. C. Kolar. Anthropometrics and art in the aesthetics of women's faces. — Clin. Plast. Surg., 14, 1987, 599-616.
5. Farkas, L. G., L. R. Munro. Anthropometric facial proportions in medicine. Springfield, Charles C. Thomas, 1987.
6. Martin, R., K. Saller. Lehrbuch der Anthropologie. Stuttgart, G. Fischer, 1957.
7. Йорданов, Й. Антропология в стоматологията. С., Медицина и физкултура, 1981.
8. Рогинский, Я. А., М. Г. Левин, Основи антропологии. Москва, Моск. унив., 1955.

Institute of Experimental Morphology and Anthropology

Acta morphologica et anthropologica, 10
Sofia•2005

Changes in the Nose with Growth on 7-17-Year-Old Schoolchildren from Sofia

Z. Filcheva, N. Kondova

Institute of Experimental Morphology and Anthropology, Bulgarian Academy of Sciences, Sofia

The results presented constitute a part of a complex anthropological study on 7-17-year-old schoolchildren from Sofia. Age changes of four nose sizes, the nose index and shape have been traced as a result of 3602 individual measurements — 1778 for the boys and 1824 for the girls. Most intensely pronounced are changes in the breadth and depth of the nose in both sexes. The per cent of the of the concave noses decreases with age while the per cent of the convex noses increases. Intersexual differences are most clearly expressed in the nose breadth as early as the age of 7.

Key words: nose, schoolchildren, age changes, intersexual differences.

Introduction

The nose is an important trait of the morphological characteristics of human face. Investigating in children and adolescents represents a special interest [1, 2, 4, 5, 6].

The aim of the present study is to trace the dynamics of age changes of four sizes and shape of the nose between the ages of 7 to 17, to record the rate of growth of the features under study and to detect the intersexual differences.

Material and Methods

The subject of the study realized as a mixed one (longitudinal-transversal) are schoolchildren aged between 7 and 17 years from five schools of Sofia. A total of 3602 individual measurements — 1778 for the boys and 1824 for the girls aged 7-17 years from five Sofia schools have been carried out after the classical method [3]. The age changes in the height, length, depth and breadth of the nose, the nose index and shape of the nose have been traced and analyzed. The methods of the t-criterion and χ^2-test have been used in the comparative analysis.

Results and Discussion

The mean values of the studies sizes of the nose grow unevenly between the ages 7 and 17 in both sexes (Table 1). The height and length of the nose in boys grow most intensely between 11 and 13 years of age and especially between 13 and 15 and in girls — 9 and 11, especially between 11 and 13. At 17 the height and length of the nose in the boys has reached 94,8% and 93,8% of the mean values for adult Bulgarians and in the girls this fact is recorded as early as 11-12 years of age. The nose depth in both sexes reaches the values for the grown-up Bulgarians as early as 10-11 years of age. The nose index in the 7 to 17-year-old boys displays the limit values of the leptorrhin-mesorrhin categories while with the girls it is in leptorrhin category. The intersexual differences in the height and length of the nose are best pronounced between 14 and 17 ($P<0,001$), in the nose breadth as early as 7 years of age ($P<0,001$) and in the nose depth — between 8 and 12 and 16 and 17 years of age ($P<0,01$). The per cent of concave noses decreases with age but straight noses prevail. Between 15 and 17 the per cent of the convex noses considerably increases as well. Intersexual differences are insignificant in the nose form ($P>0,05$).

Conclusions

The period under study — from 7 to 17 years of age is characterized with dynamic changes expressed by the more rapid growth of the nose breadth and depth as compared with its heigth and length. The per cent of the concave noses is decreasing while the one of the convex noses increases. The intersexual differences are best marked in the nose breadth as early as the 7-year-old children.

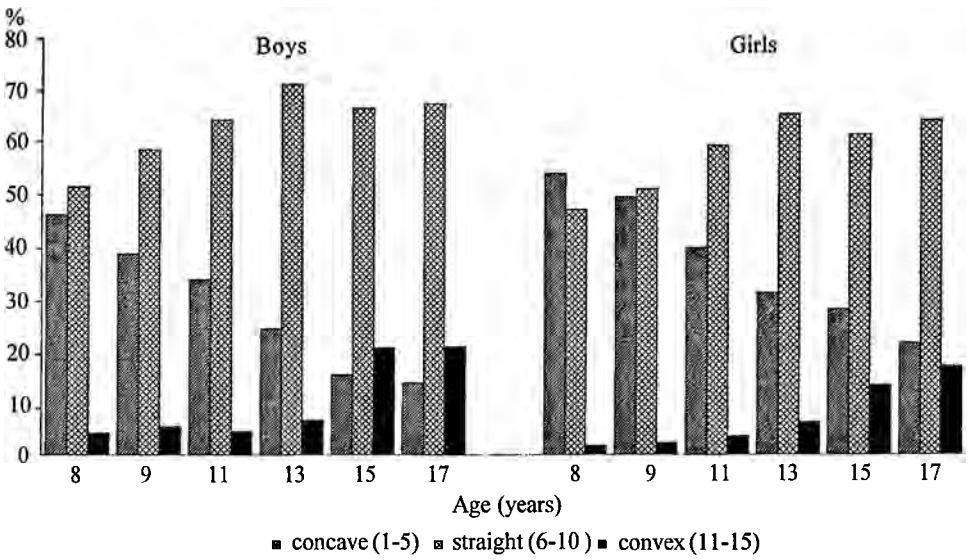

Fig. 1. Age changes in the nose shape

Table 1. Age changes in the nose measurements and in the nose index

FEATURE	AGE (years)	BOYS			GIRLS		
		n	$\bar{X}$	SD	*n*	$\bar{X}$	SD
Nose height	7	182	44.07	3.00	177	43.32	2.75
	8	190	44.49	2.90	182	44.09	2.84
	9	189	45.41	2.88	181	44.79	2.75
	10	190	46.02	3.00	186	45.59	2.93
	11	183	46.53	2.83	204	46.18	3.07
	12	172	47.73	3.08	190	47.38	3.12
	13	166	49.18	3.32	184	48.39	3.01
	14	139	49.96	3.65	138	48.15	3.19
	15	124	52.06	3.89	137	48.83	2.98
	16	133	51.69	3.13	127	48.64	2.88
	17	118	52.70	3.11	137	49.03	3.16
Nose length	7	182	41.44	3.17	177	40.72	2.97
	8	190	41.59	3.17	182	41.28	3.00
	9	189	42.64	3.05	181	42.04	2.99
	10	190	43.46	3.16	186	43.08	3.07
	11	183	44.24	2.92	204	44.15	3.11
	12	172	45.50	3.18	190	45.54	3.13
	13	166	47.11	3.46	184	46.55	3.01
	14	139	48.15	3.81	138	46.44	3.35
	15	124	50.13	3.78	137	46.93	3.09
	16	133	49.96	3.21	127	47.13	2.78
	17	118	50.92	3.16	137	47.31	3.25
Nose depth	7	182	12.48	1.38	177	12.62	1.51
	8	190	12.87	1.44	182	13.31	1.62
	9	189	14.38	1.40	181	14.71	1.66
	10	190	15.17	1.38	186	15.58	1.68
	11	183	16.02	1.68	204	16.60	1.82
	12	172	17.42	1.53	190	17.98	1.89
	13	166	18.39	1.75	184	18.70	1.86
	14	139	18.80	2.00	138	18.91	1.94
	15	124	19.58	2.52	137	19.43	1.94
	16	133	19.74	1.90	127	18.45	1.82
	17	118	20.28	2.06	137	19.26	1.88
Nose breadth	7	182	29.34	1.84	177	28.47	1.86
	8	190	30.99	1.82	182	30.04	1.83
	9	189	31.93	1.73	181	30.99	1.75
	10	190	32.48	1.64	186	31.94	1.72
	11	183	32.66	1.73	204	32.14	1.91
	12	172	33.48	1.85	190	32.98	1.89
	13	166	34.14	1.88	184	33.44	1.89
	14	139	34.55	2.07	138	33.03	1.87
	15	124	35.42	1.91	137	33.14	2.00
	16	133	35.71	2.24	127	32.65	1.77
	17	118	35.79	2.10	137	33.11	2.10
Nose index	7	182	66.85	5.79	177	65.95	5.66
	8	190	69.92	5.74	182	68.39	5.79
	9	189	70.57	5.58	181	69.46	5.82
	10	190	70.86	5.71	186	70.32	5.70
	11	183	70.42	5.40	204	69.88	6.12
	12	172	70.41	5.63	190	69.90	5.97
	13	166	69.72	5.75	184	69.34	5.62
	14	139	69.50	6.38	138	68.92	6.35
	15	124	68.45	6.66	137	68.14	6.14
	16	133	69.39	6.64	127	67.40	5.86
	17	118	68.20	6.25	137	67.82	6.28

References

1. Brůžek, J., K Hajniš. Die Entwicklung der Nase bei prager Kindern und Jugendlichen zwischen dem 10. bis 19. Lebensjahr. — Anthropologie, **XIV**, 1976, No 1,2, 5-13.
2. Jasicki, B. The development with increasing age of the head dimensions andproportions in the youth of Cracow. — Zeszyty Naukowe Universitetu Jagiellonskiego, Prace Zoologiczne, **12**, 1966, 7-35.
3. Martin, R., K. Saller. Lehrbuch der Anthropologie in sistematischer Darstellung, T. I. Stuttgart, Gustav-Fischer Verlag, 1957, 363-371, 385-429.
4. Štefančič, M. Growth of the face, nose and ear in the late chiodhood — Glasnic anthropološkog društva Jugoslavije, **18**, 1981, 121-133.
5. Štefančič, M., P. Leben-Seljak. Growth of head and face in children from Ljubljana during adolescence: mixed longitudinal study. — Anthropološki zvezki, **4**, 1996, 73-85.
6. Миклашевская, Н. Н, В. С. Соловьева, Е. З. Година. Ростовые процессы у детей и подростков. Москва, Моск. унив.,1988, 35—40.

Institute of Experimental Morphology and Anthropology

Acta morphologica et anthropologica, 10
Sofia • 2005

Distribution of the Subcutaneous Fat Tissue in Patients with Type 2 Diabetes Mellitus

A. Baltadjiev, S. Sivkov, Y. Boukov, I. Hristov, T. Matev, S. Vladeva, G. Baltadjiev

Department of Anatomy, Histology and Embryology, Clinic of Endocrinology, Medical University, Plovdiv

The aim of the present study is to determine the deposition and distribution of the subcutaneous fat tissue in patients with type 2 diabetes mellitus. Female (n=69) and male (n=36) patients with type 2 diabetes mellitus were examined. The mean age of the females was 65.2 years and of the males 65.5 years. All patients were of Bulgarian ancestry. Nine skin folds in the upper and lower limbs, thorax and abdomen were measured with skin fold calipers type Lange. The data obtained allow determining the tendency of distribution of the subcutaneous fat tissue. In the females the skin folds were thicker in the abdomen than in the thorax and in the lower limbs thicker than in the upper limbs. Males have greater deposition of subcutaneous fat tissue in the thorax than in the abdomen and in the lower limbs than in the upper limbs.

Key words: skin folds, subcutaneous fat tissue, type 2 diabetes mellitus.

Introduction

Diabetes mellitus attracts greatly the interest in the modern society [3, 5]. The relation between age, overweight, distribution of the subcutaneous fat tissue and risk of type 2 diabetes mellitus is widely discussed. The hypothesis of the relationship between type pear and type "apple" obesity in type 2 diabetes mellitus patients and severity of the associated cardiovascular syndromes has been recently proposed [1, 2, 4, 5].

The aim of the present study is to establish the deposition of distribution of the subcutaneous fat tissue in patients of both sexes with type 2 diabetes mellitus.

Material and Methods

Female (n=69) and male (n=36) patients with type 2 diabetes mellitus were examined. The mean age of the females was 65.2 years and of the males 65.5 years. All patients were of Bulgarian ancestry. Skin folds were measured with skin fold calipers type Lange in nine body areas — over the triceps and biceps brachii, in the

forearm, subscapular region, over the 10th rib, abdomen, iliac crest, in the thigh and leg. The data were analyzed in SPSS 11.0. The level of significance was accepted at $p<0.05$.

Results and Discussion

Females

The results of the descriptive statistics of the skin fold thickness are shown in Table 1.

Skin folds of the thorax and upper limb

The skin folds over the 10th rib and in the subscapular region are thickest and the difference between them does not reach statistical significance ($p>0.05$). The thickness of both skin folds is significantly greater than that over the triceps brachii, biceps brachii and in the forearm ($p<0.001$). The skin fold over the triceps is significantly greater than the skin folds over the biceps brachii and in the leg. There is no statistically significant difference between the skin folds over the biceps brachii and in the forearm ($p>0.05$).

Table 1. Descriptive statistics of the skin folds in the female patients (mm)

Variable	*n*	Mean	S.D.	max	min
sf Triceps	69	18.2913	7.6889	40.2	5.2
sf Biceps	69	11.1536	4.5528	24.4	3
sf Antebrach.	69	10.3420	3.7489	21.2	3.8
sf Subscapul.	69	23.7449	8.5139	50	9
sf Xcosta	69	24.4	7.5920	47.4	11.4
sf Abdomen	69	27.78	8.5661	42	7.8
sf Cr. Iliaca	69	18.2261	6.2219	34	5.6
sf Femur	69	17.3739	10.9906	41	4.2
sf Crus	69	17.1783	8.5239	39.2	3.3

Skin folds of the abdomen and lower limb

The skin fold of the abdomen is the thickest and significantly greater than the skin folds over the iliac crest, in the thigh and leg ($p<0.001$). The second in thickness is the skin fold over the iliac crest, which however does not differ significantly from the skin folds in the thigh and leg ($p>0.05$). The last two skin folds are of almost equal thickness.

Comparison between the skin folds of the upper and lower half of the body

The skin fold of the abdomen is the thickest and statistically greater than the skin folds in the upper part of the body and upper limbs ($p<0.001$). The difference between the skin fold of the abdomen and over the 10th rib is of moderate statistical significance ($p<0.01$). The skin folds over the 10th rib and subscapular region are significantly greater than those of the lower limb ($p<0.001$). The skin fold in the thigh is significantly greater than that over the biceps brachii ($p<0.001$) and almost equal

with that over the triceps brachii ($p>0.05$). The skin fold in the leg is almost equal with that over the triceps brachii ($p>0.05$) and significantly thicker that the skin folds over the biceps brachii and in the forearm ($p<0.001$).

The skin fold in the forearm is of lowest thickness followed by that over the biceps. Our findings show an indistinct tendency of deposition of subcutaneous fat tissue in the region of the abdomen and lower limbs. Some authors report that the subcutaneous fat in females with type 2 diabetes mellitus is laid down exclusively in the upper part of the body with tendency to "super apple" [5, 6].

Conclusions

1. The subcutaneous fat tissue deposition in the upper part of the body is greater in the thoracic region and more expressed in the chest than in the back. The subcutaneous fat deposition is less expressed in the upper limbs and especially on the back of the arm.
2. The amount of subcutaneous fat tissue is significantly greater in the region of the abdomen than in the lower limbs.
3. The subcutaneous fat tissue deposition shows a tendency to a downward decrease on the body and is more expressed in the lower than in the upper limbs.

Males

The results of the descriptive statistics of the skin fold thickness are shown in Table 2.

Skin folds of the thorax and upper limb

The thickest is the skin fold over the 10^{th} rib followed by that in the subscapular region and the difference between them does not reach statistical significance ($p>0.05$). The difference between both skin folds and the other skin folds (triceps, biceps and forearm) is statistically significant ($p<0.001$). The upper limb skin folds are of lower thickness and the difference between them and those of the thorax reaches statistical significance. The thickest is the skin fold over the triceps, which is statistically greater than the skin folds over the biceps and in the forearm ($p>0.001$).

Table 2. Descriptive statistics of the skin folds in the male patients (mm)

Variable	*N*	Mean	S D	maxi	min
sf Triceps	36	9.2472	3.3494	18.6	3.2
sf Biceps	36	6.3222	2.5738	12.4	2.6
sf Antebrach.	36	6.1583	2.9292	14	2.6
sf Subscapul.	36	19.0806	7.1612	35.8	7.8
sf Xcosta	36	21.3306	7.3925	40.2	9.8
sf Abdomen	36	19.6583	9.1793	42.4	6.2
sf Cr. Iliaca	36	11.1583	5.7402	31	4
sf Femur	36	11.5361	6.8540	27.8	4
sf Crus	36	7.2667	3.3860	19.6	3.2

Skin folds of the abdomen and lower limb

The skin fold of the abdomen is the thickest and significantly greater than the skin folds over the iliac crest, in the thigh and leg ($p<0.001$). The skin fold in the leg is of lowest thickness and the difference with the other skin folds is statistically significant ($p<0.001$). The skin folds over the iliac crest and in the leg are of almost equal thickness and significantly thinner than the skin fold of the abdomen ($p<0.001$).

Comparison between the skin folds of the upper and lower half of the body

The skin fold over the 10th rib is the thickest followed by those of the abdomen, subscapular region, thigh, iliac crest, triceps, leg, biceps and forearm.

The skin fold over the 10th rib is insignificantly greater than that of the abdomen ($p>0.05$) and significantly greater than the skin folds in the lower limb ($p<0.001$).

The subscapular skin fold is almost equal in thickness to the skin fold of the abdomen ($p>0.05$) and significantly thicker than the skin folds in the lower limb ($p<0.001$).

The skin fold in the thigh is slightly thicker than that over the triceps brachii ($p>0.05$), significantly thicker than the skin folds over the biceps brachii and in the forearm but significantly thinner than the skin folds over the 10th rib and in the subscapular region ($p<0.001$).

The skin fold in the leg is significantly thinner than that over the triceps brachii, 10th rib and subscapular region ($p<0.001$), slightly thicker that the skin fold in the forearm ($p>0.05$) and almost equal to the skin fold over the biceps brachii.

Our findings show an indistinct tendency to a greater deposition of subcutaneous fat tissue in the upper parts of the body. Horejsi et al. have reported that the subscapular and midaxillar skin folds are significantly thicker in male patients with type 2 diabetes mellitus [3]. Hence, there is a tendency to an "apple" type deposition of the subcutaneous fat tissue.

Conclusions

1. The subcutaneous fat tissue deposition in the upper part of the body is greater in the thoracic region and almost equal in the chest and in the back. The subcutaneous fat deposition in the upper limbs is more expressed on the back of the arm.
2. The amount of subcutaneous fat tissue is significantly greater in the region of the abdomen and proximal part of the lower limbs.
3. The subcutaneous fat tissue is greater in the region of the thorax than in the abdomen. The skin folds are thicker in the lower than in the upper limbs. The subcutaneous fat tissue shows a tendency to an "apple" type deposition.

Intergender differences in the skin folds

The examined skin folds are significantly greater in the female than in the male patients with type 2 diabetes mellitus ($p<0.001$). The only exception is the skin fold over the 10th rib with intergender difference failing to reach statistical significance ($p>0.05$).

It could be concluded that the deposition of the subcutaneous fat tissue is greater in the female than in the male type 2 diabetes mellitus patients.

References

1. Attvall, S. Diabetes and obesity. — Obesity, **1**, 2003, 15.
2. Goodpaster, B. H. et al. Association between regional adipose tissue distribution and both type 2 diabetes and impaired glucose tolerance in eldery men and women. — Diabetes Care, **26**, 2003, 372-379.
3. Horejsi, R. et al. Differences of subcutaneous adipose tissue topography between type-2 diabetic men and healthy controls. — Exp. Biol. Med., **227**, 2002, 794-798.
4. Isomaa, B. et al. Cardiovascular morbidity and mortality associated with the metabolic syndrome. — Diabetes Care, **24**, 2001, 683-689.
5. Moller, R. et al. Quantifying the "appleness" or "pearness" of human body by subcutaneous adipose tissue distribution. — Ann. Hum. Biol., **27**, 2000, 47-55.
6. Tafeit, E. et al. Differences of subcutaneous adipose tissue topography in type-2 diabetic (NIDDM) women and healthy controls. — Am. J. Phys. Anthropol., **113**, 2000, 381-388.

Institute of Experimental Morphology and Anthropology

Acta morphologica et anthropologica, 10
Sofia • 2005

Obesity and Overweight Prevalence of the Adult Population in the Trakya Region of Turkey

B. S. Cigali

Trakya University, Medical Faculty, Department of Anatomy, Edirne, Turkey

Purpose: To evaluate the prevalence of the obesity and overweight in the Trakya Region of Turkey.
Method: A random sample of 798 inhabitants of Edirne (382 women and 416 men) aged 18-84 years participated in our work. All participants answered a structured questionnaire comprising information on social, demographic, and behovioral and clinical aspects. When the BMI (body mass index) was > = 30 kg/m^2, the subject was considered as "obese" and if BMI was between the 25kg/m^2 and 30kg/m^2 then the subject was considered overweight. Spearmen correlation analyses were performed to determine whether BMI scores were related to other aspects.

Results: The mean BMI was 25.55 kg/m^2 and the prevalence of the obesity was 15.9 % and the overweight was 31.6%. BMI is significantly correlated with age, gender, education level, marital status, hypercolestrolemia, hypertension and diabetes. There was no correlation with smoking and alcohol intake.

Conclusion: Obesity is a major issue of public health in Trakya Region of Turkey and obese individuals have some chronic health problems. Obesity increased with age and marriage, and it is more frequent among low educated men.

Key words: obesity, overweight, body mass index, adult, Turkey.

Obesity is a growing health problem for all countries even when they are developed or developing. The fundamental causes of obesity epidemic are sedentary lifestyles, high fat and energy dense diets, despite the dissemination of a large variety of diet programs, fat free or low-fat foods. It is reported the prevelance of obesity among the adult people is increasing and today it is known that obesity is a risk factor for some diseases and mortality. On the other hand, the influence of western culture spreads even to Asian countries. As a sample in Japan fashion magazines publish articles on how to achieve the ideal (thin) body, and white models appear in 30% of television commercials and today Japanese females wish they were taller, would prefer to be blonde, and have longer legs. As a result of these kinds of expectations the desire for thinness seems to be increasing with the body/self dissatisfaction and eating disorders. BMI is a commonly used measure of body size, obtained by dividing the weight in kilograms by the square of the height in meters. A BMI over 25 kg/m^2 is defined as overweight, and a BMI of over 30 kg/m^2 as obese.

Our aim in this study is to determine the obesity prevalence in Trakya Region and to see the correlation with some diseases, social and behavioral conditions.

Methods

798 people participated our study. Sample consisted of a total of 382 (mean age 37.99 +/–15.22) female and 416 (mean age 39.45 +/–14.41) male adults. All participants answered a structured questionnaire including age, gender, height, weight, marital status, education level (no education, literate, primary school, secondary school, high school, university), cigarette smoking (never, current), alcohol consumption (never, daily, weekly, monthly) and existence of hypertension, hypercolestrolemia and diabetes. These last three conditions were accepted positive if the case was being followed by a medical establishment or using a medicine or applying a special diet for instance low salt or low fat diets. All participants randomly selected from the primer health establishments in a week to avoid the repetition. Questions were asked by educated health staff. Body Mass Index (BMI) is calculated by dividing weight in kilograms by height in meters squared. A BMI below 18.5 indicates unusual thinness and possibility of anorexia nervosa. A BMI of 25-29.9 indicates overweight status and a BMI of greater than 30 indicates obesity. Spearman correlation analyses were performed to determine whether BMI scores were related to other parameters.

Results

Regardless of gender the mean BMI was found 25.55 kg/m^2 and the prevalence of obesity was 15.9 % and the overweight 31.6 %. The mean BMI for males was 26.06 +/–3.82 and the prevalence of the obesity was 14.42% and overweight prevalence was 46.15%. The mean BMI for females was 25.00 +/–5.17 and the prevalence of the obesity and overweight were 17.8 % and 25.91%. 44.61 % of the population were smoking, 28.69 % drinking alcohol daily, weekly or monthly, and they were married 68.67%. The prevalence of the hypertension was 19.04%, hypercholestrolemia 13.91% and diabetes mellitus 6.65%. Using Spearman correlation analyses it was determined that BMI is significantly correlated to age $r = 0.455$ $p<0.001$, marital status $r = 0.399$ $p<0,001$, gender $r = -0.116$ $p<0.001$, education $r = -0.287$ $p<0.001$, hypertension $r = 0.300$ $p<0.001$, hypercolestrolemia $r = 0.255$ $p<0.001$, diabetes mellitus r = 0.182 $p<0,001$. It was not found a correlation to cigarette smoking $r = 0.051$ $p>0.05$ and alcohol consumption $r = 0.043$ $p>0.05$. The male and female population divided into three groups: obese, overweight and normal to compare the prevalence of three diseases. The results were given in the table 1.

Table 1. The prevalence of Hypertension, Hypercholestrolemia and Diabetes Mellitus for normal, overweight and obese people

Features	BMI (kg/m^2)					
	<25		25-30		>30	
	male %	female %	male %	female %	male %	female %
Hypertension	12.88	7.94	17.09	32.00	28.33	47.05
Hypercholestrolemia	7.36	7.47	12.95	20.00	21.66	36.76
Diabetes Mellitus	4.36	2.33	6.73	11.00	6.66	17.64

Discussion

The results show that obesity and overweight are spreading. The mean BMI is 25.55 kg/m^2 and 47.5% of our population exceeded the 25 kg/m^2 limit. In Turkey the oldest scientific research about anthropometry is Afet İnan's work which was published in 1947. According to this results the mean height and weight of males and females are 1652mm 62.01kg and 1522mm and 52.89kg sequentially [4]. Unfortunately she did not calculate the BMI values but it may estimated about 23kg/m^2 from these averages. Our mean height and weight are 1726.4+/–70mm, 77.69+/–12.34 kg for males and 1613.3+/–6.45mm, 64.92+/–13.16 kg for females. It is seen that our male population became longer about 7cm and females 9cm in last 67 years. But unfortunately our BMI values are also increasing comparing those years.

In literature there are lots of works about the prevalence of overweight and obesity. The obesity prevalence of adolescents was reported 2.3% in Turkey [5]. Lissau et al. searched the adolescent population of 13 European countries, United States and Israel. Their results show that the highest prevalences of overweight were found in the United States (15.1% for girls and 13.9% for boys), Ireland, Greece, and Portugal. They also concluded that the prevalence of obesity and overweight were increasing by age [6]. Yates A. et al. reported BMI values from the different ethnic groups from the USA. The mean BMI was 25.15 for whites, 24.30 for Japanese, 21.70 for Chinese and the average of all 24.90kg/m^2 [11]. Santos reported the prevalence of obesity was significantly higher in women (26.1%) than men (13.9%) among the Portuguese adults [9]. A progressive and significant increase in weight, height and BMI of the Portuguese young male population was reported between 1960 and 1990 [1]. The percentage of young males with BMI over 25 kg/m^2 was of 8.1% in 1960 and of 18.0% in 1990, while those having a BMI over 27 kg/m^2 varied between 3.6% and 6.4% in the same period, respectively. The percentage of young adult males with BMI higher than 25 kg/m^2 doubled between 1960 and 1990. In 2002 the overall prevalence of obesity was 16% and the prevalence of overweight –49.1% in Lithuanian population [3]. Reich A et al. concluded obesity is an increasing problem even among schoolchildren in Germany [8]. England has the same problem with the ratios of overweight children about 20% [7]. The mean BMI values 25.3–27.0 are reported from Poland for female adults [10]. The cumulative incidence of obesity from birth to grave was 33.8% in men and 32.4% in women in Finland [2].

It is obvious that obesity is a growing health problem for all western countries today. It is also a risk factor for some diseases such as cardiovascular, metabolic and some kinds of cancer. According to our results hypertension, hypercholestrolemia and diabetes mellitus were increasing while the BMI was increasing as well. In table 1 this increasing trend is seen more obviously for females. Obese females have 47.05 % hypertension 36.76% hypercholestrolemia and 17.64% diabetes mellitus. These results show that obesity is destructive especially for women.

Alcohol consumption and cigarette smoking was not correlated with BMI. Smoking is very common in our population, it is 52.88% among males and 35.60 among females. Smoking is one of the most important risk factors for the cancer. This addiction together with obesity may become more dangerous. Trakya region is known with the high alcohol consumption. It is 43.50 % among men and 12.56 % among women.

Education level was one of the correlated factors to BMI. Its negative correlation value ($r = -0{,}287$ $p < 0{,}001$) indicates that obesity was increasing among the low educated people.

Conclusions

Obesity is a serious problem in Turkey. It is more common between the married low educated men. Obese people are more endangered to have hypertension, hypercholestrolemia and diabetes mellitus. Alcohol consumption and cigarette smoking was not correlated to BMI.

References

1. De Castro, J. J. et al. Secular trends of weight, height and obesity in cohorts of young Portuguese males in the District of Lisbon: 1960-1990. Eur. J. Epidemiol., Apr;14(3),1998, 299-303.
2. Eriksson, J. et al. Obesity from cradle to grave. Int. J. Obes. Relat. Metab. Disord., 27, 2003, No 6, 722-777.
3. Grabauskas, V. et al. The prevalence of overweight and obesity in relation to social and behavioral factors (Lithuanian health behavior monitoring). Medicina (Kaunas), 39, 2003, No 12, 1223-1230.
4. İnan, A., Türkiye halkının antropolojik karakterleri ve Türkiye Tarihi. Ankara, Türk Tarih Kurumu Basımevi, 1947.
5. Kanbur, N. O., O. Derman, E. Kinik. Prevalence of obesity in adolescents and the impact of sexual maturation stage on body mass index in obese adolescents. Int. J. Adolesc. Med. Health. Jan-Mar;14(1), 2002, 61-65.
6. Lissau, I. et al. Body mass index and overweight in adolescents in 13 European countries, Israel, and the United States. Arch. Pediatr. Adolesc. Med. Jan;158(1), 2004, 27-33.
7. Lobstein, T. J., W. P. James, T. J. Cole. Increasing levels of excess weight among children in England. Int. J. Obes. Relat. Metab. Disord., 27, 2003, No 9, 1136-1138.
8. Reich, A. et al. Obesity and blood pressure-results from the examination of 2365 schoolchildren in Germany. Int. J. Obes. Relat. Metab. Disord., 27, 2003, No 12, 1459-1464.
9. Santos, A. C., H. Barros. Prevalence and determinants of obesity in an urban sample of Portuguese adults. Public Health. Nov;117(6), 2003, 430-7.
10. Szklarska, A., E. A. Jankowska. Independent effects of social position and parity on body mass index among Polish adult women. J. Biosoc. Sci., 35, 2003, N0 4, 575-583.
11. Yates, A., E. Edman, M. Aruguete. Ethnic diffrences in BMI and body/self-dissatisfaction among Whites, Asian Subgroups, Pacific Islanders, and African-Americans. J. Adolescent. health., 34, 2004, 300-307.

Institute of Experimental Morphology and Anthropology

Acta morphologica et anthropologica, 10
Sofia • 2005

Variations in the Body Mass Index (BMI) of Middle-Aged Men: Effects of the Occupation, Age and Social Class

E. Andreenko

Biological Faculty, University of Plovdiv, Plovdiv

In this study 860 persons (males) at the age of 30-50 years of different professions and different social status have been investigated. The basic anthropometric characteristics of each one of them were taken — height and weight, on the basis of which their BMI was calculated (kg/m^2). The results show that amongst all men studied, the relative share of men with Grade 1 overweight is highest, and that of men with Grade 3 overweight is lowest.

Kew words: BMI, overweight, males, age, socioprofessional status.

Introduction

Body weight is one of the main indicators of the physical status of man on every stage of his postnatal ontogenesis. The interpretation of this major morphological characteristic has been changing in the last decade from a criterion of good health to an indicator of accumulated inert, useless tissue due to fattening. The results of specific research in this direction unequivocally show that the excessive body weight of grown-up individuals is becoming a serious medico-biological problem, grounded in the adaptive changes of human organism to the contemporary conditions of life and work [1, 2, 3, 4]. The purpose of this study is to investigate the variations of the BMI of men in middle age, and to establish the frequency and tendency of excessive weight as related to some exogenous factors: education, monthly income, occupation and age.

Material and Methods

860 men were studied, divided into two groups according to their age, into three categories according to their education, and into three categories, according to their monthly income.The men under study represented 5 occupations — founders, carpenters, fitters, drivers and programmers. The basic anthropometric characteristics of each one of them were taken — height and weight, on the basis of which their BMI

was calculated (kg/m²). The different levels of excessive weight were determined according to the feeding norms of grown-ups, published by the WHO in 1995: normal range—BMI 18.50-24.99; Grade 1 overweight — BMI 25.00-29.99; Grade 2 overweight—BMI 30.00-39.99; Grade 3 overweight — BMI ≥ 40. The material was statistically processed on a computer using SPSS-9.0 software and descriptive analysis.

Results and Comments

The general distribution of men studied (in %), according to the values of their BMI, is illustrated in Fig. 1. The results show highest frequency of the individuals with Grade 1 overweight, representing almost half of all men studied — 390 (45.35%). Followed by those with normal weight — 281 (32.67 %). High levels of the BMI index (BMI = 30) were established in roughly one fourth of men.We can get a clearer picture of the proportion of individuals with normal weight and those with excessive weight when we look into their percentage distribution with relation to their age or social and occupational status. (Table 1, Fig. 2). The percentage of men with normal body weight (BMI 18.50—24.99) is predominant in the occupational group of software programmers (50,00 %), as well as in the groups with highest monthly income (43.02%) and those with higher education (47.94 %). Individuals with the above index can be met more often in the first period of middle age than in the second. The percentage of men with Grade 1 overweight (BMI 25.00—29.99) is highest in all occupations of physical labour — founders, carpenters, fitters, drivers; in the groups with low and medium monthly income; with primary and secondary education; and in the both periods of middle age. The frequency of men with Grade 2 overweight (BMI 30.00—39.99) is highest in two occupational groups — founders and drivers. The result is indicative in view of the occupation of these men. The higher level of BMI of founders may be explained by their bigger muscles due to their intensive physical labour, while the static character and the hypo-dynamics in the occupation of drivers most probably stimulate the accumulation of fat in their bodies. Besides, the frequency of individuals with BMI 30.00—39.99 is highest in the second period of active middle age, in the groups with primary education and with medium monthly income.From all individuals studied, the percentage of men with Grade 3 overweight (BMI = 40) is lowest. A slight tendency of rising in the frequency of this index can be noticed in occupational aspect, with the reduction of physical effort.

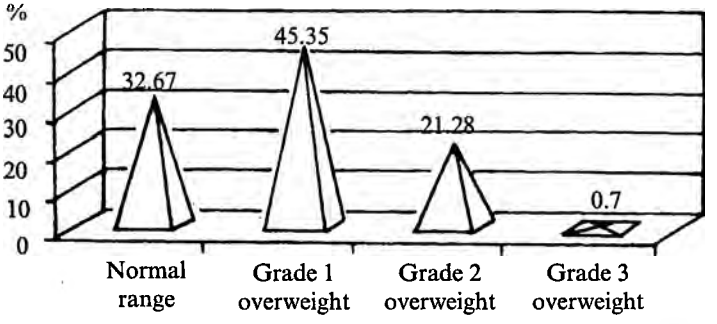

Fig. 1. Distribution of men studied according to their BMI values

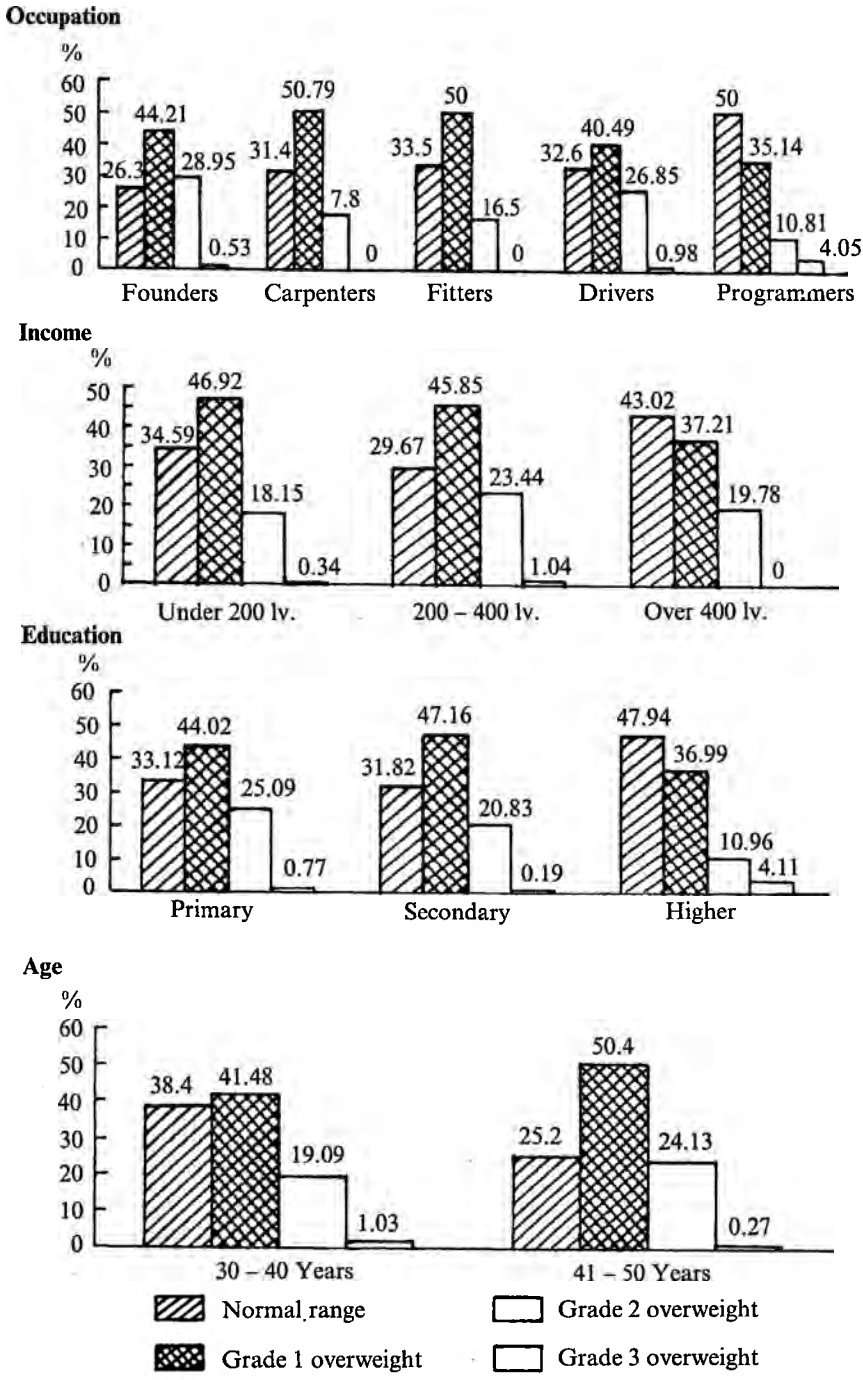

Fig. 2. Percentage distribution of men in the categories of BMI with relation to factors studied

Table 1. Distribution of men studied in the categories of BMI (%)

BMI / Factors	Normal range BMI 18.50-24.99		Grade 1 overweight BMI 25.00-29.99		Grade 2 overweight BMI 30.00-39.99		Grade 3 overweight BMI = 40	
Occupation- *n*	*N*	%	*N*	%	*N*	%	*N*	%
Founders- 190	50	(26.31)	84	(44.21)	55	(28.95)	1	(0.53)
Carpenters- 191	60	(31.41)	97	(50.79)	34	(17.80)	0	—
Fitters- 200	67	(33.50)	100	(50.00)	33	(16.50)	0	—
Drivers- 205	67	(32.68)	83	(40.49)	53	(25.85)	2	(0.98)
Programmers- 74	37	(50.00)	26	(35.14)	8	(10.81)	3	(4.05)
Income - *n*								
Under 200 lv. 292	101	(34.59)	137	(46.92)	53	(18.15)	1	(0.34)
200 — 400 lv. - 482	143	(29.67)	221	(45.85)	113	(23.44)	5	(1.04)
Over 400 lv. - 86	37	(43.02)	32	(37.21)	17	(19.78)	0	—
Education- *n*								
Primary- 259	78	(30.12)	114	(44.02)	65	(25.09)	2	(0.77)
Secondary- 528	168	(31.82)	249	(47,16)	110	(20.83)	1	(0.19)
Higher- 73	35	(47.94)	27	(36.99)	8	(10.96)	3	(4.11)
Age- *n*								
30 — 40 years - 487	187	(38.40)	202	(41.48)	93	(19.09)	5	(1.03)
41 — 50 years - 373	94	(25.20)	188	(50.40)	90	(24.13)	1	(0.27)

Conclusions

1. Amongst all men studied, the relative share of men with Grade 1 overweight (BMI 25.00-29.99) is highest, and that of men with Grade 3 overweight (BMI ≥ 40) is lowest.
2. Individuals with normal body weight are most frequent in the groups of higher social and occupational status and in the younger period of middle age.
3. The frequency of men with Grade 1 and Grade 2 overweight increases with the lowering of their social status and the advancing of age. It is higher in the occupations of greater physical effort (founders) and marked hypo-dynamics (drivers).

References

1. Gueli, N. et al. An assessment of the main variables of cardiovascular risk in a simple population of workers in Roma. — Panminevra Med., **43**, 2001, Dec., No 4, 267-277.
2. Nacheva, A., E. Lazarova, L. Yordanova. Body nutritional status in 7—17 years old schoolchildren from Sofia (Longitudinal study 1993 — 2001). — J. Anthropology, **4**, 2003, 21-25.
3. Suka, M., H. Sugimori, I. Lida. Risk factors for hypertension. A longitudinal study of middle-aged Japanese male workers. — Nopon Koshu Eisei Zasshi., **48**, 2001, Jul., No 7, 543-550.
4. Младенова, С. Динамика на растежа и развитието на деца и подрастващи от Смолянски регион и влияние на социално-икономически фактори върху техния морфологичен статус. Дисерт. труд, 2003, 151 с.
5. WHO Working Group. Physical status: The use and interpretation of anthropometry. Report of WHO Expert Committee, 1995, 452 p.

Institute of Experimental Morphology and Anthropology

Acta morphologica et anthropologica, 10
Sofia • 2005

Body Composition of Female Students Players in Volleyball

H. Al Mabruk, M. Toteva

National Sports Academy, Sofia

The preliminary morphological selection of the sportsmen is important and so is the building of a suitable body structure both a predisposition for high results. The **purpose** of our study is the investigation of the body composition of female students volleyball players. **Material and Methods** — 72 female competitors were investigated from different students teams. Sixteen anthropological features were measured — height, weight, 4 girths of the limbs and 10 skinfolds. In addition 7 parameters were calculated which characterize the main body components. **Results and Conclusion** a) Students female volleyball players compared to national competitors have lower height, weight, muscle arm girths and LBM; bigger fat mass and almost equal development of leg muscles. b) The body composition in different sports vary not only based on the differences in the exercises but on the level of this process. c) The data could be used in preliminary selection of female volleyball players.

Key words: Body composition, female students, volleyball.

Introduction

The components of the athletes' body structure considerably vary according to the differences in the sports. Their characteristics differ from those of untrained people. For this reason the preliminary morphological selection of the sportsmen is very important as well as the building of a suitable body structure which are a predisposition for high results.

There are few publications on this topic focused on volleyball competitors and there is not any information about lower qualified players that could help the selection. This defined the purpose of our study — the investigation of the body composition of female students volleyball players.

Material and Methods

Seventy-two female competitors were investigated from different Bulgarian students teams. The mean age was 21.3 years. Sixteen anthropological features were measured — height, weight, 4 girths of the limbs and 10 skinfolds. In addition 7 parameters were calculated which characterize the ratios between the main body

components: per cent fat mass (%FM), total fat mass (kg), total muscle mass (kg), muscle arm girth (cm), muscle tight girth (cm), lean body mass (LBM), body mass index (BMI).

The method of Parizkova was used for the determination of fat components. Muscle mass was calculated on the basis of main girths and the thickness of appropriate skinfolds.

The data were submitted on statistical analysis. They were compared to the results of the Bulgarian population [3] female students volleyball players and elite competitors [2]. Student's ratio was used at the level of $p< 0.05$.

Results

Students volleyball players have high stature (171.1 cm) in comparison to Bulgarian population (161.6 cm) but according to the elite Bulgarian competitors (183.7cm) they are not tall enough for this sport [2]. The data of foreign students players do not differ essentially from ours because the sport's level is relatively low. The Hungarians are 170.9 cm, Americans —176 cm, Japanese — 168.2cm and the competitors from World Students Games'77 are 173.8 cm tall (Fig. 1).

The weight of students volleyball players (61.84 kg) shows average values compared to the 21-year-old Bulgarian women (59.9 kg). They are considerably lighter than the national competitors (71.8 kg), and others from student's female teams (Fig. 2).

The fat mass quality is very important because there is negative correlation between this feature and sports achievements [1]. Our contingent has 18.85% FM which is higher than those of the national Bulgarian competitors —15.1 %, but the differences are not statistically significant. The data of the other authors are very similar — Americans 17.9%, Japanese 18.3 % (Fig. 3).

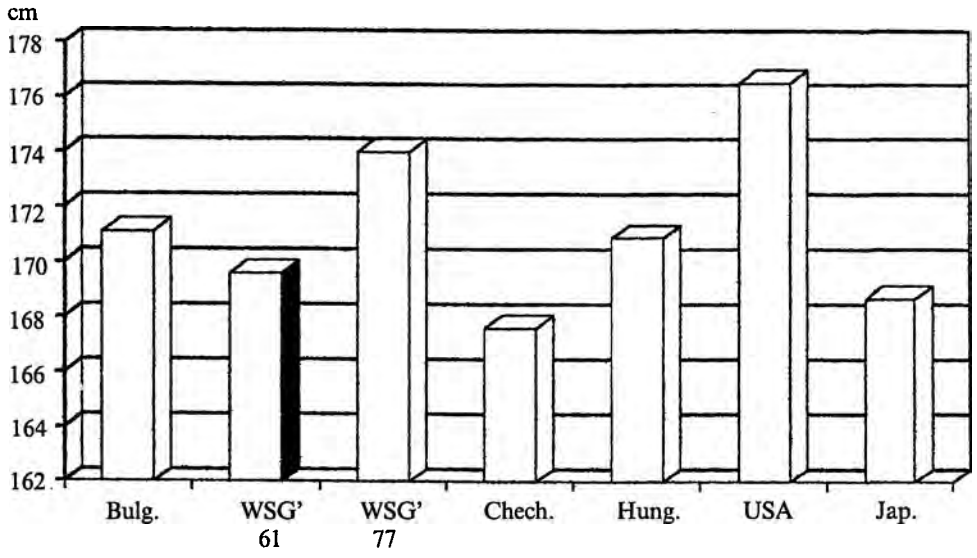

Fig. 1. Height of female volleyball players

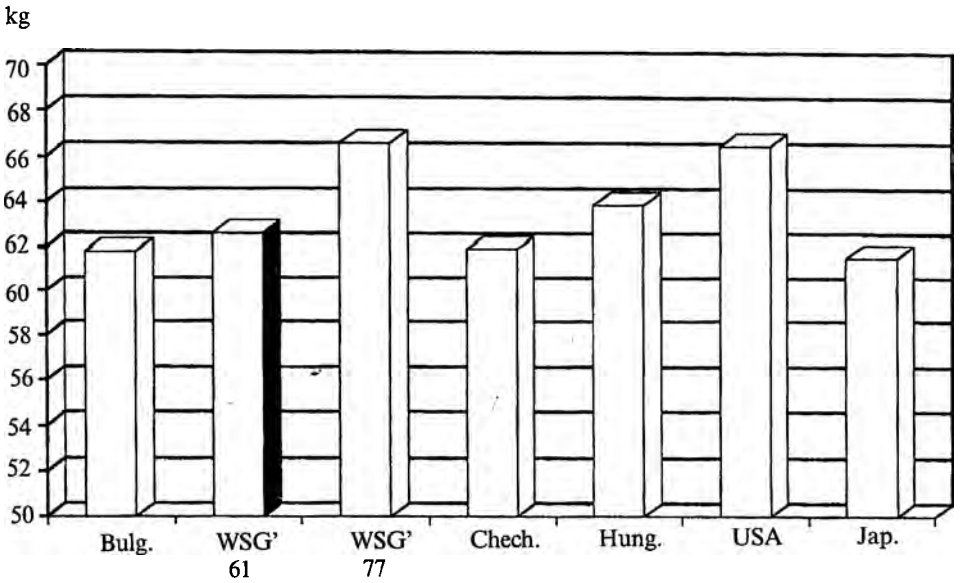

Fig. 2. Weight of female volleyball players

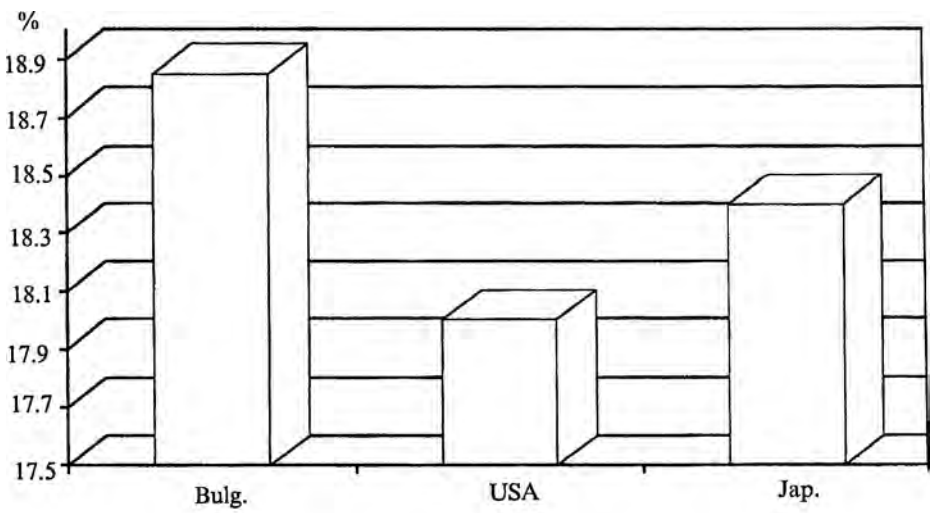

Fig. 3. Per cent body fat of female volleyball players

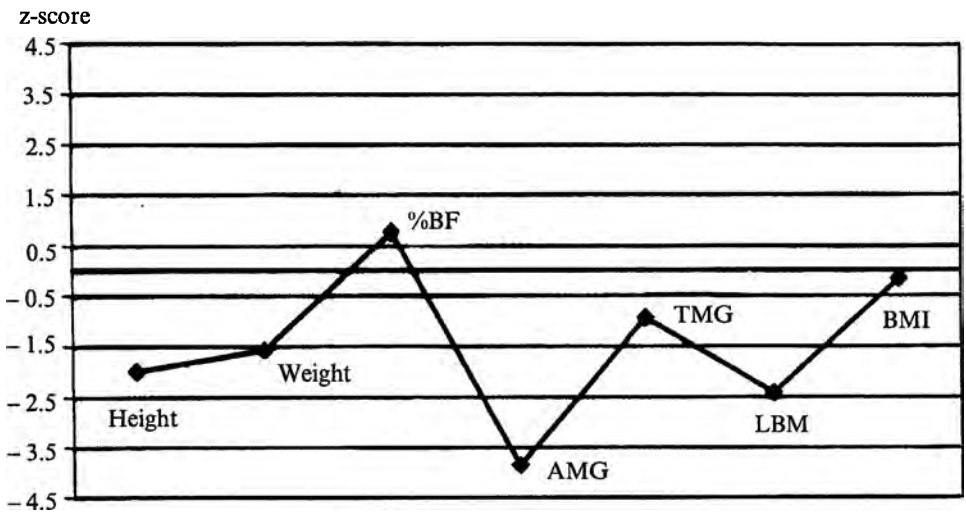

Fig. 4. Body composition of female student's volleyball players in Z-scores versus elite female volleyball players

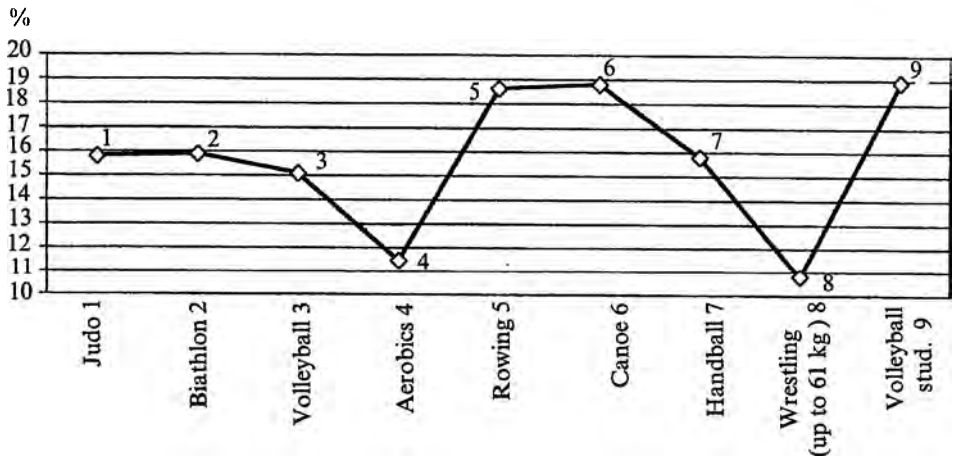

Fig. 5. Per cent body fat of elite female competitors

The body composition of students and elite volleyball players is presented in Z-scores in Fig. 4. This visualizes clearer the differences in body structure according to the level of sports qualification.

The permanent exercises play main part in the development of muscle mass, which is in great correlation with physical fitness. The muscles of higher and lower limbs are very important for success in volleyball. The muscle arm girths of the students are 17.25 cm and 21.3 cm of national competitors. The difference of

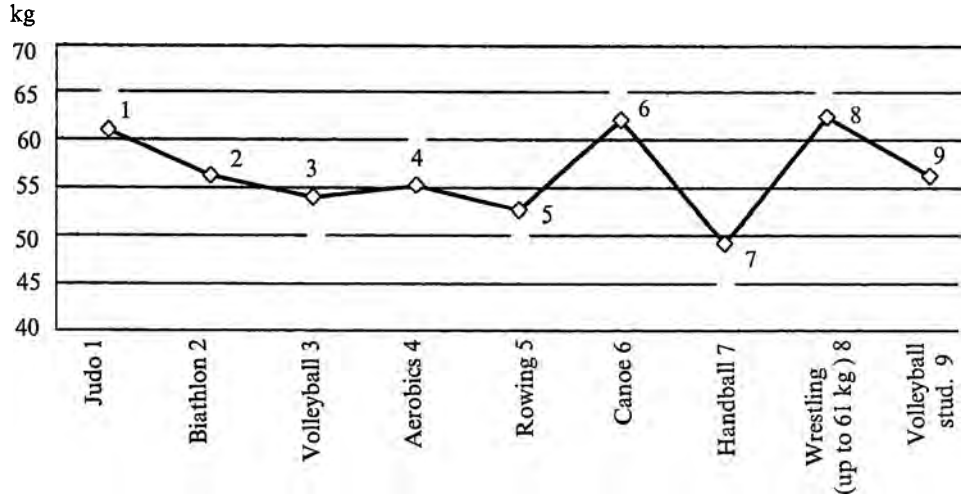

Fig. 6. Lean Body Mass of elite female competitors

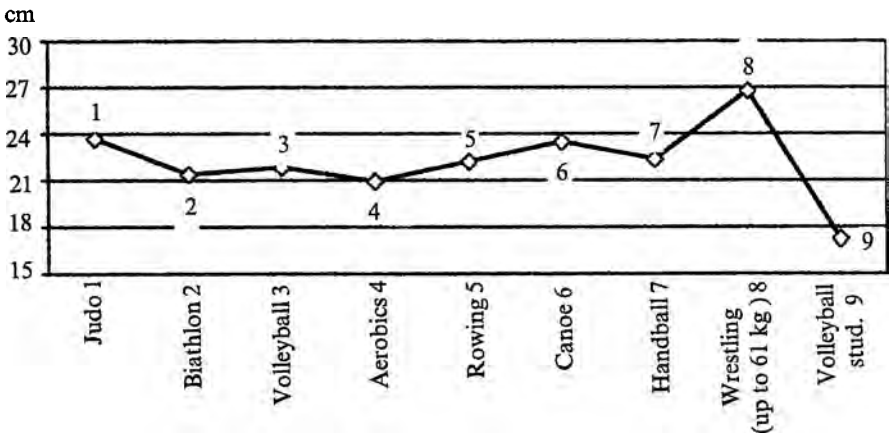

Fig. 7. Arm muscular girths of elite female competitors

4.55 cm is considerable due to the different sports level of the two groups. The muscle tight girths (51.03 cm and 53.0 cm) of these athletes do not have essential differences.

LBM is an indirect mark of muscle development. It is directly related to oxygen consumption and main characteristics of physical working capacity. We find great difference between LBM of students (49.05 kg) and elite volleyball players (60.8 kg) based on various sports practice.

BMI is not very suitable for athletes but it was calculated as an additional parameter and it shows similar values (20.86 kg /m^2 and 21.86 kg /m^2) in two contingents.

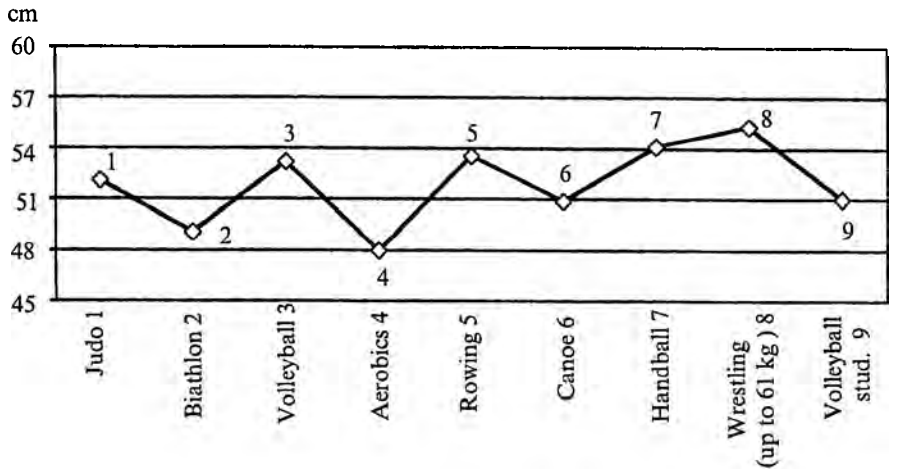

Fig. 8. Tight muscular girths of elite female competitors

Body composition of athletes is very different according to sports discipline and could be seen in figures 5-8. Students volleyball players have the highest % FM, almost equal values of these in rowing and canoe (Fig. 5). LBM is similar to this of competitors in aerobics and biathlon (Fig. 6). Muscle arm girths, which is so important for volleyball has the least values in students (Fig. 7). Muscle tight girth shows better development equal to those practising canoe (Fig. 8).

Conclusions

— Students female volleyball players compared to national competitors have lower height, weight, muscle arm girth, and LBM; bigger fat mass and almost equal development of leg muscles.

— The body composition in different sports varies not only based on the differences in the exercises but on the level of this process.

— This data could be used in preliminary selection of female volleyball players.

References

1. Siders, W. A., H. C. Lukaski. Body composition and collegiate volleyball performance. N. D. Acad. Sci., 46, 1992.
2. Игнатов, П. В. Спортна медицина. С., Нови знания, 1998.
3. Слънчев, П. и др. Физическо развитие, физическа дееспособност и нервно-психична реактивност на населението на България. С., 1992.
Световна купа по волейбол жени. Бюлетин, 2000.

Institute of Experimental Morphology and Anthropology

Acta morphologica et anthropologica, 10
Sofia•2005

Somatotype of Fasting and non Fasting Schoolboys from 14 to 16 Years of Age

I. Hristov, Y. Boukov, T. Matev, G. Baltadjiev, A. Baltadjiev, T. Petleshkova, M. Daskalova

Department of Anatomy, Histology and Embryology, Medical University, Plovdiv

Objective: The purpose of this research was to study ups and downs of some bodily indices during the period of time in boys who fast and those who do not fast. The bodily indices are 10 anthropometric dimensions needed to calculate the anthropometric somatotype using the Heath-Carter method of somatotyping. Simultaneously we traced the somatotype alteration during the adolescence.

Material and Methods: We measured 3 times 142 schoolboys, 31 of them are from Ecclesiastical Seminary — Plovdiv, the rest of them are from Vocational College — Plovdiv; 75 boys aged 14, 67 boys aged 15. Conclusions: There are no statistically significant differences in measured anthropometrical indices between fasting and non fasting boys. Almost all indices increased in all groups. Fasting boys are balanced mesomorph. Initially non fasting boys are ectomorphic mesomorph and became to balanced mesomorph. The mesomorphy in the group of 15 years old boys increased.

Key words: fasting, somatotype, anthropometric indices.

Fasting plays an important role in Eastern Christian life. Apart from Great Lent and the forty days before Christmas, most Wednesdays and Fridays, a number of days before the Feast of Saints Peter and Paul, the first fourteen days of August, Holy Cross Day and the Vigils of several other great feasts are fasting days.

Fasting is of several kinds: During Cheese Week, the week before Great Lent, no meat may be eaten, but dairy products and fish are permitted. On most fast days no meat, fish or dairy products, wine or olive oil may be used. On days of a particularly severe form of fasting, nothing is eaten except for raw vegetables or vegetables cooked in water, with salt or vinegar. A strict interpretation of the fasting rules requires complete abstinence from food on certain days in the first week of Lent and on the last days of Holy Week. When a major feast occurs during a period of fasting, fish is normally permitted. On certain fasting days oil and wine are permitted.

The purpose of this research was to study ups and downs of some bodily indices during the period of time in boys who fast and those who do not fast. The bodily indices are 10 anthropometric dimensions needed to calculate the anthropometric somatotype using the Heath — Carter method of somatotyping. Simultaneously we traced the somatotype alteration during the adolescence in order to prove findings in a lot of investigations [1, 2, 5, 7, 8].

Material and Methods

We measured 142 schoolboys, 31 of them are from Ecclesiastical Seminary — Plovdiv, the rest of them is from Vocational College — Plovdiv; 75 boys aged 14, 67 boys aged 15.

At time of first measurement the average age of boys is 14 years and 4 months and 15 years and 4 months at the second measurement respectively. The religious affiliations and keep to a fasting were evaluated by two inquiries made at one year interval.

The anthropometric measurements are 3. First measurement was provided at the beginning of November, forty days before Christmas. Second measurement was provided in the middle of May, after the end of Easter. Third measurement was done one year later. Ten anthropometric indices were evaluated using standard anthropometric equipment according Heath-Carter method of somatotyping. [6] The data were calculated by Macintosh "Stat View 4.5" statistic program.

Results and Discussion

From inquire: most college students are orthodox Christians baptized in East Orthodox Church — 76.7%, not baptized — 19.4%, Muslims — 2.9%, and from other religions — 1%. All seminarists are orthodox Christians. Fasting are boys who fast during Great Lent — 48 days and the forty days before Christmas and some of the others fasting. In a group of 14 years old Seminarists are 57. 9% and in a group of 15 years old boys they are 65. 5%. Fasting is a tradition in families of 52% in group of 14 years old boys and 55% in group of 15 years old boys who fasting.

The anthropometric data are present in table 1.

The average somatotypes are present in table 2.

Body mass index increased at every measurement but remained in a range of standard (19—24. 9).

The changes in average somatotype between first and third measurements define the somatotype dispersion distance (SDD) and the somatotype attitudinal distance (SAD):

14 years old fasting — SDD = 0. 3, SAD = 0. 1; non fasting — SDD = 1. 0, SAD = 0. 4
15 years old fasting — SDD = 1. 4, SAD = 0. 5; non fasting — SDD = 1. 5, SAD = 0. 6

Conclusions

1. There are no statistically significant differences in measured anthropometrical indices between fasting and non fasting boys.
2. The height and the body mass increased in all groups. Growth is bigger in the group of 15 years old boys.
3. In the group of 14 years old boys increased mostly biepicondylar breadth of the humerus and biepicondylar breadth of the femur on a small scale.
4. Upper arm girth and calf girth increased.
5. Fasting boys are balanced mesomorph at all free measurements.
6. Non fasting boys are ectomorphic mesomorph at the first measurement. At the third measurement the average somatotype in the group of 14 years old boys are balanced mesomorph because of gradually augmentation of endomorphy and diminution of ectomorphy. We notice the same tendency in the group of 15 years old non fasting boys, although they remain ectomorph mesomorph.
7. The mesomorphy in the group of 15 years old boys increased.

Table 1. The anthropometric data of fasting and non fasting schoolboys from 14 to 16 years of age

14 y. FASTING	*n*=38 I meas.		*n*=38 II measurement		*n*=33 III measurement		15 y. FASTING	*n*=29 I measurement		*n*=29 II measurement		*n*=25 III measurement	
	X	SD	X	SD	X	SD		X	SD	X	SD	X	SD
Height (cm)	**164.8**	9.1	**167.7**	9	**172.6**	7.8	Height (cm)	**173**	6.6	**174.2**	6.7	**175.3**	6.5
Weight (kg)	**56**	11.1	**59.4**	11.1	**64.3**	11.7	Weight (kg)	**65.2**	10.8	**67**	10.3	**70.6**	10.7
Humerus breadth (cm)	**6.5**	0.4	**6.7**	0.4	**6.8**	0.4	Humerus breadth (cm)	**6.8**	0.4	**6.9**	0.3	**6.9**	0.4
Femur breadth (cm)	**9.3**	0.5	**9.5**	0.5	**9.5**	0.6	Femur breadth (cm)	**9.7**	0.7	**9.8**	0.5	**9.8**	0.5
Biceps girth (cm)	**26.6**	3.1	**27.2**	2.7	**28.3**	2.8	Biceps girth (cm)	**29.3**	3.5	**29.6**	3.3	**31**	3.5
Calf girth (cm)	**34.1**	3.7	**34.8**	3.7	**36.1**	3.8	Calf girth (cm)	**36.1**	3	**36**	3.1	**37.5**	3.1
Triceps skinfold (mm)	**11.8**	5.7	**12.1**	5.4	**10.2**	4.3	Triceps skinfold (mm)	**10.8**	4.8	**11.7**	6.2	**11.5**	5.7
Subscapular skinf. (mm)	**9.4**	4.6	**9.4**	3.7	**9.4**	3.5	Subscapular skinf. (mm)	**10**	4.9	**9.9**	4.7	**10.4**	4.9
Subscapular skinf. (mm)	**9.6**	5.9	**9.8**	6.4	**9.7**	5.4	Supraspinal skinf. (mm)	**9.4**	5.5	**10**	6.8	**10.2**	5.7
Med. calf skinfold (mm)	**13.6**	6.5	**13.2**	6.9	**12.4**	6.1	Med. calf skinfold (mm)	**11.3**	3.9	**11.9**	4.8	**12.3**	6
14 y. NONFASTING	*n*=37 I meas. rement		*n*=34 II measurement		*n*=34 III measurement		15 y. NONFASTING	*n*=31 I measurement		*n*=38 II measurement		*n*=25 III measrement	
	X	SD	X	SD	X	SD		X	SD	X	SD	Xu	SD
Height (cm)	**167.4**	6.7	**170.4**	6.6	**173.5**	6	Height (cm)	**172.5**	5.7	**173.7**	6.2	**174.1**	6.6
Weight (kg)	**56.6**	9.5	**59.3**	9.1	**64.5**	10.8	Weight (kg)	**62.1**	9.8	**63.7**	10.1	**65.9**	10.3
Humerus breadth (cm)	**6.6**	0.4	**6.7**	0.3	**6.9**	0.3	Humerus breadth (cm)	**6.7**	0.3	**6.8**	0.3	**6.8**	0.3
Femur breadth (cm)	**9.4**	0.5	**9.5**	0.4	**9.5**	0.5	Femur breadth (cm)	**9.5**	0.5	**9.6**	0.5	**9.6**	0.5
Biceps girth (cm)	**27**	3.3	**27.2**	3.3	**29.1**	2.7	Biceps girth (cm)	**27.7**	2.2	**28.9**	2.6	**30.1**	3.1
Calf girth (cm)	**34.3**	3	**35.3**	3.4	**36**	2.9	Calf girth (cm)	**35.7**	3	**36.1**	2.7	**36.6**	2.5
Triceps skinfold (mm)	**10.3**	4.3	**10.6**	5.1	**10.7**	4.7	Triceps skinfold (mm)	**9.4**	4.2	**9.8**	4.2	**9.1**	3.7
Subscapular skinf. (mm)	**8.5**	3.4	**8.7**	4.1	**9.4**	4.2	Subscapular skinf. (mm)	**8.6**	3.6	**8.9**	4.1	**8.9**	4.2
Supraspinal skinf. (mm)	**7.7**	4.2	**8.4**	6.1	**9.5**	6.2	Supraspinal skinf. (mm)	**7.1**	4	**8.4**	6.2	**7.6**	4.2
Med. calf skinfold (mm)	**11.2**	4.6	**11.8**	5.2	**12.1**	5.7	Med. calf skinfold (mm)	**10.3**	3.9	**11**	4.6	**10.6**	4.9

Table 2. The average somatotypes of fasting and non fasting schoolboys from 14 to 16 years of age

14 y. FASTING		Endomorphy	Mesomorphy	Ectomorphy		15 y. FASTING		Endomorphy	Mesomorphy	Ectomorphy
I measurement	X	**3**	**4.1**	**3.2**		I measurement	X	**3**	**4.5**	**3.2**
	SD	1.5	1.4	1.5			SD	1.4	1.7	1.9
II measurement	X	**3.1**	**4.2**	**3.1**		II measurement	X	**3.1**	**4.4**	**3.1**
	SD	1.4	1.3	1.5			SD	1.6	1.6	1.8
III measurement	X	**2.9**	**4.2**	**3.2**		III measurement	X	**3.2**	**4.8**	**2.8**
	SD	1.2	1.4	1.7			SD	1.5	1.5	1.6
14 y. NONFASTING		Endomorphy	Mesomorphy	Ectomorphy		15 y. NONFASTING		Endomorphy	Mesomorphy	Ectomorphy
I measurement	X	**3.2**	**4.2**	**3.5**		I measurement	X	**2.5**	**3.9**	**3.5**
	SD	1.2	1	1.2			SD	1.1	1	1.3
II measurement	X	**2.7**	**4.1**	**3.5**		II measurement	X	**2.6**	**4.2**	**3.4**
	SD	1.5	1.1	1.2			SD	1.3	1.2	1.4
III measurement	X	**2.9**	**4.2**	**3.2**		III measurement	X	**2.5**	**4.4**	**3.1**
	SD	1.5	0.9	1.2			SD	1.2	1.1	1.3

References

1. Zuk, G. H. The plasticity of physique from early adolescence through adulthood. — Journal of Genetic Physiology, **92**, 1958, 205-214.
2. Bok, V., E. Tlapakova. New ways of somatotyping and their application. — Acta Universitatis Caroline (Gymnica), **18**, 1982, 5-19.
3. Boukov, Y. et al. Basic somatometric indices in three generations of children from Plovdiv. — Journal of Anthropology, **3**, 2000, 41-49.
4. Carter, J. E. L., B. H. Heath. Somatotyping — development and applications. Cambridge University Press, 1990.
5. Claessens, A., G. Beunen, J. Simons. Stability of anthroposcopic and anthropometric estimates of physique in Belgian boys followed longitudinally from 13 to 18 years of age. — Annals of Human Biology, **13**, 1986, 3.
6. Heath, B. H., J. E. L. Carter. Growth and somatotype patterns of manus children, Territory of Papua and New Guinea: application of a modified somatotype methods to the study of growth patterns. — American Journal of Physical Anthropology, **35**, 1971, 49-67.
7. Parizkova, J., J. E. L. Carter. Influence of physical activity on stability of somatotypes of boys. — American Journal of Physical Anthropology, **44**, 1976, 327-340.
8. Тотева, М. Соматотипология в спорта. София, НСА Издателско-печатна база, 1992, 54—61.

Institute of Experimental Morphology and Anthropology

Acta morphologica et anthropologica, 10
Sofia•2005

Anthropometric Indicatoris for Assessment of Body Composition

M. Nikolova, S. Mladenova***

* *Department of Human Anatomy and Physiology, University of Plovdiv, Plovdiv*
** *University of Plovdiv, Smolyan Filial, Smolyan*

This paper presents the results from the assessment of body composition made by means of some anthropometric characteristics; it also shows the changes in body composition in the growth period effected by some social factors such as the education of the mother. The research included 1174 children, of whom 597 girls and 576 boys within age range of 3-17 years. The body composition of each individual was assessed through the body mass index (BMI), the sum of skinfolds (SSKF), the upper arm muscle area (UAMA), the upper arm fat area (UAFA), the lean body mass (LBM), the body fats quantity (BF), and the body surface area (BSA). The findings show significant changes in body composition in the surveyed growth period in children of both sexes, differences in body composition in children from families of different social status, significant correlation coefficients between body dimensions and the body composition defining factors, as well as reliability of this characteristics for assessment of body composition.

Key words: body composition, anthropometric characters, social status.

Introduction

Various anthropometric methods and techniques are used to assess the growth and the nutritional status of the individual. Some authors report that the triceps skinfold, the upper arm fat area and the body fats are in positive correlation with BMI and can be the logical characteristics for determining the calorie reserve and the obesity in children and adults [10, 11]. Besides, the change in body composition influenced by various factors in the process of ontogenesis has been taken into consideration [1, 8, 7, 9].

The **aim** of this study is, by means of various anthropometric characters, to define the body composition of children and adolescents and the changes in it that occur in the growth period, taking into consideration the education level of the mother.

Material and Methods

Anthropometrical examination of 1174 children, of whom 597 girls and 576 boys within age range of 3-17 years from Smolyan region, was carried out in the period 1998-2001. By means of Martin-Saler's method [6] , the height (H,cm), weight (W, kg),

and upper arm circumference (UAC, cm) were measured; by means of GPM caliper with constant pressure of 10g/mm^2, four skinfolds were measured: the triceps (TS, mm), biceps, the subscapular and the suprailiac skinfolds.

The body composition of each individual was estimated by means of body mass index BMI (kg/m^2), the upper arm muscle area (UAMA,cm^2), the upper arm fat area (UAFA, cm^2), the sum of skinfolds (SSKF, mm), the lean body mass (LBM, kg), the body fats quantity (BF, kg), and the body surface area (BSA, m^2) calculated through special formulae [4, 3, 2, 5].

The educational level of the mother was classified as follows: 1st level — secondary education; 2nd level — special/professional education; 3rd level — higher education.

The data was processed implementing various analyses: descriptive, alternative (Z-score), correlation, and one-factor dispersion analysis (ANOVA, Tukey HSD-test).

Results

The results of this research show significant changes in the values of the characters used to determine the body composition (Fig.1-7). With girls of all age groups, high values of the fat body component comprising the sum of four skinfolds (Fig.2), the body fats (Fig. 6) and the upper arm fat area (Fig.4) have been observed. With boys, muscle development, higher values of body surface and BMI (Fig.1) are dominant, especially after their 13th year.

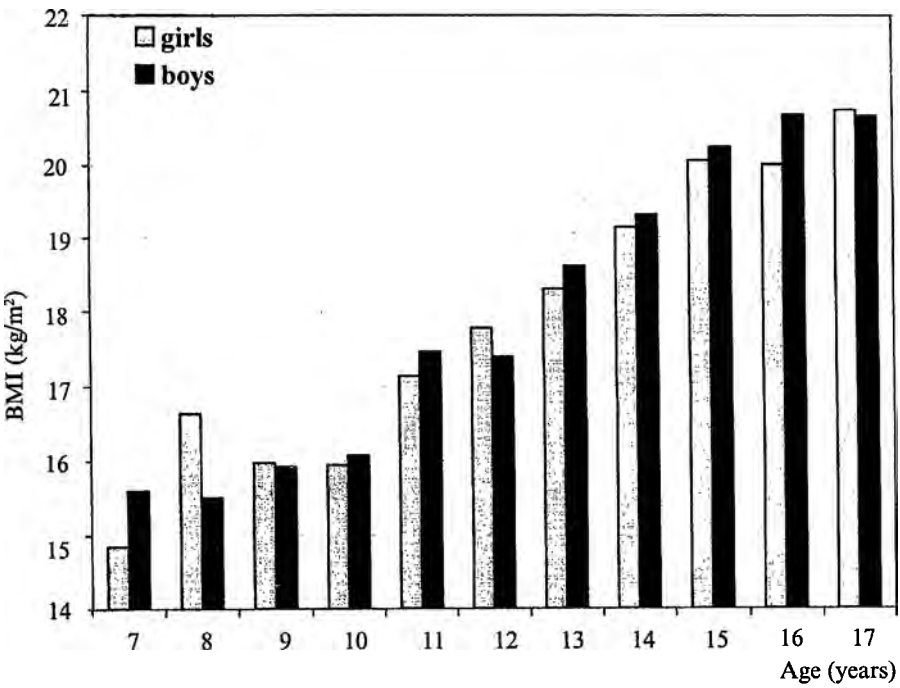

Fig. 1. Growing variations of BMI of girls and boys

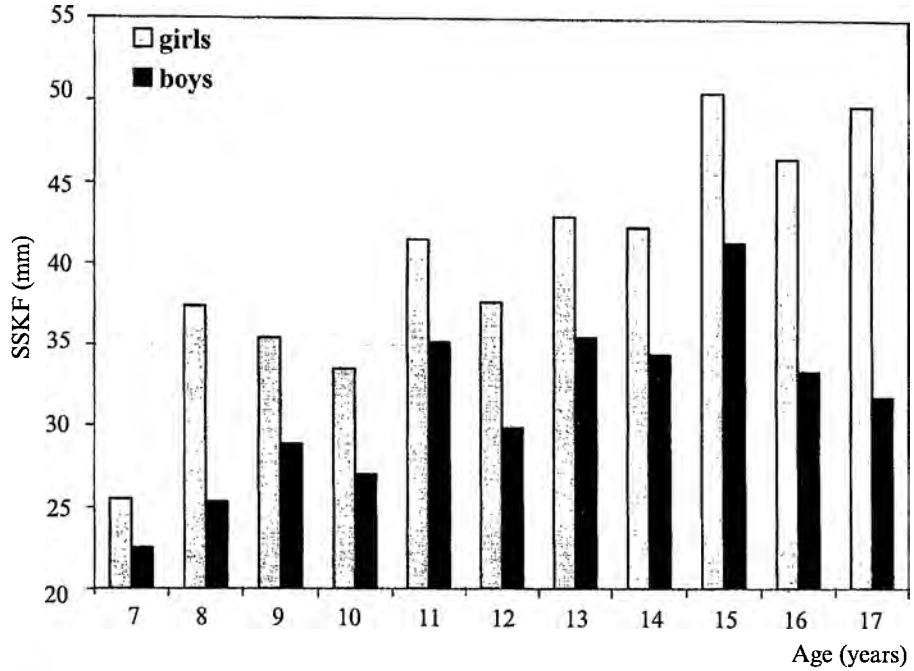

Fig. 2. Growing variations of SSKF of girls and boys

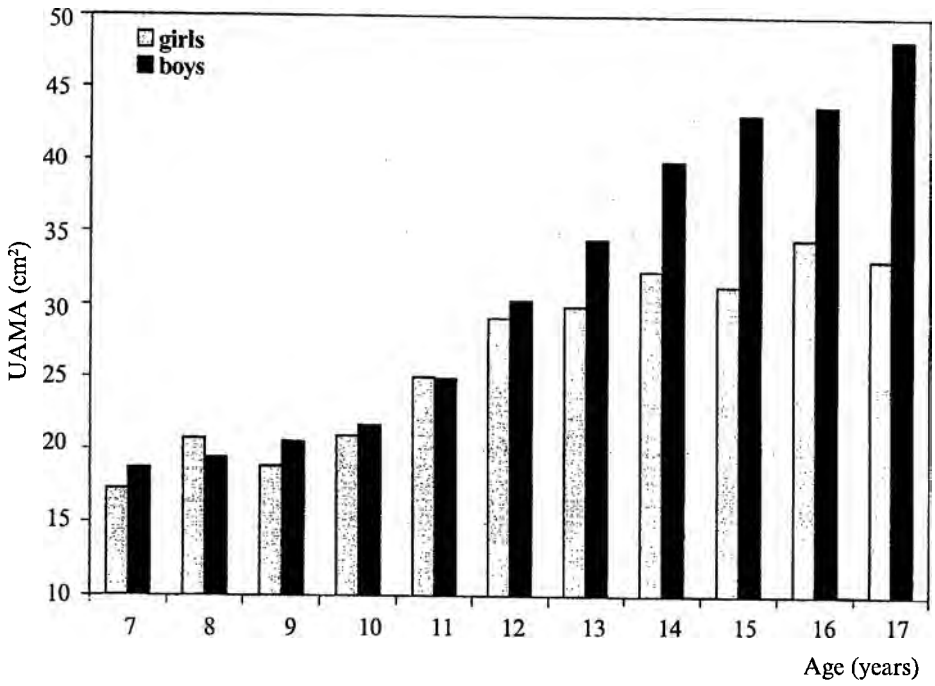

Fig. 3. Growing variations of UAMA

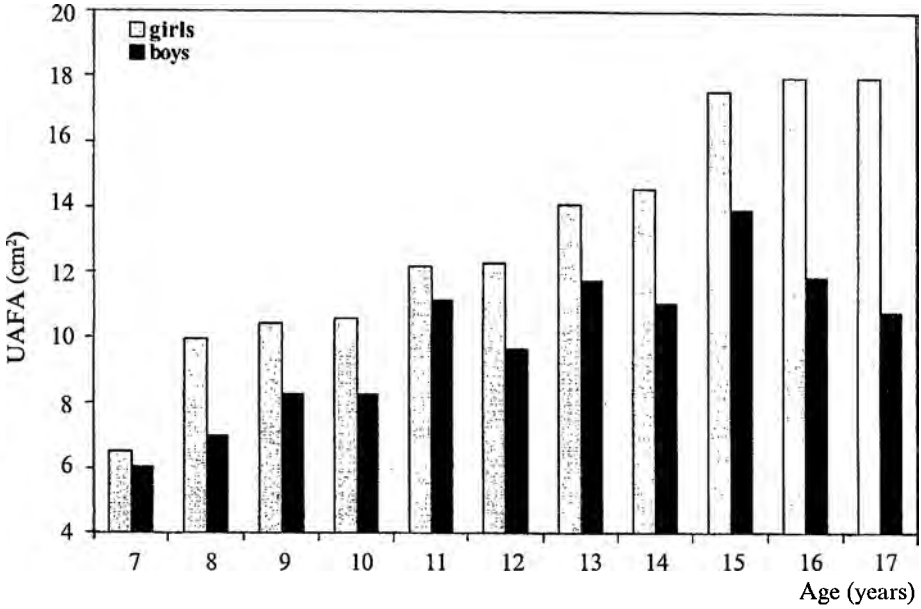

Fig. 4. Growing variations of UAFA

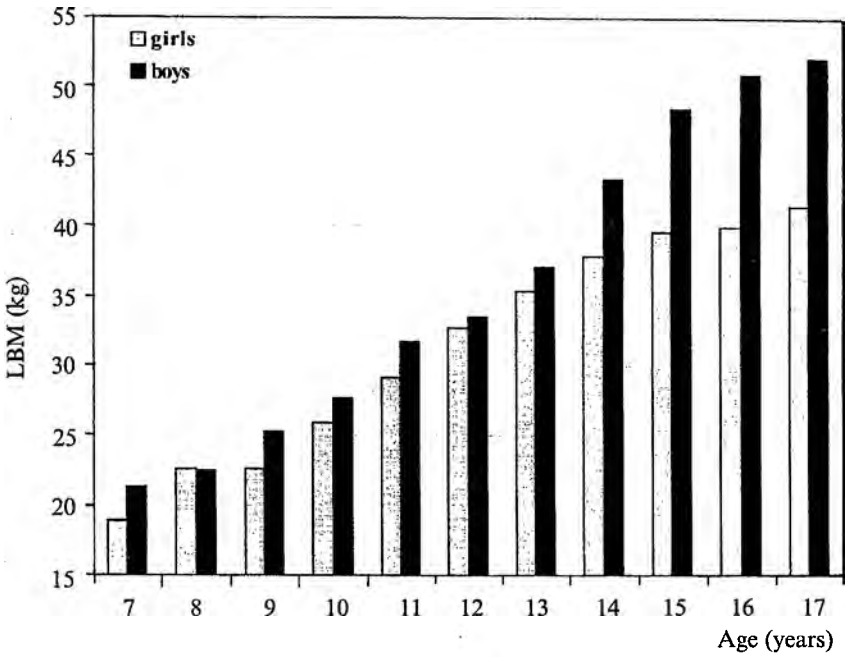

Fig. 5. Growing variations of LBM

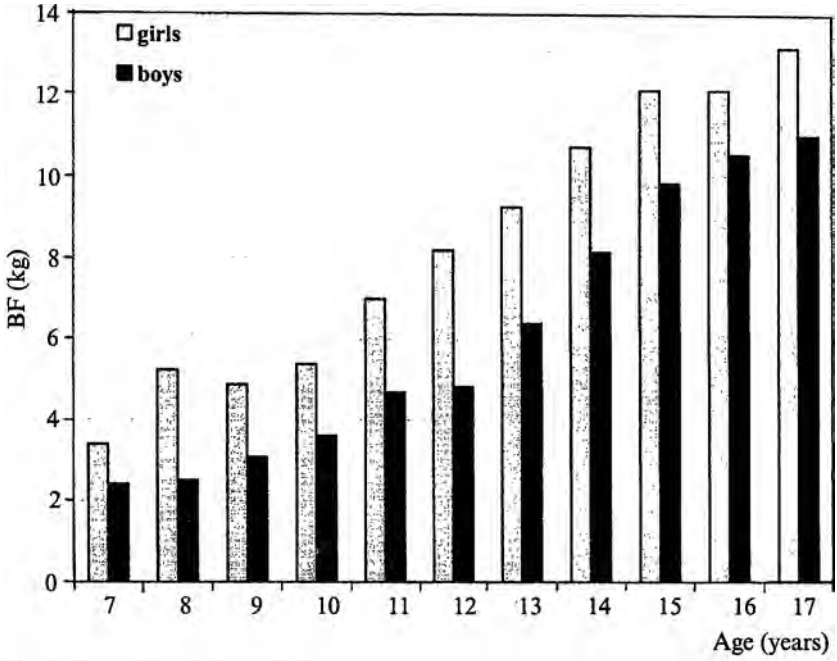

Fig. 6. Growing variations of BF

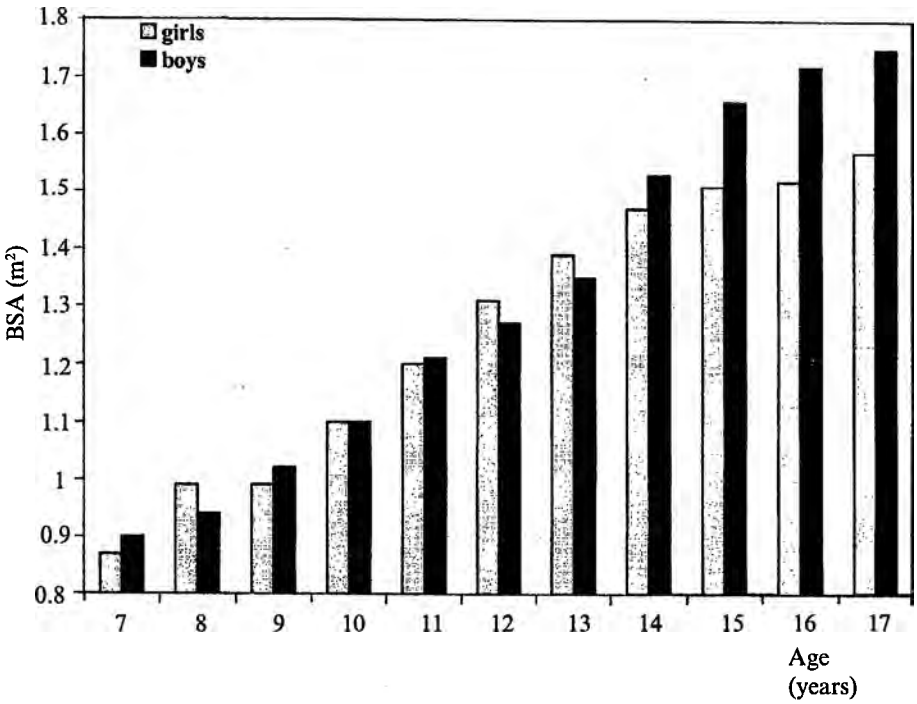

Fig. 7. Growing variations of BSA

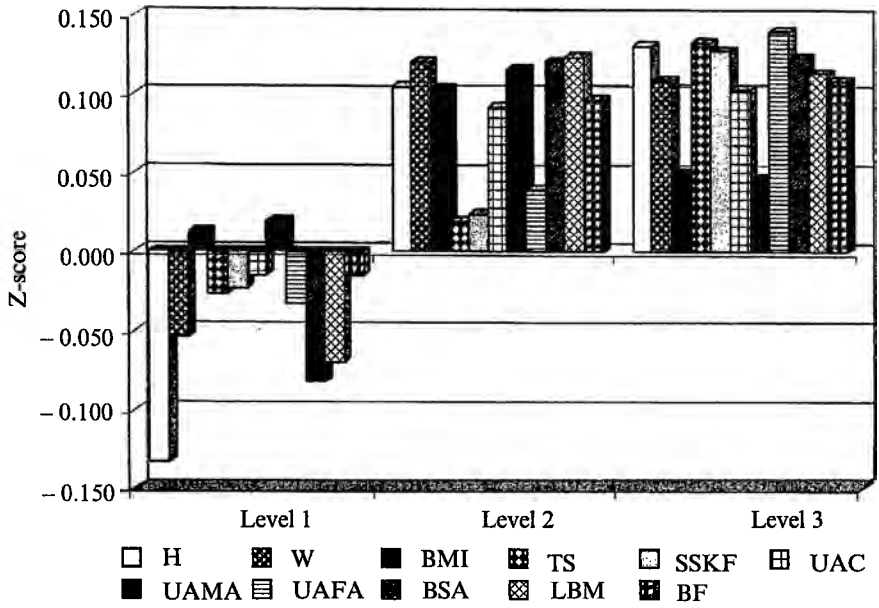

Fig. 8. Distribution of body compositon's indices of boys according to the educational level of the mother

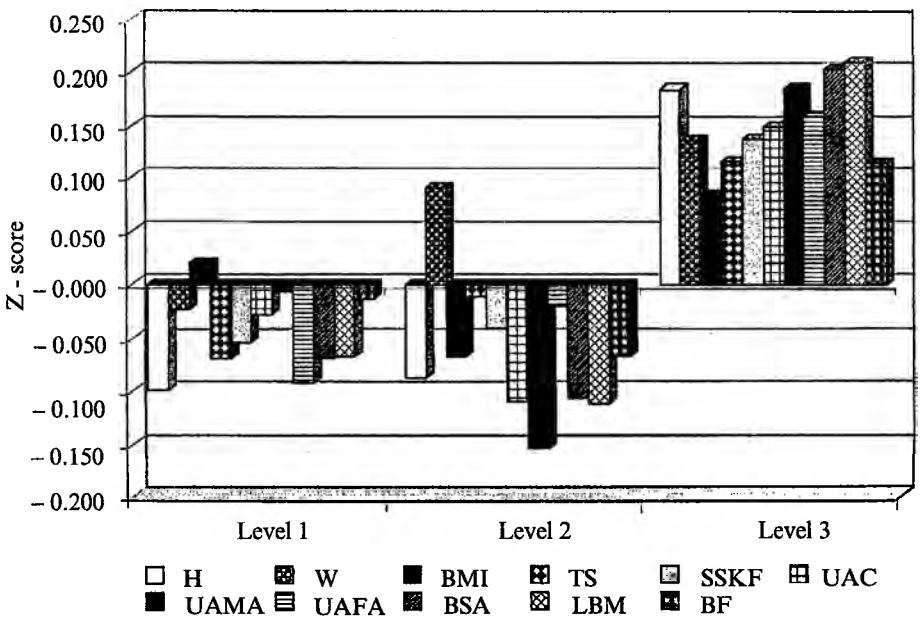

Fig. 9. Distribution of body composition's indices of girls according to the mother's educational level

The relationship between characters defining body composition and the total body dimensions (height and weight) shows that, with both sexes, the weight is in strong correlation with the body surface, the lean body mass, the body fats and BMI, while body height correlates mainly with body surface area and the lean body mass. BMI correlates with all other characters, especially with body fats, the subcutaneous fat tissues and the upper armpit circumference (Tables 1, 2).

The relationship between body composition and the educational level of the mother has shown that sons and daughters of mothers with high educational level have values of the characters being researched above the average, and vice versa. The only exception is BMI with both sexes, and the upper arm muscle area with boys.

In **conclusion**, the results show that the anthropometric characteristics used in combination with BMI are reliable instruments for assessment of the body composition in the growth period of children in connection with the social status of their families.

T a b l e 1. Pearson correlation matrix body composition's indices (marked correlations are significant at $p<0.05$)

	Weight	*Height*	*BMI*	*TS*	*SSKF*	*UAC*	*UAMA*	*UAFA*	*BSA*	*LBM*	*BF*
Weight	-	-	-	-	-	-	-	-	-	-	-
Height	0.61*	-	-	-	-	-	-	-	-	-	-
BMI	0.87*	0.18*	-	-	-	-	-	-	-	-	-
TS	0.66*	0.13*	0.73*	-	-	-	-	-	-	-	-
SSKF	0.71*	0.14*	0.80*	0.95*	-	-	-	-	-	-	-
UAC	0.85*	0.34*	0.86*	0.76*	0.80*	-	-	-	-	-	-
UAMA	0.76*	0.39*	0.89*	0.40*	0.49*	0.89*	-	-	-	-	-
UAFA	0.73*	0.18*	0.85*	0.98*	0.96*	0.85*	0.53*	-	-	-	-
BSA	0.96*	0.79*	0.72*	0.54*	0.58*	0.76*	0.71*	0.61*	-	-	-
LBM	0.99*	0.72*	0.80*	0.59*	0.64*	0.81*	0.74*	0.66*	0.99*	-	-
BF	0.94*	0.35*	0.95*	0.75*	0.81*	0.88*	0.73*	0.83*	0.82*	0.87*	-

T a b l e 2. Pearson correlation matrix Z-score of body composition's indices of girls (marked correlations are significant at $p<0.05$)

	Weight	*Height*	*BMI*	*TS*	*SSKF*	*UAC*	*UAMA*	*UAFA*	*BSA*	*LBM*	*BF*
Weight	-	-	-	-	-	-	-	-	-	-	-
Height	0.61*	-	-	-	-	-	-	-	-	-	-
BMI	0.91*	0.25*	-	-	-	-	-	-	-	-	-
TS	0.73*	0.24*	0.77*	-	-	-	-	-	-	-	-
SSKF	0.73*	0.21*	0.78*	0.83*	-	-	-	-	-	-	-
UAC	0.89*	0.38*	0.90*	0.79*	0.76*	-	-	-	-	-	-
UAMA	0.72*	0.35*	0.70*	0.40*	0.60*	0.82*	-	-	-	-	-
UAFA	0.74*	0.24*	0.77*	0.89*	0.94*	0.81*	0.63*	-	-	-	-
BSA	0.88*	0.69*	0.72*	0.58*	0.76*	0.75*	0.76*	0.74*	-	-	-
LBM	0.89*	0.65*	0.74*	0.60*	0.74*	0.77*	0.77*	0.76*	1.00*	-	-
BF	0.87*	0.35*	0.89*	0.69*	0.86*	0.83*	0.79*	0.86*	0.88*	0.90*	-

References

1. Bar-O r, O. et al. Physical activity, genetic and nutritional consideration in childhood weight management. — Med. Sc. for Sport. Exersice, **30**, 1998, 2-10.
2. Bolzant, A., L. Guimarey, A. Frisancho. Study of growth in rural school children from Buenos Aires, Argentina using upper arm muscle area by height and other anthropometric dimensions of body composition. — Ann. Hum. Biol., **26**, 1998, 185-193.
3. Frisancho, A. New standards of weight and body composition by frame size and height for assessment of nutritional status of adults and elderly. — Am. Journ. of Clinical Nutrition, **40**, 1984, 808-819.
4. Frisancho, A., S. Garn. Skinfold thickness and muscle size:implications for developmental status and nutritional evaluation for children from Honduras. — Am. Journ. of Clinical Nutrition, **24**, 1971, 541-554.
5. Hu, Ch., R. Kneusel, G. Barnas. Body surface area, body mass index, lean body mass. Online clinical calculator,Division of general internal medicine, MCW HealthLink, 1999. Available to: . http://www.halls.md/body-mass-index/leanbody. html
6. Martin, R., K. Saller. Lehrbuch der Anthropologie. T. 1. Stuttgart, Gustav Fischer Verlag, 1957, 661.
7. Malina, R. M., Y. C. Huang, K. H. Brown. Subcutaneous adipose tissue distribution in adolescents girls of four ethnic groups. — Intern. Journ. Obesity, **19**, 1995, 793-797.
8. Mesa, M. S. et al. Body composition in rural and urban children from thr central region of Spain. — Ann. Hum. Biol., **23**, 1996, No 3, 203-212.
9. Moussa, M. A. A. et al. Factor associated with obesity in school children. — Int. Journ. Obesity, **18**, 1994, 513-515.
10. Rolland-Cachera, M. Body composition during adolescence: methods, limitations and determinants. — Hormonal Research, **39**, 1993, 25-40.
11. Walker, S. et al. Anthropometry in adolescent girls in Kingston, Jamaica. — Ann. of Human Biology, **23**, 1996, 23-29.

Institute of Experimental Morphology and Anthropology

Acta morphologica et anthropologica, 10
Sofia • 2005

Body Mass Index, Some Circumference Indices and their Ratios for Monitoring of Physical Development and Nutritional Status of Children and Adolescents

S. Mladenova, M. Nikolova**, D. Boyadzhiev****

* *University of Plovdiv, Smolyan Filial, Smolyan*
** *Department of Anatomy and Physiology, University of Plovdiv, Plovdiv*
*** *Department of Mathematics and Informatics, University of Plovdiv, Plovdiv*

The aim of this paper is to construct modern age/sex-specific percentile norms of body Mass Index (BMI, kg/m^2), waist circumference (WC, cm), and its ratio with that of the hips (WHR) for monitoring of the physical development and for assessment of the nutritional status of children and adolescents from Smolyan region. The percentile norms have been developed using the database of the height, weight, waist and hip circumferences of 1174 children from Smolyan region (597 girls and 577 boys). The database was collected after an anthropometric transversal study conducted in the period 1998-2001. The anthropometry used the method of M a r t i n-S a l e r [7], while the derivatives were calculated by means of formulae. The percentiles were constructed on the basis of the empirical distribution of the characters and the following levelling by means of the method of the smallest squares. The graphic norms offered can be used in the clinics and schools for monitoring of the physical development and for assessment of the nutritional status of the children and adolescents from Smolyan region.

Key words: growth monitoring, nutritional status, undernutrition, overweight, obesity, abdominal obesity.

Introduction

For assessment of the physical development and the nutritional status of children and adolescents [13, 11, 3, 4, 5, 12, 8, 9] are used more methods, but the most widely used are based on different anthropometric characters, among which is the body mass index (BMI kg/m^2), waist circumference (WC), its ratio with hip circumference (WHR) and others. BMI used for diagnosing undernutrition and obesity in children and adolescents [12, 13, 11, 5, 1], and for intra-group and inter-group comparisons [2, 10, 1]. WC and WHR are indicators of abdominal (central) obesity and they are largely responsible for the risk of cardio-vascular illnesses, of increase of fats in the upper body segment, and the higher risk of metabolic dysfunctions, and of various illnesses [8, 9, 6, 1].

The specific features in the physical development and nutritional status of children and adolescents of different populations require the monitoring to be realized

on the the modern assessment norms, which have been constructed within specific time and space coordinates, i.e. the time (secular) alterations should be registered on the basis of populational (local) material.

In this context, the **aim** of this paper is to construct modern age/sex-specific percentile norms of BMI, WC and WHR for monitoring of the physical development and of assessment of the nutritional status of children and adolescents from Smolyan region.

Material and Methods

The percentile norms have been developed using the database of the height, weight, waist and hip circumference of 1174 children from Smolyan region (597 girls and 577 boys). The database was collected after an anthropometric transversal study conducted in the period 1998-2001. The anthropometry used the method of Martin-Saller [7] in which the database of directly measured metric characters was used to calculate the body mass index (BMI), and the waist-hip ratio (WHR). The percentile curves for the three characters were constructed on the basis of their empirical distribution and the following levelling by means of the method of the smallest squares.

Results

As a result of the created norms for BMI (Fig. 1, 2), the following categories for assessment of the nutritional status of the children from Smolyan region have been defined: undernutrition (BMI $\leq P_3$); nutritional disorders and risk of undernutrition ($P_3 - P_{10}$); slightly-under-the norm weight ($P_{10} - P_{25}$), normal body weight ($P_{25} - P_{75}$), slightly-over-the norm weight ($P_{90} - P_{97}$), overweight ($P_{90} - P_{97}$), and obesity ($\geq P_{97}$). In the clinical and school practice, however, classifying a child to one or other category according to BMI, should be done with care and after taking into consideration other body composition characters, such as development of the muscle or fat component, etc.

The waist circumference values (WC, Fig. 2, 3) and the waist/hip ratio (WHR, Fig. 3, 4) ranging between $\geq P_{90}$ and $\leq P_{97}$ are indicative of extra abdominal i.e. central body fats, while values $\leq P_{97}$ — the central or abdominal obesity.

Values of BMI, WC and WHR ranging between P_3 and P_{10} signal the beginning of growth dysfunctions probably and nutritional disorders, while values under P_3 signal obvious growth disturbances and undernutrition.

Children with values of the three indices above P_{90} and under P_{10} are a risk group for development of various illnesses at a greater age, that is why they should be under regular monitoring.

In **conclusion**, we suggest that the constructed percentile norms should be used in clinical and school practice for monitoring of the physical development and for assessment of nutritional status of children and adolescents from Smolyan region.

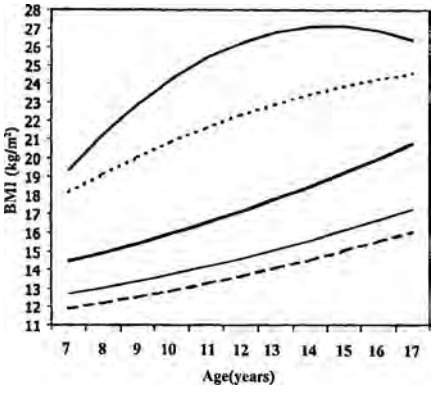

Fig. 1. BMI — girls

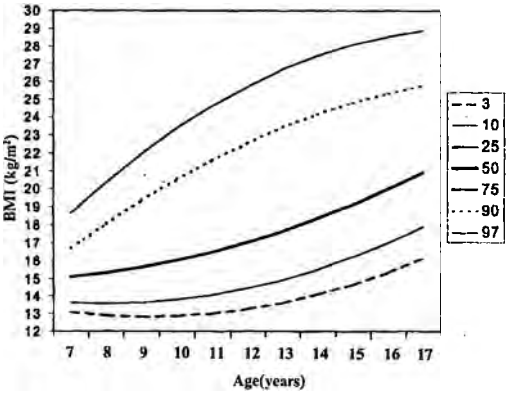

Fig. 2. BMI — boys

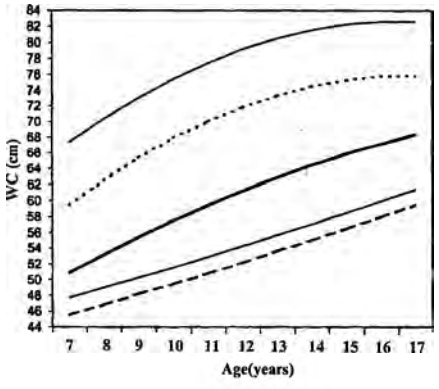

Fig. 3. Waist circumference — girls

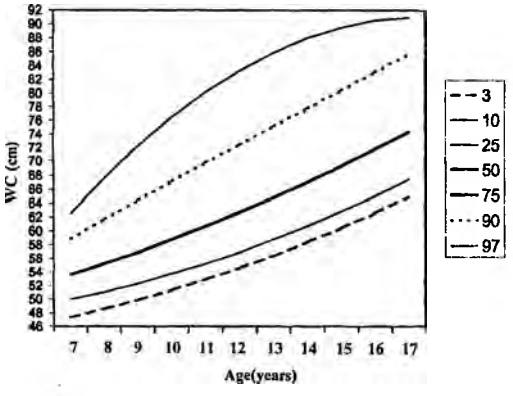

Fig. 4. Waist circumference — boys

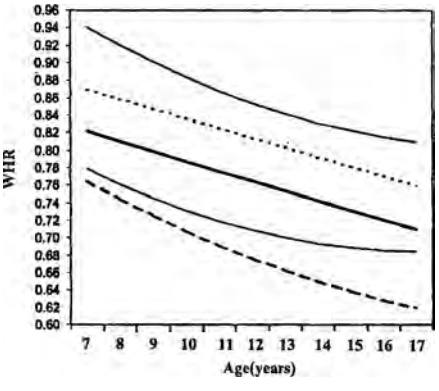

Fig. 5. Waist/Hip ratio — girls

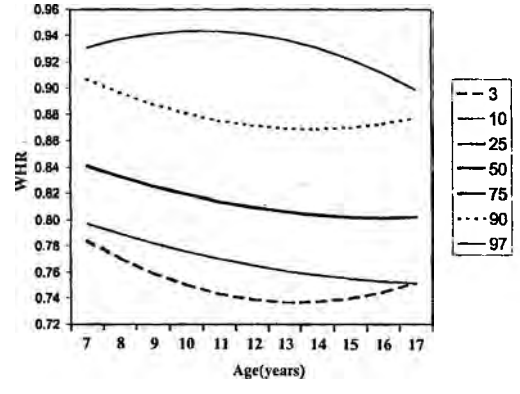

Fig. 6. Waist/Hip ratio — boys

References

1. Armstrong, J. The prevalence of obesity and undernutrition in Scottish Children: growth monitoring within the Child Health Surveillance Programme. — Scottish Medical Journal, **48**, 2003, No 2, 32-37.
2. Cole, T. Y., M. Y. Roede. Centiles of body mass index for Dutch children aged 0-20 years in 1980 a baseline to assess recent trends in obesity. — Ann. Hum. Biol., **126**, 1999, No 4, 303-308.
3. Cole, T. J. Statistical constructs of human growth: new growth charts for old. Anthropometry: the Individual and the Population, Cambridge: Cambridge Univ. Press, 1994, 78-98.
4. Cole, T. J. The use of Z-scores in growth reference standards. The Eighth International Congress of Auxology. Philadelphia, 1997, 33.
5. Cole, T. J. et al. Establishing a standard definition for child overweight and obesity worldwide: International survey. — British Medic. Journ., **320**, 2000, No 5, 1-6.
6. Goran, M. I., B. A Gower. Relation between visceral fat and disease risk in children and adolescents. — Am. Journ. of Clin. Nutrit., **70**, 1999, 1495-1565.
7. Martin, R., K. Saller. Lehrbuch der Anthropologie. T. 1. Stuttgart, Gustav Fischer Verlag, 1957, 661.
8. McCarthy, H. D., S. Ellis, T. Cole. Central overweight and obesity in British youths aged 11-16 years: cross sectional surveys of waist circumference. — British Medic. Journ., 2003, 326 (7390): 624.
9. McCarthy, H. D., K. V. Jarrett, H. F. Grawley. Development of waist circumference percentiles in British children aged 5.0-16.9y. — Eur. Journ. of Clin. Nutr., 2001, 55, 902-907.
10. Nacheva, A., E. Lazarova, L. Yordanova. Body nutritional statius 7-17 years old school-children from Sofia. — Journ. of Anthrop. Sofia, 4, 2003, 21-25.
11. Obesity: preventing and managing the global epidemic. Report of a WHO consultation on obesity. June, 305, 1997. WHO, Geneva. Aviable at: http:// dosei.who.int/uhtbin/cgisirsi/ Wed+Nov+21+23:21:20+MET+2001/0/49.Accessed April, 18, 2002.
12. Rolland-Cachera, M. F. Body mass Index References. The Cambridge Encyclopedia of Human Crowth and Development, Cambridge, Cambridge Univ. Press., 1998, 68-69.
13. World Health Organisation. Physical status: the use and interpretation of anthropometry. Report of a WHO Expert Committee, Geneva, 1995, 854.

Institute of Experimental Morphology and Anthropology

Acta morphologica et anthropologica, 10
Sofia•2005

Body Composition and Body Nutritional Status in Bulgarian Students at the Beginning of the 21st Century — Anthropological Assessment

Y. Zhecheva

Institute of Experimental Morphology and Anthropology, Bulgarian Academy of Sciences, Sofia

The aim of the present work is to characterize anthropometrically the body composition and the body nutritional status during the transitional age between youth and maturity in Bulgarian students at the beginning of the 21st century. Anthropometrically are examined % Body Fat (% BF), total Body Fat in kg (BF), Lean Body Mass (LBM), waist/hip circumference ratio (W/H) and BMI in 142 students — 72 male and 70 female aged 19-20 years. Males have lower per cent Body Fat and higher per cent Lean Body Mass compared to females. In males the mixed and android type of Subcutaneous Fat Tissue distribution prevails, and almost all females have gynoid type. According BMI none of the investigated individuals belongs to the II and III overweight categories. Highest is the per cent of normal body nutritional status in them.

Key words: body composition, body fat, body nutritional status, obesity, students.

Introduction

The basic anthropological features, which determine the physical development of human body, are those of the various body components and their proportions that indicate the body nutritional status and the obesity of the individual, as well.

The **Aim** of the following work is to characterize anthropometrically the body composition and the body nutritional status during the transitional age between youth and maturity (19-20 years) in Bulgarian students at the beginning of the 21st century.

Material and Methods

The material is collected during the period March — May 2002. Anthropometrically are examined 142 students — 72 males and 70 females aged 19-20 years. The investigation was taken at the University of Sofia "St. Kliment Ohridsky" and the Technical University of Sofia where students from all around the country are studying. The

anthropometrical investigation was conducted according to the classical method of Martin and Saller [2]. For the assessment of body composition and body nutritional status are used the following features: % Body Fat (% BF), total Body Fat in kg (BF), Lean Body Mass in kg (LBM), waist/hip circumference ratio (W/H). These features give general idea of the male and female types of subcutaneous fat tissue accumulation and distribution, as well as, of BMI that is accepted by the WHO as unified indicator about body nutritional status and obesity.

The features for determination of body composition and body nutritional status are estimated by the following formulas:

% BF male = 17,305 × lg SF triceps + 12,012 × lg (SF subscapular + SF X-th rib)+ +6,293 × lg SF abdomen — 20,9 [3];

% BF female = 9,367 × lg SF tricepsc + 13,462 × lg (SF subscapular + SF X-th rib)+ +5,298 × lg SF abdomen — 16,2 [3];

BF = $\frac{\text{body weight x \% BF;}}{100}$ **LBM** = body weight — BF;

BMI = weight (kg) / stature (m^2)

The intersexual differences are evaluated by the ISD data according to the formula:

$$ISD = \frac{\bar{x}_{female}}{\bar{x}_{male}}.100$$

The evaluation of the established intersexual differences is done the by T-criteria of Student at $P < 0.05$.

Results

According to literature data about body composition the ratio between body fat and lean body fat vary significantly during the different ages. Largest is the percentage of LBM in the 20 years old indivduals, whose body fat percentage is lowest [4].

➢ **Per cent Body Fat** (Table 1, Fig. 1). At the age of 19-20, the studied young males have16.58 % BF, and the females — 17.59 % BF. The 30-40 years old Bulgarian males (unpublished data by National Anthropological Program) have 23.1 % BF, and the adult female — 24.7 % FT. The comparative evaluation shows that at the age of 19-20 males have 6.52 % BF and females 7.11 % less BF than their 30-40 years old contemporaries. It is interesting that although the amount of body fat is different in 19-20 years old and 30-40 years old individuals, the intersexual differences have almost equal character in both age groups. In adults the males have 1.6 % less body fat than females, and the sexual differences for 19-20 years old individuals are 1.1 %.

➢ **Body Fat** (Table 1, Fig. 1). The average value of this feature for young males is

Table 1. Data about body composition and body nutritional status

No	Features	Males				Females				T-test	ISD
		$\bar{x}$	SD	$s\bar{x}$	V	$\bar{x}$	SD	$s\bar{x}$	V		
1	%BF	16.58	4.99	0.59	30.10	17.59	2.94	0.35	16.71	1.47	106.09
2	BF	11.90	4.53	0.53	38.07	9.34	2.65	0.32	28.37	4.12*	78.49
3	LBM	58.51	6.04	0.71	10.32	43.04	4.85	0.58	11.27	16.85*	73.56
4	W/H	0.85	–	–	–	0.76	–	–	–	–	89.41
5	BMI	22.04	2.56	0.30	11.62	19.44	2.21	0.26	11.37	6.48*	88.20

* $P < 0.05$

11.90 kg BF and for young women — 9.34 kg BF. The intersexual differences are statistically significant. ISD shows that BF is with 21.51 % more for males than females.

➢ **Lean Body Mass** (Table 1, Fig. 1). LBM includes all non-fat tissues (bones, muscles, other soft tissues, liquids). Of all non-fat tissues, most eco-sensitive are the muscles therefore it is considered that data about LBM give information of its development. The average value of this component for the studied males is 58.51 kg, and for the females — 43.04 kg. The intersexual differences are statistically significant. ISD indicates that LBM is with 26.44 % more for males, than females.

➢ **W/H ratio** (Table 1, Fig. 1, 2). The W/H ratio determines two basic models of fat tissue distribution: android (abdominal) and gynoid (gluteofemoral). There is also a third one — mixed type of fat tissue distribution. The average value of this ratio for males is 0.85 (mixed type), and for females 0.76 (gynoid type). ISD indicates that W/H ratio is with 10.59 % more for males, than females.

➢ **Body mass index** (Table 1, Fig. 1, 3). The average values of this index are 22.04 kg/m^2 for men and 19.44 kg/m^2 for women. The intersexual differences are statistically significant. ISD indicates that the BMI for males is with 11.8% more than for females. Depending on the categorization of body nutritional status of the stud-

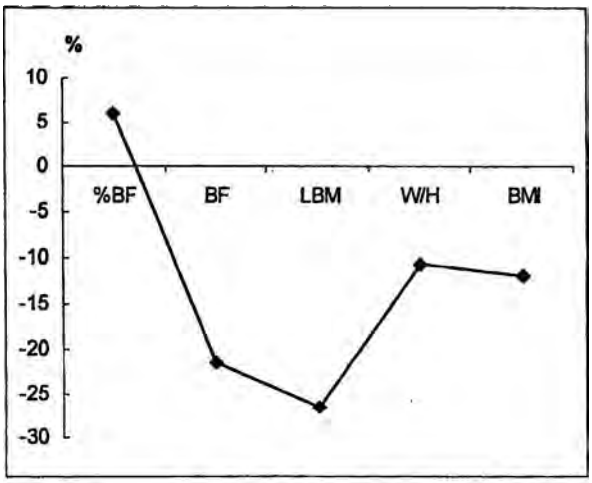

Fig. 1. Intersexual differences of body composition and body nutritional status (data by ISD)

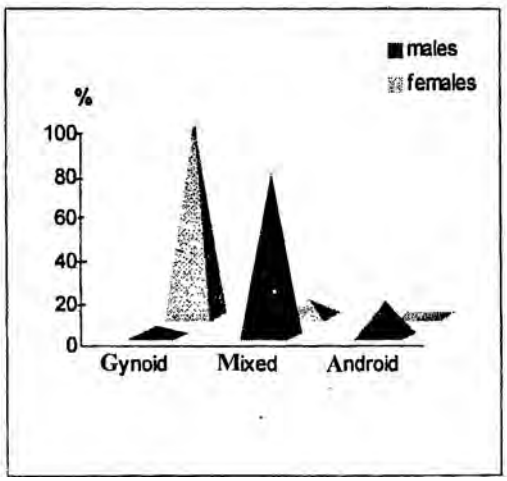

Fig. 2. Distribution of individuals according to W/H ratio

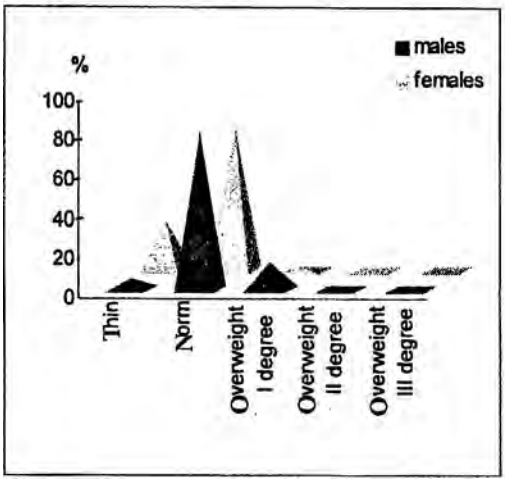

Fig. 3. Distribution of individuals according to BMI categories

ied students, according to the WHO categories elaborated by J. Garrow [1], none of the investigated individuals belongs to the II-nd and III-rd overweight categories. Biggest is the per cent of young men with normal body nutritional status — 80.56 %, 13.89% are I-st degree overweight, and the rest 5.55 % are categorized as thin. From the young women — 72.86 % are with normal body nutritional status, 25.71 % are belonging to the category "thin" and the rest 1.43 % are I-st degree overweighed.

Conclusions

- The 19-20 years old males have lower per cent Body Fat and higher per cent Lean Body Mass compared to the 19-20 years old females.
- The data about W/H ratio show that in young males the mixed and android type of Subcutaneous Fat Tissue distribution prevails, and almost all young females have gynoid type of Subcutaneous Fat Tissue distribution.
- The assessment of body nutritional status in males and females aged 19-20 years according to the WHO criteria about BMI shows that to the II-nd and III-rd overweight categories belongs none of the investigated individuals. Highest is the per cent of these with normal body nutritional status — 70-80 %, 13.9 % from males and 1.4 % from females are I-st degree overweighed.

Generalized the results obtained in the present paper give information about the specific peculiarities of basic characteristics in the individual's physical development namely about body composition and body nutritional status in the investigated 19-20 years old men and women who are a part of the young Bulgarian population living at the beginning of 21st century.

References

1. Garrow, J. S. Treat obesity seriously — a clinical manual. Edinburgh, Churchill Livingstone, 1981.
2. Martin, R., K. Saller. Lehrbuch der Anthropologie in sistematischer Darstellung. T. I. Stuttgart, Gustav Fischer Verlag, 1957.
3. Möhr, M. Eine körperbautypologische Gliederung der Industrie — Arbeiter und Arbeiterinnen der DDR. — Ernährungsforschung, 14, 1969, No 3, 197-223.
4. Parizkova, J. Body fat and physical fitness. Prague, 1977, 1-279.

Institute of Experimental Morphology and Anthropology

Acta morphologica et anthropologica, 10
Sofia • 2005

Distribution of Subcutaneous Fat Tissue in 9-15-Year-Old Schoolchildren from Sofia

Z. Mitova

Institute of Experimental Morphology and Anthropology, Bulgarian Academy of Sciences, Sofia

In the present study the intersexual and inter-age differences in the topical distribution of subcutaneous fat tissue in 9-15 year-old schoolchildren was evaluated anthropometrically. The investigation was carried out during 2001-2003 in three Sofia schools. The results obtained show that between 9 and 14 years of age clearly expressed, non-changing and sex-determined differentiation of subcutaneous fat tissue distribution across trunk and extremities has not yet occurred. The sexually associated differentiation, typical of adults, begins in the 15th year both for boys and girls.

Key words: skin folds, body fat distribution, intersexsual differences.

Introduction

Intensive changes in the human body configuration and composition occur during the "border period" between childhood and adulthood — the puberty period. These changes are markedly manifested in the thickness of subcutaneous fat tissue and contribute to the typical of adult males and females anthropometrical characteristics [1, 2].

The aim of the present study is to evaluate anthropometrically, the intersexual and inter-age differences in the topical distribution of subcutaneous fat tissue in 9-15-year-old schoolchildren. This age period includes the end of pre-pubertal and the pubertal ages.

Material and Methods

The investigation was carried out during 2001-2003 in three Sofia schools.

Nine skin folds (SF) of the trunk and extremities in 566 boys and 570 girls (9-15 years of age), were measured with a Holtan caliper. The typical features in the topical distribution of subcutaneous fat tissue (SFT) were evaluated:

• the relative share of the thickness of each skin fold to the total quantity of the measured SFT [($\bar{X}$ thickness of every skin fold• 100)/($\bar{X}$ total sum from thickness of 9 SF)];

• the comparison between the relative share of the thickness of 4 SF on the trunk (subscapular SF + suprailiac SF + 10^{th} rib SF + abdominal SF) and 4 SF on the extremities (triceps SF+ biceps SF+ thigh SF + medial calf SF), as opposed to their total sum (8 SF).

The statistically significant differences were evaluated by the Student's t-test ($p<0.05$).

Results and Discussion

The results show that there are no significant intersexual and inter-age differences of the ratio (skin fold thickness)/(total SFT thickness) in the age interval 9-15yr., (Table. 1, 2).

Table 1. Absolute values (mm) of skin fold thicknesses

Skin folds	Boys							Girls						
	Age (years)							Age (years)						
	9	10	11	12	13	14	15	9	10	11	12	13	14	15
	n 81	n 80	n 82	n 84	n 80	n 83	n 80	n 81	n 80	n 80	n 85	n 83	n 82	n 82
subscapular	8.4	9.1	11.1	10.1	9.7	10.1	9.4	10.3	11.5	11.4	10.2	12.2	13.7	12.4
10^{th}- rib	6.1	6.2	7.4	6.8	7.0	7.4	7.6	7.5	8.7	8.6	7.6	9.6	10.3	9.5
suprailiac	7.1	7.4	8.5	7.6	8.0	8.7	8.3	8.6	10.1	10.3	9.3	10.9	11.3	10.9
abdomen	13.2	14.0	16.1	14.0	14.4	15.2	13.8	15.0	17.8	17.7	16.3	18.3	20.4	19.3
triceps	10.5	10.6	12.2	11.1	11.3	10.8	9.5	12.4	13.1	12.9	12.6	13.9	14.2	1.2
biceps	6.0	5.9	6.8	5.8	5.7	5.4	4.36	6.5	7.2	6.9	6.3	6.9	7.1	6.3
forearm	6.2	6.3	6.2	5.9	5.7	5.6	5.0	6.7	6.5	6.7	6.1	6.9	7.0	6.4
thigh	16.7	16.7	19.9	17.1	18.0	17.5	14.7	20.4	21.1	21.8	20.2	22.5	24.1	23.8
calf	12.1	12.0	14.7	13.5	14.2	13.9	11.7	14.6	15.7	16.9	15.6	17.7	18.1	16.6
Sum of 9 SF	86.7	88.0	102.7	91.8	93.9	94.6	84.4	102.0	111.7	113.1	104.1	119.0	126.2	119.4

Table 2. Relative share (%) of skin fold thicknesses

Skin folds	Boys							Girls						
	Age (years)							Age (years)						
	9	10	11	12	13	14	15	9	10	11	12	13	14	15
	n 81	n 80	n 82	n 84	n 80	n 83	n 80	n 81	n 80	n 80	n 85	n 83	n 82	n 82
subscapular	9.7	10.0	10.3	10.3	10.0	10.6	11.2	9.5	9.8	9.7	9.7	10.0	10.6	10.3
10^{th}-rib	7.0	6.9	7.0	7.2	7.5	7.9	9.0	7.0	7.2	7.2	7.2	7.9	7.9	7.9
suprailiac	7.8	8.1	8.0	8.1	8.4	9.0	9.4	8.2	8.9	8.9	8.8	9.0	8.9	8.9
abdomen	14.7	15.3	15.3	14.9	15.2	15.9	15.9	14.4	15.7	15.6	15.6	15.4	16.3	16.0
triceps	12.6	12.4	12.3	12.5	12.1	11.6	11.3	12.5	12.0	11.6	12,1	11,7	11,3	12,0
biceps	7.1	6.8	6.8	6.4	6.1	5.9	5.3	6.6	6.5	6.1	6.0	5.9	5.6	5.3
forearm	7.9	7.7	6.6	7.0	6.6	6.5	6.4	7.1	6.3	6.3	6.1	6.0	5.7	5.5
thigh	19.2	19.1	19.4	18.7	19.0	18.2	17.4	20.3	19.3	19.7	19.6	19.3	19.4	20.3
calf	14.1	13.7	14.4	14.9	15.2	14.5	14.1	14.5	14.3	15.0	15.0	15.0	14.4	13.9

Table 3. Distribution of SFT on the trunk and extremities

Boys														
Age	**9**		**10**		**11**		**12**		**13**		**14**		**15**	
	mm	**%**	**mm**	**%**	**mm**	**%**	**mm**	**%**	**mm**	**%**	**mm**	**%**	**mm**	**%**
trunk - 4SF	39	43	40	44	40	43	41	44	41	44	43	46	46	49
extremities - 4 SF	53	57	52	56	53	57	52	56	52	56	50	54	48	51
Suma - 8 SF	92		92		93		93		93		94		94	
Girls														
Age	**9**		**10**		**11**		**12**		**13**		**14**		**15**	
	mm	**%**	**mm**	**%**	**mm**	**%**	**mm**	**%**	**mm**	**%**	**mm**	**%**	**mm**	**%**
trunk - 4SF	39	42	42	44	41	44	41	44	42	45	44	46	43	46
extremities - 4 SF	54	58	52	56	52	56	53	56	52	55	51	54	51	54
Suma - 8 SF	93		94		94		94		94		94		95	

However, the 15-year- old children already exhibit the SFT distribution characteristic of the adults — males have larger relative share of trunk SFT, while adult females have larger one on the extremities. For example, the 15 yr boys display a larger relative thickness of skin folds on the chest (subscapular and 10th rib) and around area suprailiaca (Fig. 1, 2, 3). Through the age-period 10-15yr girls show a larger relative SFT in the medium part of the abdomen at the umbilicus level.

When the upper extremities are considered, the relative SFT in both sexes is lower with increasing age. This process is more clearly expressed in the boys, which have thicker skin folds on the upper arm and forearms. Increasing SFT is observed in girls after the age of 14. This is illustrated by the crossed curves on the figures showing the relative share of the thickness of the triceps by years (Fig. 4).

Specific intersexual differences of relative SFT on the lower extremities (Fig. 5) are manifested in the skinfolds of the thigh. Throughout the studied age period, girls though not significantly display a larger relative SFT of the thigh than boys. At the age of 15 the intresexual differences for this features show greatest values as compared to the other analyzed features.

A general evaluation of the topical distribution of SFT on the trunk and the extremities may be obtained by the comparison between the relative share of the sum of thicknesses of 4 SF on the trunk and 4 SF on the extremities (Table 3 and Fig. 6).

Through the investigated age period (9-14yr) girls display a larger relative SFT on the trunk and the boys on the extremities. Between 14 и 15 yr the age-curves are crossed, illustrating that the thickness of SFT on the trunk is already larger in boys and the girls on the extremities.

Conclusions

The results obtained show that between 9 and 14 years of age clearly expressed, non-changing and sex-determined differentiation of subcutaneous fat tissue distribution across trunk and extremities has not yet occurred. The sexually associated differentiation, typical of adults, begins in the 15th year both for boys and girls.

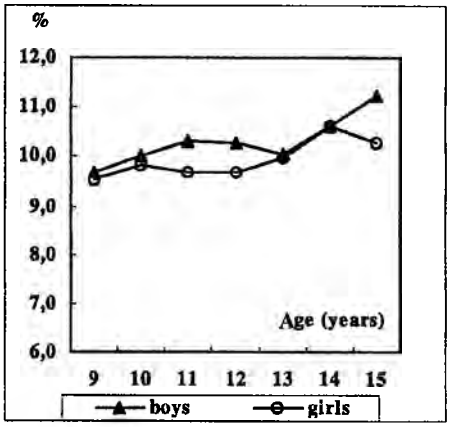

Fig. 1. Subscapular SF

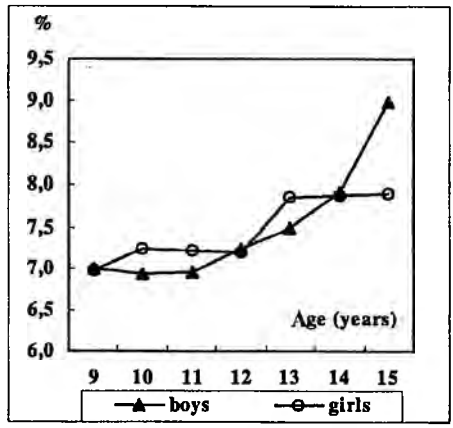

Fig. 2. 10^{th} — rib SF

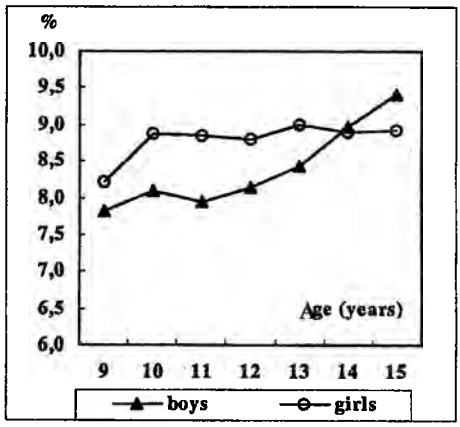

Fig. 3. Suprailiac SF

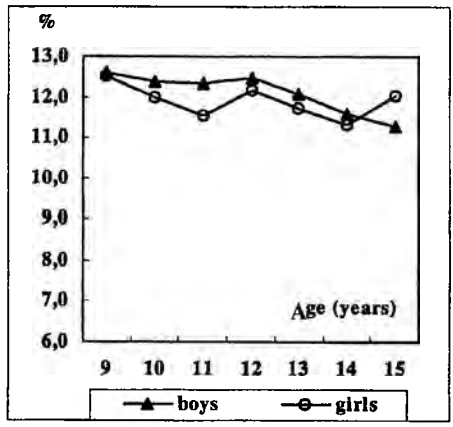

Fig. 4. Triceps SF

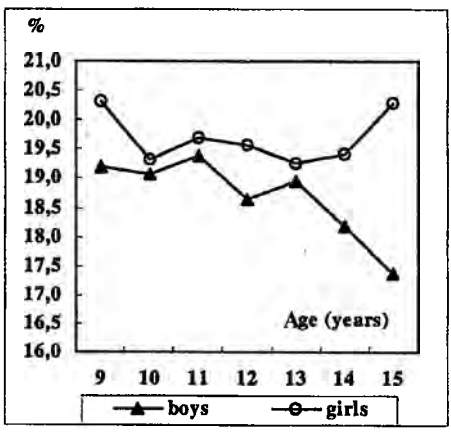

Fig. 5. Thigh SF

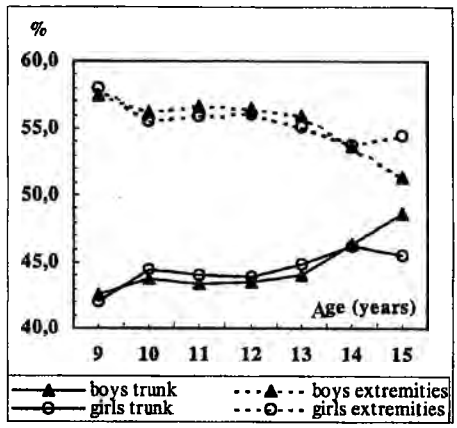

Fig. 6. Distribution of the SFT on the trunk and extremities

References

1. Malina, R. M. Regional Body Composition: Age, Sex, and Ethnic Variation. —In: Human Body Composition (Ed. Al. Roche, St. Heymsfield, T. Lohman). USA, Human Kinetics, 1996, p. 217-255.
2. Van Loan, M. D. Total Body Composition: Birth to Old Age. — In: Human Body Composition (Ed. Al. Roche, St. Heymsfield, T. Lohman). USA, Human Kinetics, 1996, 205-215.

Institute of Experimental Morphology and Anthropology

Acta morphologica et anthropologica, 10
Sofia•2005

Dermatoglyphic Indexes, Menarche and Menopause in Females

M. Pirinska-Apostolu, V. Angelova

Faculty of Biology,Department of Zoology and Anthropology, Sofia University "St. Kliment Ohridski"

The purpose of the present research is to be detected probable correlation between the digital dermatoglyphic features and the occurrence of menarche and menopause in females as well as to be accomplished anthropological characterization of the population by these traits. The examined sample includes women from various age groups. There has been made 437 dermatoglyphic prints out of 217 females. Data about the occurrence of menarche and menopause has been collected from 225 females by the inquiry method. On the basis of the received data it has been established that loops are presented with higher frequencies as fingerprint patterns in the examined population. Correlation between fingerprints and menarche/menopause is not significant.

Key words: females, fingerprints, menarche, menopause, correlation.

Introduction

All the dermatoglyphic traits, as well as the sex maturity are genetically determined features. During the end of the third prenatal month the sexual characteristics have already been developed. By the same time the dermatoglyphic features have been formed too [1]. Maturational timing associated with sex chromosomes as a factor in dermatoglyphic variation has been also suggested [2, 7]. The purpose of the present research is to be detected probable correlation between the digital dermatoglyphic features and the occurrence of menarche and menopause in females as well as to be accomplished anthropological characterization of the population by these traits.

Material and Methods

The research has been undertaken in the territory of the Belogradchik city and the adjacent villages. The examined sample includes women from various age groups. There has been made 437 dermatoglyphic prints out of 217 females. The diagnosis of the fingerprints has been accomplished by the means of the Cummins and Midlo methods [3, 4]. Three basic features have been used: loops-L, whorls-W and

arcs-A. Data about the occurrence of menarche and menopause has been collected from 225 females by the inquiry method. Early or late first menarche and menopause is calculated according to Meier, Meier et al. [5, 6] (Table 2 and 3).

Results and Discussion

Fingerprints. Among the digital dermatoglyphic features of Belogradchic females, loops (U+R) have shown the highest concentration (64.03%) and arcs (A+T) the lowest-8.30%. Ulnar loops are more frequent than radial ones for both hands (60.46 and 3.26 respectively). The first are also more frequent on the III and V fingers, especially on the V (82.49%). The lowest concentration of ulnar loops has been found in respect of the II finger (34.10%). The conclusions made on the basis of the data analysis indicates that whorls are more frequent on the I finger for both hands. Arcs have been found to be the most rare fingerprint feature in comparison with loops and whorls.

The most variable fingerprint feature is proved to be ulnar loops. In the examined population this trait varies from 32.74 % (referring to the II finger of the right hand) to 83.40% (referring to the V finger of the same hand) (Table 1).

Menarche. The occurrence of the menarche among the examined females varies from 9 to 14 years old, with a value of 11.60 ±1,17 as a mean. About 62.30% of them belong to the interval between 10.43 and 12,77 years old. 15.7% of the sample has an early maturity [7] (from 9 to 10.43 years old). In addition, late maturity show 21.99% of the sample (between 12.77 and 14 years old) (Table 2). A group of nonmature girls including 34 persons has a mean age of 10.62 years, whereas the limits of its age variation are 10 and 13 respectively. Among the schoolgirls first menarche

Table 1. Frequency of the digital dermatoglyphic features (in %)

Type of feature	Fingers														
	I			II			III			IV			V		
	L	R	L+R	L	R	L+R	L	R	L+R	L	R	L+R	L	R	L+R
A+T	6.45	3.23	4.61	20.74	17.97	19.15	15.67	7.37	11.52	4.15	1.84	3.00	3.23	2.30	2.77
R	0.92	0.92	0.92	14.29	13.82	14.06	0.46	–	0.23	0.46	1.38	0.92	–	0.46	0.23
U	57.14	53.46	55.30	32.72	35.48	34.10	66.82	76.50	71.66	60.83	56.68	58.75	83.40	81.57	82.49
W	35.48	42.40	38.94	32.26	32.72	32.49	17.05	16.13	16.59	34.56	40.09	37.33	11.36	5.67	14.52
L(R+U)	58.06	54.38	56.22	47.01	49.30	48.16	67.28	76.50	71.89	1.29	8.06	59.68	83.40	82.03	82.72

Table 2. Classification of relative maturity defined by age at menarche

Category	*N*	%	Range of age
Early maturers	30	15.71	9–10.43
Late maturers	42	21.99	12.77–14

Table 3. Classification by age at menopause

Category	*N*	%	Range of age
Early	11	18.33	39–41.98
Late	10	16.67	50.72–57

Table 4. Menarche and menopause according to seasons

Groups		Total		Seasons			
				winter	spring	summer	autumn
Schoolgirls under 20 years old		98	*n*	32	15	23	28
			%	32.65	15.31	23.46	28.57
20 — 40 years old		35	*n*	6	9	8	12
			%	17.14	25.71	22.86	34.29
Above 40 years old	Menarche	58	*n*	7	19	11	21
			%	12.07	32.76	18.97	36.21
	Menopause	60	*n*	16	18	17	9
			%	26.67	30.00	28.33	15.00

Table 5. Correlation between digital dermatoglyphic features and occurrence of menarche/menopause

Spearman's correlation		W	L	A
menarche	Correlation Coefficient	0.055	—0.072	0.053
	Sig.	0.449	0.321	0.466
	N	191	191	191
menopause	Correlation Coefficient	—0.026	0.054	—0.098
	Sig.	0.842	0.0684	0.457
	N	60	60	60

** Correlation is significant at the .01 level (2-tailed).
* Correlation is significant at the .05 level (2-tailed).

occurs in winter more frequently (32.57%) and only rarely in spring (15.31). The groups from 20 to 40 years old and above 40 show higher rates of menarche occurrence in autumn (43.29% and 36.21% respectively). For the representatives of these two groups the lowest percentage values of first menarche have been established in winter (17.14 and 12.07 respectively) (Table 4).

Menopause. In 26.67% of the examined females above 39 years old menopause has already occurred. The estimated mean value of the feature is 46,35 ± 4,37 years, with limits of variation ranged from 39 to 57 years old (table 4). Occurrence of menopause is observed more frequently in spring (30%) in addition with autumn (15%).

Correlation. In order to be found out if digital dermatoglyphic features and occurrence of menarche and menopause are connected, Spearman's correlation coef-

ficient has been calculated. The received data shows that this kind of correlation is statistically insignificant, although from Fig. 1 and Fig. 2 can be established the fact that girls with early menarche have more loops as fingerprint patterns, as well as women with late menopause (Table 5).

Conclusions

On the basis of the received results it has been found out that the Belogradchik female population is characterized by:

— Relatively high frequency of loops as fingerprint features
— Mean age of first menarche equal to 11.6 ± 1.17 years

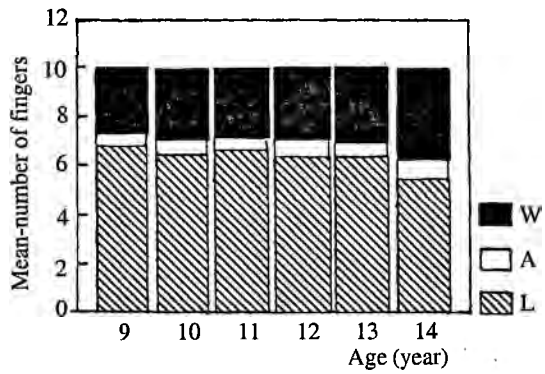

Fig. 1. Dependence between 1st menarche and dermatoglyphic patterns of fingers

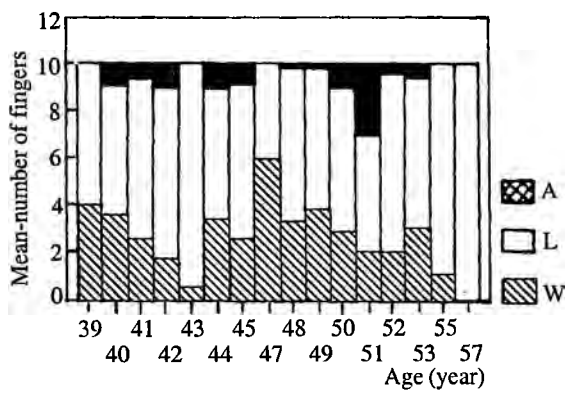

Fig. 2. Dependence between menarche and dermatoglyphic patterns of fingers

— Mean age of menopause equal to 46.35 ±4.37 years

— Occurrence of menarche and menopause of the various examined age groups set up at different seasons.

— Statistically non-significant correlation between fingerprints and menarche / menopause.

References

1. Babler, W. J. Prenatal selection and dermatoglyphic patterns. — Am. J. Phys. Anthrop., **48**, 1978, 21-27.
2. Barlow, P. The influence of inactive chromosomes on human development. — Human genetics, **17**, 1973, 105-136.
3. Cummins, H. The topographic history of volar pads (walking pads, Tastballen) in the human embryo. — Carnegie Insitute of Washington, **20**, 1929, No 1, 123-126.
4. Cummins, H., C. Midlo. Finger Prints, Palms and Soles. Dover, New York, 1961.
5. Meier, R. J. 1981 Sequential developmental components of digital dermatoglyphics. — Human Biol. 53, 557-573.
6. Meier, R. J., C. Sorenson Goodson, E. M. Roche. Dermatoglyphic Development and Timing of Maturation. — Human Biol., **59**, 1987, No 2, 357-373.
7. Netley, C., J. Rovet. Verbal deficits in children with 47, XXY and 47, XXX karyotypes: A descriptive and experimental study. — Brain and Language, **17**, 1982, 58-72.

Institute of Experimental Morphology and Anthropology

Acta morphologica et anthropologica, 10
Sofia • 2005

Morphological Peculiarities of Head and Face Structure in Patients with Neuro-Muscular Diseases

P. Borissova, S. Tornjova*, I. Turnev***

* *Institute of Experimental Morphology and Anthropology, Bulgarian Academy of Sciences, Sofia*
** *Departure of Neurology, Medical University, Sofia*

The cephalometric status of patients with Congenital Cataracts Facial Dysmorphism Neuropathy syndrome (CCFDN), Hereditary Motor and Sensory Neuropathy — Lom (HMSNL) and Congenital Myasthenic Syndrome (CMS) type Ia and of healthy Gypsies is studied. The investigation includes 38 patients with CCFDN, 54 patients with HMSNL, 19 patients with CMS type Ia and 77 healthy Gypsies. The program of the study includes 20 cephalometric features and 5 cephalometric indices. Generalized the patients from both sexes showed a tendency towards less head and face measurements compared to the healthy persons. Compared to the healthy persons, the patients from both sexes have longer face, relatively less wide forehead, but larger head length than bizygomatical diameter. The male patients have relatively wider head breadth and upper face part, while the female patients have relatively bigger head length and narrower upper face part.

Key words: neuromuscular diseases, cephalometric features.

Introduction

The hereditary neuromuscular diseases are a heterogeneous group of diseases attacking the skeletal musculature and the peripheral nerves. Among these diseases are also the congenital cataracts facial dysmorphism neuropathy syndrome (CCFDN), the hereditary motor and sensory neuropathy — Lom (HMSNL) and the congenital myasthenic syndrome (CMS) type Ia. The investigated diseases are genetically determined (with autosome-recessive type of inheritance) and spread only among Gipsy families. Up to the present days a wide investigations thoroughly in medical aspect of the diseases are made [2, 3]. The **aim** of the present study is to analyse the inter group differences in the cephalometric status of patients with CCFDN, HMSNL and CMS type Ia and healthy Gypsies.

Material and Methods

Subject of the study are 38 patients (18 males and 20 females) with CCFDN, 54 patients (26 males and 28 females) with HMSNL, 19 patients (5 males and 14

females) with CMS type Ia and 77 healthy Gypsies (36 males and 41 females). The program of the study includes 20 cephalometric features and 5 indices (Table 1), taken by the methods of Martin, Saller [1]. The statistical significant differences are assessed by the one-way analysis of variance (ANOVA) with post hoc tests by Bonferroni and Tamhane for multiple comparisons (after the rejection of the null hypothesis by ANOVA).

Table 1. Investigated cephalometric features and indices

Cephalometrical features		Cephalometrical indices
Head length (gl-op)	Nasal-subnasal length (n-sn)	Head index
Head breadth (eu-eu)	Nasal-pronasal length (n-prn)	*I = (eu-eu) / (g-op) *100*
Minimal frontal diameter (ft-ft)	Nose protrusion (sn-prn)	Morphological face index
Bizygomatical diameter (zy-zy)	Philtrum length (sn-sto)	*I = (n-gn) / zy-zy) *100*
Bigonial diameter (go-go)	Labrale sup.-labrale inf. distance (ls-li)	Jugofrontal index
Trichion-nasion distance (tr-n)	Interocular diameter (en-en)	*I = (ft-ft) / (zy-zy) *100*
Physiognomical face height (tr-gn)	Biocular diameter (ex-ex)	Transversal cephalo-facial index
Morphological face height (n-gn)	Nose breadth (al-al)	*I = (zy-zy) / (eu-eu) *100*
Morphological upper face height (n-pr)	Lip length (ch-ch)	Jugomandibular index
Physiognomical upper face height (n-sto)	Head circumference (g-op)	*I = (go-go) / (zy-zy) *100*

Results and Discussion

The comparative between group analyses shows a common for both sexes tendency towards smaller head and face measurements in the patients, compared to the healthy individuals (Fig. 1). This tendency is most strongly expressed in the patients with CCFDN, and most slightly — in the patients with HMSNL. Applying the dispersion analysis and suitable post hoc procedures about multiple comparison, 14 feature for men and 13 for women are distinguished in which the patients mean values differs significantly from those of the healthy persons (Table 2). The differences are more strongly expressed to a large degree in women than in men. For both sexes more frequent are the significant differences between healthy individuals and CCFDN patients than between healthy individuals and HMSNL and CMS type Ia patients.

Significant differences of the cephalometric indexes' characteristics in the healthy and diseased individuals are available. The data about head index (Fig. 2)

Table 2. Statistical significant differences between investigated subgroups of patients and healthy persons

	Groups	Features																			
		head circum.	g-op	eu-eu	ft-ft	tr-n	zy-zy	go-go	tr-gn	n-gn	n-sto	sto-gn	n-sn	al-al	n-prn	sn-prn	sn-sto	ls-li	ch-ch	en-en	ek-ek
Males	healthy / CCFDN	*	*	*	*	*		*				*						*	*		
	healthy / HMSNL							*	*	*		*									
	healthy / CMS						*	*						*					*		*
	CCFDN / HMSNL					*													*		
	CCFDN / CMS																				
	HMSNL / CMS													*					*		*
Females	healthy / CCFDN	*	*	*	*	*	*	*	*			*		*		*			*		
	healthy / HMSNL	*					*														
	healthy / CMS							*											*		
	CCFDN / HMSNL	*	*			*	*		*					*					*	*	*
	CCFDN / CMS		*		*	*	*														
	HMSNL / CMS							*											*	*	

*Statistical significant differences ($P<0.05$)

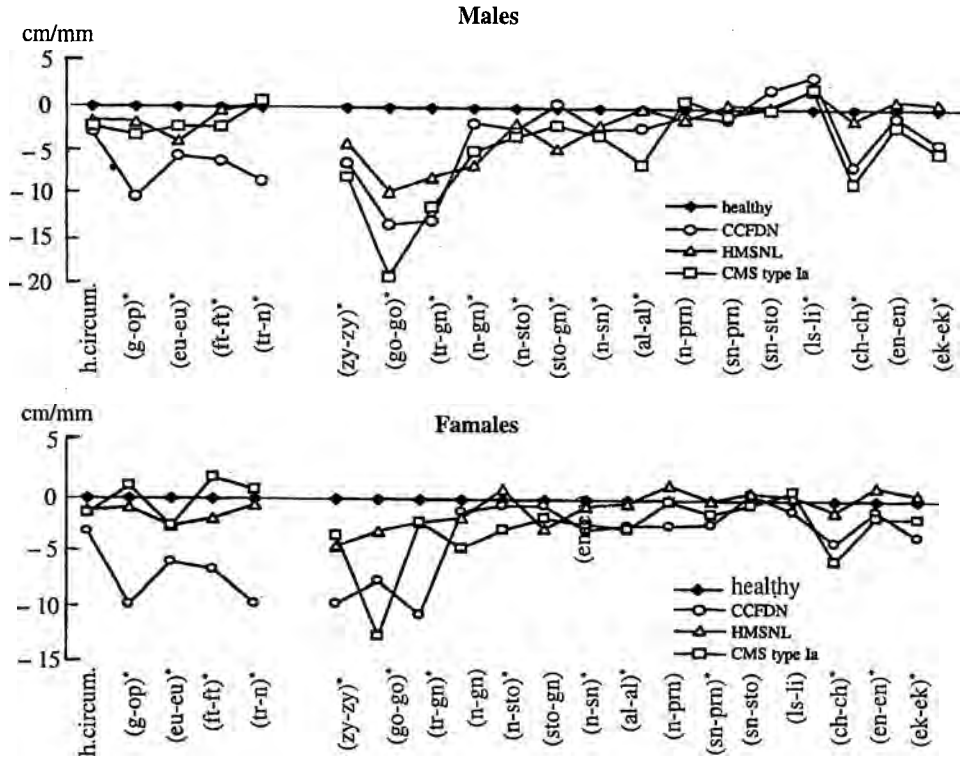

Fig. 1. Differences between mean values of the investigated cephalometric features in patients with CCFDN, HMSNL, CMA type Ia and healthy persons

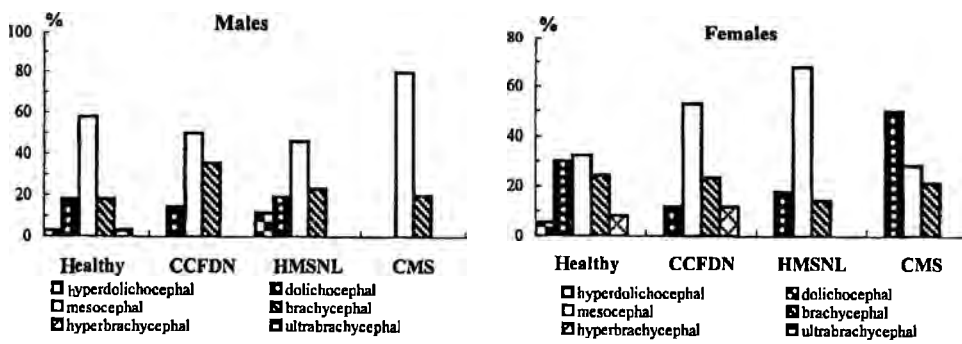

Fig. 2. Distribution of the investigated patients and healthy persons by head index categories

show that males and females with CCFDN, as well as the males with CMS type Ia have relatively higher head width while the males and females with HMSNL and the females with CMS type Ia have relatively higher head length. The CCFDN males basically distinguish by higher frequency of brachycephal forms, the HMSNL males — by higher frequency of dolichocephal and hyperdolichocephal ones, and the CMS

type Ia males — by very high frequency of mesocephal, as well as, by total absence of dolichocephal and hyperdolichocephal forms. As the CCFDN females basically distinguish by higher frequency of mesocephal and lower frequency of dolichocephal forms, the HMSNL females — by lower frequency of brachycephal forms and higher frequency of mesocephal forms while the CMS type Ia females — by higher frequency of dolichocephal forms. Analyzing the jugofrontal index in the patients from both sexes, a tendency for relatively higher forehead width compared to the bizygomatical diameter is established (Fig. 3). In the male and female patients, the frequency of very wide forms in higher, and the frequency of the wide forms are near or less to those in the healthy ones. The data about transversal cephalo-facial index show that the patients from both sexes have relatively less bizygomatical diameter compared to the head length (Fig. 4). A tendency of higher frequency about middle and below middle forms than those about over middle and large forms is observed. According to the data about jugomandibular index, the CCFDN, HMSNL and CMA type Ia males, as well as the CMS type Ia females have brighter upper face part in relation to the lower part (Fig. 5). Opposite, the CCFDN and HMSNL females have relatively narrower upper face part than the lower one. In the ill males and the CMS type Ia females is established a lower frequency of short and very short forms, and

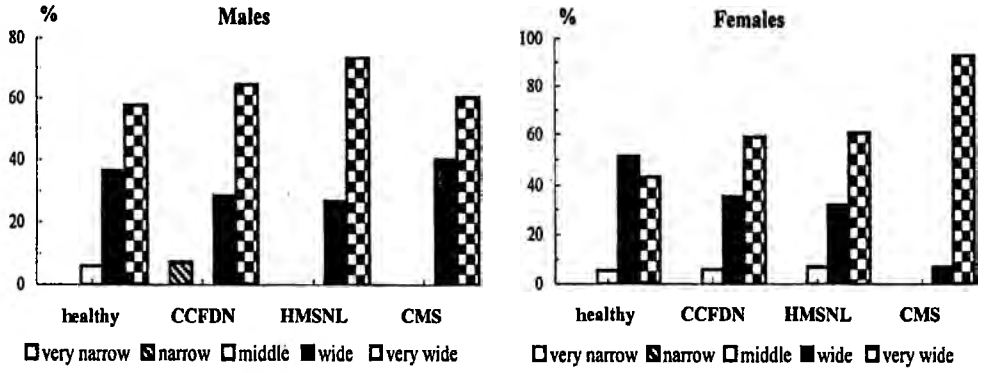

Fig. 3. Distribution of the investigated patients and healthy persons by jugofrontal index categories

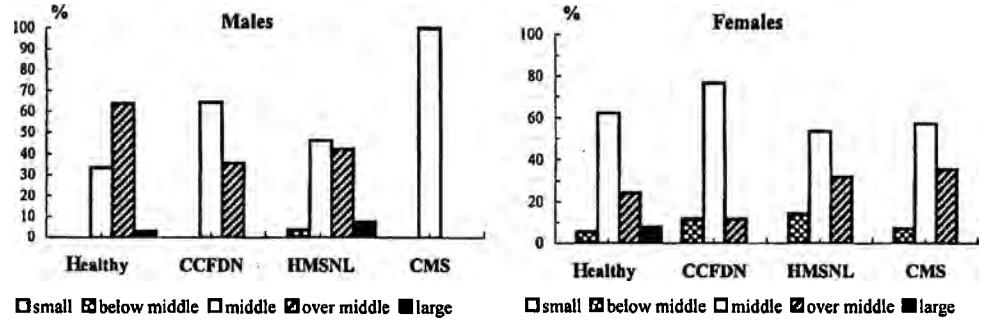

Fig. 4. Distribution of investigated patients and healthy persons by transversal cephalo-facial index categories

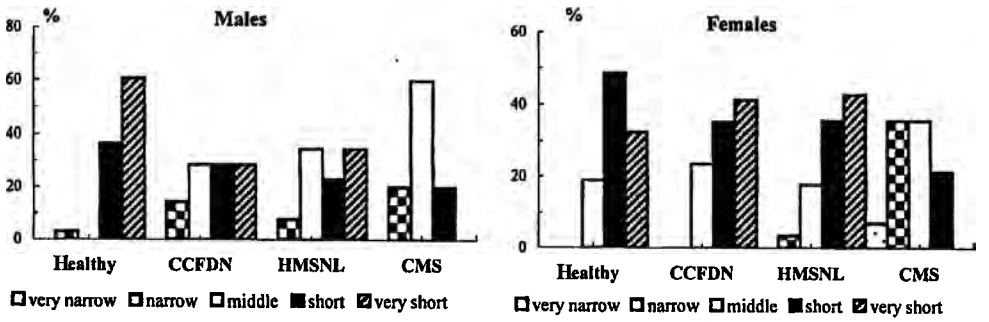

Fig. 5. Distribution of investigated patients and healthy persons by jugomandibular index categories

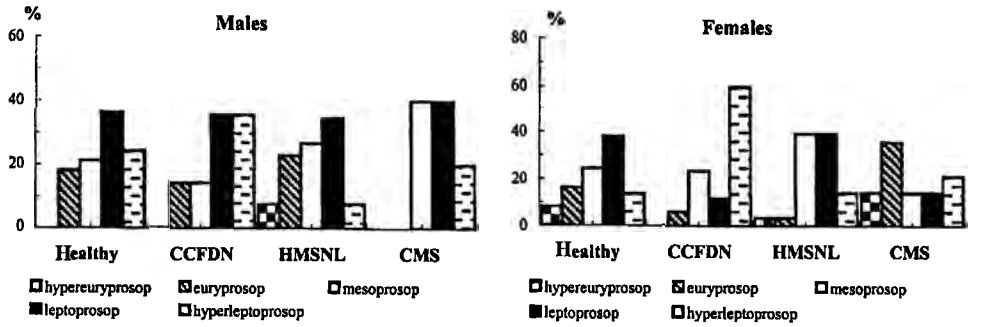

Fig. 6. Distribution of investigated patients and healthy persons by morphological face index categories

considerably higher frequency of middle and narrow forms. The HMSNL and CCFDN females have a higher frequency of very short forms. For the patients from both sexes, a tendency toward longer faces as a whole, and separately for the upper face part is established. According to morphological face index data, the patients more frequently are mesoprosopes, leptoprosopes and hyperleptoprosopes, and less frequently euryprosopes and hypereuryprosopes (Fig. 6).

Conclusions

A common tendency towards less head and face measurements in the patients from both sexes compared to the healthy persons is available. This tendency is strongly expressed in the CCFDN patients and slightly — in the HMSNL ones. In males reliable differences are established only between the HNSNL and CCFDN patients, as well as between the HMSNL and CSM type Ia patients. For females reliable differences are established between all subgroups of patients.

Compared to the healthy individuals, the patients from both sexes have longer face, relatively less forehead width, but larger head length than bizygomatical diameter. The male patients have relatively wider head breadth, while the female patients have relatively bigger head length.

References

1. Martin, R., K. Saller. Lehrbuch der Anthropologie in sistematischer Darstellung. T. I. Stuttgart, Gustav Fischer Verlag, 1961, 322-324.
2. Tournev, I. et al. Congenital cataracts facial dysmorphism neuropathy syndrome, a novel complex genetic disease in Balkan Gypsies: clinical and electophysiological observations. — Annals of Neurology., 45, 1999, 742-750.
3. Търнев, И. Клинико-генетично и епидемиологично проучване на шест новооткрити наследствени невро-мускулни заболявания сред ромите в България. Дисерт. труд. С., Медиц. академия, 2000.

Institute of Experimental Morphology and Anthropology

Acta morphologica et anthropologica, 10
Sofia•2005

Phenotypic and Genetic Frequency of the Erythrocyte Enzyme Systems ADA and AK in Bulgarians Living in the South Central Region of Bulgaria

S. Baltova

Department of Human Anatomy and Physiology, Faculty of Biology, University of Plovdiv, Plovdiv

For the study of ADA and AK we made parallel investigations. We took blood samples from 2368 individuals with Bulgarian origin, males and females, at the age from 18 to 45, clinically healthy and without family relationships among them. The phenotypes of ADA and AK were determined through horizontal electrophoresis of haemolysates on starch gel, according to the method of Radam and Strauch [1968]. The most frequently phenotypes are ADA 1-1 — 85.35% and AK 1-1 — 93.54% followed by the heterozygous. The genetic frequencies of the alleles from ADA and AK are as follows: ADA^1 =0.9240, ADA^2 =0.0760; AK^1 =0.9675, AK^2 = 0.0325.

Key words: polymorphism, ADA, AK, phenotype, gene frequency.

Introduction

We still do not have sufficient information for the expression of the genetically determined polymorphism of the enzymes of the Bulgarian population.

There are population and genetic studies of the erythrocyte enzyme systems adenosine-desaminase (ADA) and adenylat-kynase (AK) for certain cities — Sofia and Plovdiv but there is missing data about other regions in Bulgaria. [1, 7, 8].

The aim of the present study is to determine the phenotypic distribution and the genetic frequency of ADA and AK for the clarification of the genetic status of the Bulgarian population in the South central region of Bulgaria and to make a comparison with other populations.

Material and Methods

For the study of ADA and AK we made parallel investigations. We took blood samples from 2368 individuals with Bulgarian origin, living in the South Central region of Bulgaria, males and females, at the age from 18 to 45, clinically healthy and without family relationships among them. The distribution of the investigated indi-

viduals in sub-populations is as follows: the region of Plovdiv — 1508 individuals, the region of Stara Zagora — 450 and the region of Haskovo — 410.

The phenotypes of ADA and AK were determined through horizontal electrophoresis of haemolysates on starch gel, according to the method of Radam G., Strauch [5, 6].

Results and Discussion

In all the investigations we found out only the classic types of ADA and AK (Table 1). The phenotype 1-1 of ADA and AK has the greatest distribution in the studied quota — 2368 individuals. It is found respectively in 2021 individuals (85.35%) for ADA and in 2215 individuals (93.54%) for AK. The phenotypic distribution in the different sub-populations shows that phenotype 1-1 for both enzymes decrease its frequency in direction — regions of Plovdiv, Stara Zagora and Haskovo.

In Table 2 we represent the genetic frequencies of the enzymes ADA and AK. The genes from locus ADA and AK that determine homozygous phenotypes 1-1 and 2-2 are characterized from alleles with frequency for the population of the whole studied region respectively: $ADA^1 = 0.9240$, $ADA^2 = 0.0760$ and $AK^1 = 0.9675$, $AK^2 = 0.0325$. For the different sub-populations we observe increase of the genetic frequency of the allele ADA^1 and AK^1 in direction - regions of Plovdiv, Stara Zagora and Haskovo.

Table 1. The observed and expected phenotype frequencies in ADA and AK enzyme system in the samples studied

Region	Parameters	ADA			AK		
		phenotype 1-1	phenotype 2-1	phenotype 2-2	phenotype 1-1	phenotype 2-1	phenotype 2-2
Plovdiv	Observ.	1306	196	6	1419	88	1
	%	86.60	13.00	0.40	94.10	5.84	0.06
	Expect.	1307.08	193.74	7.18	1419.46	87.20	1.34
Stara Zagora	Observ.	376	70	4	419	31	0
	%	83.55	15.56	0.89	93.11	6.89	—
	Expect.	375.36	71.26	3.38	419.57	29.89	0.54
Haskovo	Observ.	339	68	3	377	33	0
	%	82.68	16.59	0.73	91.95	8.05	—
	Expect	339.37	67.29	3.34	377.70	31.64	0.66
Total region	Observ.	2021	334	13	2215	152	1
	%	85.35	14.10	0.55	93.54	6.42	0.04
	Expect.	2021.74	332.58	13.68	2216.58	148.92	2.50

Table 2. The gene frequencies in ADA and AK enzyme systems in samples studied

Alleles	Plovdiv $n = 1508$	Stara Zagora $n = 450$	Haskovo $n = 410$	Total region $n = 2368$
ADA^1	0.9310	0.9133	0.9098	0.9240
ADA^2	0.0690	0.0867	0.0902	0.0760
$\chi 2$	0.0264	0.0223	0.0075	0.0061
	$0.05<P<0.20$	$0.5<P<0.80$	$0.99<P<0$	$0.05<P<0.20$
AK^1	0.9702	0.9656	0.9598	0.9675
AK^2	0.0298	0.0344	0.0402	0.0325
$\chi 2$	0.0073	0.0412	0.5400	0.5820
	$0.05<P<0.20$	$0.05<P<0.20$	$0.20<P<0.50$	$0.01<P<0.05$

Table 3. Distribution of gene frequencies of ADA and AK by others populations

Population	Locus ADA			Locus AK			Authors
	No	ADA^1	ADA^2	No	AK^1	AK^2	
Sofia	138	0.8623	0.13760,	138	0.9637	0.03620,	Ananthakrishnan, et al. (1972)
	402	0.9440	0560	310	0.9710	0390	Попвасилев, И. (1980)
	2694	0.9311	0.0689	—	—	—	Ненков, Н. (1981)
Plovdiv	1508	0.9310	0.0690	1508	0.9702	0.0298	Ours studies
	116	0.9138	0.0862	—	—	—	Ненков, Н. (1981)
St. Zagora	450	0.9133	0.0867	450	0.9656	0.0344	Ours studies
Haskovo	410	0.9098	0.0902	410	0.9598	0.0402	Ours studies
Kyustendil	100	0.9500	0.0500	—	—	—	Ненков, Н. (1981)
Gipsy	171	0.8655	0.1345	—	—	—	Ненков, Н. (1981)
Germany	2925	0.9460	0.0540	1067	0.9610	0.0390	Schel, H-G. (2001)
Hungary	654	0.9450	0.0550	654	0.9680	0.0320	Pap, M. (2000)
Europe	—	0.9400	0.0600	—	0.9500	0.0500	Lewontin, R.C. (1974)
Africa	—	0.9700	0.0300	—	1.0000	0.0000	Lewontin, R.C. (1974)
India,Pakistan	—	0.8600	0.1400	—	0.8700	0.1300	Lewontin, R.C. (1974)
Andi-redskin	—	1.0000	0.0000	—	1.0000	0.0000	Lewontin, R.C. (1974)

We used the criterion of Pierson and we compared the distribution among the observed and the expected values and we found out that the difference is not significant — $P>0.05$, $\chi^2=0.402$ for ADA and $\chi^2=0.9648$ for AK. The correlation between the observed and the expected values is good and according to the law of Hardy-Weinberg shows that the studied population is in genetic balance concerning the enzymes ADA and AK.

We compared the results of the present study with these of other populations made by different authors according to literary data (Table 3).

The values of the frequency of the allele ADA^2 is zero in Negroes, South-American Indians and from 0.11-0.16 for South Asia. For Europe the ADA^2 frequency in the different populations vary in narrow borders (0.05-0.09) and it has certain tendency to increase from North to South [3, 6, 8].

In Europe we have predominantly the gene AK^1. The frequency of the alleles AK^1 and AK^2 in the European populations has certain stability — AK^1 - 95-97% and AK^2 — 2.9-4.5%. In the Negroid and Mongoloid populations the frequency of the allele AK^2 is considerably lower than in the Europoid populations.

Conclusions

1. The most frequently phenotypes are ADA 1-1 — 85.35% and AK 1-1 — 93.54% followed by the heterozygous. The genetic frequencies of the alleles from ADA and AK are as follows: $ADA^1=0.9240$, $ADA^2=0.0760$; $AK^1=0.9675$, $AK^2=0.0325$.

2. The frequency of the iso-enzyme variations in the studied Bulgarian population does not differ substantially from the European populations. We observe a tendency of west-east and north-south geographic distribution.

References

1. Ananthakrishnan, R., H. Walter, L. Tsacheva. Red Cell Enzyme Polymorphisms in Bulgaria. — Humangenetik, **15**, 1972, 186-190.
2. Lewontin, R. C. The genetic Basis of Evolutionary Change. — Columbia University Press., 1974, 381-398.
3. Pap, M. Population genetic research in Hungary. — Acta Biologica Szegediensis, **44**, 2000, No 1-4, 129-133.
4. Radam, G., H. Strauch. Populationsgenetik der Adenylatkinase (EC 2.7.4.3). — Humangenetik, **6**, 1968, 90.
5. Radam, G., H. Strauch. Beitrag zur Populationsgenetik der Adenosindesaminase. — Humangenetik, **12**, 1971, 173.
6. Scheil, H.-G., W. Huckenbeek. Hämogenetische Studienim im Regierungsbezirk Köln (Nordrhein-Westfalen, Deutschland). — Anthrop. Anz., **58**, 2000, 155-169.
7. Попвасилев, И., Хр. Близнаков. Кръвногрупови системи у човека. С., Медицина и физкултура, 1980, 186—195.
8. Ненков, Н. Популационно-генетични и съдебно-медицински аспекти по полиморфната система аденозиндезаминаза. Дисерт. труд. С., 1981, 28.

Institute of Experimental Morphology and Anthropology

Acta morphologica et anthropologica, 10
Sofia • 2005

Correlation of Some Palm Papillary Patterns with the Phenotypes of ABO Blood Group Systems

S. Baltova

Department of Human Anatomy and Physiology, Faculty of Biology, University of Plovdiv, Plovdiv

For the study we took blood samples from 626 individuals of Bulgarian origin, at the age from 18 to 60, clinically healthy, without family relationships among them.The determination of the blood groups was made using the classical method. We took palm-prints from both hands of the same individuals using the typographic method. The representations of the palms were deciphered using the methodology of Cummins and Midlo. The correlative relations vary from moderate to significant between the phenotypes of the system ABO and the papillary palm representations.We did not find out significantly expressed bilateral and intersexual relationships.

Key words: blood-group systems ABO, palm papillary patterns.

Introduction

The problem of the correlation between the dermatoglyphic indices and the phenotypes of the blood-group systems is not sufficiently studied and the different authors have controversial opinions. [3, 6, 7].

Most publications concern the papillary representations of the fingers.

The aim of the present study is to investigate the correlative relations between the blood-group system ABO and the papillary representations of the palm in Bulgarians.

Material and Methods

For the study we took blood samples from 626 individuals of Bulgarian origin, living in South Central and South-East region of Bulgaria, males 330 and females — 296, at the age from 18 to 60, clinically healthy, without family relationships among them.

The determination of the blood groups was made using the classical method. We took palm-prints from both hands of the same individuals using the typographic method. The representations of the palms were deciphered using the methodology of Cummins, Midlo [1]. The data were processed according to the methods of the variation and correlation analysis.

Results and Discussion

Among the studied 626 individuals we found out 6 phenotype combinations of the blood groups ABO with frequency as follows: A_1 (41.85%); A_2 (5.75%); B (18.21%); A_1B (5.43%); A_2B (0.31%) and O (28.43%). The genetic frequencies that we found are for p_1 =0.2873; p_2=0.0514; q =0.1497, and r =0.5332. We used the criterion of Pierson and we compared the distribution among the observed and the expected values and we found out that the difference is not significant (p>0.05).

The analysis of the frequency of the representations of the Thenar (Th) shows slight bilateral differences in lines III and IV (in males) IA and slight differences between sexes only in Th/I IA.

The per cent distribution of the palm representations in the studied individuals is similar to those compared with literary data from other authors [2, 4, 5, 8].

The data of the correlation analysis is presented in Table 1.

We determined strong correlative relations between phenotypes A_2, A_1B and B and palm representations — open arc (O), loops (Ld) on Th in I,II,III and IV IA with great extent of reliability (p>0.95 and p>0.99).

We found out significant correlative relation between phenotypes A_2 A_1B and B. In phenotype A_2 there is relation with O on Th /II for males and on Th/I for females on the left hand as well as with Ld on Th/IV for left hand in males and Th/III for right hand in females.

In phenotype A_1B we found relation with Ld on Th/III on the right hand in both sexes and in phenotype B — only in males with O on Th/II for both hands.

Moderate correlative relation is found in phenotypes A_2, A_1B and the palm representations in both sexes and phenotype B in males.

We determine this relation in phenotype A_2 with O on Th/III on left hand in males, with O on Th/I on right hand, O on Th/I on both hands and with Ld on Th/I on both hands in females. In phenotype A_1B there is relation also with O on Th/I on right hand in males and both hands in females, as well as O on Th/III on left hand in females. In males with phenotype B we found moderate correlation with O on Th/II on right hand and with Ld on Th/IV on left hand.

There is slight correlative relation in phenotype A_1B with O on Th/III on right and Th/I on left hand in males. We observe tendency of increasing of r for individuals

Table 1. Per cent frequencies of palmar patterns in males and females

Th	Pat-tern	Males (n = 330)						Females (n = 296)					
		right			left			right			left		
		n	%	Sp	n	%	Sp	n	%	Sp	n	%	Sp
Th/I	Au	2	0.61	0.43	6	1.82	0.74	2	0.68	0.48	2	0.68	0.48
	Ar	52	15.76	2.01	56	16.97	2.07	26	8.78	1.64	32	10.81	1.80
	Lu	—	—	—	2	0.61	0.43	—	—	—	—	—	—
	Lr	6	1.82	0.74	10	3.03	0.94	10	3.38	1.05	14	4.73	1.23
	Lc	6	1.82	0.74	8	2.42	0.85	6	2.03	0.82	4	1.35	0.67
	W	4	1.21	0.60	2	0.61	0.43	4	1.35	0.67	4	1.35	0.67
	Ws	—	—	—	16	4.85	1.18	16	5.41	1.31	22	7.43	1.52
	V	164	49.70	2.75	148	44.85	2.74	82	27.70	2.60	84	28.38	2.62
	O	96	29.09	2.50	82	24.85	2.38	150	50.68	2.91	134	45.27	2.89
Th/II	Ld	18	5.45	1.25	14	4.24	1.11	26	8.78	1.64	10	3.38	1.05
	V	16	4.85	1.18	2	0.61	0.43	14	4.73	1.23	2	0.68	0.48
	O	296	89.70	1.67	314	95.15	1.18	256	86.49	1.99	284	95.95	1.15
Th/III	Ld	222	67.27	2.58	108	32.73	2.58	156	52.70	2.90	98	33.11	2.74
	V	14	4.24	1.11	48	14.55	1.94	10	3.38	1.05	36	12.16	1.90

Table 2. Correlation between phenotypes of ABO blood groups and some palmar patterns

Th	Pattern	Side	MALES (n = 330)									
			A_1		A_2		B		A_1B		O	
			r	χ^2	r	χ^2	r	χ^2	r	χ^2	r	χ^2
I	V	R	–0,0973	0,67	–0,2109	0,45	–0,2549	1,82	–0,4363	1,52*	–0,1857	1,66
		L	–0,0851	0,35	–0,2701	0,73	–0,1355	0,51	–0,1812	0,26	–0,2056	2,03
	O	R	0,1139	0,92	–0,2909	0,85	–0,0416	0,05	–0,1812	0,26	–0,0007	0,00
		L	0,1891	2,54	–0,1462	0,21	–0,1054	0,31	–0,2870	0,66**	0,0580	0,16
II	Ld	R	0,3871	10,6	–	–	0,1320	0,49	–	–	0,1806	1,57
		L	0,3178	10,6	–	–	0,0951	0,25	–	–	0,2459	2,90
	V	R	0,3511	8,75	–0,0376	0,01	0,1320	0,49	–	–	0,2459	2,90
		L	0,4168	12,3	–		–	–	–	–	–	–
	O	R	–0,4318	13,6	–0,0289	–	–0,5839	9,55**	0,0357	0,01	0,4841	11,3
		L	–0,4913	17,1	–0,6727	4,53*	–0,5839	9,55**	0,0357	0,01	–0,5661	15,4
III	Ld	R	–0,2125	3,21	–0,4312	1,86**	–0,3645	3,72	–0,5026	2,02*	–0,3925	7,40
		L	0,0737	0,39	–0,1257	0,16	0,0416	0,05	–0,1812	0,26	–0,0948	0,43
	V	R	0,3871	10,6	–0,0864	0,08	0,0599	0,10	–	–	–	–
		L	0,2659	5,02	–0,0864	0,08	0,0951	0,25	–0,1812	0,26	0,1188	0,68
	O	R	0,1267	1,14	–0,2102	0,44	–0,2162	1,31	–0,2856	0,65**	0,0381	0,07
		L	–0,0445	0,14	–0,4993	2,49*	–0,4469	5,59	–0,3725	1,11**	–0,1325	0,83
	W	R	–	–	–	–	–	–	–	–	–	–
		L	0,4168	12,3	–	–	–	–	–	–	–	–
IV	Ld	R	0,0860	0,53	–0,4304	1,85**	–0,1049	0,09	–0,2851	2,28	0,0981	0,46
		L	–0,0860	0,03	–0,5653	3,20**	–0,3388	0,92**	–0,4618	5,97	–0,1325	0,83
	V	R	0,3547	8,93	–	–	0,0599	0,03	0,0734	0,15	0,2036	1,99
		L	0,2396	4,08	–	–	–0,0083	0,00	–0,1771	0,88	0,1188	0,68
	O	R	–0,1487	1,57	–0,2701	0,73	–0,3636	1,06**	–0,4363	5,33	–0,3873	7,20
		L	0,0867	0,53	–0,2125	0,45	–0,0734	0,04	0,0734	0,15	–0,0952	0,44
	W	R	–	–	–	–	–	–	–	–	–	–
		L	0,4027	11,5	–	–	–	–	–	–	–	–
			FEMALES (n = 296)									
I	V	R	–	–	–	–	–	–	–	–	–	–
		L	–	–	–	–	–	–	–	–	–	–
	O	R	–0,0395	0,99	–0,4471	1,60*	–0,3511	3,58	–0,4700	1,19*	–0,1652	1,12
		L	0,0344	0,07	–0,5347	2,29*	–0,3019	2,64	–0,3198	0,92**	–0,1652	1,12
II	Ld	R	0,2628	4,14	–0,1712	0,24	0,1578	0,72	–0,1456	0,19	–	–
		L	0,3504	7,37	–0,0660	0,04	0,1578	0,72	–	–	–	–
	V	R	0,3850	8,27	–	–	0,1284	0,48	–0,0468	0,02	0,2002	1,64
		L	–	–	–	–	–	–	–	–	0,2499	2,56
	O	R	–0,4038	9,78	–0,5347	2,29*	–0,5595	9,08**	–0,4700	1,99*	–0,5410	12,0
		L	–0,4941	14,7	–0,6084	2,29*	–0,5986	10,4**	–0,6821	4,19**	–0,5806	13,8
III	Ld	R	–0,0931	0,52	–0,5347	2,29*	0,2753	2,20	–0,5423	2,65*	–0,1860	1,42
		L	0,2592	4,03	–0,3592	1,03**	–0,1335	0,52	–0,2336	0,49	–0,1001	0,41
	V	R	0,3640	7,95	–	–	0,1284	0,48	–	–	0,2499	2,56
		L	0,2766	4,59	–0,1712	0,24	0,0552	0,09	–0,0468	0,02	0,1737	1,24
	O	R	–0,0408	0,10	–0,1712	0,24	–0,1892	1,04	–0,1456	0,19	–0,1860	1,42
		L	–0,1751	1,84	–0,1712	0,24	–0,2753	2,20	–0,4011	1,45**	–0,2049	1,72
	W	R	0,3850	8,89	–	–	–	–	–	–	–	–
		L	0,3850	8,89	–	–	–	–	–	–	–	–
IV	Ld	R	0,1014	0,62	–0,2742	0,60**	–0,1892	1,04	–0,4011	1,45**	–0,1436	0,85
		L	–0,0854	0,44	–0,3892	1,21**	–0,2745	2,19	–0,4011	1,45**	–0,2879	3,4
	V	R	0,3298	6,53	–	–	0,0879	0,22	–	–	0,2002	1,64
		L	0,2766	4,59	–0,0660	0,04	0,0552	0,09	–0,0468	0,02	0,2224	2,03
	O	R	0,0202	0,03	–0,3892	1,21**	–0,2436	1,72	–0,3198	0,92**	–0,1860	1,42
		L	0,0509	0,16	–0,2742	0,60**	–0,1323	0,51	–0,2336	0,49	–0,0362	0,05
	W	R	0,3640	7,95	–0,0660	0,04	–	–	–	–	–	–
		L	0,3640	7,95	–	–	–	–	–	–	0,2499	2,56

** $P > 0.99$ * $P > 0.95$

with phenotype A_2B and A_1B with O on Th/II on left and right hand in females and with O on Th/Iv on right hand in both sexes ($p>0.99$).

We found out that in all phenotypes of the system ABO there are correlative relations and **r** varies from —0.7 to —0.2 but not all of them are reliable. There is considerable correlation but the extent of reliability is not so significant ($p>0.92$).

We suppose that the observed correlative relations are due to the presence of genetic relations among the individuals and perhaps there are general factors for their determination that vary independently one from the other.

Conclusions

1. The dermatoglyphic analysis of the palm representations shows presence of slight bilateral and intersexual differences.

2. The correlative relations vary from moderate to significant between the phenotypes of the system ABO and the papillary palm representations.

3. We did not find out significantly expressed bilateral and intersexual relationships.

References

1. Cummins, H., C. Midlo. Finger prints, palms and soles. An introduction to dermatoglyphics. — Philadelphia, Blakinstone. 1943 (Reprinted: New York, Dover, 1961, 319).
2. Otto, P. A., M.M. Bozoti. Digital dermatoglyphics and blood-groups. — Lancet, **11**, 1968.
3. Tornjova-Randelova, S., D. Paskova-Topalova. Some uncommon dermatoglyphic features in Bulgarians. — J. Anthropology, **3**, 2000, 177-190.
4. Tornjova-Randelova, S., D. Paskova-Topalova. Dermatoglyphic patterns and accessory triradii on the palmar interdigital areas in Bulgarians. — J. Anthropol. **4**,2003, 86-95.
5. Гладкова, Т. Д., М. О. Битадзе. Заметки о связи некоторых признаков дерматоглифики с групами крови системы АВО. — Вопр. Антроп., **69**, 1982.
6. Колодченко, В. П. Взаимосвязы показателей конституции с групами крови системы АВО. Генетические маркеры в антропогенетике и медицине. Хмелницкий, 1988.

Institute of Experimental Morphology and Anthropology

Acta morphologica et anthropologica, 10
Sofia • 2005

Dermatoglyphics of Children with Family-Hereditary Deafness — Fluctuating Asymmetry

S. Tornjova-Randelova, D. Paskova-Topalova, P. Borissova

Institute of Experimental Morphology and Anthropology, Bulgarian Academy of Sciences, Sofia

The fluctuating asymmetry level of finger ridge count, palm ridge count, *atd* angle and finger patterns type on the homologous digits is studied in children with family-hereditary deafness. The investigation encloses 53 boys and girls with family-hereditary deafness, as well as a control group of 260 healthy boys and girls. The results show a trend to higher fluctuating asymmetry level of *palm ridge count, angle atd* and *finger patterns type* for the children with family-hereditary deafness compared to the healthy ones, while those of *finger ridge count* is lower. The diversions of fluctuating asymmetry level between deaf and healthy children, are not very high. This fact indirectly leads to the conclusion that the disturbances' degree of homeostasis development of the organism for the deaf children is not very appreciable, as well.

Key words: dermatoglyphic features, fluctuating asymmetry, children with family-hereditary deafness.

Introduction

The fluctuating asymmetry, random deviations from organism's bilateral symmetry, is accepted as one of the best indicators about developmental homeostasis. On the basis of this understanding is grounded the idea that the genetically factors, or the environmental factors leading to disturbances in the normal development of organism, exert a negative influence on the control when bilateral morphological structures are formed. So, the disturbances' degree of perfect body bilateral symmetry, assessed by the fluctuating asymmetry, gives possibilities of the mechanisms that control the homeostasis to be defined.

The aim of the present investigation is to be assessed the fluctuating asymmetry level of four dermatoglyphic features (finger ridge count, palm ridge count, *atd* angle and finger patterns type) in children with family-hereditary deafness.

Material and Methods

Object of the investigation are 53 children (30 boys and 23 girls) with family-hereditary deafness (FHD). The papillar patterns are read by the method of Cummins and Midlo [1] and the *atd* angle is evaluated by the criterion of Sharma [2].

The fluctuating asymmetry level of finger and palm ridge count and *atd* angle is determined by the *coefficient of indetermination (I-r²)*, and for the finger patterns — by the degree of finger patterns discordance on pair fingers [3].

The data about fluctuating asymmetry (FA) for the dermatoglyphic features of FHD children are compared with analogous data for healthy children (129 boys and 131 girls) [4].

Results and Discussion

The correlation coefficients between ridges count on homologous fingers; right and left "a-b", "b-c" and "c-d" palm ridge count and *atd* angle are determined in connection with the assessment of FA about the three quantitative dermatoglyphic features (Table 1). The comparative analysis of coefficient values shows presence of big correlation dependence between the bilateral indices of the three features, as for the healthy, so for the FHD children. Available is a common tendency to more high correlation degree about finger ridge count in the FHD children, and about palm ridge count and *atd* angle — in the healthy ones. Highest inter-group difference ($P<0.05$) for boys is established between the correlation coefficients about ridge counts on the V digit pairs and the total ridge count, as for the girls it is highest about "c-d" ridge count.

Opposite to the presented results about correlation analysis, a common tendency to lower fluctuating asymmetry level is available for finger ridge count in the FHD children, and for palm ridge count and *atd* angle — in the healthy ones (Table 2). The homologous fingers arrangement according to the fluctuating asymmetry level for the FHD children (♂ — II>I>III>IV>V; ♀ — II>IV>I>III>V) considerably differ from this for healthy ones (♂ — I>II≥ V >III>IV; ♀ — III>I>II>IV>V). For the FHD children from both sexes highest FA is established

Table 1. Correlation between finger ridge count, palm ridge count and atd angle of children with family-hereditary deafness and healthy children

Features	Correlations (r)							
	boys				girls			
	FHD	controls	t	*P*	FHD	controls	t	*P*
Finger ridge count								
I	0.7095	0.6715	0.3607	*P*>0.05	0.7726	0.6963	0.6223	*P*>0.05
II	0.6845	0.7108	0.2740	*P*>0.05	0.5537	0.7294	1.2621	*P*>0.05
III	0.8046	0.7275	0.8012	*P*>0.05	0.8125	0.6455	1.4305	*P*>0.05
IV	0.8541	0.7600	1.2260	*P*>0.05	0.7382	0.7651	0.2839	*P*>0.05
V	0.8814	0.7124	2.3040	***P*<0.05**	0.8505	0.7969	0.6410	*P*>0.05
I-V	0.9528	0.8657	2.3516	***P*<0.05**	0.9241	0.8968	0.4751	*P*>0.05
Palm ridge count								
a-b	0.8270	0.7027	1.4148	*P*>0.05	0.7032	0.5877	0.7885	*P*>0.05
b-c	0.6715	0.7561	0.8181	*P*>0.05	0.5550	0.6632	0.6654	*P*>0.05
c-d	0.6306	0.6923	0.4701	*P*>0.05	0.2718	0.6992	2.4792	***P*<0.05**
a-d	0.8410	0.8486	0.1544	*P*>0.05	0.6371	0.7405	0.7998	*P*>0.05
***atd* angle**	0.3523	0.6485	1.9499	*P*>0.05	0.5641	0.5650	0.0565	*P*>0.05

Table 2. Fluctuating asymmetry measure of finger ridge count, palm ridge count and atd angle of children with family-hereditary deafness and healthy children

Features	Coefficient of indetermination ($1-r^2$)					
	boys			girls		
	FHD	controls [C]	difference [FHD-C]	FHD	controls [C]	difference [FHD-C]
Finger ridge count						
I	0.4966	0.5491	-0.0525	0.4031	0.5152	0.1121
II	0.5315	0.4948	0.0367	0.6934	0.4680	0.2254
III	0.3526	0.4707	-0.1181	0.3398	0.5833	-0.2435
IV	0.2705	0.4224	-0.1519	0.4551	0.4146	0.0405
V	0.2230	0.4925	-0.2695	0.2766	0.3650	-0.0884
I-V	0.0921	0.2506	-0.1585	0.1461	0.1958	-0.0497
Palm ridge count						
a-b	0.3160	0.5062	-0.1902	0.5056	0.6546	-0.1490
b-c	0.5490	0.4283	0.1207	0.6919	0.5602	0.1317
c-d	0.6023	0.5207	0.0816	0.9261	0.5111	0.4150
a-d	0.2926	0.2799	0.0127	0.5942	0.4517	0.1425
***atd* angle**	0.8759	0.5794	0.2965	0.6818	0.6808	0.0010

about II digit pairs, and lowest — about V digit pairs. Diverse from the FHD children, in the healthy boys FA is highest for I digit pairs, and in healthy girls — for III ones. The lowest FA for IV digit pairs are found in the healthy boys and for the V digit pairs — in the healthy girls. The trend to which the fluctuating asymmetry levels of palm ridge count decreases for FHD and healthy children differ considerably, as well. For the FHD boys and girls the FA decreases in the same direction submitted in the descendent formula: "c-d" > "b-c" >"a-b". In contrast to the FHD children, for healthy boys the FA decreases in the direction "c-d" >"a-b" >"b-c", and for healthy girls it is "a-b" >"b-c" >"c-d".

The data analysis of the investigation shows a trend toward lower coincidence degree of the papillary patterns' type on the homologous fingers in the FHD children compared to the healthy ones (Table 3). The FA calculated by the discordance level of papillary patterns' type on homologous fingers is higher in the FHD children than in the healthy ones (Table 4). The consecutiveness of homologous fingers for the FHD and the healthy boys and girls according to the FA differs insignificantly. For the FHD boys it decreases in the direction II>I=III>IV>V homologous digits, as for the FHD girls it is II>III>I=IV>V. For the healthy boys the FA decreases in the direction II>I>III=IV>V homologous digits, as for the healthy girls it is II>III>IV>I>V.

Conclusions

The results from the elaborated by us dermatoglyphic investigation show a trend to higher fluctuating asymmetry level of *palm ridge count, angle atd* and *finger patterns type* for the children with family-hereditary deafness compared to the healthy children. The fluctuating asymmetry level of *finger ridge count* for the children with family-hereditary deafness is predominantly lower than for the healthy ones. The variations of dermatoglyphic fluctuating asymmetry follow the same direction for both sexes of the studied FHD and healthy children. As is well known, the fluctuating asymmetry level is assumed as an indicator of different unfavorable (endogenous and/or exogenous) factors for the developmental homeostasis, as well as for its ability to overcome the influence of such factors. Along these lines the higher values

Table 3. Coincidence of finger patterns for homologous fingers of children with family-hereditary deafness and healthy children

Homologous fingers	Boys						Girls					
	FHD		controls		t	*P*	FHD		controls		t	*P*
	X	SD	X	SD			X	SD	X	SD		
I	0.6562	0.4826	0.7132	0.4540	0.5891	*P*>0.05	0.6800	0.4761	0.7752	0.4191	0.8997	*P*>0.05
II	0.6250	0.4919	0.5581	0.4985	0.6693	*P*>0.05	0.5600	0.5066	0.4961	0.5019	0.5587	*P*>0.05
III	0.6562	0.4826	0.7519	0.4336	0.9966	*P*>0.05	0.6000	0.5000	0.7209	0.4503	1.0850	*P*>0.05
IV	0.6875	0.4709	0.7519	0.4336	0.6846	*P*>0.05	0.6800	0.4761	0.7519	0.4336	0.6767	*P*>0.05
V	0.7812	0.4200	0.8295	0.3776	0.5779	*P*>0.05	0.9200	0.2769	0.8605	0.3478	0.9194	*P*>0.05

Table 4. Discordance of finger patterns for homologous fingers of children with family-hereditary deafness and healthy children

Homologous fingers	Boys			Girls		
	FHD	controls [C]	Difference [FHD-C]	FHD	controls [C]	Difference [FHD-C]
I	0.3438	0.2868	0.0570	0.3200	0.2248	0.0952
II	0.3750	0.4419	—0.0669	0.4400	0.5039	—0.0639
III	0.3438	0.2481	0.0957	0.4000	0.2791	0.1209
IV	0.3125	0.2481	0.0644	0.3200	0.2481	0.0719
V	0.2188	0.1705	0.0483	0.0800	0.1395	—0.0595

of the fluctuating asymmetry about more features in the children with family-hereditary deafness could be accepted as an indicator about genetic control disturbances along the formation of their dermatoglyphic features, i.e. as an indicator for developmental homeostasis. The diversions of fluctuating asymmetry level for the deaf children towards this for the healthy ones, are not very high. This fact indirectly leads to the conclusion that the degree of disturbances in the developmental homeostasis of the organism for the children with family-hereditary deafness is not very appreciable, as well.

References

1. Cummins, H., C. Midlo. Finger prints, palms and soles. Ann. Introduction to Dermatoglyphics. Philadelphia, Blakinstone, 1943 (Reprinted: New York, Dover, 1961).
2. Sharma, A. Comparative methodology in dermatoglyphics. Delhi, 1964.
3. Mellor, C., S. Dermatoglyphic evidence of fluctuating asymmetry in schizophrenia. — British Journal of Psychiatry, **160**, 1992, 467-472.
4. Торньова-Ранделова, С. Дерматоглифика при здрави деца и деца със зрителна, слухова и интелектуална недостатъчност. Дисерт. труд. С., 1986, 214 с.

Institute of Experimental Morphology and Anthropology

Acta morphologica et anthropologica, 10
Sofia • 2005

Quantitative Dermatoglyphic Indexes in Monozygotic and Dizygotic Twins

V. Angelova, M. Pirinska-Apostolu

Department of Zoology and Anthropology, Faculty of Biology,
Sofia University "St. Kliment Ohridski"

For the aims present research there have been tested 140 twin pairs (56 pairs monozygotic and 84 pairs dizygotic). The zygotic status was determined by a complex of somatic features as well as blood group indexes of the ABO system and Rh factor. Dermatoglyphic material was processed according to Cummins and Midlo's method [1].
There have not been observed considerable differences in quantitative indexes between the two examined groups.

Key words: ridge number, thenar corners, monozygotic and dizygotic twins.

Introduction

Researching of twins always interested scientists of different areas of science.

The method of twins allows to be analyzed the degree of influence of the hereditary factors as well as the environmental ones and their connection with different features of the organism [3]. Dermathoglyphic analysis is included as a part of the twin's method. Pappilar features are referred as multilocus hereditary features.

Quantitative dermatoglyphic indexes give the opportunity to use them when a need to settle the degree of similarity occurs [2, 4, 5]. The aim of the present research is to settle down variations of the examined indexes taken down from monozygotic and dizygotic twins, and to calculate intragroup correlation between twin pairs by the researched features.

Material and Methods

There have been investigated 140 twin pairs (56 pairs monozygotic and 84 pairs dizygotic). The zygotic status was determined by a complex of somatic features and blood group indexes of the ABO system and Rh factor. Prints from the volar surface were obtained by topographic ink.

From the present research there have been used the following quantitative features:

I. Digital features:

— ridge number of I to V finger; sum of ridge number; total ridge number

II. palmar features:

— ridge number to interdigital triradius; sum of ridge number; total ridge number; size of the corners atd; ctd; bad; adt; atb; bac

Dermathoglyphic material was treated by the means of Cummins and Midlo's method [1].

Results and Discussion

There have not been observed considerable differences in monozygotic and dizygotic groups according to the finger ridge number. The higher mean values of this feature are observed about DT of the I finger of the right hand (21.9) and the lower ones about MT of the V finger of the same hand (12.4). Slightly higher mean values according to the total and sum ridge number of the MT in addition with the DT group have been estimated (Fig. 1). The differences in palm ridge number of the two exam-

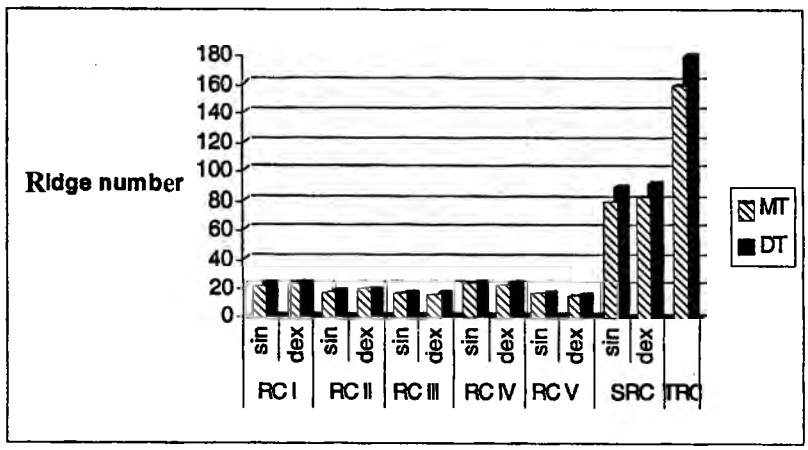

Fig. 1. Mean values of the digital ridge number

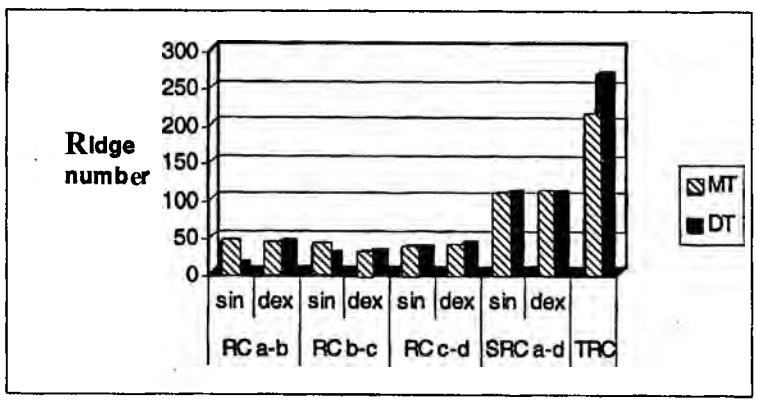

Fig. 2. Mean values of the palmar ridge number

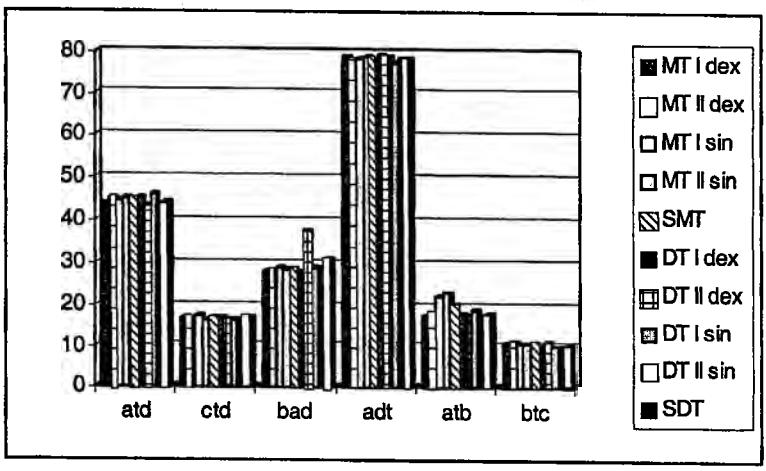

Fig. 3. Mean values of the palmar corners

ined groups are statistically insignificant. The only exception is observed about the ridge number of the interdigital triradius a-b and b-c of the left hand, where higher levels of significance are given in MT group (a-b — 40.8; b-c — 36,1) in comparison with DT group (a-b — 12.8; b-c — 26,8) (Fig. 2). After comparing the feature si of thenar corners, the two basic researched groups were divided into two basic subgroups in order of birth time. The mean values of the size of thenar corners between the compared two groups are almost the same. Differences were observed in the size

T a b l e 1. Correlation coefficient between the ridge number of the homologic fingers in MT and DT

Features	Monozygotic twins		Dizygotic twins	
	dex	sin	dex	sin
I	0.77	0.75	0.34	0.66
II	0.84	0.74	0.21	0.17
III	0.71	0.88	0.23	0.19
IV	0.76	0.74	0.42	0.13
V	0.91	0.92	0.22	0.31

T a b l e 2. Intergroup corcllation coefficent according to the size of the palmar corner

Indexes	Order of birth time	Monozygotic twins		Dizygotic twins	
		I	II	I	II
atd	dex	0.83	0.62	0.50	0.47
	sin	0.68	0.68	0.55	0.53
ctd	dex	0.61	0.56	0.35	0.49
	sin	0.61	0.55	0.08	0.43
bad	dex	0.78	0.83	0.50	0.47
	sin	0.57	0.55	0.34	0.51
adt	dex	0.55	0.52	0.38	0.42
	sin	0.56	0.53	0.19	0.51
atb	dex	0.58	0.50	0.49	0.21
	sin	0.50	0.50	0.20	0.54
btc	dex	0.74	0.74	0.54	0.16
	sin	0.59	0.73	0.34	0.46

of the corner bad in II twin (corner bad 37.62) from DT groups (Fig. 3). The calculation of intragroup correlation between homological fingers from both hands gave the following results: in the group of monozygotic twins the estimated correlation is very high, as well as significance ($p<0.05$). In dizygotic twins it was observed lack of correlation within the group and low correlation for I finger of the left hand (Tabl. 1).

The received data from the intragroup correlation by the size of thenar corners confirm high levels of correlation in MT, in comparison with DT.

The highest correlation values observed are about the me, atd and bad for the right hand in the group of MT (Tabl. 2).

Conclusions

Considerable differences in the values of the quantitative dermatoglyphic indexes in MT and Dt are not observed.

There have been calculated high levels of correlation between the examined features in the group of MT and low correlation rates in the group of DT.

References

1. Cummins, H., C. Midlo. Finger Prints, Palms and Soles. New York, Dover, 1961.
2. Cantor, R. M. et al. Analysis of the covariance structure of digital ridge counts in the offspring of monozygotic twins. Genetics Society of America, 1983, 495-509.
3. Vagel, J., A. G. Motulsky. Human genetics. Москва, Мир, 1989, 275—300.
4. Дэрфлио, Р. У., Л. И. Тегако. Пальцевой гребневой счет у монозиготных и дизиготных близнецов. — Вопросы антропологии. Вып. **54**, 1976, 131—140.
5. Никитюк, Б. А. Количественные показатели дерматоглифики близнецов. — Вопросы антропологии. Вып. **50**, 1975, 68—83.

Institute of Experimental Morphology and Anthropology

Acta morphologica et anthropologica, 10
Sofia•2005

Evolution of the Distal Humerus and Elbow Joint

A. Katsarov, Y. Yordanov

Institute of Experimental Morphology and Anthropology, Bulgarian Academy of Sciences, Sofia

Hominid evolution started about 23 million years ago in the early Miocene. The elbow joint structure underwent many changes for that period of time but from 2,5 million years rests unchanged.

In our study we reveal the evolutionary stages of distal humerus supported by analysis of well-known fossil evidences.

Key words: humerus, elbow, human, distal humerus, evolution, joint.

Introduction

Humerus is the bone of the arm. It is divided into three parts [3, 4]. Central part is known as humeral body. Others are proximal and distal ends. It brings its origin from mesenchyme 4 to 6 week of the prenatal development [2].

Distal end of the humerus is a part of the elbow joint, which is the connection between the shoulder and hand, makes possible the mobility and transfers generated forces in both directons — proximal and distal.

Anatomy of the distal humerus responds to this dual function — rounded head of radius and spheric capitellum take part in wide range of the rotational movements — pronation and supination, while the specific configuration of the humeroulnar joint and the collateral ligaments form stability of the elbow joint [5].

A great part of the characteristics of human elbow' structure are known far before the appearance of Homo sapiens. Recent anthropologic evidences give us the possibility to trace the morphology of the distal humerus back in time, to the common ancestor of humans and apes — at about 15-20 mln years ago.

Material and Methods

Distal humerus of pelycosaurus was with bulb like capitellum stretched medially and laterally (late Paleozoic period — 255 — 235 mya). Articulation with ulna was accomplished by two separate surfaces — slightly concave ventral and a flat dorsal. Its proximal articular surface is separated in the same way at two surfaces crossed by low ridge [1].

The humerus was held more or less horizontal and the elbow was flexed, so they walked with limbs spread outside of the body. The locomotion was possible because of the rotation of the humerus around its axis and at the same time by straightening of the forearm in vertical direction. Having in mind that, we could say that flexion and extension in the elbow were necessary only in side-to-side motion. This shows that the stability was more imortant than the mobility [7].

A closer group of mammal ancestors, cynodonts, started to move with limbs underneath their bodies (235—160 mya). The distal articular surface was formed by lateral and medial epicondyles separated by a shallow groove. The proximal surface of the ulna for articulation had an elongate spoon shape. The lateral edge of the ulna for articulation with radius was separated from this surface by a low ridge. The ridge articulated with the groove between radial and ulnar condyles and represents the earliest evolutionary stage in the development of the recent humeroulnar articulation in mammals.

Early mammals from Triassic (210—160 mya) and Jurassic (160—130 mya) periods have still not well-developed radial and ulnar epicondyles, although the radial is more protuberant than the ulnar and the ulnar was more linear and obliquely oriented. The two condyles were separated by an intercondylar groove. Oblique orientation of humeroulnar joint helped to keep the forearm in sagittal plane, while the humerus acts in adduction, elevation and rotation during locomotion.

Widening of the intercondylar groove and the development of a ridge within it determine the development of pulley — like distal humeral articular surface. The articular surface of proximal ulna is also oblique in orientation.

Most small noncursorial mammals retained the spiral shape of the trochlear articular surface as in early mammals. In larger and more cursorial mammals, the trochlea could be with various ridges and grooves. It is very narrow to provide stability but sustain the join mobility.

Only in hominoid primates (chimpanzee, gorilla, orangutans, gibbons and humans) the trochlea is really trochleariform. Other monkeys could have cylindrical, conic or pulley-like trochlea. In most species the articular surface of trochlea spreads posteriorly to olecranon fossa. In larger monkeys the lateral edge of the posterior trochlear surface forms a ridge that extends proximally forming the lateral wall of the olecranon fossa. The articular surface of the capitellum spreads further onto the posterior surface of the distal humerus in human and chimpanzee, which results in larger range of extension in elbow joint, in contrast to baboon [1, 7].

In apes, so formed lateral ridge is a continuation of the lateral trochlear ridge and helps for shaping of more vertical lateral wall of the olecranon fossa. The distal articular surface is deeper with well-expressed medial and lateral edges. The ideal articular configuration for load bearing includes proximal orientation of the trochlear ridge nevertheless it restricts the elbow flexion. The differencies in humeroulnar joint in primates are determined most of all by the different kind of movements in which the upper extremity takes part.

It is not surprising that the most stable position of humeroulnar joint in most monkeys is in partial flexion, due to the development of the medial trochlear ridge anteriorly and distaly, and lateral ridge — posteriorly.

Anterior orientation of the trochlea is a direct adaptation to weight bearing in partially flexed elbow, but such spacial situation of the trochlea restricts the elbow motion to some extent.

Big apes (chimpanzee, gorilla, orangutan) and the lesser ones (gibbon) move to some degree in manner that differs from the monkeys. To achieve these movements, the humeroulnar joint with it deeply socketed articular surface and well developed

medial and lateral ridges is constructed to sustain maximum stability during the whole range of motion.

The use of overhead suspensory postures in apes brought to evolutionary larger volume of extension in elbow joint, while the apes hold their elbow joints extended in their quadrupedal locomotion.

The ideal joint configuration for resistance to transarticular stress with fully extended elbow must be with trochlear notch directed proximally. In this position it serves as a cradle and supports the humerus during the act of locomotion. However, the proximal orientation of the trochlear notch restricts significantly the elbow flexion, because it is in contact with the distal articular surface. The anteroproximal orientation of the trochlear sulcus in monkeys is some kind of compromise in extension stability during motion, but without restricting the flexion range [8].

Elbow is a complex joint. As it is known, it is composed of 3 joints — humeroulnar, humeroradial and proximal radioulnar joint. All the movements are possible due to that structure — flexion, extension, pronation, and supination. In the apes, in contrast with monkeys, the capitellum spreads far more posterior, giving the radius possiblity for orientation along with the ulna in full extension.

The zone between capitellum and trochlea (zona conoidea) is relatively flat and ends distaly in most of the monkeys. Lateral lip of the radial head comes into maximum congruence with zona conoidea. It gives maximum stable joint configuration [8].

We could mention some additional features in elbow joint structure in common. In human and apes radial neck is relatively long. In apes it is connected with the demand of powerful elbow flexion to raise the center if mass of the body during climbing and suspensory postures in locomotion. Although the radial tuberosity is situated more or less anteriorly in most of the apes, in human is situated more medially. It increases the range of supination.

In apes and human the olecranon process is relatively short. This is determined by the need of fast extension during suspensory locomotion.

A significant biomechanical characteristic is the presence of so called "carrying angle". It is the acute angle formed by the long axis of the humerus as the long axis if the ulna projects on the plane containing the humerus- normally 10—20° in human. The presence of carrying angle is due to the need of moving the center of mass of the body under the sustaining arm in the locomotion. This resembles the valgus in human's knee, which moves the foot closer to the center of mass of the body during the single step in walkling.

Some differencies in elbow morphology between human and apes due to the elimination of the forearm from the locomotion [8].

In human, the lateral epycondyle is distally positioned and with not so expressed supracondylar ridge, in contrast with apes, because of the restricted volume of the extensory misculature of the hand and brachioradial muscle. The bending if ulna and radius is not so big in human, which is a result of the strenghtened lever action of pronator and supinator muscles of the forearm. And finaly the restircted size of trochlear ridges and oblique lateral ridge of the olecranon fossa in human are result of the total decrease of weight bearing in elbow and significantly greater need of elbow stability during all phases of motion.

Results

When exactly the elbow joint originate and how old is the structure of recent human elbow? To answer these questions we need to look at the various fossil evidences.

We could not say exactly, which of known Miocene (23—5 mya) species is the common ancestor of hominids. There are some unknowns concerning individual evolutionary histories of chimpanzee, gorilla, gibbon and human.

Dendropithecus macinnesi, Limnopithecus legetet and Proconsul heseloni (Africa) are among the hominoid species from early Miocene (23—16 mya). Distal humerus of the first two species resembles structure of the distal humerus in Cebus (capuchin monkeys). The trochlea is without prominent lateral ridge and the zone conoidea is relatively flat. The trochlear notch is situated anteriorly and the radial head is oval shaped and well-developed lateral ridge. It is considered that these characteristics are primitive for the rest of higher primates (monkeys, apes and humans).

Proconsul heseloni has some of the characteristics of later hominids. Its distal humerus has round capitellum, well-developed medial and lateral ridges and deep zone conoidea. This suggests significant stability of the joint in parallel to other mentioned two species. The limited and incomplete fossil material from the late Miocene (16—5 mya) suggests that many hominoid species; includings members of geners Dryopithecus (Europe), Sivapitehcus (Europe and Asia) and Oreopithecus (Europe) have the same characteristics in elbow morphology as modern human. Although it is possible that these features in structure to originate in different genera, the most probable explanation is that it is inherited from an early ancestor similar to Proconsul heseloni. Having in mind the listed characteristics and analysed fossil records we could affirm that the recent structure of the elbow joint originated 15 mya ago. The bigger part of paleoanthropologists agrees that the human is most closely related to the African apes (chimpanzee and gorilla) and these two lines are formed in late Miocene or early Pliocene (10—4 mya).

The earliest known fossil evidences of immediatae human ancestors are dated from the early Pliocene (4 mya). Three genera of these early hominids are known — Ardipithecus, Paranthropus and Australopithecus. Best studied is the last one because of its well-known representative — "Lucy" from Hadar, Ethiopy (Australopithecus afarensis) [9].

The genus Homo, to which we belong, origins 2,5 mya ago in East Africa. The earliest representative is Homo habilis. It is suggested that this species is predecessor of Homo erectus — 1,6 mya. It is considered that Homo erectus is an ancestor of all later hominoids, including Homo sapiens.

Fossil evidences could be divided in two groups according to the shape of the distal humerus, situation of the epicondyles and articular surface configuration.

First one is characterized by weakly projecting lateral epicondyle placed distaly, almost to the level of the capitellum and moderately developed lateral trochlear ridge. These characteristics are similar to modern human ones and because of that this group is referred to early Homo.

The second group includes Paranthropus and Australopithecus and is characterized by a well-developed lateral epicondyle more proximally situated. It is similar to modern apes.

In overview, as a result of the achievements of the comparative anatomy and fossil record it is known that the modern human elbow originated from the elbow of a common ancestor who lived 15—20 mya ago.

Discussion

The functional analysis suggests that the structural characteristics arose in primate ancestors as a need of providing elbow stability during the locomotion and to achieve wide range of motion of the forearm. As a consequence originated changes connected with upright posture and bipedal locomotion in the earliest representatives of hominids. The elbow joint and the forearm decrease their participation in locomotion but increase the elbow stability in all positions.

The fossil record indicates that our ancestor Homo habilis first appeared 2 mya ago and from then the structure of the distal humerus remained essentially unghanged during all subsequent stages of human evolution.

References

1. Aiello, L. C., M. C. Dean. An Introduction to Human Evolutionary Anatomy. London, Academic Press, 1990.
2. Bardeen, C. R., W. H. Lewis. Development of the limbs, body wall and back in man. — Am. J. Anat., **1**, 1960.
3. Clemente, C. Clemente Anatomy: A Regional Atlas of the Human Body. 4th edition, Lippincott, Williams & Wilkins, 1997, 83-192.
4. Grant, J., C. Boileau. Grant's Atlas of Anatomy. 9th edition. Springer, 1991, 299-482.
5. Gray, H. Anatomy of the Human Body. 20th edition, Philadelphia: Lea & Febiger, Renewed, 1996, 123-157.
6. Leakey, R. E. F. Further evidence of lower Pleistocene hominids from East Rudolf, Northern Kenya. Nature, **237**, 1972, p. 264.
7. Morrey, B. The elbow and its disorders. 3rd edition, London, W. B. Saunders Company, 2000, 3-10.
8. Rose, M. D. Another look at the anthropoid elbow. — J. Hum. Evol., **17**, 1988, p. 193.
9. Stern, J. T. Jr., R. L. Susman. The locomotor anatomy of Australopithecus afarensis. — Am. J. Phys. Anthropol., **60**, 1983, p. 279.

Institute of Experimental Morphology and Anthropology

Acta morphologica et anthropologica, 10
Sofia•2005

Three-Dimensional Reconstruction of the Head after the Skull, Morphological Data and their Applications

Y. Yordanov

Institute of Experimental Morphology and Anthropology, Bulgarian Academy of Sciences, Sofia

The basic role and meaning of the skull morphological information and the way of its application in the 3-D reconstruction of the head soft tissues are pointed out. The methodological principles about the use of morphological data are traced out. The peculiarities and the difficulties in the re-creation of the lateral face parts are pointed out, as well.

Key words: skull, plastic reconstruction, face.

The motives underlying this presentation are the reports submitted to the 1st International Conference on Reconstruction of Soft Facial Parts held in Potsdam, Nov. 10-12, 2003 [21]. Sufficient grounds are also provided by my 30-year long practice and experience in the application of the plastic anthropological reconstruction of the head after the skull dating back to 1974 [7].

Anthropological plastic reconstruction of the head after the skull renders the possibility for visualization in three dimensions the image of the individual whose skull has served as basis for the reconstruction. This is a specific activity in which the human face is restored on the basis of anatomo-topographic and anthropological data obtained in the study of the concrete cranium. The reconstruction of the head after the skull is based on established dependencies between the thickness and relief of the soft tissues of the face, on the one hand, and the anatomical peculiarities of the cranial bones and the relief of their surfaces, on the other. This approach can be expressed in the unity of three parameters of the metric (quantitative) characterization of the skull (anthropometry, craniometry) ⇔ thickness of the soft tissues in the variety of spots and portions of the head ⇔ descriptive characteristics of the skull (cranioscopy, relief of the skeletal surfaces). The existing linkage is confirmed by a multitude of the studies and statistical data obtained in the measurement of the thickness of the soft tissues on many sites of the head in individuals differing in sex, age, morphological types and nationality [1, 2, 4].

My profound and final conviction is that plastic anthropological reconstruction of the head after the skull must be categorically based on the complete morphological information obtained from it (and from the postcranial skeleton as well).

The main approach in the collection, registration and analysis of the data from the skull studies and their utilization in the reconstruction is the anatomo-topographical one. The most important data are in the field of anatomical achievements. The layer by layer topography, holotopy, syntopy and skeletotopy as well as the differences between the representatives of both sexes and the changes taking place with growth and ageing are of practical importance in the analysis of the dependences between shape, size and interrelationships of the soft tissues of the head and the cranial bones in the human [2, 5, 6, 8, 9, 10]. It should be emphasized that the application of this approach gives the opportunity of encompassing all parts of the human head taking into account the influence of all (the deep ones including) morphological structures on its outside relief (glandula parotis, the fatty body of the cheek, the submandibular saliva gland, etc) [21].

— Each human face displays an individual logical construction of its outside relief and as a rule the combination of the separate facial features follows this logic. If the balanced shape of the human head, face respectively is assumed as initial basis i.e. the mean statistical ratio between lengths, widths and heights its change towards elongation or shortening would account for the situation and size of the facial elements and partially the soft tissue relief. Taking into account the logic of the human face the individual peculiarities defining the concrete instructions for the soft tissue underlying bone linkage should not be ignored.
— The manifestation and degree of asymmetry and symmetry respectively of the human face yield to the greatest degree its individual characteristics — an imperative in their investigation and observation in the 3D anthropological reconstruction. It should be borne in mind that the degree of asymmetry manifestation in the facial cranial part (according to the studies for most sizes asymmetry is in the right direction being in that sense a partial case of the total body asymmetry) is greater in parts formed by several bones, for example the orbital entrance [12, 13, 14, 15, 18].
— There exist concrete relations of identity and differentiation between the sizes of the different elements of human head which are directly maid use of in the anthropological reconstruction of the head after the skull. This relation between the values of constant anatomical dimensions in the facial cranial part, human face respectively has been long well-known and its beginning can be found in the canons of the fine art. In the practical application of the existing dependencies their manifestation should be obligatorily taken into account in both sexes and the age-related changes [3, 5, 6, 10, 11, 17, 19].
— The accepted values of the soft part thickness in the different regions and sites of the head and face in particular taking into account their differences due to sex, age and racial type of the individuals only stress upon and confirm the unity of the human species using the classical methods of His, Kollman and Büchli and modern techniques of ultra-sound investigation and computerized scanning tomography.

From the above-presented it becomes clear that the morphological information obtained from the studies on the skull is the scientific and solid basis for undertaking a 3D reconstruction of the soft parts of the head i.e. this is the methodology.

When applied in the practice it renders possibilities for: usage not enough precise which is a methodological error; precise usage but with incorrect technical equipment which is a personal error of the author; and the worst variation is the combination both the methodological and personal errors.

The widely accepted term used for naming this activity is "reconstruction of the soft parts of the face" based on data from the skull. "Plastic anthropological recon-

struction of the face", "reconstruction of the face", "three-dimensional reconstruction of the face", etc. are other terms often used. Here I can express two opinions of mine:

— Reconstruction (restoration) of the soft tissues I would assume as the right one since it reflects the essence of the process and the term "plastic" is unnecessary the relief of the head being in itself plastic. Besides "plastic" in this sense is "three-dimensional".

— The reconstruction of the soft tissues based on data from the skull is their morphological reconstruction, considering the anatomical and anthropological information and is obligatory referred to as a whole to the head and face in particular.

Besides, the reconstruction of the neck and its upper part in particular is absolutely obligatory because it is of great importance. In the extended program the use of information from the extracranial skeleton, in our case the cervical compartment of the spine, sternum, claviculae, shoulders, etc. is recommended.

More appropriate though a bit wider is the definition "reproduction of the soft tissues of head and neck based on data from the skull and skeleton".

In the method described and applied by M. Gerasimov [1, 2] the reconstruction of the soft tissues of the head is performed on one half of the head, the other one being used as a source of information. It is quite appropriate for the modelling to be carried out on the whole skull because [4]:

— It is impossible to reconstruct for example the half of the outside nose, half of the mouth or half of the chin.

— The modern materials for imprinting and casting give an almost absolute precision in the production of the copy of the skull serving as a basis for the reconstruction. Thus, the authentic cranium remains as a tool for observation and measurements, while the modelling is carried out on its copy.

Graphic reconstruction of the profile introduced by M. Gerasimov [2] which takes into account the data about the soft tissue thickness after the profile and observing the bone base is an objective and relatively fast method for obtaining visual information. But the graphic drawing of this profile is already rife with in exactness since it is two-dimensional and the extent of the shadow (white-gray-dark-black) is exceptionally subjective and in many cases untrue. The graphic reconstruction of the profile and the half-profile (introduced by myself) [20] should be used but only to the degree of its outlined control.

In certain skulls, of the Americans for example, the modelling of regio parotideo masseterica is carried out "en masse", i.e. the soft tissue thickness is recorded and applied from the surface of the mandibular angle, ramus respectively, including the body of m. masseter, the tissues underlying the skin and the skin itself. This approach, however, ignores the information about the size and thickness of muscle body, the direction and situation of its two parts (superficial and deep) about which there is objective information — the ratio between the two dentures, the two jaws respectively, i.e. of the mandibulae to the facial part of the skull; the relief of angulus mandibulae and the characteristics of tuberositas masseterica; the development, situation and relief of the lower edge of arcus zygomaticus. The right approach is when the genuine chewing muscle is modelled individually together with the temporal one and the other muscles of the neck and the soft tissues lying over.

In some other techniques certain muscles of the mimic are modelled — for example m. orbicularis oculi; orbicularis oris, m. zygomaticus major, m. zygomaticus minor, m. levator anguli oris, mm. levator anguli oris et alaeque nasi, etc. Their mass, volume (with certain exeptions) is very small and when taking the data, their thick-

ness is registered "en masse". That is why their reconstruction is due to be made in the same way — "en masse". The development of some of them — m. zygomaticus major et minor might be judged about from the relief of their insertion places on the cheek-bone and the maxilla. Their development affects the relief and mimic of the face but not its shape. For example the development of the relief in the surroundings of glabella may yield information about the characteristics and function of m. procerus and m. corrogator supercilii which can be reflected in the facial relief but not in the thickness of the surrounding tissues in the glabella region.

There is a lot of data collected about many elements in the facial area; the techniques for their reproduction are elaborated but the case with the cheek area (regio buccalis), i.e. the lateral part of the face makes an exception. That is why my mentioning the deeper structures such as the fatty body of the cheek (corpus adiposum buccae) and glandula parotis was not incidental in summing up the morphological principles of the reconstruction.

The complexity in the reproduction of this part of the human face becomes still greater owing to the lack of metric data about the soft tissue thickness in regio buccalis as well as its transition in the adjacent regio nasalis, regio orbitalis, regio oralis, regio mentalis and regio parotideomasseterica. The relief of the lateral facial part is formed on the borders between them. From above along the Frankfurt horizontal plain the thickness of the soft tissues (arcus zygomaticus, orbital edge) has been restored starting from the medial side — from the lateral edges of apertura piriformis and from angulus oris; underneath — from the lower edge of the mandibulae, behind — from m. masseter. The area between them is only left. The assessment of the development of m. buccinator and m. rizorius on one hand and the development of m. zygomaticus major et minor and the volume of corpus adiposum buccae on the other is of great importance. Information about these elements from the lateral facial part can be found in the relief the underlying bone surfaces. The relief of the lateral facial part is also characterized with the presence and expression of sulcus nasolabialis passing through its medial side which is most often reflects the vertical and horizontal profiling of the face.

The above thesis sets the modest task of presenting the morphological consideration on the reconstruction of the soft parts covering the head and face respectively, taking into account all data about the bone matrix.

References

1. Герасимов, М. Восстановление лица по черепу. — Труды Инст. Этнографии, Новая серия, **XXVIII**, 1955.
2. Герасимов, М. Основы восстановления лица по черепу. М., Советская наука, 1949.
3. Йорданов, Й., В. Крумова. Връзка между размерите на твърдото небце и някои от основните размери на главата у човека. — Стоматология, **1**, 1989, № 35—41.
4. Йорданов, Й. Възстановяване на главата по черепа. С., Акад. изд. „Проф. М. Дринов", 2000.
5. Йорданов, Й. За връзката между формата и големината на лицето и горните централни резци. — Стоматология, **51**, 1969, № 2, 156—159.
6. Йорданов, Й. За връзката на някои лицеви измервания с височината на захапката. — Стоматология, **48**, 1966, № 6, 438—444.
7. Йорданов, Й. Портретна реконструкция по женски череп от IX в. — В-к „Народно дело", бр. 117, Варна, 1975.
8. Петков, В., П. Екимов, Й. Йорданов. Възрастова характеристика на височината на захапката. — Стоматология, **52**, 1970, № 6, 475—479.
9. Bojanov, B., K. Bernstein, Y. Yordanov. Anthropometrische Bestimmung der Bisshoche, D. Zah. Zeitschrift, München, **23**, 1968, No 11, 1126-1129.

10. Dimitrova, B. The shovel shaped character in the maxillar incisors of modern Bulgarian population. — Acta Morph. et Anthrop., 7, 2002, 133-138.
11. Filcheva, Z., N. Kondova, Y. Yordanov. Cephalometric characteristics of children from the city of Sofia in beginner school age. — Acta Morph. et Anthrop., 5, 2000, 133-137.
12. Kadanoff, D., Y. Yordanov. Die Asymmetric Bau des Mittelteiles des Gesichtsschadels, Morph. Jahrbuch, Leipzig, 124, 1978, No 3, 305-321.
13. Kadanoff, D., Y. Yordanov. Die Asymmetrie in der Form und Grosse des Aditus Orbitae beim Menschen. — Verb. Anat. Ges., 71, 1977, 1283-1288.
14. Kadanoff, D., Y. Yordanov. Die Symmetrie und Asymmetrie der das Gebiss Tragengen Teile des Oberund Unterkieferknochens. — Verh. Anat. Gess., 74, 1980, 795-797.
15. Kadanoff, D., Y. Yordanov. Die Symmetrie und Asymmetrie im Bau des Gesichtsschadels. — C.R. del'Akademie Bulgare de Sciences, 31, 1978, No 6, 775-778.
16. Yordanov, J., L. Tsacheva. Anthropometric characteristics of the hard palate in twins and certain correlations with metric features of the face. — C.R. Acad. Bulg., Sci., 23, 1970, No 2, 233-236.
17. Yordanov, Y. et al. Anthropometric characteristics of nose of adult Bulgarian. — Acta Morph. et Anthrop., 4, 1995, 71-77.
18. Yordanov, Y., B. Dimitrova. Data about human face asymmetry. — Acta Morph. et Anthrop., 4, 1997, 79-83.
19. Yordanov, Y., B. Dimitrova. Differences and degree of identity between certain face dimensions. — Acta Morph. et Anthrop., 2, 1991, 31-36.
20. Yordanov, Y. Graphic reconstruction of the semi-profile. — Acta Morph., 5, 1984, 61-71.
21. Yordanov, Y. Morphological principles of tri-dimensional head reconstruction on the skull — results in Bulgaria. — In: 1st International Conference on Reconstruction of Soft Facial Parts (10-12 November, Potsdam, Germany, 2003).

Institute of Experimental Morphology and Anthropology

Acta morphologica et anthropologica, 10
Sofia • 2005

Comparative Studies upon the Infraorbital Canal and the Mandibular Canal in Dogs from Different Cephalic Types

A. Dechev, G. Kostadinov, A. Vodenicharov

Department of Veterinary Anatomy, Histology and Embryology, Faculty of Veterinary Medicine, Thracian University, Stara Zagora

Comparative studies on infraorbital canal and mandibular canals as well as on infraorbital and mental foramina have been performed in 26 canine skulls (with mandibulae) from dolichocephalic dogs. Nineteen of them belonged to various breeds: Miniature Pinscher, Dachshund, Poodle, Drathaar, Collie, German Shepherd, Caucasian Ovcharka, Belgian Sheepdog, Dogue, Rottweiler and Shar Planinets. Another 7 skulls of mixed-breed dogs, obtained from the Stara Zagora Community Kennel were furthermore studied. It was found out that contrary to the infraorbital canal, the mandibular canal was with irregular margins. It was stated that the index infraorbital canal length/nasal bones length (Nasion/Rhinion) was with identical value only in Dachshunds (0.23). It was also observed that the ration of mandibular canal length and mandibular length varied within very narrow limits in purebred dogs as well as in mixed-breed dogs, being 0.58-0.62 and 0.59-0.62 respectively.

Key words: infraorbital and mandibular canal, dog, cephalic types.

Introduction

Data referring to the anatomy of canine breeds are still insufficient and are primarily about the dimensions of the foramen magnum [9, 10], cephalometric indices in growing and adult shepherd dogs [7, 8] as well as diagnostic imaging studies of normal nasal cavities and the paranasal sinuses in mesaticephalic dogs [2].

It is known that both the infraorbital and the mandibular canals are important from a clinical point of view, because the blood vessels and the nerves responsible for the blood supply and the inervation of teeth are located inside them. The biggest part of reported literature data are about the location of those foramina and canals in the dog as a species, without considering the type and breed-related peculiarities. There is not a uniform opinion about the number of mental foramina [3, 6, 11]. Also, there are no data about the ratio of both canals' lengths vs the length of nasal bones and the mandibula, respectively.

This motivated our interest in studying the particularities of both canals in dogs from different cephaic types as well as in mixed-breed dogs.

Material and Methods

Twenty-six canine skulls were included in the study. Nineteen skulls were obtained from different cephalic type canine breeds as follows: Miniature Pinscher, Dachshund, Poodle, Drathaar, Collie, German Shepherd, Caucasian Ovcharka, Belgian Sheepdog, Dogue, Rottweiler and Shar Planinets. Another 7 skulls of mixed-breed dogs, obtained from the Stara Zagora Community Kennel.

All skulls were taken from dead or euthanasized dogs. After skinning, they were soaked for several hours in running water. Afterwards, the heads were boiled in water, the soft tissues were removed and the skulls dried at room temperature. Then they were defatted in an ether/chloroform mixture (1:1) and bleached in 4% hydrogen peroxide solution.

Osteological investigations on the shape and the location of the infraorbital foramen, the mandibular foramen and the mental foramina were performed in all skulls. Using a caliper-gauge and Wilkins compasses, the following measurements were taken: ratio of the infraorbital canal to the biggest nasal bone length and ratio of the mandibular canal to the mandibular length.

The infraorbital canal length was taken between the maxillar and the infraorbital foramina and the mandibular canal length - between the mandibular foramen and the foramen magnum that in all cases was the middle foramen. The greatest nasal bones length was measured from the caudal margin of the frontonasal suture in the median plane (Nasion) to the rostral end of nasal process (Rhinion) according to the skull morphometry proposed by several authors [1, 4, 5, 8, 9, 12]. The length of mandibula was obtained between the caudalmost point of the condylar process to the rostralmost median mandibular point.

Both canals were examined on radiographs as well as on whole and previously bisected skulls and mandibulae in a lateromedial view. Into the canals of 3 mixed-breed dogs skulls, warmed 10% Pb_3O_4 solution in gelatine was injected. After the polymerization of gelatine, the skulls were bisected along the median plane and radiographs in lateromedial views were taken.

Results and Discussion

The radiological studies after the application of saturated lead tetroxide solution in aqueous gelatine in the arterial system of the head showed that both canals were distinctly differentiated from the adjacent bone tissue. Their shadow was more radiolucent due to the presence of air and soft tissues (blood vessels and nerves) within. Only the shadows of the filled infraorbital and mandibular alveolar arteries were dense and well visible. Only the apical parts of roots of carnassial teeth, P_4 and M_1 respectively, were bended inward to the cavity of canals (Fig. 1).

The osteological and osteoscopic studies revealed that in all skulls, the infraorbital foramen was located in the transverse plane between the third and the fourth premolars. The shape of the foramen was similar to an isosceles triangle in most breeds (Fig. 2). Only in Dachshunds, the foramen's shape was eliptical. The location of the infraorbital foramen could be detected via palpation through the skin in all cases.

The mental foramina in almost all studied mandibulae were three, the middle one being with the biggest dimensions, so we suggest that it could be specified as foramen magnum. The other two foramina, located anterior to and posterior to the foramen magnum, could be designated as rostral and caudal mental foramina, re-

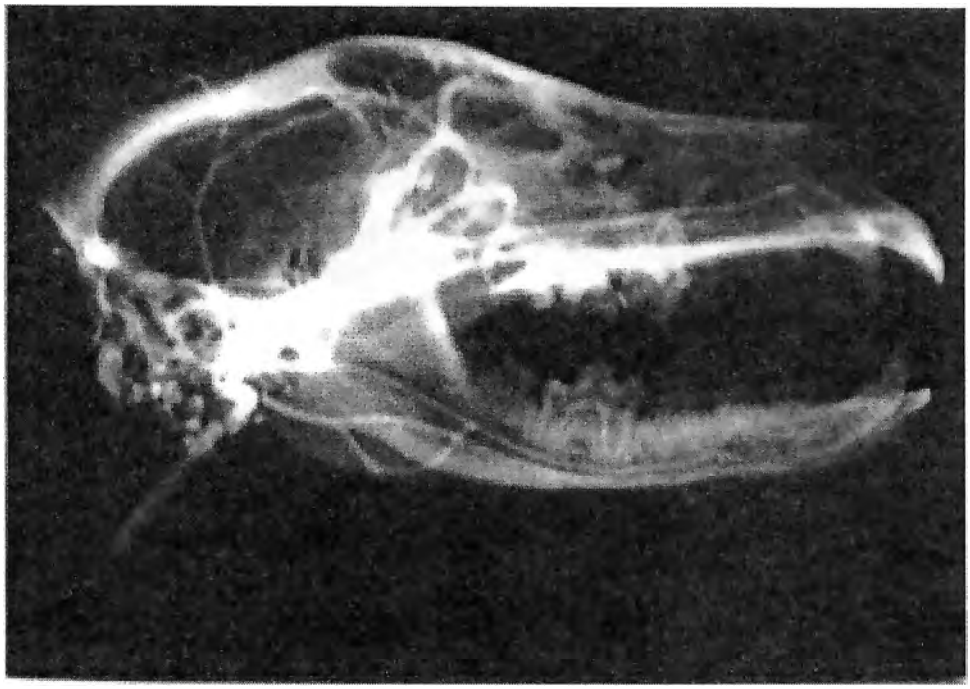

Fig. 1. Radiograph of a canine skull from a mixed breed following application of saturated lead tetroxide solution in aqueous gelatine in the arteries. The margins of the infraorbital and the mandibular canals with the respective arteries are seen

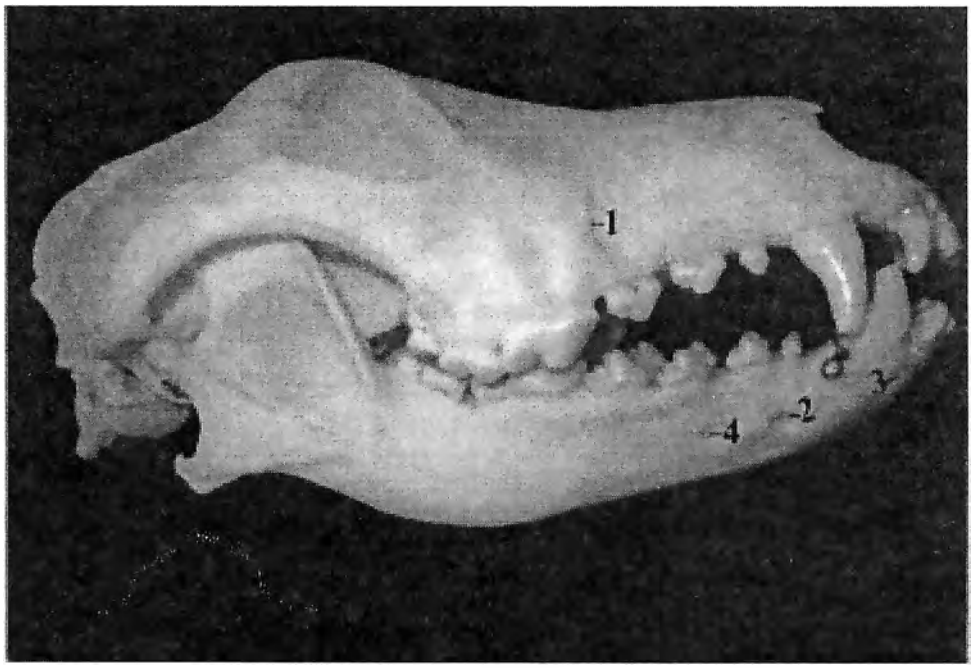

Fig. 2. Skull of German Shepherds: 1 — For. infraorbitale; 2 — For. mentale magnum; 3 — For. mentale rostrale; 4 — For. mentale caudale

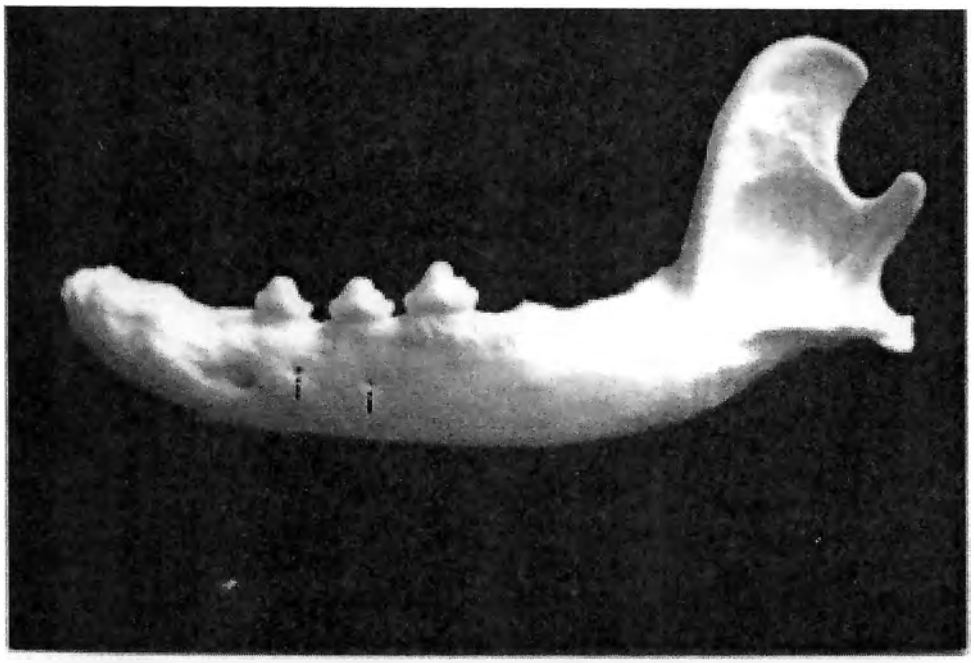

Fig. 3. Left mandibula of a Labrador with two caudal mental foramina (i)

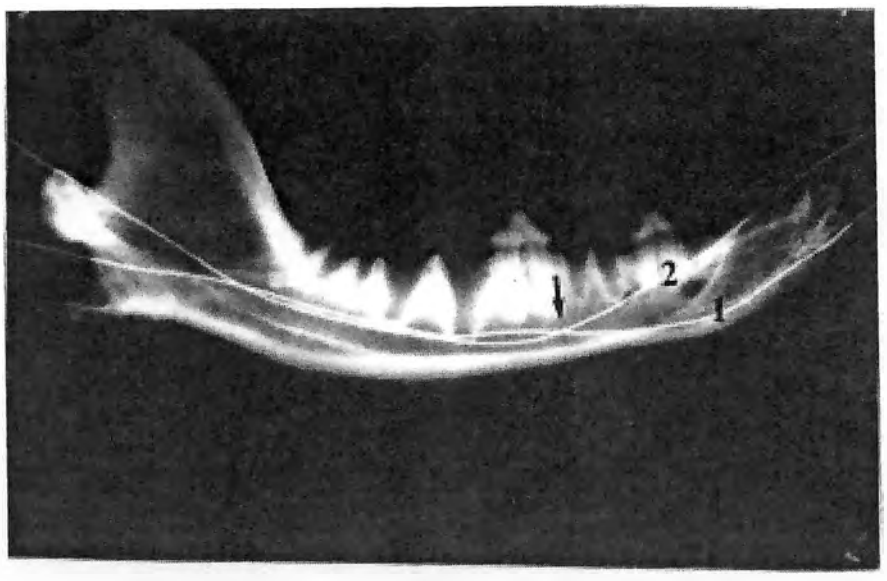

Fig. 4. Radiograph of the mandibula of a Labrador. A wire is inserted through the rostral and caudal mental foramina, that leaves through the mandibular foramen. The beginning (arrow) of canals for the rostral (1) and caudal (2) openings is visible

spectively. Only in one Labrador, two caudal mental foramina were observed on the left mandibula, located under the caudal halves of P_1 and P_2 at the level of the upper margin of the foramen magnum. The foramen magnum in Collies, German Shepherds, Belgian Sheepdogs and Caucasian Ovcharkas was situated at the rostral root of P_2, whereas the caudal mental foramen was positioned by the rostral root of P_3. In Dachshunds, American Pitbull Terriers and Dogues, the foramen magnus was under P_1 and in German Shorhaired Pointer — anterior to P1. The other two mental foramina were situated as followed: rostral mental foramen —between I_1 and I_2 and the caudal mental foramen — between the rostral root of P_3, i.e. in a manner such that in already mentioned breeds. The radiological studies of the mandibular canal (following preliminary introduction of a wire in rostral and caudal foramina) showed that the canals originated considerably behind the foramen magnus — in the transverse plane passing through the anterior contact surface of the third premolar (Fig. 4).

The data about the ratio of infraorbital canal /Nasion-Rhinion lengths showed that it varied in relatively large limits in studied skulls: from 0.23 to 0.39. The lowest value was observed in Miniature Pinschers (0.23) and the highest — in Collies (0.39). It was interesting that the index was considerably variable in skulls of mixed-breed dogs (0.26 — 0.36). Various ratios were obsetained in Dogue skulls — 0.27, 0.30 and 0.32 respectively as well as in German Shepherds (0.29 and 0.33), Caucasian Ovcharkas (0.28) and Belgian sheepdogs. For the other studied breeds, the index was as followed: 0.31 in Drathaars, 0.32 in Shar Planinets and 0.28 in Rottweilers. Furthermore, information about the shape of the infraorbital foramen is reported for the first time — except for Dachshunds, in the skulls of all other studied breeds (including mixed-breed dogs), it was similar to an isosceles triangle. This fact could be important from a clinical point of view as well.

The index reflecting the ratio of mandibular canal and mandibular lengths was less variable. In purebred dogs it was between 0.58-0.62 and in mixed-breed dogs — between 0.59-0.62. The lowest value of the index was obtained in the Shar Planinets breed (0.58) and the highest one — in Dachshunds and Belgian Sheepdogs (0.62).

The data of our investigations evidenced that mandibular canal values were considerably less variable than those of the infraorbital canal. Because of the relatively few number of purebred canine skulls, a statistical analysis of data was not performed. Yet, the obtained results allowed us to assume that the mandibula and the mandibular canal were in more constant association compared to the index presenting the infraorbital canal/Nasion-Rhinion ratio.

References

1. Constantinescu, G. The head. — In: Clinical Anatomy for Small Animal Practitioners. Blackwell Publishing Company, Iowa State Press, Ames, 2002, 67-135.
2. De Rycke, L., J. Saunders, I. Gielen, H. van Bree, P. Simoens. Magnetic resonance imaging, computed tomography, and cross-sectional views of the anatomy of normal nasal cavities and paranasal sinuses in mesaticephalic dogs. — American Journal of Veterinary Research, 64, 2003, No 9,1093-1098.
3. Dyce, K., W. Sack, C. Wenshing. The Head and Ventral Neck of the Carnivores. — In: Texbook of Veterinary Anatomy (Ed. D. Peterson). Philadelphia, W. B. Saunders Company, 1987, 370-389.
4. Lignereux, Y., S. Regedon, C. Pavaux. Typologie céphalique canine. — Revue Médicine Veterinarie, **142**, 1991, 469-480.
5. Lignereux, Y., S. Regedon, B. Personaz, C. Pavaux. Typologie céphalique du Chien et ostéo-archéologie: a porpos d'une population canine du XVII[e] siécle Toulousain. — Revue Médicine Veterinarie, **143**, 1992, 143-149.

6. Evans, H., A. de Lahunta. The Head. The Skull. — In: Miller's Guide to the Dissection of the Dog. Fourth Edition. Philadelphia, W. B. Saunders Company, 1996, 250-263.
7. Onar, V. A morphometric study on the skull of German shepherd dog (Alsatian). — Anatomia, Histologia, Embryologia, **28**, 1999, 253-256.
8. Onar, V., S. Özgan, G. Pazvant. Skull typology of adult male Kangal dogs. Anatomia, Histologia, Embryologia, **30**, 2001, 41-48.
9. Regedon, S., A. Robina, A. Franco, J. Vivo, Y. Lignereux. Détermination radiologique des types morphologiques crâninens chez le Chien: *Doligocéphalie*, *Mésocéphalie* et *Brachycéphalie*. — Anatomia, Histologia, Embryologia, **20**, 1991, 129-138.
10. Simoens, P., P. Poels, H. Lauwers. Morphometric analysis of the foramen magnum in Pekinese dogs. — American Journal of Veterinary Research, **55**, 1994, No 1, 34-39.
11. Simoens, P., P. Poels, Ph. Vyt, H. Lauwers. Variabiliteit van het foramen magnum en occipitale dysplasie bij de hond. — Vlaams Diergeneeskd Tijdrschr, **63**, 1994, 44-53.
12. Sisson, S. Carnivore Osteology. Skull. — In: The Anatomy of Domestic Animals (Ed. R. Getty). Philadelphia, W. B. Saunders Company, 1975, 1467-1482.
13. Von de Driesch, A. A guide to the Measurement of Animal Bones from Archaeological Sites. Peabody Museum Bulletin 1. Cambridge, MA: Harvard University, 1976.

Institute of Experimental Morphology and Anthropology

Acta morphologica et anthropologica, 10
Sofia•2005

Is There a Difference between the Human Height before and after Death?

D. Radoinova, I. Ivanova**, I. Krasnaliev****

* *Department of Forensic Medicine, Medical University of Varna*
** *Department of Internal Medicine, Medical University of Varna*
*** *Department of Pathology, Medical University of Varna*

The purpose of this study is to find out if there is a difference in the human stature before death and post mortem. The height of 160 dead people was measured and then compared to the height stated in their identification cards. For individuals older than 45 years of age an ageing correction has been applied and, subsequently, the actual height of the person was compared to the post mortal height. There is a statistically significant, but practically insignificant difference between the human heights measured during lifetime and after death. This difference is considerably smaller when comparing the actual and the post-mortal height than when the comparison is made between the height recorded in the identification cards and the height after death. The rigor mortise of the body does not affect the body length. The accuracy of the height post mortem depends primarily on the used methods for measuring and the precision in reporting the data.

Key words: living stature, post-mortal height, forensic stature.

The human stature is one of the fundamental attributes of physical development, which gives us a general idea of the size of the human body. The increase of the body length follows a particular genetic model, with typical growth line-graphs and with predictably changing growth speed.

After people have reached their maximal height at the age of 18-20, there is a long period of stability. After the age of 45 the length of the body begins to reduce by 1 mm per year with minimal differences for the two genders.

There are some physiological hesitations in a person's height on a daily basis. These hesitations can reach as much as 2,2 cm and depend on many factors [2]. The question of whether there is a difference between the human height before death and post mortem has not been studied sufficiently. The standpoints expressed by different authors are conflicting [1, 3, 5, 7, 8, 9, 10].

The ***purpose*** of this study is to determine whether there is a difference between the human height measured during lifetime and that one measured after death. In order to answer this question, the height of people is measured after their death and then compared to the height recorded in their identification cards. The same comparison is made between the post-mortal height and the actual height after an age correction was made.

Material and Methods

The subjects of this study were 160 people who have died at the Department of Forensic Medicine at the Medical University of Varna. 37 of the studied individuals are women, 123 are men, all of them between 18 and 87 years of age. The subjects did not have any mechanic, thermal, or other damages, which could affect the height. The information about the height during lifetime was taken from the individuals' identification cards where the persons themselves stated their height. The post-mortal height was taken before the autopsy, using a graphed table while the body was in a supine position and after cutting of the Achilles' tendons. Whenever it was possible, multiple measurements were made: from 1-2 hours after the death to 3-4 days, i.e. before the rigor mortis, while it was in process and after it had finished. For all the subjects older than 45 years of age the Giles and Borcan age correction was used according to the individuals' gender. The correction compensates the height reduction due to aging. Thus, two parallel comparisons were made: 1) between the height during lifetime forms the identification cards and the height after death and 2) between the actual height before and after death. The statistical estimates and calculations of the collected data were made using Excel, the double t-test and the SPSS software.

Results and Discussion

The average age of the studied persons was 54.8 ± 1.7 years old. All the calculations were made using 95% accuracy level. The average height of the male individuals was 170,9 cm, which coincides with the data reported for Varna city in the national anthropological study (1992). The studied female individuals' average height was 160.1 cm whereas the national anthropological program is 158.9 cm. The age correction that was made was within the 0-4.2 cm interval or, averagely, 1.35± 0.10 cm. The post-mortal height of the male subjects of the study was 169.7 cm, i.e. lower by 1.25 cm. The females' height after death was 157.8 cm or lower by 1.68 cm.

Table 1. Basic characteristic of the measurements

Parameters	Male (n=123)	Female (n=37)
mean stature from personal cards [cm]	171.91±0.64 SD=7.08	160.13±0.98 SD=5.96
mean age correction [cm]	1.35±0.10 SD=1.21	
mean real stature [cm]	170.66±0.66 SD=7.35	158.45±1.09 SD=6.60
mean postmortal stature [cm]	169.71±0.65 SD=7.24	157.76±1.13 SD=6.87
difference between st. card/postm. st. [cm]	-1.25	-1.68
difference between real st./postm. st. [cm]	-0.95	-0.69

The difference between the human height before death and postmortem was much smaller when the actual human height was compared to the post-mortal height: It was respectively —0.95 cm for the men and —0.69 cm for the female subjects of the study. Such differences are practically insignificant because they are within the range of the margin of error.

The double T-test was used to compare the differences between the height during lifetime, stated in the identification cards, and the post-mortal height.

Furthermore, the T-test was also used to measure the difference between the actual lifetime height and the post mortal height (Fig. 1) The differences in the measured height levels for men were significant ($P<0,0001$) in both cases. Although the statistically significant differences, the height measured post mortem was much closer to the actual (the true) human height than to that stated in the identification cards (Fig. 2). Furthermore, these results indirectly confirmed those people frequently state unrealistic and imprecise height, more often the maximal or close to the maximal height. The study proved that the differences in the women's height levels are also significant.

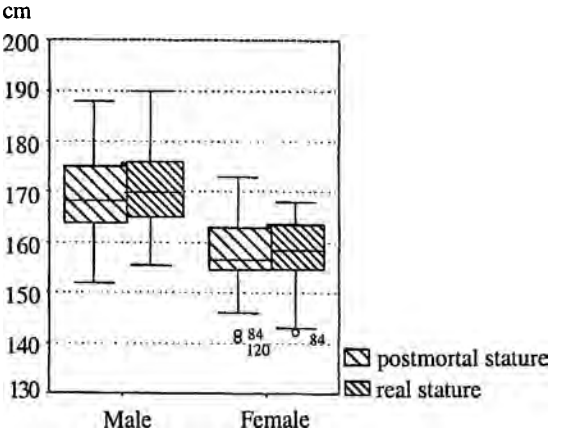

Fig. 1. A comparison between the height stated in the identification cards and the post-mortal height of the two genders

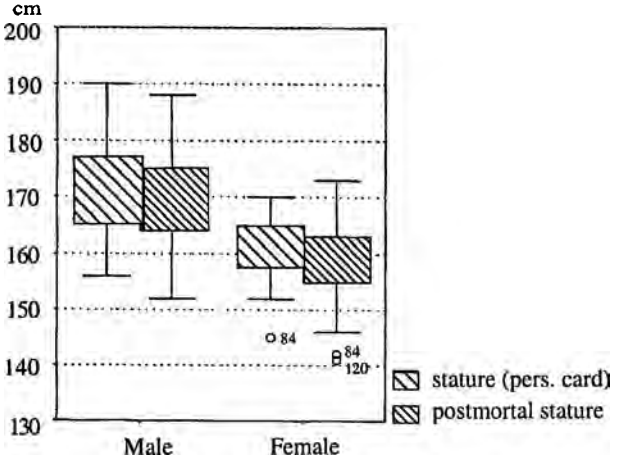

Fig. 2. A comparison between the actual height and the post-mortal height of the two genders

In any case, the average post-mortal height levels for the two genders were smaller than the average height levels during lifetime, regardless of whether those levels were compared to the height in the identification cards or the actual height. This could be explained with the effect of the rigor mortis and with the daily variation of the human height. We did not encounter a scientific explanation of this fact in the literature. The influence of the methods used as well as the precision of the data reporting cannot be ignored.

The results of the study are contradictory to the most "classical" assumptions. Manouvrier [3], Telkka [8], Pearson [5] have assumed that the height after death is greater than the height of the living individual with 1.3 to 2 cm. However, they used a different methodology - they measured the height of the dead bodies while they were hanging down as opposed to lying on a counter.

On the other hand, Todd and Lindala [9], who measured a large group of dead bodies, pointed out, "...the heights of the dead bodies are perhaps a little smaller compared to those of the living people standing up freely, but the difference does not exceed the margin error of the measurement...." A similar assumption was supported by Trotter and Gleser [8] who believed that a correction between the height during lifetime and after dead is not necessary and the possible difference only results from the differing methods of measurement. According to Dupertius and Hadden [1], the difference between the height post mortem and during lifetime could only result from subjective reasons. Apparently, these viewpoints correspond to the results of our study. Our opinion is that the realistic and precise measurement of the human height after death depends essentially on the methodology, the precision of the reporting of the data, the accurate graphing of the table, the cutting of the Achilles' tendons, and the vertical positioning of the head.

Conclusions

1) The difference between the human height before and after death is statistically significant but practically insignificant. 2) The average difference between the persons' height stated in their identification cards and their height measured post mortem is —1.25 cm for the men and —1.68 cm for the women. The difference between the actual height during lifetime (after the correction for ageing) and the height measured after death is much smaller: —0.95 cm for the men and 0.69 cm for the women. 3) The rigor mortis after death practically does not affect the post mortal height. 4) The accuracy of the measurement of the human height post mortem depends essentially on the methodology of the measurements and the precision in the reporting of the data. 5) For the purposes of the forensic medicine, the actual height of each individual needs to be measured and a correction for the height reduction due to ageing needs to be calculated, especially for the elderly individuals.

References

1. Dupertuis, W., J. Hadden. On the Reconstruction of Stature from long Bones. — Am. J. Phys. Anthropol., 9, 1951, 15-53.
2. Kobayashi, M., M. Togo. Twice-Daily Measurements of Stature and Body Weight in Two Children and One Adult. — Am. J. Hum. Biol., 5, 1993, 193-201.
3. Manouvrier, L. La dètermination de la taille d'apres les grands os des membres. — Mem. de la soc. d'anthopol. de Paris. 2 ser., 4, 1892, 347-402.

4. O u s l e y, S. Should We Estimate Biological or Forensic Stature. — J. Forensic Sci., **5**, 1995, No 40, 768-773.
5. P e a r s o n, K. On the reconstruction of stature of prehistoric races. Mathematical Contributions to the Theory of Evolution. V. On the reconstruction of stature of prehistoric races. — Philos. Transa. Roy. Soc. London (Biol), **192**, 1899, 169-245.
6. R a d o i n o v a, D. Estimating actual height in older individuals. — J. Anthrop., **4**, 2003, 154-157.
7. R o l l e t, E. De la mesuration des os longs des membres dans ses rapports avec l'Anthropologie la Clinique et la Médecine judiciaire. Lyon, 1888.
8. T e l k k a, A. On the Prediction of Human Stature from the Long Bones. — Acta Anat. Basel, **9**, 1950, No 1-2, 103-117.
9. T o d d, T., A. L i n d a l a. Dimensions of the body; Whites and American Negroes of both sexes. — Am. J. Phys. Anthropol., **12**, 1928, 35-119.
10. T r o t t e r, M., G. G l e s e r. Estimation of Stature from Long Bones of American Whites and Negroes. — Am. J. Phys. Anthropol., **10**, 1952, No 4, 463-514.

Institute of Experimental Morphology and Anthropology

Acta morphologica et anthropologica, 10
Sofia•2005

From Mummification to Plastination

D. Sivrev, A. Georgieva, N. Dimitrov

Department of Anatomy, Faculty of Medicine, Stara Zagora
Thracian University, Stara Zagora

The authors analyze and systematize the principals and the methods of embalmment and some factors that were used for conservation of the of corpses through the ages and now.

Key words: Mummy, Mummificatin, Plastination, Biodur.

Introduction

For many centuries scientists have tried to create effective and safe for human health method of conservation and long-lasting preservation of corpses. Mummies and anatomic preparations created in the past have had many disadvantages, which is the reason for the continuation of research in this area. There is a succession between mummification and plastination as a modern scientific method for conservation of organic matter.

Basic information

The Mummies of Chinchoros. A u f d e r h e i d e et al. [3] inform about seven mummies from the northern Chilean coast. One of the bodies is the oldest naturally preserved mummy aged 9000 years. A l l i s o n [1] and S t a n d e n [12] describe in detail the funeral techniques used by Chinchoros in 149 well preserved mummies. Embalmers took out the internal organs, remove soft tissues and replace them with texture. There are two styles of mummification [2]: **1) "Black style"**(manganese mask). The earliest well preserved mummy of this style "The child of valley Camarone", situated 70 kilometers south of city Arica in Chile, is from 5050 BC; **2) "Red style"** (red ochre cover). The child from El Morro near Arica is in this style.

Pacific mummies. A u f d e r h e i d e [4] describes 14 of the well-preserved pacific mummies from Melanesia, Papua New Guinea, Australia and the islands of Torres.

Embalmers take out fats and internal organs, smoke the body and rub into the skin its own fats and red ochre. Few times a day the body is massaged until it has

dried out. Big part of the preserved Pacific mummies is kept in Maclean Museum in Australia or in American collections [11].

The Siberian Ice princess. Russian scientists discovered in 1993 a richly dressed mummy [7] in pazaryk tomb in Altai. Ossification of the skull on X-ray pictures proves that the mummy is one of a 25 years old woman, and examination with radioactive carbon that it is buried 500 BC.

Internal organs, brain and all other parts that rotten quickly are removed after the death, during the process and replaced with natural conservatives: tree barks containing tannin, and peat, which acid has anti-bacterial and mummification working [5].

The mummies of Chachapoyas. They are discovered in the jungle of Northern Peru in November 1996 in the area named "The Cloudy Forest" at 3658 m above the sea level.

There was more than 200 mummies in six tombs, hewn into the cliff coast of the Laguna de Los Condores. Every tomb is 3.5 meters tall, has a wooden platform, where the mummies are placed. The tombs are dry and well protected against the bad weather.

X-ray study in the improvised laboratory in Leimembamba, where they are still kept, shows that organs of the dead ones have been removed. The skin and the internal cavities are treated with few different balsams, but their type has not been discovered yet [4].

Egyptian mummies. The ritual of embalmment lasted 70 days. The body is placed on a straight cloth, called "ibu" and washed with "water from Nile" and "aromatic palm wine".

Embalmers scooped out the brain through the nose and take out the internal organs with the exception of the heart. After 40-days drying with natron (carbonates, bicarbonates, and chloride salts of sodium) they are placed in special containers and 17 cuts were made on different parts of the skin to compensate the shrinking when drying [6, 8].

Embalmers would fill the inside of the mummies with linen cloth soaked with aromatic resins, the skin is treated with oils and impregnated with wax. This process lasted 10-15 days, and after that "the corpse is dressed". Embalmers used linen bandages soaked in conservative solutions [9, 10].

Plastination technologies. Plastination method of von Hagens, besides the 3 typical processes of ***fixation***, ***dehydration*** and ***impregnation*** includes a stage of drying. The most commonly used dehydrator is acetone and impregnators are different modifications of Biodur depending on the organ.

Discussion and Conclusions

In more of ancient mummies the internal organs, the brain and the fats have been removed. The methods used in ancient times such as fixation, dehydration and impregnation are base of newest preserving methods of the modern science for preparation, keeping and long-time preservation of anatomical preparations for the requirements of education.

The ancient principles of embalmment use also in modern plastination technologies — plastination with the products of type "Biodur Sn" executed for first time in anatomical practice by Gunther von Hagens in 1979.

References

1. Allison, M. Chile's Ancient Mummies. — Natural History, **94**, 1995, No 10, 74-81.
2. Arriaza, B. Beyond Death: The Chinchorro Mummies of Ancient Chile. — Smithsonian Institution Press, 1995, 164-182.
3. Aufderheide, A. C., I. Munoz, B. Arriaza. Seven Chinchorro mummies and the prehistory of northern Chile. — Am. J. Phys Anthropol, **91**, 1993, No 2, 189-201.
4. Aufderheide, A. The Scientific Study of Mummies. — Cambridge University Press, 2003, 277-286.
5. Campbell, M. Ice Maiden of The Steppes. — World Press Rev., 1994, 6-19.
6. Colombini, P. et al. Characterization of the balm of an Egyptian mummy from the 7th century BC. — Studies in conservation., **1**, 2000, 19-29.
7. Davis-Kimball, J. Chieftain or Warrior Priestess. — Archaeology, **3**, 1997, 40-41.
8. Kaup, Y., M. Schmid, A. Middleton. Borate in mummification salts and bones from Pharaonic Egypt. — J. Inorganic Biochemistry, **94**, 2003, No 3, 214-220.
9. Koller, J. et al. Effective mummification compounds used in pharaonic Egypt. — J. Chem. Sci., **58**, 2003, No 5, 462-480.
10. Koller, J. et al. Ancient materials — Analysis of a pharaonic embalming tar. — Nature, **425**, 2003, No 6960, 784-784.
11. Pretty, G. The Maclean Museum mummy from Torres Straits: A Postscript to G. Eliot Smith and the diffusion controversy. — In: Man, 1969, 24-43.
12. Standen, V. Temprana complejidad funeraria de la cultura Chinchorro (norte de Chile). — Latin American Antiquity, **8**, 1997, No 2, 134-156.

Institute of Experimental Morphology and Anthropology

Acta morphologica et anthropologica, 10
Sofia • 2005

Morphofunctional Aspects of Phonetics

E. Evgenieva, V. Radeva

Department of Special Education, Sofia University "St. Kliment Ohridsky", Sofia

The establishment of a holistic approach in the work on problems related to man will allow of their live description and analysis. The previous strong differentiation of the sciences of language has led to accumulation of extremely varied and vast information. However, this information is still away from the real language practices. The development of an approach for description of the morphofunctional aspects of phonetics will be a step toward the process of building up a specific level of the science of language and of bringing life to it.

Key words: interdisciplinary approach, universal (abstract) sound potential, unique (individual) modified sound variant, discrepancies between the different levels of language modification.

The problem to be dealt with poses a challenge because it is on the boundary of several fields of science — functional morphology, psychology and linguistics, in addition it expands the ontogenetic description of the language/speech phenomenon and it also has an applied contribution to the therapy and rehabilitation of a number of communication disorders.

The place of the problem among all these sciences is determined by the necessity to look at man and his identification as an individual using the holistic approach instruments. The existing differentiation of sciences makes it necessary to find out bridges between them in order to achieve a common theoretical and practical analysis of the problem. The study of the personality from a morphofunctional, psychological and linguistic points of view is expected to give a full picture of a definite level of the individual's self-fulfilment — the language/speech level. The presentation of the development process of the individual aims to describe the level of self-fulfilment, which corresponds to the idea of the level reached in ontogenesis. It should also be taken into account that the strongly changing environment (including the social one) brings about changes, though slow ones, of the individual. In many cases they are insignificant from a morphofuctional viewpoint, but examined in the light of psychology and linguistics they give a possibility to find out tendencies in the process of development. For example, the considerable changes resulting from the introduction, first, of the alphabet and, second, of electronic media have led to considerable changes in the model of social behaviours, as well as in the activity of sensory channels for perception of the surrounding reality. However, work on this issue starts with a description and observation of the changes

in the social realisation at the morphofunctional level of a communication model. The reason is that, firstly, these changes are related mostly to the individual's adaptation to the new environment, secondly, to the process of developing a purposeful applied model of interaction and of provoking a socially productive behaviour (in this case development of a communication level). It is only then that changes at the morphofunctional level are taken into account. It takes long for the changes imposed by the environment to have an effect on the individual's development and social functioning. This leads to a logical alternation of the state of differentiating the sciences dealing with such descriptions and their subsequent integration in quest of an overall approach for description of the observations. This understanding has made it necessary to look at the problem in question from the viewpoint of several sciences — phonetics (linguistics), functional morphology and psychology.

Dealing with the above problem is planned in the light of the phonetic aspects which correspond to the structural division of the science of language sound composition — phonetics, phonematics, speech pathology and speech therapy.

Phonetics is a science of the sound essence of the language reality. Its subject matter is *the universal sound potential* of Homo sapiens. Each individual and national language seizes or *partially* acquires this reality. The acquired portion of the universal sound potential is the one that is necessary and sufficient for the corresponding (national or individual linguistic practice). This partial acquiring leads to a definite level of modification of sounds.

Phonematics is a science of the phonologically determinable linguistic realities. Such a reality is usually described for every single language. At the same time, *every individual* realises it as a *unique variant*. Of key importance for clarifying the status of phonetics and phonematics are the concepts universal (understood as abstract language) and unique (understood as individual acquiring and modification). The interrelation between these can be found out with every individual. On the one hand, an individual can produce, create every single phoneme of the abstract language, and modify it accordingly, on the other, at the level of national realisation and mostly at the level of individual realisation. Evidence of this modification is the speech (pattern) of Bulgarians who have lived abroad for a long time. In their case a modification of the phonemic composition of the national language is observed at an individual level by bringing in of tempo-rhythmic elements of the foreign language. This shows the flexibility of the mechanisms of phoneme production, as well as the individual's unlimited process of modifying.

Logopaedia registers the difference and discrepancies between the specific sound reality of a concrete language and the specific modification on the part of an individual. Taking into account the universal-unique relation, the so-called deviation (from the concrete native language) could also be looked at as an unlawful borrowing from the universal sound reality whose potential bearer the individual is.

The morphofunctional aspects are related to a description of the instruments (organs) whose function is to carry out the production of sounds and is an object of their functional morphology (in the biological sense). It is viewed not only as a function of the voice-forming organs, but also as a result of the functions of definite brain structures and their relation to the former.

The viewpoints brought forward will be of broader significance if subjected to description and analysis on definite psychological grounds. The individual's communication ability (a considerable part of which is made up of the phonetic level development) is dealt with in the context of the higher psychic functions and their role in rationalising the information received and the individual's verbal response to it.

The description of the morphofunctional aspects of phonetics has its linguistic origin. The pragmatic aspect of the individual's communication ability defined as a linguistic manifestation is a precondition for the morphofunctional and psychic interpretation of the problem. This is what outlines the tasks of logopaedia in the existing private science practice.

The projected base points, which the viewpoint system is to be built on, cannot start co-functioning without giving reasons for the way in which they interact and without grounds that are wide enough for this interaction to develop. For the purposes of this interpretation of the problem the differentiated scientific theories interact in two basic ways: a) two by two and b) the three of them at a time. The interaction *in pairs* has already been developed and subject to a broad comment. There is knowledge of a number of discoveries achieved by supplementing the morphofunctional plan of analysis and its psychic correspondence. Traditional phonetics has described the major articulation and acoustic characteristics of speech by combining the morphofunctional and logopaedic analysis. A wide scope of questions focuses on description of the psychic peculiarities of the process of communication (production and perception, understanding and mastering of a language). These already developed relations will serve as a point of departure in the description and systematisation of the set morphofunctional basis of phonetics. The addition to this already existing theory is the work done at the level of *triple* supplement to the above fields of science. The most important peculiarity of the quest of a theoretic description of this triple interaction is its real existence in the linguistic practice. For this reason its description has been incomplete so far, which has had an effect on the pragmatic aspect of the morphofunctional aspects that are being developed. Without a detailed description of this really existing interaction it is impossible to develop adequate (live) methods for purpose-oriented formation of this important level of the communication competence.

Rationalisation of this problem is a challenge to a future study.

References

1. Spinnler, H., L. A. Vignolo. Impaired Recognition of Meaningful Sounds in Aphasia. — Cortex, **2**, 1966, 337-348.
2. Shankweiler, D. P., K. S. Harris. An experimental Approach to the Problem of Articulation in Aphasia. — Cortex, **2**, 1966, 277-292.
3. De Renzi, E., A. Pieczuro, L. A. Vignolo. — Cortex, **2**, 1966, 50-73.
4. Винарская, Е. Н., А. М. Пулатов. Дизартрия и ее топико-диагностическое значение в клинике очаговых поражений мозга. Ташкент, Медицина, 1973, 9—49.
5. Современая американская лингвистика: Фундаментальные направления. (под. ред. А. А. Кибрика, И. М. Кобозевой и И. А. Секеринов). Москва, 2002, 168-203.

Institute of Experimental Morphology and Anthropology

Acta morphologica et anthropologica, 10
Sofia • 2005

The Etruscan Skulls of the Rostock Anatomical Collection — an Attempt to Compare Them with a Hallstatt-Celtic Population from North Bavaria and with Other Skeletal Findings of the First Thousand Years BC

*H. Claassen**, *A. Wree***.

* *Institut für Anatomie und Zellbiologie der Martin-Luther-Universität Halle-Wittenberg, Halle, Germany*
** *Institut für Anatomie, Universität Rostock, Rostock, Germany*

Seven skulls in Rostock's anatomical collection belong to the ancient population of the Etruscans. After determination of age and sex the following measurements were taken among others: maximum skull breadth and ear bregma height. Morphological and metrical traits of the seven Etruscan skulls were compared biometrically to the Celtic population in North Bavaria using the measurements of Claassen and to other Celtic populations. All the Etruscan skulls were found to be masculine, their age ranging from 20 to 60 years, with an average age of about thirty. A significant difference between the Etruscan and the Celtic in North Bavaria could be demonstrated: the Etruscan skulls were narrower (maximum skull breadth) and not as large in height (ear bregma height) as the Celtic ones in North Bavaria. However, the Etruscans showed similarities in these metrical traits with Celtic skulls from Manching in South Bavaria and Hallstatt in Austria. Due to the similarities of the Etruscan skulls with some Celtic skulls from South Bavaria and Austria it seemed possible that the Etruscans are more original inhabitants of Etruria than immigrants from Asia Minor.

Key words: skulls, Etruscan, Celtic, North Bavaria.

All the seven Etruscan skulls were found in Corneto Tarquinia in the years 1881 and 1882 and were given as a present to Rostock's anatomical collection in 1882. The origin of the Etruscan who were contemporary with the Celts whether the were original inhabitants or had immigrated from Asia Minor to Italy is discussed controversially. To put the Etruscan skulls of Rostock's anatomical collection in an ethnological grid it seemed interesting to compare them with skeletal remains of the first thousand years BC, especially with a Hallstatt-Celtic population in North Bavaria [2, 3].

Etruscans and Hallstatt-Celts were contemporary having their cultural climax approximately from 800 to 500 BC. The Latène-Celtic skeletal remains were dated to a period from 500 to 0. The Early Bronze Age skeletal remains from Moravia are

Fig. 1. Map with skeletal findings used for comparison: Etruscan skulls from Corneto-Tarquinia, Hallstatt-Celtic skulls from Beilngries, Dietfurt and Schirndorf, Hallstatt-Celtic skulls from different places in Baden-Württemberg and Hallstatt, Early Bronze Age skulls from Mähren, Latène-Celtic skulls from Manching

dated to 1800 to 1600 BC. The local origin of the populations is described on a map (Fig. 1). Tarquinia is located 70 km in north western direction to Rome. The Hallstatt-Celtic cemeteries of Beilngries [2], Dietfurt [3] and Schirndorf [3] are located in the north of the Danube river. The Hallstatt-Celtic populations used for a comparison originated from different places in Baden-Württemberg [9] and from Hallstatt [8] in Austria in the near of Salzburg. The Latène-Celtics came from Manching [11] in the south of the Danube river and the Early Bronze Age skeletons came from different places in Mähren [10] today in the Czech Republic.

Concerning the cultural background of the Etruscans and Celts [4], both population had the idea that the deceased needs something for the life after. Therefore the

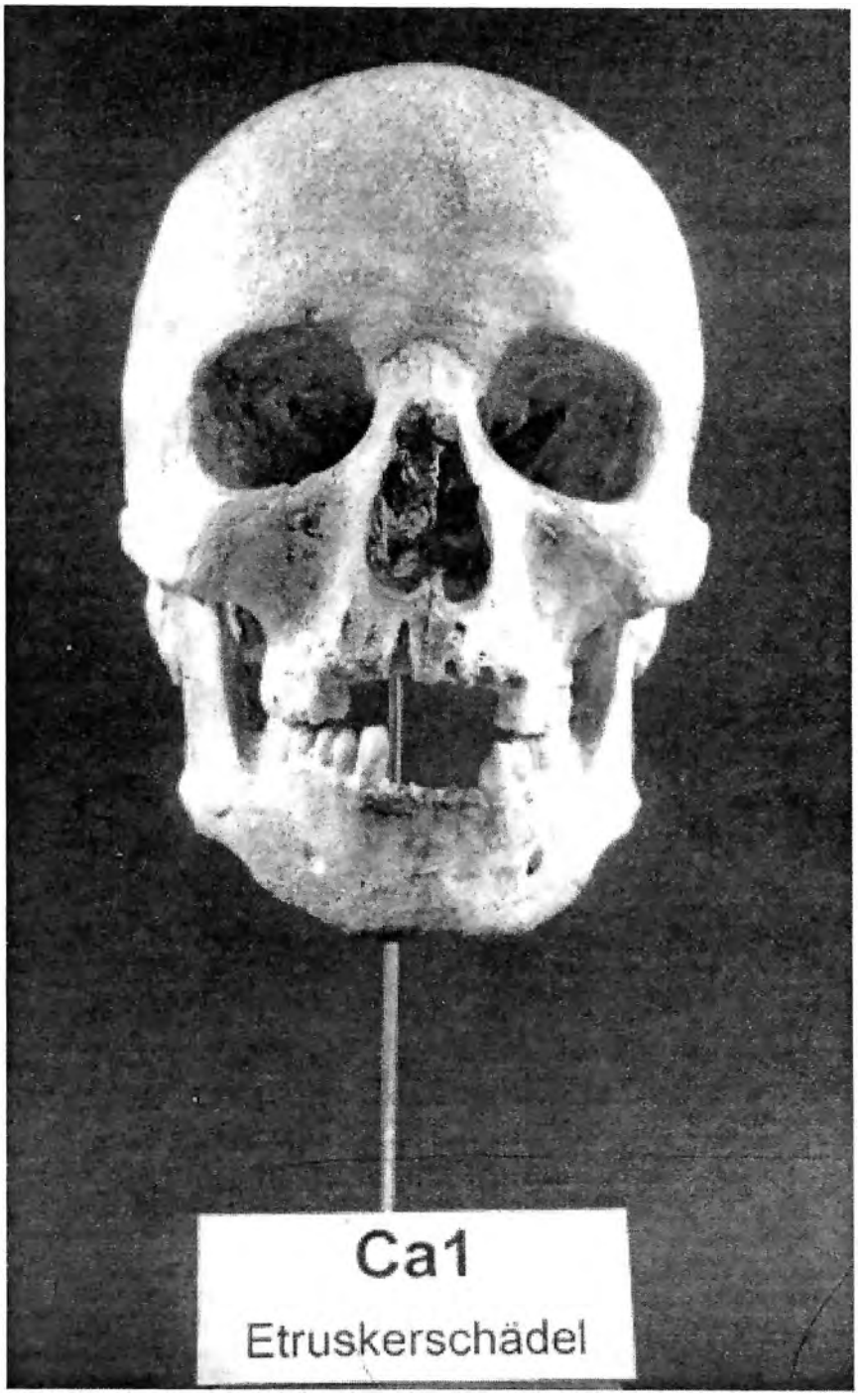

Fig. 2. Etruscan skull Ca1 from Corneto-Tarquinia in frontal view

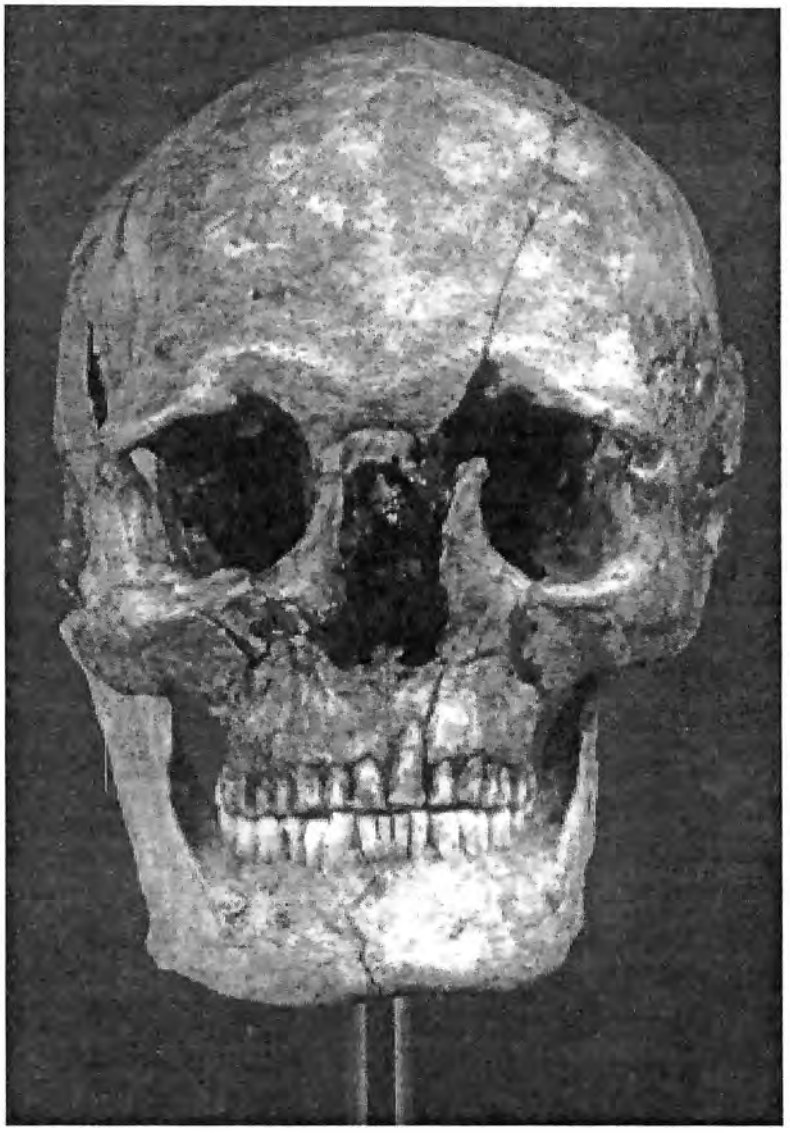

Fig. 3. Hallstatt-Celtic skull 13/1 from Dietfurt in frontal view

tombs of the Etruscans were decorated with wall-paintings, for example with flute players. On the other side, the Celts laid down the deceased on a sofa bed and gave him an amphora with wine and pieces of beef in ceramics, sometimes placed in a wodden car, for his journey from here to there. Further on, the ceramics of the Etruscans was decorated with figures, for example with figures of the marine flora like the well known motive of pirates turned into dolphins. In contrast, the celtic ceramics was decorated with geometric ornaments as it is known from the early Greeks.

The skull with the catalog number Ca1 (Fig. 2) comprises the general outfit of the Etruscan sculls from Corneto-Tarquinia and is approximately 20 to 30 years old

(for determination of age see 5). Like the other Etruscan skulls of Rostock's anatomical collection its sex is male. It was found in an Etruscan tomb together with a golden earring. In the frontal view, the maximum skull breadth and the bizygomatical breadth are narrow, upper facial height is middle-high, orbital breadth is middle-broad, orbital height is middle-high and nasal height is high — skull measurements according to Martin and Saller [12] were classified according to Breitiner [1]. In the lateral view maximum skull length is middle-long and basion bregma height is low. Taken together, a common feature of this and other Etruscan skulls is that the broad measurements are less developed.

In comparison to an exemplary Hallstatt-Celtic skull from Dietfurt (Fig. 3) in North Bavaria especially maximum skull breadth and minimum frontal breadth show higher values in in the Celtic ones. In addition, upper facial height and orbital height are higher in the Celtic specimen compared to the Etruscan ones. In the lateral view the basion bregma height of the Celtic skull is higher in comparison to the Etruscan skull. Due to the aspect of the zygomatic bone, the maxilla and the mandibula the Etruscan skulls are gracile.

Some Hallstatt-Celtic skulls show archaic traits [6], for example, a gable-shaped skull roof, box-shaped orbitae and a right-angled transition of the zygomatic bones into the maxilla.

These features are characteristic for the early specimen of Homo sapiens sapiens found in Oberkassel or Cromagnon. However, these archaic traits were missed at the seven Etruscan skulls.

The mediansagittal outlines of the Etruscan skulls were similar to one another. The skull with catalog number Ca4 has a very prominent glabella, therefore the frontal part of its outline is located a little bit outside of the other skulls. By comparison of the mediansagittal outlines of the Etruscan skulls with grouped mediansagittal outline of the male Hallstatt-Celtic skulls of Dietfurt and Schirndorf in North Bavaria it is observed that the Etruscan skulls are smaller and lower than the Hallstatt-Celtics. Additionally, the results of the t-test show in the same direction. The values for maximal skull breadth, minimal frontal breadth, ear bregma height, bizygomatical breadth and orbital breadth are significantly lower at the Etruscan skulls when compared with Hallstatt-Celtic ones of North Bavaria.

It was tried to put the Etruscan skulls in an ethnological grid by comparing them with skeletal remains of the first thousand years BC (7). A metrical comparison of the variables maximum skull breadth and ear bregma height in the Etruscan skulls with contemporary skeletal populations showed that they did not share similarities with Hallstatt-Celtics from North Bavaria and Baden-Württemberg but shared similarities with Hallstatt-Celtics from Hallstatt. Hallstatt-Celtics from Hallstatt are not as robust as Hallstatt-Celtics from North Bavaria. This robusticity is reflected in the fact that Hallstatt-Celtics from North Bavaria have the highest values for maximum skull breadth and ear bregma height among all the skeletal samples.

Among the chronologically adjacent skeletal remains the Etruscan skulls from Tarquinia shared more similarities with Latène-Celtic skulls from Manching than with Early Bronze Age skulls from Mähren. The shorter chronological and geographic distance of Tarquinia from Manching in relation to Mähren seemed to be the reason for the unexspected similarity of the Etruscans from Tarquinia with the Latène-Celtics from Manching.

In conclusion, the Etruscan skulls from Tarquinia were gracile and showed similarities in metrical traits with Hallstatt-Celtic skulls from Hallstatt in Austria and Latène-Celtic skulls from Manching in South Bavaria. Due to these similarities with

neighbouring skeletal remains on the other side of the Alps the hypothesis could be supported that the Etruscan are more original inhabitants of Etruria than immigrant from Asia Minor.

Acknowledgement. We would like to thank Mr. G. Ritschel (Anatomical department of Rostock university) for the excellent schematic drawings.

References

1. Breitinger, E. Gruppenrisse vom Hirnschädel. — Anthrop. Anz., **15**, 1938, 298-319.
2. Claassen, H., G. Ziegelmayer. 1989a Die anthropologischen Befunde aus dem hallstattzeitlichen Grabhügelfeld von Beilngries, "Industriegebiet". Lkr. Eichstätt, Oberbayern. Bericht der Bayerischen Bodendenkmalpflege., **28/29**, 1987/1988, 106-134.
3. Claassen, H. Untersuchungen zur Anthropologie und Paläopathologie des hallstattzeitlichen Menschen in der Oberpfalz. Thesis, Universität München, 1989.
4. Claassen, H. Paläopathologische Befunde am hallstattzeitlichen Menschen der Oberpfalz — Rückschlüsse auf seine Umwelt. — Anthropologischer Anzeiger., **49**, 1991a, 217-229.
5. Claassen, H. Methoden zur Lebensaltersbestimmung am menschlichen Skelett, dargestellt am Beispiel von hallstattzeitlichen Körper- und Brandbestattungen. Zeitschrift für Gerontologie., **24**, 1991b, 316-318.
6. Claassen, H. Neandertaloide Merkmale am Stirnbein — ein auffälliger hallstatt-zeitlicher Schädel aus dem Grabhügelfeld von Dietfurt/Oberpfalz. — Anthropologischer Anzeiger., 49, 1991c, 3-21.
7. Claassen, H., A. Wree. The Etruscan skulls of the Rostock anatomical collection — How do they compare with the skeletal findings of the first thousand years B.C.? — Ann. Anat., **186**, 2004, 157-163.
8. Ehgartner, W., A. Kloiber. Das anthropologische Material. — In: Das Gräberfeld von Hallstatt, Textband (Ed. K. Kromer). Firenze, 1959, 29-34.
9. Ehrhardt, S., P. Simon. Skelettfunde der Urnenfelder — und Hallstattkultur in Württemberg und Hohenzollern. — In: Naturwissenschaftliche Untersuchungen zur Vor- und Frühgeschichte in Württemberg und Hohenzollern (Ed. S. Schiek). Stuttgart, 1971.
10. Jelinek, J. Anthropologie der Bronzezeit in Mähren. Anthropos N. S. 2. Brno, 1959.
11. Lange, G. Die menschlichen Skelettreste aus dem Oppidum von Manching. — In: Die Ausgrabungen von Manching (Ed. W. Krämer). 7. Wiesbaden, 1983.
12. Martin, R., K. Saller. Lehrbuch der Anthropologie. 1, 3. Aufl. Stuttgart, 1957.

Institute of Experimental Morphology and Anthropology

Acta morphologica et anthropologica, 10
Sofia•2005

A Case of Variation of the Left Common Carotid Artery

M. Batinova, T. Kitova, S. Sivkov

Department of Anatomy, Histology and Embryology, Medical University, Plovdiv

Aortic arch variation occurs due to disorders of the development of primitive double aortic arch system. During anatomic dissection on adult cadaver we investigated the variability of appearance of brachiocephalic trunk and left carotid artery. Both these arteries originate together such as first branch of the aortic arch. The second one is the left subclavian artery. It arises from the backside of common carotid artery. The special attention was paid also to ductus arteriosus (Botali). It is thick — 2.5/2 cm, and connects pulmonary trunk and aortic arch, below the left subclavian artery. The literature is reviewed and the clinical significance of aortic arch variations is discussed.

Key words: aortic arch, embryonic development, common carotid artery, variation.

Introduction

Variations of human body attract interest not only as a descriptive finding but also because of their particular clinico-anatomical value [1,2,3]. The relatively high incidence with coinciding abnormal topography of the blood vessels attracts the interest of morphologists and clinicians. The experimental and clinical studies show that developmental anomalies differ depending on the period of critical exogenous or endogenous influence [1]. Development anomalies of the aortic arch result from disturbances in the formation of the primary aortic arch in the early embryonic stages. There are a number of publications in literature presenting a variety of variations of the aortic arch and its branches [4,5]. In the present communication is described an anomalous finding of the brachiocephalic trunk and the left common carotid artery concerned with the topography and dimensions of the vessels. The anomaly is considered a result of embryonic dysmorphogenesis of the primary aortic arches.

Material and Methods

During a routine dissection of a cadaver of adult male in the Department of Anatomy, Histology and Embryology, Plovdiv uncommon topography and dimensions of the heart and large arterial and venous blood vessels was recognized after

exposing the elements in the root of the neck and superior mediastinum. Variation of the aortic arch branches was present.

Results

Dissection exposed normal topography of the elements in the superior mediatinum — i.e., lymph nodes, loose connective tissue, venous vessels, remnant of the thymus, and considerably dilated superior vena cava — circumference 8.5 cm and diameter 3.5 cm. The left brachiocephalic vein was with normal dimensions but the thoracic duct was thickened — 2.5cm/2.0cm. The aortic arch was found deeper beginning at the level of the second right sternocostal joint, bending upward and backward from right to left, locating in front of the trachea, and then turning downward and backward to the fourth thoracic vertebra. The convexity of the arch was at higher level and 15 cm in length while the length of the concavity was 6.5 cm. The aortic arch circumference was 12.5 cm and the diameter — 5 cm.

The branches of the aortic arch were two — the brachiocephalic trunk and the left common carotid artery (LCCA) beginning with a common stem and the left subclavian artery. The common stem was 9 cm wide. LCCA branched immediately above the aortic arch, ascended in front of the trachea lodging between the left side of the trachea and the left recurrent laryngeal nerve. LCCA was 3 cm wide, the right common carotid artery 2.8 cm and the right subclavian artery 5.5 cm.

Fig. 1. The brachiocephalic vein lying on the V-shaped structure and dilated thoracic duct

Fig. 2. The common stem of the brachiocephalic trunk and left common carotid artery and the vertical portion of the left subclavian artery parallel to the left border of the trachea

The left subclavian artery was the second branch of the aortic arch beginning from its posterior aspect at 2.5 cm from the LCCA. It passed behind the left brachicephalic vein, ascended to the level of the left recurrent laryngeal nerve and bent sharply to the left towards the interscalenic space. The artery was 7.0 cm wide and 3.0 cm long up to the bent and its length from the bent to the interscalenic space was 2.5 cm.

The persistent ductus arteriosus with 1.8 cm circumference and 2.0 cm length connected the pulmonary trunk and aortic arch opposite the origin of the left subclavian artery.

Discussion

The anomalies of the aortic arch result from maldevelopment of the primary aortic arches in the early week 4 of gestation. The remnants of the arterial vessels are paired. They leave the heart through the aortic sac, which is the anterior part of the common arterial trunk. From the arterial trunk begin the two ventral aortae, which join the six aortal brachial arches. In further development of the arterial vessels in the cervical region part of the aortic arches reduce and the remaining ones follow an irregular growth [2]. Not all of the aortic arches exist at one and the same time [1]. The first two aortic arches degenerate before the next arches appear. From their roots are formed the two common external carotid arteries [1]. The third and fourth arches form in the beginning of the week 5 of gestation at 5-mm embryo. The carotid arteries develop from the third aortic arch. From the proximal part of the third arch forms the common internal carotid artery and from the distal part the dorsal aorta is formed [1]. The fourth pair aortic arches gives rise to the distal part of the definite aortic arch on the left and the right subclavian artery on the right side. The aortic bag gives origin to the common carotid artery, ascending aorta, the proximal part of the aortic arch and brachiocephalic trunk. Variations are more frequently seen in the initial part of the left common carotid artery than in the right carotid artery [7]. The distance between the initial part of the branches of the aortic arch can increase or decrease with LCCA approaching the brachiocephalic trunk being the most frequent variation [6].

Conclusions

1. The described variation can be due to the common origin of the aortic sac and third aortic arch, which supported by the findings of other authors. Its is possible that an inhibiting noxious factor prevents the cell reaction to induction signal. The anomaly (right shift) of the LCCA could be a compensatory mechanism for the embryo surviving. This suggests more profound studies. Harmful factors of various natures could be a subject of investigation.

2. The right marginal vessels are narrower with approximately 5 mm in their circumference than the left ones, which suggest a tendency to insufficient blood supply of the corresponding regions — the right upper limb and right half of the head and neck.

3. Due to the changed origin of the LCCA the position of the left recurrent laryngeal nerve is changed from lateral to medial with 12 mm. This change in the nerve topology should be taken into consideration in the surgical practice.

References

1. Heinech, R., A. Mohiuddin. Handbook of human embryology. Edinburgh and London, E&S. Livingstone Ltd., 1970, 112-115.
2. Davies, D., V. R. Coupland. Gray's anatomy. New York, Thirty-fourth edition, Longman's, 1984, 784-777.
3. Lucev, N. et al. Variations of the great arteries in the carotid triangle. — Otolaryngol. Head Neck Surg., **122**, 2000, No 4, 590-591.
4. Nelson, M. L., C. Sparks. Unusual aortic arch variation:distal origin of common carotid arteries. — Clin. Anat., **14**, 2001, No 1, 62-65.
5. Sadler, T. Langman's medical embryology. — Baltimore, Williams & Wilkins, Sixth Edition, 1990, 214-215.
6. Turgut, H. et al. Patent ductus arteriosus, large right pulmonary artery and brachiocephalic trunk variations. — Surg. Radiol. Anat., **23**, 2001, No 1, 69-72.
7. Георгиев, И. Ембриология на човека. С., Медицина и физкултура, 1975, 77—79.

Institute of Experimental Morphology and Anthropology

Acta morphologica et anthropologica, 10
Sofia•2005

Lunate Bone-Types and Morphological Characteristics

S. Dyankova

Department of Anatomy, Histology and Embryology, Medical University, Varna

One hundred macerated lunate bones were researched for the number of the joint facets on the distal and the proximal surfaces. Four types of lunate bones were classified according to their relationship with the bones situated proximally and distally:
1. **Type I (−)** — contacting with the radius and the capitate bone — 10%.
2. **Type I (+)** — contacting with the radius, discus articularis and the capitate bone — 24%.
3. **Type II (−)** — contacting with the radius, the capitate and the hamate bone — 16%.
4. **Type II (+)** — contacting with the radius, *discus articularis*, the capitate and the hamate bone — 50%.
The metrical characteristics suggest that the type that undergoes the greatest pressure is Type II (+).

Key words: os lunatum, types, morphology, morphometry.

Introduction

The lunate bone plays an important role in the statics and biomechanics of the wrist joint complex. Some anatomical variations affect the translation of pressure from the metacarpal bones and, therefore, affect its biomechanics and pathology [6]. Different classifications of the *os lunatum* types can be found according to the method of research [2, 3, 11, 12, 13]. In this report we aim to study the different types of *os lunatum* and their morphological and metrical characteristics.

Material and Methods

One hundred macerated lunate bones were studied scopically for the number of the joint facets on the distal and the proximal surface and, metrically, after Martin-Saller [5] (10 indicators) following which a descriptive statistical analysis was made.

Results and Discussion

The scopical observations of the lunate bones revealed that 34% of them had one facet on the distal joint surface for the capitate bone (type I, according to Viegas et al. [10] and 66% of them had two facets for the capitate and the hamate bones (type II, according Viegas et al. [10] (Fig. 1, 2).

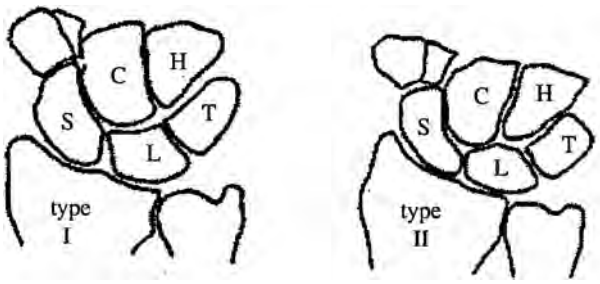

Fig.1. Lunate bone type I and II (Viegas et al., 1990)

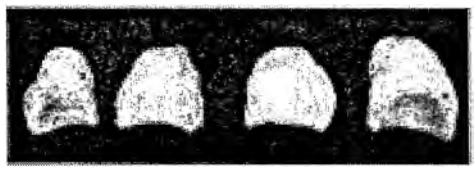

Fig. 2. Lunate bone type II

This direct research of bones excludes the probability of misdetermination of type II as type I unlike roentgenological, MRI and arthroscopy. Therefore, there is some difference in the data obtained (Table 1).

The analysis of the metrical characteristics of *os lunatum* type I and type II (Table 2) shows:

1. All measurements after Martin and Saller [5] except indicator No 6 are greater at the *os lunatum* type II. The difference is statistically significant in indicators No 1 and 7;
2. The width of the joint facet for *os capitatum* in type I is greater than the same of type II (indicator No 7a). The difference is statistically significant.
3. The width of the joint facet for *os capitatum* in type II is always greater than the width of the joint facet for *os hamatum*.

Table 1. Os lunatum types

Method	Authors. years	type I – %	type II – %
Macerated bones	**Dyankova S. (2004)**	34 %	66 %
Dissection of wrists	**Dyankova S. (unpublished data)**	44 %	56 %
	Viegas S. F. et al. (1990 a)	39.3 %	60.7%
	Viegas S. F. et al. (1990 b)	34.5 %	65.5%
	Viegas S. F. et al. (1993)	27 %	73 %
MRI and arthroscopy	**Malik A. M. et al. (1999)**	42.5 %	57.5 %
Roentgenography of wrists	**Viegas S. F. et al. (1990 b)**	46.1%	53.9%
	Tsuge S. R. Nakamura (1993)		
	Contralateral unaffected wrists of patients with trauma		42%
	Contralateral unaffected wrists of patients with Kienböck's disease		37%
	Bilateral wrists of volunteers		35%
MR arthrography	**Pfirrmann C. W. A. et al. (2002)**	50%	50%

Table 2. Measurements of os lunatum type I and type II — mean and standard error, mm

Indicator after R. Martin and K. Saller	Indicator No	type I (n=34)	type II (n=66)
Length	1	15.62 ± 0.29*	16.35 ± 0.22*
Greatest width	2	13.24 ± 0.28	13.68 ± 0.22
Greatest height	3	16.35 ± 0.26	16.44 ± 0.28
Greatest height of the proximal surface	4	14.16 ± 0.31	14.73 ± 0.23
Greatest width of the proximal surface	5	11.93 ± 0.31	12.57 ± 0.24
Greatest height of the distal surface	6	13.16 ± 0.19	13.11 ± 0.19
Width of the distal surface in the middle	7	9.26 ± 0.17**	9.98 ± 0.13**
Width of the joint facet for *os capitatum*	7a	9.26 ± 0.17**	7.89 ± 0.11**
Width of the joint facet for *os hamatum*	7b	0	3.34 ± 0.12
Greatest depth of the distal surface	12	3.65 ± 0.10	3.81 ± 0.12

*$p<0.05$; **$p<0.0025$

The scopical observation of the lunate bones revealed that 26% of them had one facet on the proximal joint surface, and 74% of the lunate bones had two joint surfaces with margins for contact with the radial bone and *discus articularis*. Having only one facet on the proximal surface does not mean that the lunate bone does not contact *discus articularis*. In a case of adduction in the radiocarpal joint, the lunate bone is always in contact with *discus articularis* whereas, in neutral position and abduction, they would probably not contact. Zapico's results [13] for the frequency of one facet only on the proximal joint surface (30%) are similar to ours.

We can classify four types of relationships of the lunate bone with the bones situated proximally and distally, based on the present of one or two facets on the proximal and on the distal joint surfaces:

1. Lunate bone **type I (–)** — with one facet on the proximal and one facet on the distal joint surface contacting only the capitate bone — 10%.

2. Lunate bone **type I (+)** — with two borderline facets on the proximal and one facet on the distal joint surface for a contact only with the capitate bone — 24%.

3. Lunate bone **type II (–)** — with one facet on the proximal and two facets on the distal joint surface for a contact with the capitate and hamate bones — 16%.

4. Lunate bone **type II (+)** — with two borderline facets on the proximal and two facets on the distal joint surface for a contact with the capitate and hamate bones — 50% (Fig. 3).

The measurements of the four types show that Type II (–) (except indicator No 6) and Type II (+) (except indicator No 3 and No 6) are greater than the same measurements of Types I. The difference between the greatest height of the proximal surface of *os lunatum* type II (–) and (+) is statistically significant ($p<0,05$) (Table 3).

Fig. 3. Zunate bone type I (–), I (+) and II (—), II (+)

Table 3. Measurements of the os lunatum type I and type II (–) and type I and type II (+) — mean (mm)

Indicator after R. Martin and K. Saller	type I (–) (n=10)	type II (–) (n=16)	type I (+) (n=24)	type II (+) (n=50)
Length (1)	15.59	16.01	15.63	16.45
Greatest width (2)	12.92	13.77	13.38	13.64
Greatest height (3)	15.80	16.03	16.58	16.57
Greatest height of the proximal surface (4)	13.40	14.06*	14.48	14.94*
Greatest width of the proximal surface (5)	11.46	12.57	12.13	12.56
Greatest height of the distal surface (6)	13.11	12.37	13.18	13.15
Width of the distal surface in the middle (7)	9.10	10.07	9.32	9.95
Width of the joint facet for *os capitatum* (7a)	9.10	7.82	9.32	7.91
Width of the joint facet for *os hamatum* (7b)	0	3.62	0	3.25

*p<0.05

The lunate bone is subject to pressure both from the proximal and the distal direction. In specilised literature this pressure from both sides is known as "the phenomenon of the nut-cracker" [1]. The "nutcracker's phenomenon" is also considered to play an important role in the development of Kienböck's disease. The pressure varies with the anatomical type of the lunate bone. This pressure from the distal direction on the lunate bone type II comes not only from the capitate and respectively from the II-nd and III-rd metacarpal bones, but also from the hamate and respectively from the IV-th and V-th metacarpal bones. Thus there is probably a significant pressure increase on a unit area of the lunate bone type II. As the mean value of the greatest width of the proximal and the distal joint surface is lower in the lunate bone Type II (+), the pressure this type suffers is probably the greatest.

Conclusions

Our investigations suggest that the type that undergoes the greatest pressure is Type II (+).

References

1. Chuinard, R. G., S. C. Zeman. Kienböck's disease: An analysis and rationale for treatment by capitate-hamate fusion. — *Orthop. Trans.*, **4**, 1980, 18.
2. Gupta, A., N. M. Al-Moosawi. Lunate morphology. — *J. Biomech.*, **35**, 2002, 1451-1457.
3. Kato, H., R. Nakamura. Lunate Morphology of Kienböck's disease on X-Ray Study. — *J. Hand Surg.*, **4**, 1999, 75-79.
4. Malik, A. M. et al. MR imaging of the type II lunate bone: frequency, extent, and associated findings. — *Am. J. Roentgenol.*, **173**, 1999, 335-338.
5. Martin, R., K. Saller. Lehrbuch der Anthropologie. Bd.I, 1957, Bd.II, 1958 Stuttgart. G. Fischer Verl.
6. Nakamura, K. et al. Motion analysis in two dimensions of radial-ulnar deviation of type I versus type II lunates. — *J. Hand Surg.*, **25**, 2000, 877-888.
7. Pfirrmann, C. W. A. et al. The hamatolunate facet: characterization and association with cartilage lesions — magnetic resonance arthrography and anatomic correlation in cadaveric wrists. — *Skeletal Radiol.*, **31**, 2002, 451-456.
8. Tsuge, S., R. Nakamura. Anatomical risk factors for Kienböck's disease. — *J. Hand Surg.*, **18B**, 1993, 70-75.
9. Viegas, S. F. The lunatohamate articulation of the midcarpal joint. — *Arthroscopy*, **6**, 1990a, 5-10.

10. V i e g a s, S. F. et al. Medial (hamate) facet of the lunate. — *J. Hand Surg.*, **15**, 1990b, 564-571.
11. V i e g a s, S. F. et al. Wrist anatomy: incidence, distribution, and correlation of anatomic variations, tears, and arthrosis. — *J. Hand Surg.*, **18**, 1993, 463-475.
12. W a t s o n, H. K., M. Y a s u d a, P. M. G u i d e r a. Lateral lunate morphology: an x-ray study. — *J. Hand Surg.*, **21**, 1996, 759-763.
13. Z a p i c o, J. M. Malacia del Semilunar. Thesis doctoral. Universidad de Valladolid, 1966, Industrias y Editorial Sever Cuesta, Valladolid.

Institute of Experimental Morphology and Anthropology

Acta morphologica et anthropologica, 10
Sofia • 2005

Vertebral Artery Arising from Aortic Arch. Embryological Basis and Clinical Implication

S. Novakov, N. Yotova, S. Muletarov, M. Tufkova

Department of Anatomy, Histology and Embryology, Medical University, Plovdiv

Anatomic variation and routine clinical job are closely related. The detailed knowledge of vascular variations is quite important for the physician. Our study reveals frequently met variation of left vertebral artery found during regular student dissection on an embalmed cadaver. The artery arises directly from the aortic arch and enters the transverse foramen at the level of fifth cervical vertebra. It has a longer course compared with standard one. The authors suggest embryologic basis of its frequency and emphasize the clinical importance. In conclusion we consider that the described variation is an important fact for the physician and should be included in students' anatomy textbooks.

Key words: vertebral artery, variations, aortic arch, embryology.

Introduction

Human anatomy variations are not so rarely found and therefore their clinical significance is reported by many authors [7, 8]. The detailed knowledge of vascular variation is quite important for a physician during his routine work. The vertebral artery unusual beginning is not so often discovered: for the right one the beginning from aortic arch is in 3% [3], while for the left is 4.1% [4]. This study reveals a case of left vertebral artery arising from the aortic arch.

Description

During routine student dissection of a 72 years old male cadaver no vertebral artery was found arising from subclavian artery. The next stage of our work revealed the aortic arch with four branches including the left vertebral artery. The right vertebral artery had normal beginning and course.

The vertebral artery arises from the upper and posterior part of the first part of the subclavian artery. It ascends through the foramina in transverse processes of all the cervical vertebrae save the seventh, winds behind the lateral mass of the atlas, enters the skull through the foramen magnum, and, at the lower border of the pons joins the vessel of the opposite site to form the basilar artery.

The vertebral artery consists of four parts. The first part runs upwards and backwards between the longus colli and the scalenus anterior and behind the common carotid artery. In front, it is related to the common carotid artery and vertebral vein, and is crossed by the inferior thyroid artery. On the left side it is crossed also by the thoracic duct. Behind, it is related to the transverse process of the seventh cervical vertebra, the cervicothoracic ganglion and the ventral rami of the seventh and eighth cervical nerves.

The second part ascends through the transverse foramina of the upper six cervical vertebrae, with a large branch derived from cervicothoracic sympathetic ganglion, and by a plexus of veins, which unite to form the vertebral vein. It lies in front of the ventral rami of the cervical nerves (C2-C6), and pursues an almost vertical course as far as the transverse process of the axis, through which it runs upwards and laterally to the transverse foramen of the atlas.

The third part issues from the foramen on the medial side of the rectus capitis lateralis, and curves backward behind the lateral mass of the atlas, the ventral ramus of the first cervical nerve being on its medial side. It then lies in the groove on the upper surface of the posterior arch of the atlas, and enters the vertebral channel by passing below the lower, arched border of the posterior atlanto-occipital membrane. This part of the artery is covered by the semispinalis capitis and is contained in the suboccipital triangle. The dorsal ramus of the first cervical nerve lies between the artery and the posterior arch of the atlas.

The fourth part pierces the dura and arachnoid mater, ascends in front of the roots of the hypoglossus nerve and inclines medially to the front of medulla oblongata where, at the lower border of the pons, it unites with opposite artery to form the basilar artery.

In our case variation is found of the aortic arch having four branches (Fig. 1). The first branch is the brachiocephalic trunk which appears on 23 mm from the beginning of the aortic arch and its diameter is 13 mm. Upwards it bifurcates into right subclavian (9 mm in diameter) and right common carotid (7.5 mm in diameter) arteries. The second branch is the left common carotid artery (7.5 mm in diameter) lying 14 mm from the previous branch. The third branch is the variable vertebral artery arising 3 mm to the second branch and being 5mm in diameter. The fourth branch is the left subclavian artery 10 mm in diameter. The left vertebral artery arises from the upper part of the aortic arch between the left common carotid and left subclavian arteries. In its prevertebral part climbs upwards between the left brachiocephalic vein in front, and the thoracic duct behind. Craniad medially and behind are the trachea, esophagus and the left laryngeal nerve, while in front is the inferior thyroid artery. Further the artery lies between the scalenus anterior muscle and the longus colli muscle and behind the left common carotid artery. It enters the transverse foramen at the level of fifth cervical vertebra. The entire length of the left vertebral artery in its prevertebral part is 77 mm. The normal right vertebral artery is 44 mm in length.

Discussion

Many variations occur in number and position of vessels arising from the aortic arch. There may be as few as one or as many as six branches. The usual combination of three branches is reported in 80% of cases, right brachiocephalic, left common carotid and left subclavian [3]. If a vertebral is present, the left more frequently than the right vertebral, then the variation of four vessels has a frequency of about 5% [3].

Fig. 1. Left vertebral artery arising from aortic arch

The frequency of the left vertebral artery arising from the aortic arch is: Pelligrini — Examined 104 specimens and noted the variation 3 times; Bean — Examined 129 specimens and reported the variations 3 times; Canivares — Examined 40 subjects and 80 individual hearts and noted the variation 2 times; Dubreuil-Chambardel — Examined 250 subjects and found the vertebral artery arising 2 times from the aortic arch [3]. In our case the founding belongs to the variation of aortic branches, which is second by frequency. The role of this study is to accentuate the significance of the embryologic basis as an explanation for the high frequency of this variation and its clinical importance for the medical practice.

Embryologic basis

The anomalies and variations of the aortic branches are based on the deviation of the transformation of the aortic arches. The aortic arches of the human embryo have great significance when viewed comparatively. Five or more pairs of arches are

provided in connection with the functional gills of fishes and either three or four pairs serve the same purpose in tailed amphibians. In higher vertebrates there is both a reduction in number and an extensive transformation into vessels more appropriate to air-breathing animals. In the embryos of man and other mammals six pairs of aortic arches developed but all are not present at one time. The primitive internal carotid arteries begin with the third arch and continue by way of the dorsal aorta to the head region. Both fourth arches persist, but their histories differ. On the left side the arch becomes the permanent arch of the aorta. On the right side a right portion of the aortic sac elongates into the brachio-cephalic trunk.

The vertebral arteries are an important pair of vessels, which arise as secondary developments from two series of dorsal rami belonging to the neck (Fig. 2). These rami undergo longitudinal linkage just dorsal to the ribs (postcostal anastomosis). All of their original stalks then atrophy except the most caudal one in the series. The resulting longitudinal vessel is a vertebral artery. The latter together with subclavian artery begins from the six intersegmental artery [2].

We suppose that the rising of the left vertebral artery directly from the aortic arch is due to the higher beginning (fifth or fourth intersegmental artery) of the 'postcostal anastomosis' and persistence of the part of each intersegmental artery which appears to be the origination of the vertebral artery. In connection with the faster growth craniad of the adjacent structures the root of the left subclavian as well as the proximately placed variable left vertebral artery shift considerably higher on the permanent aortic arch.

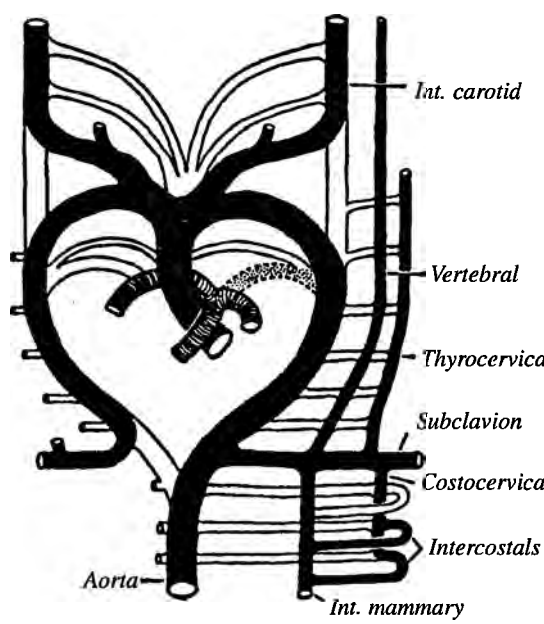

Fig. 2. Derivatives of the dorsal branches of the human aorta in the vicinity of the subclavian artery

Clinical implications

The knowledge of the structures connected with brain blood supply and their relations in the superior mediastinum and the neck is very important with clinical diagnosis and especially with vertebro-basilar syndrome [6]. According to the available data [5] our case is essential for the surgeon during operation for metastases and lymph nodes of esophageal cancer and malignant vertebral tumors. Very significant are the relations of the aorta and its branches during total aortic arch replacement [1]. To know about this finding seems to be very important not only in diagnosis (angiography, color coded Doppler sonography) but also in surgical and endovascular treatment.

Conclusion

The variation described by the authors is not infrequently found which is suggested by our embryologic interpretation. The last conclusion together with the undoubted clinical importance of the variant vertebral artery makes it an important fact for the physician. We consider that the described variation should be included in students' anatomy textbooks.

References

1. Apaydin, A. Z. et al. Experience with cerebral perfusion in total aortic arch replacement. — Med. Sci. Monit., **8**, CR, 2002, No 12, 801-804.
2. Arey, L. B. (editor). Developmental Anatomy. A textbook and laboratory manual of embryology. — Philadelphia and London, W. B. Saunders Company, 1965, 350-356.
3. Bergman, R. A. et al. Compendium of human anatomic variation. — Munich: Urban and Schwarzenberg, 1988.
4. Nelson, M. L., C. D. Sparks. Unusual aortic arch variation: distal origin of common carotid arteries. — Clin. Anat., **14**, 2001, No 1, 62-65.
5. Reijiro, S. et al. Esophageal cancer associated with right aortic arch: report of two cases. — Jpn. J. Surg., **29**, 1999, 1164-1167.
6. Tzvetkova, A. et al. A rare variant of the vertebral artery directly arises from the arch of the aorta in connection with a vertebro-basilar syndrome. — 85th Anniversary of the Department of Anatomy and Histology. Anatomical Collection., 2003, 91.
7. Willan, P. L., J. R. Humperson. Concept of variation and normality in morphology: important issues at risk of neglect in modern undergraduate medical courses. — Clin. Anat., **12**, 1999, No 3, 185-190.
8. Zucconi, W. B., M. Guelfguat, N. Solounias. Approach to the educational opportunities provided by variant anatomy, illustrated by discussion of a duplicated inferior vena cava. — Clin. Anat., **15**, 2002, No 2, 165-168.

Institute of Experimental Morphology and Anthropology

Acta morphologica et anthropologica, 10
Sofia•2005

MP Joint of the Thumb — Thickness of the Subchondral Zone of Mineralization and Subchondral Bone Density

S. Terzieva

Department of Anatomy, Histology and Embryology, Medical University, Varna

75 anatomic preparations of the MP joint of the thumb were studied by means of computed tomography-osteoabsorptiometry (CT-OAM). The results reveal the predominance of the polymorph type (type A) of distribution of the density maximums in caput ossis metacarpalis and the prevalence of type C (maximums are located mainly in the dorsal and/or radial area) in basis phalangis proximalis.

The results of the investigation of the thickness of the subchondral zone of mineralization of the histological slices of the anatomic preparations of the MP joint of the thumb prove the existence of three types of distribution of the maximums of this parameter: type A — polymorph type, type B — maximums are located mainly in the center and type C — maximums are located in the dorsal and/or radial area.

Key words: subchondral bone, density, thickness.

Introduction

The simultaneous investigation of two morphological parameters reflecting the long-term stress in the joint provides richer information concerning its mechanical situation.

The CT —OAM method can be applied to patients and the data collected can be used in the process of diagnosing of some mechanically predetermined joint diseases. The method by means of which the thickness of the subchondral zone of mineralization was defined was additional and controlling.

Material and Methods

1. Determination of the thickness of the subchondral zone of mineralization 4 anatomic preparations were put in methylmetakrylat (MMA) and anatomic slices were made — 100 μm in thickness. By means of Vidas — an image analyzing system — the thickness of the subchondral zone of mineralization was determined — this process was carried out perpendicularly to the joint surface. The values achieved were used for creating images — aggregates of isocrasides (Fig. 1). The isocrasides are lines that connect points with the same thickness.

Schemes were made based on these images showing the location of the highest values of the parameter studied.

2. Determination of the subchondral bone density by means of the CT-OAM [1, 2, 3, 4, 5].

75 anatomic preparations of the MP joint of the thumb were investigated. By means of the computer tomograph (Picker) CT-slices were prepared 1 mm in thickness each. Afterwards the slices were digitalized with the computer program Analyse®. The purpose of the computer processing was to achieve colour image of the different layers of subchondral bone density (Fig. 6). In this way the distribution of the subchondral bone density was determined for both joint surfaces — caput ossis metacarpalis and basis phalangis proximalis. For better interpretation of the results schemes were drawn based on the colour images. These schemes show the location of the areas with highest bone density.

Results and Discussion

The results from the investigation of the subchondral zone of mineralization prove the existence of three types of distribution of the maximums of this parameter.
Type A — polymorph (Fig. 2)
Type B — maximum located mainly in the center (Fig. 3)
Type C — maximums located in the dorsal and/or radial area (Fig. 4)
The results of the investigation of the distribution of the subchondral bone density reveal the following types of distribution:
Type A — polymorph type (Fig. 2)
Type B — maximum located mainly in the center (Fig. 3)
Type C — maximums located mainly in the dorsal and/or radial area (Fig. 4)
Type D — maximums located mainly in the palmar area (Fig. 5).

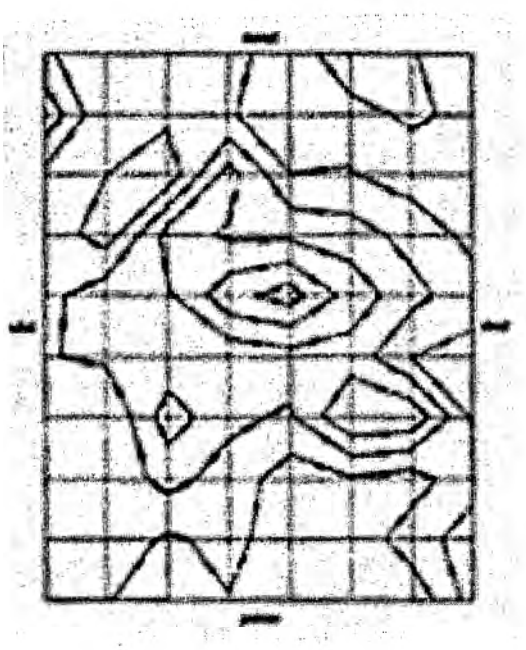

Fig. 1. Isocrasides

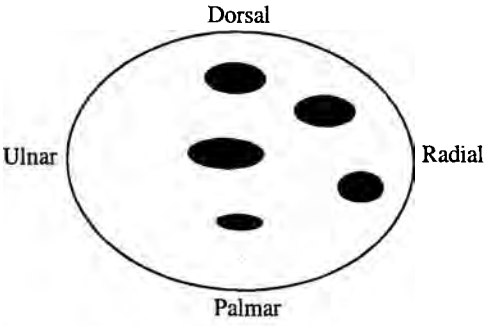

Fig. 2. Type A — polymorph

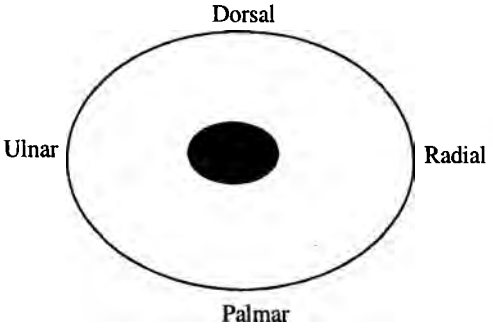

Fig. 3. Type B — maximum located mainly in the center

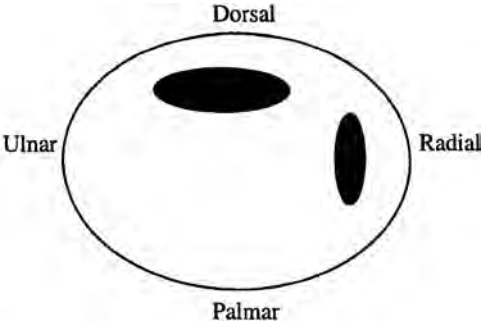

Fig. 4. Type C — maximums located in the dorsal and/or radial area

Caput ossis metacarpalis — it was concluded that the polymorph type of distribution of the density maximums is prevailing.

Basis phalangis proximalis — the results show that the maximums are mainly located in the dorsal and/or radial area of the joint surface.

These results illustrate the way of adapting of the joint surfaces to the long-term stresses.

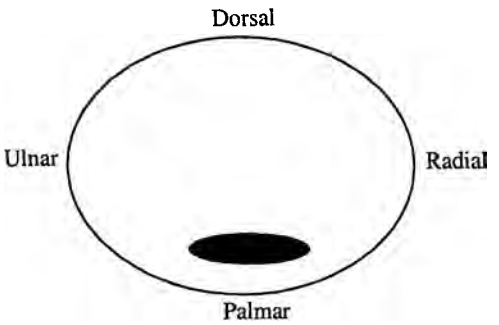

Fig. 5. Type D — maximums located mainly in the palmar area

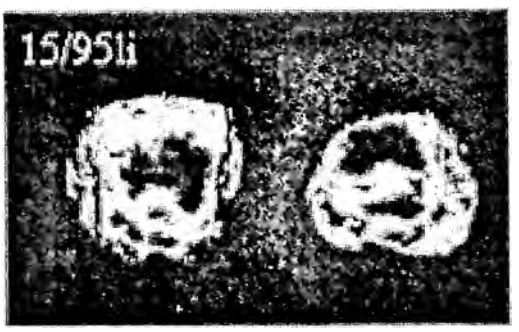

Fig. 6. Determination of the subchondral bone density by means of the CT-OAM

We suggest that the necessity for quick transition and combination of movements has been the leading factor in the formation of the models of distribution of the thickness of the subchondral zone of mineralization and bone density.

References

1. Müller-Gerbl, M. et al. Computed tomography-osteoabsorptiometry for assessing the density distribution of subchonddral bone as a measure of long-term mechanical adaptation in individual joints. — Skelet. Radiol., **18**, 1989, 507-512.
2. Müller-Gerbl, M. et al. Computed tomography-osteoabsorptiometry: a method of assessing the mechanical condition of the major joints in a living subject. — Clin. Biomech., **5**, 1990, 193-198.
3. Müller-Gerbl, M. et al. Die Darstellung der subchondralen Dichtemuster mittels der CT-Osteoabsorptiometrie (CT-OAM) zur Beurteilung der individuellen Gelenkbeanspruchung am Lebenden. Z. Orthop., **128**, 1990, 128-133.
4. Müller-Gerbl, M., R. Putz, R. Kenn. Demonstration of subchondral bone density patterns by three-dimensional CT Osteoabsorptiometry as a noninvasive method for in vivo assessment of individual long-term stresses in joints. — J. Bone Miner. Res., 7, 1992, N0 2, S411-S418.
5. Müller-Gerbl, M., R. Putz. Verteilung der subchondralen Knochendichte als morphologischer Parameter der Beanspruchung im Hüftgelenk. — In: Aktuelle Aspekte der Osteologie (Hrsg: Ittel, HAT, Siebert HG, Matthiaß HH). Berlin-Heidelberg-New York, Spinger, 1992.